SPATIO-TEMPORAL VARIATIONS IN PHYSICOCHEMICAL WATER QUALITY AND THE IMPACT OF LAND USE/LAND COVER CHANGE IN RIVER ATHI BASIN, KENYA.

OGBONNA VINCENT ANABORO

A Thesis Submitted in Partial Fulfillment of the Requirements for the Degree of Doctor of Philosophy (Ph.D.) In Environmental Management at South Eastern Kenya University

2025

DECLARATION

I understand that plagiarism is an offense and I, therefore, declare that this thesis is my original work and has not been presented to any other University or Institution for any other award.

Signature: 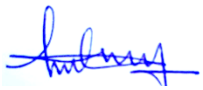 Date: 01-09-2025

Ogbonna Vincent Anaboro

B502/MAI/30016/2021

This thesis has been submitted for examination with our approval as the university supervisors.

Signature: ……. Date: ……

Dr. Charles Ndung'u.

Department of Environmental Science and Land Resources

South Eastern Kenya University

Signature: ……. Date: ……

Dr. Matheaus K. Kauti.

Department of Environmental Science and Land Resources

South Eastern Kenya University

ACKNOWLEDGEMENT

First and foremost, I extend my wholehearted and eternal gratitude to God Almighty, "in whom I live, think, move, and have my being." I am profoundly grateful for His boundless love, grace, and mercy that have guided me throughout my journey and provided me with the extraordinary privilege to conduct my Ph.D. research at South Eastern Kenya University. To Him be all the glory and honor forever.

I also express my heartfelt gratitude to the University of Port Harcourt and the Tertiary Education Trust Fund (TETFund) Nigeria for granting me the opportunity to advance my academic pursuits. This generous scholarship has enabled me to broaden my knowledge, explore new ideas, and realize my potential beyond Nigeria, and I am deeply thankful for this opportunity.

I would like to extend my heartfelt gratitude to my supervisors, Dr. Charles Ndungu and Dr. Mattheaus Kauti, for their invaluable guidance, dedication, and constructive feedback, which have significantly contributed to the success of this study. Your commitment to my academic development has been truly inspiring - “Asante.”

I also wish to thank the Department of Environmental Science and Land Resources Management, the School of Agriculture, Environment, Water and Natural Resources Management, and the entire staff at South Eastern Kenya University. Your direct and indirect support has been instrumental in my research journey, especially the library and ICT staff. Your dedication to assisting me has made a significant difference, and I pray that God Almighty abundantly rewards you all for your efforts.

To my beloved wife, Mrs. Peace Vincent Ogbonna, and children, including Mrs. Mercy Chibundu Iwedi and Dr. Oriji Onuoha, I owe an immense debt of gratitude for your patience, support, and constant presence when I needed it most. Your timely advice, unwavering prayers, and encouragement have profoundly shaped my actions and decisions during critical moments of this journey. Once again, I extend my deepest

gratitude to everyone who has played a role in my academic journey. Your contributions have not gone unnoticed, and I am forever thankful for your support.

DEDICATION

I humbly dedicate this degree to God Almighty, who has been my unwavering source of strength and guidance throughout this program. His constant support has inspired me to persevere in my academic journey and pursue knowledge with dedication.

To my family, I dedicate this work as a reflection of the love, understanding and support that have guided me throughout this journey. This degree is also dedicated in memory of my late parents, Mr. and Mrs. Anaboro Isaac Ogbonna, who lovely brought me into this world but never lived to celebrate this crown together.

TABLE OF CONTENTS

CHAPTER THREE

CHAPTER FOUR

CHAPTER FIVE

CHAPTER SIX

LIST OF TABLES

LIST OF FIGURES

LIST OF APPENDICES

LIST OF PLATES

ABBREVIATIONS AND ACRONYMS

AAS	**:**	Atomic Absorption Spectroscopy
ANOVA	**:**	Analysis of Variance
AOI	**:**	Area of Interest
APHA	**:**	America Public Health Association
ASALs	**:**	Arid and Semi-Arid Lands
BOD	**:**	Biological Oxygen Demand
CA	**:**	Cluster Analysis
CM	**:**	Centimeter
COD	**:**	Chemical Oxygen Demand
DEM	**:**	Digital Elevation Model
EPA	**:**	Environmental Protection Agency
ETM	**:**	Enhanced Thematic Mapper
FABP	**:**	Final Athi Basin Plan
FAO	**:**	Food and Agriculture Organization
GEE	**:**	Google Earth Engine
GOK	**:**	Government of Kenya
GPS	**:**	Geographic Positioning System
IWMI	**:**	International Water Management Institute
JICA	**:**	Japan International Cooperation Agency
K	**:**	Potassium
KAC	**:**	King Abdullah Canal
KNBS	**:**	Kenya National Bureau of Statistics
LULC	**:**	Land Use/Land Change
MALFC	**:**	Ministry of Agriculture, Livestock, Fishery and Corporation
MEWNR	**:**	Ministry of Environment Water and Natural Resources
Mg/L	**:**	Miligram per Litre
MODIS	**:**	Moderate Resolution Imaging Spectrometer
MOH	**:**	Ministry of Health
MWSI	**:**	Ministry of Water, Sanitation, and Irrigation

MWSSP	**:**	Ministry of Water and Sanitation Strategic Plan
NASA	**:**	National Aeronautics and Space Administration
ND	**:**	Not Detected
NDVI	**:**	Normalized Difference Vegetation Index
NEMA	**:**	National Environmental Management Authority
NEP	**:**	National Environmental Policy
NIR	**:**	Near Infrared
NO3	**:**	Nitrate
NWSS	**:**	National Water Service Strategy
PCA	**:**	Principal Component Analysis
PO4	**:**	Phosphate
QAQC	**:**	Quality Access /Quality Control
S/m	**:**	Siemens per Meter
SDGs	**:**	Sustainable Development Goals
UN	**:**	United Nations
UNEP	**:**	United Nation Environment Programme
UNESCO	**:**	United Nation Educational, Scientific and Cultural Organization
WASREB	**:**	Water Services Regulatory Board
WHO	**:**	World Health Organization.
WRA	**:**	Water Resources Authority
WWAP	**:**	World Water Assessment Programme

ABSTRACT

The growing impacts of natural processes and human activities on water quality at global, regional, and local scales are raising concerns. The River Athi Basin natural gravitational flow toward lower elevations, ultimately reaching the Indian Ocean, facilitates waste disposal practices among the residence located along the river bank. This study sought to determine the Spatiotemporal Variations in Physicochemical Water Quality and the Impact of Land Use/Land Cover Change in the Mid Reaches of River Athi Basin, Kenya by; 1) examining the influence of land use/land cover change in river Athi Basin from 2015 to 2023. (2) Determining seasonal variation in the physicochemical water quality of the river Athi Basin. (3) Assessing the spatial variation in physicochemical water quality of the river Athi Basin. The study examined the influence of LULC changes from 2015 to 2023 using Landsat 8 imagery, GIS, remote sensing, and GPS technologies for data extraction, image processing, and LULC analysis. Pearson correlation analysis assessed spatial differences of land use land cover impacts on water quality across six sampling stations in the basin. Interview survey was used to supplement the water quality dataset. The studies applied multivariate analysis for spatial and temporal reduction of the multidimensional dataset and identification of pollution sources. Seasonal variations in the physico-chemical water quality of River Athi Basin was determined using eight physicochemical parameters (pH, EC, TDS, NO_3, K, PO_4, BOD, and COD) and two heavy metals (Cd and Cr). Data collection was carried out during two distinct seasonal periods: the short dry and rainy season (August-September for dry, November-December for rainy) in 2023, and the long dry and rainy season (January-February for dry, April-May for rainy) in 2024. An independent T-test was used to compare the mean levels of water quality parameters between dry and rainy seasons. The study assessed spatial variation in the physicochemical water quality of the river basin, covering six sampling stations. One way analysis of variance (ANOVA) compared the mean values of variables of the sampling stations. Multiple linear regression tested the influence of pH, EC, TDS, NO_3, K, and PO_4 on BOD and COD (oxidation parameters) and cadmium and chromium (heavy metals). The Pearson Product-Moment Correlation Coefficient (PPMCC) assessed the relationships between water physicochemical parameters and heavy metals in seasonal and spatial variations in water quality of the river basin. The findings on LULC analysis show notable shifts in land use from 2015 to 2023. Between these periods, the overall built-up increased to 0.29%, bare-lands declined by 7.06%. Farmlands, forests, and grasslands were elevated by 0.52%, 4.54%, and 2.77%, with decline in open waters by 1.24%. Spatial LULC difference with correlation analysis reveal higher amounts of EC, TDS, Cd, Cr, NO_3, and PO_4 influencing water quality. Interview survey revealed settlements, agriculture, and climate conditions as the main causes of degradation of water quality. Seasonal finding reveal significant fluctuations in pollution, with the dry season exhibiting higher pollution levels. February demonstrate proliferated temporal pollution, characterized by high concentrations of EC, TDS, BOD, and COD. Spatial finding demonstrated significantly higher pollution signatures in Athi River Town, Stony Athi, and NYS stations, while NYS contribute to higher levels of nutrients, organic pollutants, and heavy metals. In contrast, the control station and Kibwezi Bridge station demonstrates effective self-purification processes. Multivariate analysis revealed pollution sources over time and space in the River Basin.

The stable pH levels over time and space was influenced by the buffering capacity. Multiple regression analysis indicates that physicochemical parameters, such as pH, EC, TDS, NO_3, K, and PO_4, explain 62% of BOD variation and 70% of COD variation, as well as 36% of both Cd and Cr variations. Pearson correlation analysis shows strong links between EC, TDS, BOD, and heavy metals (Cd, Cr), with significant associations among nutrients and other water quality indicators. Natural and anthropogenic activities are pivotal drivers of the water quality degradation of River Athi Basin over time and space. This study recommends that the National Environmental Management Authority (NEMA) and the National Environmental Policy (NEP) strengthen regulations on environmental management, water resource conservation, sustainable land use, public health protection, irrigation control, forest preservation, and aquatic ecosystem conservation in order to support global efforts toward achieving Sustainable Development Goals (SDGs).

CHAPTER ONE

1.0 INTRODUCTION

This chapter sets the context of the research question by presenting the background of the study, statement of the problem, research objectives and hypothesis. Furthermore, it outline the significance of the study and its scope, it addressed the study limitations and clarified the assumptions made. Finally, it provided an overview of the study organizations.

1.1 Background to the Study

Water, a transparent, odorless, tasteless, and colorless chemical substance, is a ubiquitous and essential element on Earth. The increase in human population, coupled with rapid technological advancements and economic development, has propelled a pivotal phase in the degradation of natural water quality. These trends have intensified over the years, subjecting humanity to current and impending global water quality crises, leading to greater risks of hunger, disease, and mortality. Agriculture, industry, and human settlement have emerged as major drivers of water pollution globally (FAO & IWMI, 2017; UN-Water, 2011). Water quality deteriorate with agricultural activities surpassing contamination from settlements and industries, leading to the degradation of inland and coastal waters (FAO & IWMI, 2017). Approximately 78% of global eutrophication in marine and freshwater systems is due to intensive agricultural fertilization (Poore & Nemecek, 2018), affecting 415 coastal areas and contributing to 70% of nutrient pollutants from runoff (GIWS, 2022; One Earth, 2022).

Global industrialization and urbanization contribute significantly to the introduction of pollutants such as heavy metals, chemicals, and nutrients into rivers, lakes, and oceans, leading to widespread pollution. It is estimated that 300-400 megatons of industrial effluents are discharged into water bodies annually (One Earth, 2022). The combination of industrial and agricultural effluents, including solid waste and wastewater, introduces substantial amounts of organic and inorganic toxins into these water bodies. Approximately 80 percent of wastewater, including 40 million liters from various sources, is believed to be left untreated in water bodies worldwide (One Earth, 2022; UNESCO, 2021; Conserve

Energy Future, 2020). Plastics and micro plastics are growing global concerns, affecting both freshwater and marine ecosystems. It is estimated that about five trillion pieces of plastic are floating in the oceans, and this number has been increasing since 2009 (Sutherland *et al*., 2019). The aftermath of these threats to water quality is disastrous, with consequences for Gross Domestic Product (GDP), including food shortages, damage to economic productivity, commercial fisheries, and tourism, decreased ecosystem functions, and a decline in potable water supply, alongside the increasing cost of drinking water treatment (UNESCO, 2021; Shortle *et al.,* 2019). These incidence are influenced by trends in spatial and seasonal cycle induced by day to day anthropogenic activities and climate factors worldwide. In light of this, Maja & Ayano (2021) envisions future catastrophes stemming from the causal nexus of global population increase, increasing development pressure, industrial productive capacity, and intensive agriculture and land use conversion. However, UNEP and WHO emphasize monitoring spatio-temporal dynamics to guide water management under climate stress (UNEP, 2022; UN, 2016).

Water quality variation is a multifaceted issue shaped by regional environmental conditions, including geographic location, climatic variability, and evolving land use patterns (Huang *et al*., 2022). These factors converge to influence the chemical, biological, and physical attributes of water bodies, producing spatial disparities in water quality outcomes. A major driver of this variability is transboundary pollution, wherein pollutants originating from one region cross borders and impact neighboring ecosystems. This has escalated tensions between communities and governments, highlighting the urgent need for cooperative and integrated water resource management. In particular, the pursuit of economic growth fueled by agriculture and industrial activity, has led to increased wastewater discharge, nutrient loading, and consequentially, the rise of eutrophication (Pericherla *et al*., 2020). As demand for industrial and agricultural products intensifies to meet global market needs, water systems bear the brunt. These sectors, contributing significantly to national GDP and GNP, are also responsible for substantial environmental degradation. Approximately 80% of anthropogenic activities rely on water, with agriculture being especially influential in developing countries (Connor & Chaves, 2024). This dependency manifests in widespread contamination, especially in regions lacking

adequate water governance. Eutrophication, a direct result of nutrient enrichment, has reached alarming levels globally, affecting over half of lakes and reservoirs in Asia and Europe, and close to half in North America, South America, and Africa (Global Institute for Water Security, 2022). Climate dynamics exacerbate these problems. In monsoon regions of Asia, heavy rainfall drives runoff and pollutant transport, while in arid areas like Sub-Saharan Africa, drought concentrates contaminants, aggravating toxicity levels (Ngatia *et al*., 2023; Eze *et al.,* 2018). Industrial activity and underlying geology also influence regional concentrations of heavy metals in water, adding complexity to the spatial variation narrative (Ling *et al*., 2017). In African oil-producing nations like Nigeria, little has been done to address regional transboundary effects of oil pollution on water quality. This persistent "business as usual" mentality has jeopardized water quality degradation, public health and environmental integrity. Given that 64% of African river basins are transboundary, regional collaboration is no longer optional, it is imperative for water security (UN-Water, 2021). Population growth further strains surface water systems, intensifying the consequences of poor land use and waste management (Liyanage & Yamada, 2017). In response to these challenges, regional policies have emerged. The African Water Vision 2025, led by the African Union and its partners, outlines a strategy for equitable access, sustainability, and cross-border cooperation in water governance (Economic Commission for Africa, 2012). This initiative reflects a continent-wide recognition of the need for integrated water resource management.

In Kenya, water quality degradation stems from intensified agriculture, industrial activity, and urban expansion (Water.org, 2023). Irrigation and agrochemical runoff disrupt aquatic ecosystems, while land use changes from deforestation to sand harvesting compound the issue (Wilson *et al*., 2021; Chepkorir *et al*., 2021). The Athi River Basin, originating from the Ngong Hills and flowing through Nairobi to the Indian Ocean, embodies Kenya's water challenges. Traversing diverse agroecological zones, the river faces pollution from agricultural runoff, urban waste, and industrial discharges (Kitheka *et al*., 2022). Informal settlements and commercial hubs near the riverbanks contribute nutrient loads, raw sewage, plastics, and heavy metals, all of which travel downstream and impair water quality. To this end, the Kenyan government has implemented strategic policies to curb water pollution

and ensure access to safe water for all. Part 2 of the 2010 Constitution of Kenya, Article 43(1)(b) & (d), provides that access to reasonable standards of sanitation and safe water in adequate quantities is an economic and social right for every person (Constitution of Kenya, 2010). Vision 2030 aims to ensure that improved water and sanitation are accessible and available to all citizens by the year 2030 (GOK, 2007), alongside the protection of wetlands and watercourses from indiscriminate waste disposal. The Ministry of Water and Sanitation Strategic Plan 2018-2022 targeted increasing the percentage of the national population with access to safe water from 60% to 80% between 2017 and 2022 (GOK, 2018). The Government, under the National Environmental Policy (NEP), also asserted a policy to improve the management and conservation of potable water supply sources and promote technologies for safe water use, particularly wastewater use and recycling (GOK, 2013). Additionally, the Water Act of 2016, Section 36(c), states that a permit is required to discharge a pollutant into any water resource (GOK, 2016). The effectiveness of these legislations and policies can only be demonstrated by reducing water pollution levels without conflicts of interest among the ministries.

In light of the foregoing, the unprecedented scale and persistent nature of water quality degradation and pollution, at global, regional, and local scales demands an effective set of stricter policies, technology, and scientific advances, in tackling this menace. However, the United Nations (UN) recognized the centrality and importance of water to humanity and, in its 6th Sustainable Development Goal (SDG), set 6.3 target of ensuring access to safe and affordable drinking water and curbing pollution globally by 2030 (UN, 2016). Thus, if the progress made by the UN in addressing water quality and potable water is measured annually from 2015 to the present, considering recent developments and existing challenges at global, regional, and local scales, it could undermine the efforts made over the past nine years and impede further attainment. In its July 2024 report, the UN High-level Political Forum on Sustainable Development (HLPF) recommitted to the zero draft and pledged to redouble or intensify their efforts to achieve a more sustainable world and commit to bold, ambitious, accelerated, just, and transformative action in the remaining six-year agenda (IISD, 2024). Based on this HLPF recommitment and the United Nations (UN) report on the challenges facing low and middle-income countries in attaining the

sixth SDG. It is evident that low-income countries face issues such as poor ambient water quality, inadequate levels of wastewater treatment, and a lack of water quality data, meanwhile, higher-income countries are secondarily dealing with agricultural runoff only (UN, 2023).

However, several studies have been undertaken on water quality within the River Athi Basin, focusing on microbiological, physicochemical, and hydrological characteristics. For example, Away et al. (2017) examined the suitability of Athi River water for irrigation in Athi River Town and its surroundings, while Wambugu (2017) investigated antimicrobial susceptibility among *Escherichia coli* strains in Machakos County. Masime et al. (2022) and Ratemo (2018) explored physicochemical pollution in the upper reaches of the Athi River. Kitheka (2019) examined salinity dynamics, and Kitheka et al. (2022) evaluated hydro-climatic influences on sediment yield and discharge. Kithiia (2021) analyzed basin-wide water quality degradation, and Wilson et al. (2021) linked horticultural activity to pollution levels in the Maumau Stream, a Nairobi River tributary.

To this ends, several gaps exists of which many of these studies do not address, including temporal depth, integrated statistical analysis, and spatial linkage with dynamic land use and land cover (LULC) patterns. Data fragmentation across scales, insufficient spatiotemporal monitoring, and poor connection between pollution gradients and SDG targets further challenge basin-wide water quality management. These shortcomings underscores the urgent need for more integrated, spatiotemporal approaches to water quality assessment, mainly in vulnerable catchments like the River Athi Basin. However, this study addresses these gaps by examining the impacts of land use activities on water quality in the mid-reaches of the River Athi Basin. Specifically, it investigates spatiotemporal variation in water quality and the impacts of LULC change.

In conclusion, the persistent degradation of global water quality, driven by rapid population growth, economic intensification, and widespread land use transformations, has produced multifaceted environmental challenges across global, regional, and local scales. Despite international frameworks like SDG 6.3 and national-level water policies aimed at securing

clean water and curbing pollution, progress remains limited. Much of the attention has focused on strategic planning and presentation, with inadequate emphasis on data-driven monitoring, implementation, and transboundary cooperation.

1.2 Statement of the Problem

The River Athi Basin is undergoing a steady decline in water quality due to a combination of rapid urbanization, industrial discharges, poor waste management, agricultural runoff, and climatic influences. These pressures are compounded by land use and land cover (LULC) changes, as well as natural processes like the weathering of bedrock. The situation is further aggravated by insufficient sewerage infrastructure and indiscriminate waste disposal, particularly in densely populated and industrially active zones (WRA, 2020).

Although previous studies like Ngatia *et al*., 2023; Masime *et al*., 2022; Waturu *et al*., 2022; Kithiia, 2021, have explored various anthropogenic impacts, ranging from industrial effluents and agricultural runoff to sedimentation (Kitheka *et al*., 2022). Hence, spatiotemporal water quality dynamics within the basin remain inadequately monitored and poorly understood. As a result of localized, outdated, or fragmented available data, limiting the capacity for holistic analysis and basin-wide management.

Seasonal variations such as droughts and floods further influence water quality, yet their interaction with land use dynamics and pollution trends across space and time remains underexplored. Critical factors such as topography, settlement expansion, and LULC transitions are rarely examined in tandem, leaving a significant gap in understanding how these variables collectively shape water quality at different points along the basin, upper, middle, and downstream.

This lack of integrated, spatially aware knowledge inhibits policymakers, regulators, and stakeholders from crafting targeted interventions and long-term solutions. A systematic, multivariate approach to assessing spatiotemporal trends, anchored in statistical analysis and remote sensing, is urgently needed to inform sustainable water resource management.

Accordingly, this study aims to bridge these knowledge gaps by investigating the relationships between land use changes and water quality variability across the River Athi Basin. The findings will contribute to more informed decision-making in support of Kenya's national development goals and international environmental commitments.

1.3 General Objective

The general objective of this study was to determine spatiotemporal variations in physicochemical water quality and the impact of land use/land cover change in River Athi Basin, Kenya.

1.3.1 Specific Objectives

i. Assess the influence of land use/land cover change on water quality of River Athi Basin from 2015-2023.
ii. Determines the seasonal variation in physicochemical water quality of River Athi Basin.
iii. Assess the spatial variation in the physicochemical water quality of River Athi Basin

1.4 Hypothesis

i. There is a statistically significant spatial differences in LULC change in water quality parameters across sampling stations of River Athi Basin.
ii. There is a statistically significant seasonal variations in the physicochemical water quality of River Athi Basin
iii. There is a statistically significant spatial variation in the physicochemical water quality of River Athi Basin.

1.5 Significance of the Study

The areas selected for this study are located at the urban, peri-urban, and rural interface of Machakos and Makueni counties, which lack adequate pollution control mechanisms despite multiple legislations. Due to changes in precipitation, runoff, agricultural practices, internal environmental factors, and other variables, the water quality of River Athi Basin

fluctuates both annually and seasonally (during the rainy and dry seasons). The river basin is extensive, with study stations spanning 170 km and encompassing various land uses inducing negative impacts on the water quality. Each of these locations contributes to water pollution in different ways. The study identified pollution hotspots and demonstrated how water quality changes along the river's course from the upper mid-reaches Athi River Town to downstream Kibwezi Bridge.

Land use land cover (LULC) changes contribute to watershed destructions, livelihood sources, displaced habitat, and future flood risk (Nimi *et al*., 2018). This study will serve as a foundation or benchmark for the public, including governmental and non-governmental organizations and policymakers. To gather data for specific strategies in urban planning, pollution control, sustainable agriculture, and industrial waste management. Scholars, students, all Kenyan citizens, and foreign researchers will have access to the results for further research and control strategies. The ASAL (Arid and Semi-Arid Lands) region, in particular, will benefit greatly from the study's mechanism to limit irrigation activities near most rivers, which will serve as future water supply reservoirs.

1.6 The Scope and Limitation

This study was confined to the mid-reaches of the River Athi Basin due to limited funding, which constrained access to research materials and logistics over a span of 170 km. The selected area encompassed parts of Machakos, Makueni, and Kitui counties, with sampling conducted at six key sites: Athi River Town, Stony Athi, the National Youth Service (NYS), River Kyawango Confluence, River Thwake Confluence, and Kibwezi. These locations provide a comprehensive representation of mid-reaches river segments, showcasing various pollution sources and land use impacts. The chosen sites encompass a diverse range of land use activities, including commercial, industrial, agricultural, urban, and rural settlements.

It is anticipated that these activities will lead to significant contamination of the river. By examining these areas, the study documented how different land use patterns affected water quality, enabling an analysis of both natural and human influences throughout the basin.

However, the study's focus on these six sites highlights the variety of pollution sources and land use impacts, offering a balanced depiction of mid-reaches river sections. This comprehensive examination allowed the study to capture the effects of various land use patterns on water quality, considering both natural and anthropogenic influences throughout the basin.

1.7 Assumption of the Study

The study assumes that water quality in the Athi River Basin has been significantly impacted by changes in land use and land cover (LULC) between 2015 and 2023. Deforestation, industrialization, urbanization, and agricultural practices are predicted to be major contributors to changes in water quality parameters.

It is assumed that both natural and human factors affect the Athi River's water quality, which varies over time and space. Bimodal seasonal rainfall patterns and changes in land use are anticipated to drive variations in physicochemical parameters and heavy metal concentrations.

Various land use activities, including industry, agriculture, and settlements, are thought to introduce significant pollutants into the river. Different sampling stations along the river are expected to show varying pollution levels due to their proximity to different activities.

The six chosen sampling stations namely Kibwezi, Stony Athi, NYS, River Kyawango Confluence, River Thwake Confluence, and Athi River Town, homogeneously represented the mid reaches of the River Athi Basin. These stations were specifically selected to monitor changes in water quality levels due to unsustainable land use activities and the impacts across the selected sampling stations.

1.8 Organization of the Study

The organogram in Figure 1, outlines the structure of this research, it provides a clear and systematic representation of the chapters and their respective sections. Each chapter is designed to address specific aspects of the study, ensuring a comprehensive and logical flow of information.

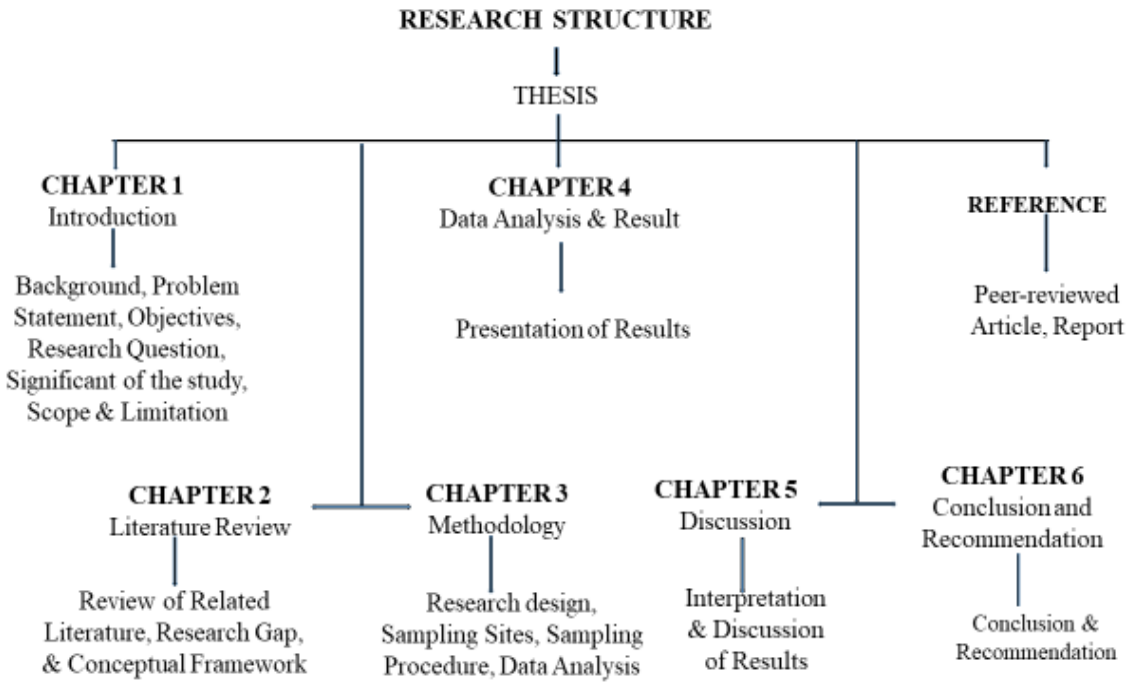

Figure 1: Organizational structure of the research study

CHAPTER TWO

2.0 LITERATURE REVIEW

2.1 Introduction

This literature review examines the impacts of land use/land cover (LULC) changes on water quality, exploring the spatio-temporal and seasonal variations influenced by both natural processes and anthropogenic activities. Findings from multiple studies suggest that water quality is highly dynamic, with both temporal (seasonal) and spatial factors playing crucial roles in its distribution.

2.2 Empirical Review of the Impacts on Water Quality of the River Athi Basin

The River Athi Basin, which traverses urban centers, suburban zones, and rural landscapes, faces complex water management challenges due to its proximity to settlements, diverse land uses, and hydrological characteristics. Numerous empirical studies have assessed the basin's water quality, revealing widespread degradation linked to anthropogenic activities. Wilson et al. (2021) found elevated pollution levels in the Maumau Stream of the Nairobi River, attributed to horticultural farming. Aywa et al. (2016) reported high concentrations of *Escherichia coli* in Athi River Town, raising concerns about its suitability for irrigation. Wambugu et al. (2017) further highlighted public health risks by identifying antimicrobial-resistant *E. coli* strains in Athi River water in Machakos County. Musyoki (2013) documented waterborne bacterial pathogens in the Nairobi River, with downstream implications for communities along the Athi River.

Long-term assessments by Kithiia (2007) revealed significant pollution trends in water quality, sediment, and riverine vegetation across the Athi and Nairobi River Basins. More recently, Ahogle et al. (2023) identified bacterial pathogens such as *Shigella spp.*, *Vibrio cholerae*, and *E. coli* in irrigation streams, alongside physicochemical indicators like pH and BOD. Bagnis et al. (2019) conducted an environmental risk assessment of pharmaceutical contaminants in the Nairobi River, detecting active pharmaceutical ingredients (APIs) with ecotoxicological implications. Masime et al. (2022) linked water quality degradation to effluents from settlements, industries, and agricultural activities

throughout the basin. Ratemo (2018) observed spatial pollution gradients in Machakos County, with higher concentrations upstream that declined downstream. Kithiia (2021) emphasized sediment and water pollution in the Athi River drainage basin, projecting future water stress due to increasing demand. Njuguna et al. (2017) analyzed the Nairobi River's water quality and found elevated levels of macrophytes, heavy metals, and nutrients, further underscoring the basin's vulnerability to contamination. Collectively, these studies illustrate the multifaceted impacts of land use, urbanization, agriculture, and industrial discharge on the River Athi Basin's water quality, with serious implications for public health, irrigation, and ecological sustainability.

2.3 Influence of Land Use/Land Cover Change on Water Quality

Land use and land cover (LULC) changes have been widely recognized as major anthropogenic drivers of ecosystem degradation and water quality deterioration. Numerous studies have demonstrated that LULC dynamics significantly influence the spatiotemporal variation in water quality parameters across diverse geographical contexts. For instance, He et al. (2008) emphasized the role of LULC changes in shaping water quality patterns, while Langat et al. (2019) reported a substantial increase in agricultural and built-up areas in Kenya's Upper Tana River Basin, accompanied by a decline in open land, vegetation, and water bodies between 1987 and 2015.

Agricultural expansion has consistently emerged as a key contributor to water pollution, with Crooks et al. (2021) linking agricultural land in Rural North Wales to elevated levels of nitrate, coliform, and phosphorus. Similarly, Gobry et al. (2023) found strong correlations between cultivated land and water quality indicators such as nitrate, phosphate, and chlorophyll-a in Tanzania's Mindu Dam drainage. In Kenya's Nyando River Basin, Olang et al. (2011) observed a 20% decline in forest cover and a 16% increase in agricultural land between 1973 and 2000. Studies by Akintunde-Alo et al. (2020) and Tahiru et al. (2020) further confirmed the adverse effects of agricultural activities on soil and water quality in Romania and Ghana, respectively.

Urbanization also plays a critical role, with Toriman et al. (2018) identifying urban and agricultural land uses as major pollution sources in Malaysia's Nerus River. Wafula et al. (2018) attributed nutrient loading in East Africa's Mara River to human activities, while Putri et al. (2021) linked agricultural practices and construction to water quality degradation in Indonesia's Tambayakbayan River. In Kenya, Wambugu et al. (2017) and Chepkorir et al. (2021) documented seasonal and spatial variations in water pollution driven by urban and agricultural land use. Ming et al. (2023) found high concentrations of TN, TP, and NH_3-N in China's Huai River associated with built-up and cultivated land. Molekoa et al. (2021) reported declining land cover in South Africa's Mokopane area due to urban encroachment.

Industrial activities contribute significantly to water quality degradation, as evidenced by Lie et al. (2021) in Germany's Stör catchment and Huang et al. (2013) in China's Chaohu Lake Basin. Apudo et al. (2014) and Gituara (2021) highlighted the impact of industrial zones on pollution levels in Kenya's Itare and Nairobi Rivers, respectively. Collectively, these studies underscore the profound influence of LULC changes, particularly agriculture, urbanization, and industrialization, on the quality of surface water across various regions.

2.4 Seasonal Variations in Physicochemical Parameters of Water Quality

Seasonal variations in water quality are strongly influenced by shifts in land use patterns, including agriculture, industry, urbanization, and peri-urban development, as well as climatic differences between rainy and dry seasons (Molekoa *et al*., 2021). These fluctuations affect key physicochemical parameters such as biochemical oxygen demand (BOD), dissolved oxygen (DO), nutrient concentrations, and sediment loads, which are shaped by pollutant discharge, redox conditions, and hydrological dynamics. Numerous studies have documented seasonal pollution trends in surface waters, highlighting the vulnerability of water bodies to anthropogenic pressures (Samlafo *et al*., 2022; Rahman *et al*., 2021; Mkude *et al*., 2018).

Agricultural productivity, which depends on consistent water quality, is particularly impacted by seasonal nutrient imbalances and pollution risks. Sudarshan et al. (2019) found

elevated pollutant and nutrient levels in Hebbal Lake, India, while Li et al. (2022) linked total phosphorus (TP) and water temperature (WT) to harmful algal blooms in Lake Qilu, China, reducing irrigation potential and aquatic biodiversity. In Benin's Okpara Basin, Lanmandjèkpogni et al. (2018) reported soil leaching and farmland degradation due to seasonal nutrient pollution. Marthe et al. (2015) observed that agriculture and urbanization influenced water use in Côte d'Ivoire's Potou Lagoon across wet and dry seasons. Seasonal nutrient dynamics were also evident in the Yenisei River (Tokareva *et al*., 2022) and Northwestern USA Watershed (Sigleo & Frick, 2003), with higher nutrient concentrations during wet seasons. Xu et al. (2022) found elevated TN and TP levels in Lake Yangzong during winter, while Padedda et al. (2022) reported seasonal peaks in cyanobacteria and phytoplankton in a Mediterranean lake. Mukherjee et al. (2022) assessed seasonal suitability of Temple Pond in India for aquatic life and recreation.

Industrial operations, which rely on stable water sources, are also disrupted by seasonal water quality changes. Kitheka (2019) reported increased salinity during dry seasons in Kenya's Athi River Basin, affecting industrial processes. Duong et al. (2022) found seasonal shifts in nutrient and coliform levels in Vietnam's Hau River, raising water treatment costs. Kokoi et al. (2015) and Samlafo et al. (2022) identified high turbidity and heavy metal concentrations during dry seasons in Nairobi and Tordzie Rivers, respectively, complicating industrial purification efforts.

Urban expansion and infrastructure development are similarly affected by seasonal water availability, especially in regions with poor governance and inadequate policy enforcement. Ojok et al. (2017) observed higher pollutant loads during rainy seasons in Uganda's River Rwizi, while Sudarshan et al. (2019) linked elevated BOD, EC, and TDS levels in Hebbal Lake to urban sanitation challenges. Long-term assessments by Kithiia (2007) in Kenya's Athi and Nairobi River Basins revealed persistent seasonal fluctuations in water quality, vegetation, and sediment pollution, underscoring the cumulative impact of urbanization and industrialization over time.

2.5 Spatial Variations in Physicochemical Parameters of Water Quality

Spatial variations in water quality are shaped by a complex interplay of anthropogenic activities and natural processes, with pollution gradients often intensifying from upstream to downstream due to land use pressures. These variations are further influenced by seasonal changes, urbanization, agricultural practices, and industrial discharges (Islam *et al.,* 2018; Barakat *et al.*, 2016). For example, Kaniz et al. (2014) reported elevated concentrations of BOD, DO, COD, TSS, and pH in Malaysia's Merbok Estuary during the dry season, reflecting both pollutant loads and buffering capacity.

Urbanization exacerbates spatial disparities in water quality, fragmenting river health into zones of stress and recovery. Li et al. (2018) observed significant spatial differences in DO and NH_3-N levels in Shanghai's river systems, while Huang et al. (2022) linked EC, TP, NO_3-N, Fe, and fecal coliform concentrations to urban wastewater in Hong Kong. In Kenya, Ontumbi and Sanga (2018) found increasing pollution in the River Sosiani due to urban and agricultural discharge, and Zhang et al. (2017) identified higher TN concentrations in urban zones of the Fuyang River during dry seasons. Eneji et al. (2012) reported 100% variance in TSS across sampling stations in Nigeria's River Benue, underscoring spatial pollution dynamics.

Agricultural activities contribute significantly to nutrient enrichment and sedimentation, with FAO and IWMI (2017) noting that agricultural pollution often surpasses urban and industrial sources in middle-income countries. Zelenakova et al. (2018) found spatial declines in BOD, NH_4, and NO_3 along Slovakia's River Laborec due to reduced farming. An et al. (2023) and Chu et al. (2021) linked excess nutrients and heavy metals in China's Wanquan and Ganjiang Rivers to agricultural and domestic wastewater. Kilonzo et al. (2013) revealed spatial differences in pH, EC, TN, and TP across tributaries of Kenya's Mara River Basin, while Ma et al. (2020) traced COD, NH_3-N, TN, and TP trends in East China's Qinhuai River to agricultural land use.

Industrial activities also drive spatial pollution, introducing heavy metals, toxic compounds, and thermal waste into aquatic systems. Ismail et al. (2016) identified Cu, Cr,

and Pb contamination in the Straits of Malacca from mining and shipping, and Hou et al. (2022) reported high pollutant loads from high-tech manufacturing sectors. Ren and Li (2021) found significant reductions in COD and NH_3-N emissions in China's Beijing-Tianjin-Hebei region due to regulatory interventions. Zhou (2022) assessed heavy metal risks in Jieshi Bay, China, noting seasonal peaks in Hg concentrations. Mkude et al. (2018) documented spatial variations in EC, pH, WT, DO, and BOD in Tanzania's Wami River linked to industrial waste discharge, while Mei et al. (2014) observed long-term declines in multiple pollutants across rural, suburban, and urban zones in Eastern China's Wen-Rui Tang River watershed. Collectively, these studies highlight the spatial complexity of water quality degradation, driven by land use intensity, pollution sources, and regulatory effectiveness.

2.6 Research Gap

Despite extensive studies on the River Athi Basin, critical gaps persist in understanding the long-term dynamics of water pollution and the influence of climate variability on pollutant cycles. While previous research has largely focused on assessing water quality and identifying pollutant concentrations, it has often overlooked the underlying sources of contamination and the complex interactions between land use/land cover change (LULCC) and water quality. In particular, there is limited integration of spatial and temporal analyses that capture how LULCC affects water quality across different zones of the basin and during varying seasonal conditions. Additionally, few studies have employed predictive modeling or multivariate techniques to explore the cumulative and synergistic effects of anthropogenic activities, such as agriculture, urbanization, and industrial discharge, on physicochemical parameters. This study aims to bridge these gaps by examining the impact of LULCC on water quality in the River Athi Basin through a combination of field-based physicochemical analysis and stakeholder interviews. It will monitor water quality variations across both short-term (dry and wet seasons) and long-term (multi-seasonal) periods, applying multivariate statistical methods to uncover spatial patterns, temporal trends, and pollution sources. By doing so, the research will offer a more holistic and policy-relevant understanding of the basin's water quality dynamics in the context of land use transformation and climate variability.

2.7 Conceptual Framework

The conceptual framework (Figure 2) illustrates the relationship between anthropogenic activities, their sources, and the pathways through which they influence water quality. It identifies various land use activities known as independent variables, that generate pollutants, which then move from their sources to processing units and pathways, both point and non-point sources. These pollutants eventually find their way into water bodies (e.g., rivers, streams, and lakes) via surface runoff, leaching, soil and sediment transportation, wastewater discharge, atmospheric deposition, and incorporation into the food web known as Intervening variables. At the processing stage, human activities release significant loads of organic and inorganic pollutants. These discharges from point sources (e.g., factories and wastewater treatment plants) and non-point sources (e.g., agricultural runoff, urban storm water, and vehicular release) contributes to water contamination. The pollutants entering water bodies (Dependent variable) initiate processes like eutrophication, during which dissolved organic and inorganic pollutants release chemical substances into aquatic environments. These processes degrade water quality, adversely impacting aquatic life and human use of the water. This integrative approach provided a comprehensive understanding of the interplay between land use and water quality changes in the River Athi Basin as illustrated in Figure 2.

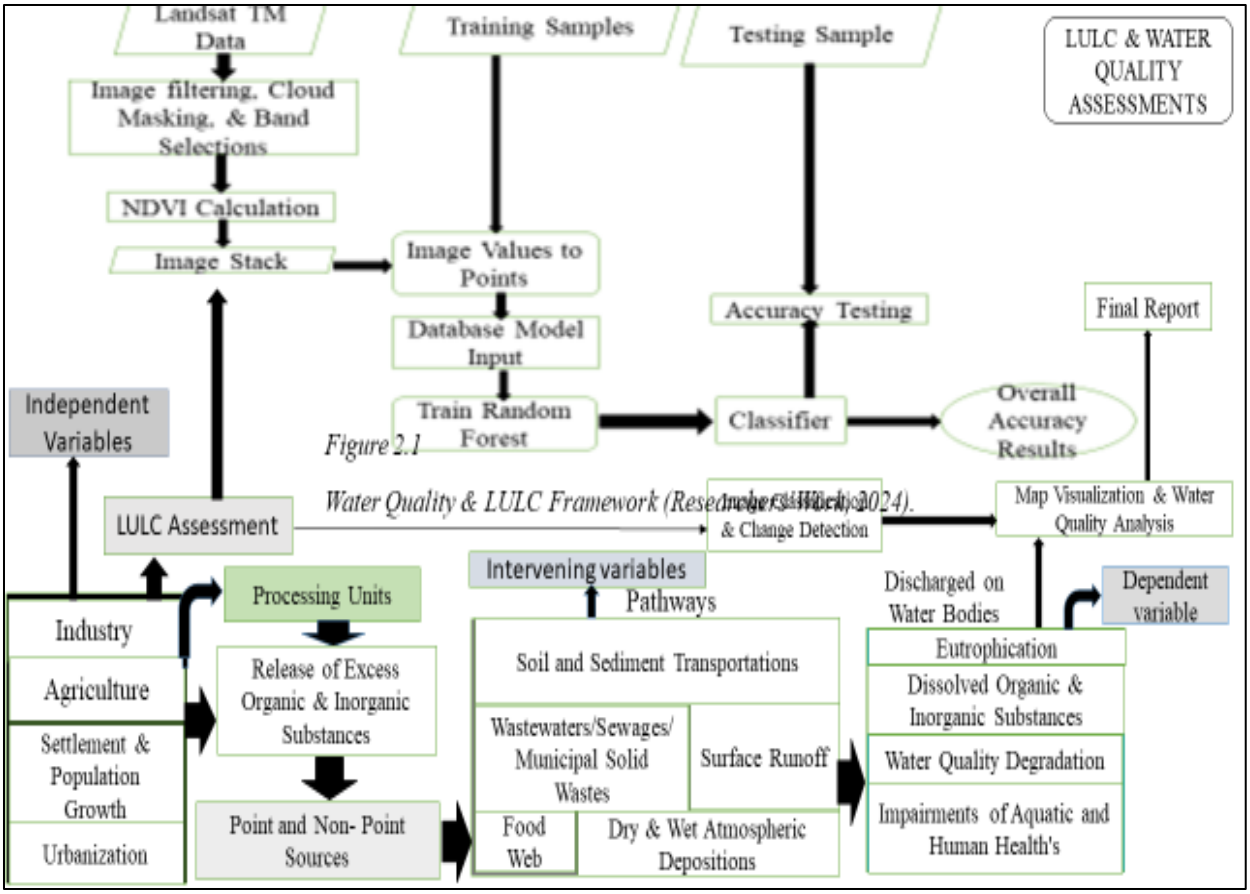

Figure 2: Conceptual Framework

Source: Author (2024)

CHAPTER THREE

3.0 RESEARCH METHODOLOGY

3.1 Introduction

This chapter provides a comprehensive overview of the land use patterns, climate, and geography of the study area, and their influence on water quality. It outlines research methodology and design employed to evaluate water quality in the Athi River Basin. Data collection procedures for land use and land cover changes, as well as water quality parameters, are described. The chapter justifies the sampling locations, measurement parameters, and analytical methods used in the study. It outlines the analytical techniques and equipment employed to assess trends in water quality in the study areas.

3.2 Study Area

The study area is located at latitude 1 26' 38 29"S and longitude 36 58' 52.49"E, down to Kibwezi, at latitude 2 12' 09.45"S and longitude 38 03' 30.36"E (Figure 3). The River Basin has an area of 66, 559 km^2 covering 11 % land surface and borders Tanzania to the south, the Indian Ocean coastline to the east, the Tana basin to the north, and the Rift Valley basin to the west.

The Athi River is the second largest river system in Kenya and it is sourced from the Central Kenya highlands at the southern region of the Aberdare ranges and the Ngong Hills (Kitheka *et al*., 2022). The river flows through the plains and valleys of Kenya, forming notable features such as the Fourteen Falls, before meandering through Nairobi and passing through Tsavo National Park. Along its course, the Athi River travers's informal settlements and industrial areas within cities and towns, including Nairobi and Machakos, as well as suburban and rural communities, where it collects various forms of effluents. The river traverses approximately 390 km from Ngong Hill through the semi-arid southeastern region of Kenya, serving as a vital resource for millions of people along its course and empty in Indian Ocean (WRA, 2022). Its waters are extensively utilized for various purposes, including agriculture, domestic use, and livelihoods. Ultimately, the river empties into the Indian Ocean, highlighting its significance not only as a source of water

but also as a crucial ecological and economic lifeline for the surrounding communities and the broader region.

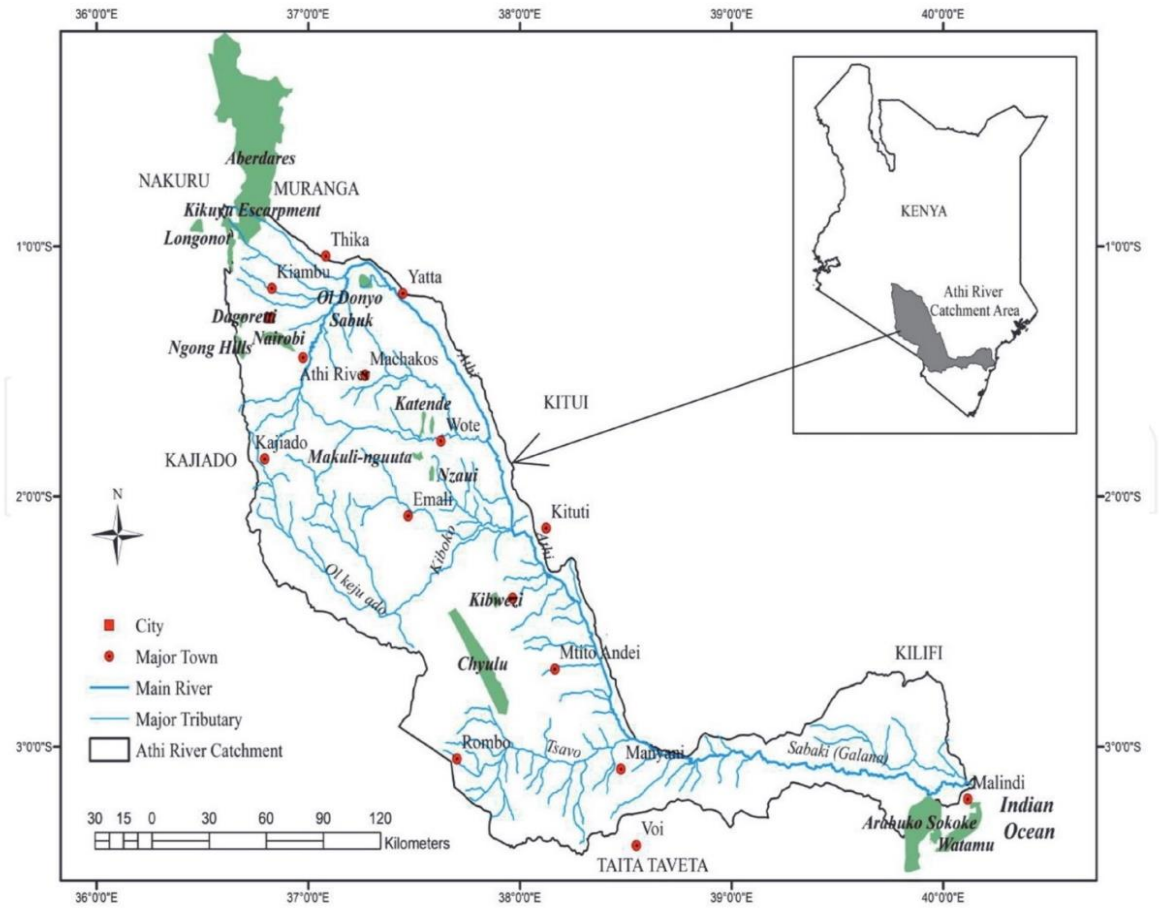

Figure 3: Map of Athi River Basin, Adapted from Kitheka (2021).

3.2.1 Climate

The climate of the Athi Basin is primarily influenced by the topography of the basin, the proximity to the ocean, and to the equator. These factors contribute to the range and variability in precipitation and temperature regimes (MWSI and WRA, 2020). The climate is mild (i.e., warm and temperate), summers are short, warm, and overcast, and winters are short, cool, dry, and partly cloudy.

3.2.1.1 Rainfall

The Athi River Basin in Kenya experiences a close interplay between rainfall and temperature patterns, which strongly influence the hydrological dynamics of the region.

Rainfall in the basin is seasonal and largely bimodal, with two main rainy periods such as the long rains occurring from March to May and the short rains from October to December. These rainy seasons are critical for replenishing surface and groundwater levels, sustaining agricultural activities, and maintaining river flow in the Athi River, which is essential for local ecosystems and water supply. The region's rainfall patterns, however, show considerable variability due to climatic factors like the El Niño-Southern Oscillation (ENSO), which can lead to fluctuations in annual and seasonal rainfall volumes.

The headwaters of the Athi River Basin originate in the high-rainfall central Kenya highlands, which receives between 1,800 and 2,250 mm of annual rainfall. Kikuyu is located in the northwestern part of the central highlands, which benefits from intense orographic rainfall due to its steep terrain and position relative to prevailing winds. Southern Aberdare range ~1,200 to 2,000 mm, mean while Ngong Hills range ~1,250mm (Okoth, 2003).

The basin also includes high-altitude regions such as the Southern Aberdare Range, ranging from 1,800 to 3,000 meters above sea level, and the Ngong Hills, whose elevation spans from 2,200 to 2,400 meters (GOK, 2012). The altitude, Inter-Tropical Convergence Zone (ITCZ), and the Orographic effects of high mountains and hills control rainfall in the basin (Kitheka *et al*., 2022). The total annual rainfall in the basin ranges from 481mm to 1764 mm (Wambugu *et al*., 2017).

3.2.1.2 Temperature

Temperature in the Athi River Basin also plays a significant role in shaping water availability. Warmer temperatures, particularly during the dry season, increase evaporation rates, which reduces surface water levels and accelerates soil moisture depletion. This effect is especially pronounced in the basin's semi-arid areas, where high temperatures combined with lower rainfall contribute to water scarcity.

Temperature varies between 28^0C to 32^0C in some months in dry season. During the day, the normal temperature is around 23^0 C and at night it is around 17^0 C. The basin

experiences dry periods from July to September (Kitheka *et al*., 2022; Kithiia, 2006). On average, April is the wettest month with 159mm (6.3 inches) of precipitation. July is the driest month with 11mm (0.4 inches) of precipitation (Kithiia, 2006), while the basin experiences low rate of harmattan in January and September.

3.2.2 Geology

The basin's geological characteristics include the presence of Precambrian basement complex rocks, Quaternary extrusive and intrusive rocks, and Tertiary rocks, including Tertiary extrusive and intrusive rocks (Kitheka *et al*., 2022). Most of the semi-arid southern zone is made up of Precambrian basement complex rocks, whereas the upper highland zone is made up of Quaternary extrusive and intrusive (volcanic) rocks. Tertiary rocks, including the Phonolites of the Kapiti plains and Amphibolites, are found in the middle upper zone. These rocks are both intrusive and extrusive (Prasol Training Ltd, 2012). Because the rocks weather and produce soils with different levels of erodibility, the basin's geology is significant. Sandy loamy soils that are extremely erodible are produced by Precambrian rocks in particular.

The semi-arid lower part of the sub-basin features sandy alluvium and red sandy soils, interspersed with patches of vertisols and gravelly lateritic materials. In contrast, the southern zone contains soils with low organic matter, resulting in low fertility and high erodibility (Prasol Training Ltd, 2012). The soils in the basin are spatially non-uniform, with nitisols predominantly found on the slopes of the Aberdare ranges and Kikuyu Plateau in the upper zones (Kitheka *et al*., 2022).

3.2.3 Hydrology

The Athi River is the main river in the Athi Basin, draining about 57% (38 170 km^2) of the basin, covering Kiambu, Nairobi, Machakos and Makueni Counties. It is the second longest river after the Tana River and has a total length of 390 km (MWSI & WRA, 2020; JICA, 2012).

The Lumi River originates in the Athi Basin in Kenya along the Eastern slopes of Kilimanjaro, and flows across the border into Tanzania, while the Umba River flows from Tanzania into the Athi Basin south of Mombasa (Kithiia, 2021; MWSI & WRA, 2020). Athi Basin includes major wetland systems such as Olngarua swamp, Ol Keju Ado, Ndumato, Mamanga Esokota, Jipe, Mangeri swamp, and the mangrove swamps along the coast (MWSI & WRA, 2020). Others are Mwachi, Pemba, Rare, and Ramisi Rivers that empties into the Indian Ocean (Kitheka *et al*., 2022; Kithiia, 2021).

The upper tributaries of the Athi River, such as those originating from Ngong Hills, Ndarugu, and Mathare, drain the Kikuyu Escarpment, flow through Nairobi City, and converge near Kilimambogo (also known as Donyo Sabuk) to form the main Athi-Sabaki River, as shown in Figure 4. The basin covers a total area of 58,639 km^2, which corresponds to 10.2% of the country's total land area. The main tributaries are Ruiru and Ndarugu. Other minor tributaries but of great hydrological importance are Ngong, Nairobi, Mathare, Mbagathi, Riara and Gitathuru (Kithiia, 2021).

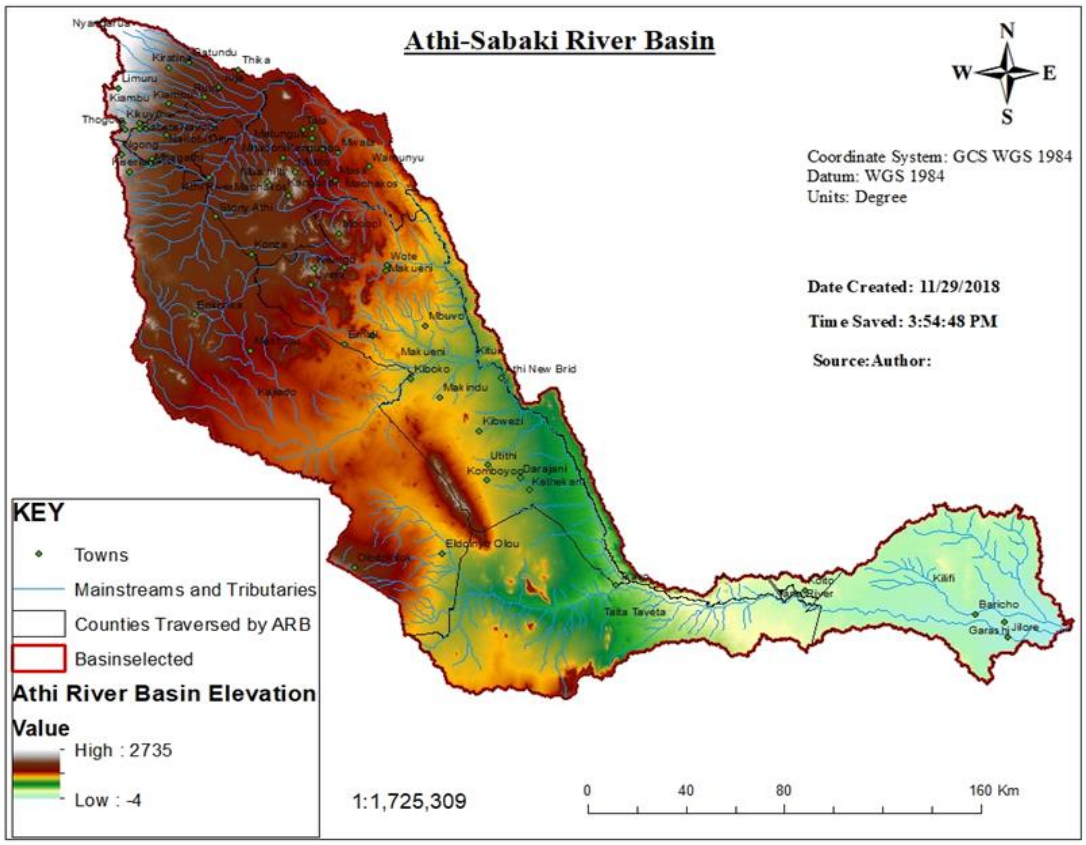

Figure 4: Athi river basin elevation level. Adapted from Kitheka (2019).

3.2.4 Soil

The semi-arid lower part of the sub-basin features sandy alluvium and red sandy soils, interspersed with patches of vertisols and gravelly lateritic materials. In contrast, the southern zone contains soils with low organic matter, resulting in low fertility and high erodibility (Prasol Training Ltd, 2012). The soils in the basin are spatially non-uniform, with nitisols predominantly found on the slopes of the Aberdare ranges and Kikuyu Plateau in the upper zones (Kitheka *et al*., 2022).

3.2.5 Topography

The topography of the Athi River Basin is diverse, ranging from sea level at the Indian Ocean coastline to approximately 2,740 meters in the highlands of the Aberdare Range (WRA, 2022). This higher elevations, from 1,800 meters to 2,740 meters above sea level, include the Aberdare Range, Ngong Hills, and surrounding regions. The mid-reaches,

ranging from 1,200 meters to 1,800 meters above sea level, cover areas such as Nairobi, Kajiado Town, Machakos, Makueni, and Kitui. The lowest elevations, from 0 to 1,200 meters above sea level, include the Sabaki River Mouth, Mombasa, Kilifi Town, Malindi, and the river's estuary at the Indian Ocean (Figure 4).

3.2.6 Vegetation

The upper basin boasts a variety of vegetation types, including woodland, savanna grasslands, scrub/bushlands, woodlands, and forests. The lower basin is dominated by savannah vegetation, much of which is degraded due to extensive settlement, cultivation, deforestation, and overgrazing (WRA, 2022). Land use in the basin includes commercial/transportation, agriculture, urbanization, and industry. Small-holder mixed farming is common in high rainfall zones, varying by sub-basin. Other significant land uses include human settlements, nature conservation, livestock grazing, quarrying, and large-holder farming, primarily tea and coffee (Wambugu *et al*., 2017).

3.2.7 Population

The River Athi Basin is home to 13.43 million people, with a population density of 202 people per km² (WRA, 2022). Machakos and Makueni counties cover significant portions of the study area. Machakos County has 1,421,932 residents, with a density of 235 people per km² and an annual growth rate of 2.47% based on the 2019 census. Machakos has 402,466 households with an average size of 3.5. The Athi River in Machakos has 322,499 residents living along the river, with 5% intersex based on sub-county census results (KNBS, 2019). Makueni County has 244,669 households with an average size of 4.0 and a total population of 987,653. The county has a population density of 121 people per km², with unknown number of people living in Thwake and Kibwezi study areas, accessing River Athi water (KNBS, 2019). The river basin serves as the primary water source for domestic, agricultural, and other uses.

3.3 Research Design

The study used mixed-method research design for qualitative and quantitative analysis (Kemper *et al*., 2003). The study first assessed land use/land cover changes in the River

Athi Basin to provide context for the water quality analysis. Geographic Information Systems (GIS) and Remote Sensing (RS) techniques were utilized for this purpose. This was followed by conducting an interview survey (open-ended question) and participant observations**.** The qualitative component gathered detailed insights into local perspectives and practices related to land use and water quality.

A descriptive research design was adopted to characterize the study area, including land use activities, which provide essential field data for analysis. A quasi-experimental research design was employed to examine and compare changes in the study variables across different spatial and seasonal conditions, without random assignment. The study utilized inferential statistical methods for hypothesis testing. ANOVA and Independent T-test.while multiple linear regression and Pearson correlation assessed relationships and measure the impact of various factors (Frankfort-Nachmias & Nachmias, 2009; Gopalan *et al*., 2020; Shadish *et al*., 2002). The study also employed Mann-Kendall test to analyze trend in rainfall Data obtained from meteorological stations over eight (8) months (Muia *et al*., 2024). Multivarate analysis with principal component and cluster analysis were employed to identify pollution sources in water quality (Marín Celestino *et al*., 2018; Shrestha & Kazama, 2007).

3.3.1 Land Use/ Land Cover Sampling Method and Data Acquisition

The study investigated land use and land cover (LULC) change within the river basin using Landsat 8 imagery model for data accusation from USGS Earth explorer database dating back to 1973 (Sidhu *et al*., 2018). Remote sensing (RS) and Geographic Information System (GIS) were applied in monitoring spatiotemporal land-use change trends. The study employed historic data for land cover change from Enhanced Thematic Mapper (ETM) Landsat 8, from January 5th to December 31st 2015, 2020, and 2023.

3.3.2 Unstructured Interview Survey

The study employed face to face interpersonal open-ended interview to identify the drivers or factor inducing change in water quality of mid reaches of River Athi basin. The interview questions administered includes;

1. Community Perception of Athi River Water Quality Issues
2. The drivers of water pollution of Athi River Basin

The study purposively targeted 120 respondents in the mid reaches river across the sampling sections. Based on the disparity in the knowledge of the water quality and availability of respondents in each stations. The targeted respondents were the age 18 years and above including gender and occupational statues. These respondents have the knowledge of the water quality of the river basin and land use activities. The study targeted to interview 20 respondents in each sampling stations due to disparities in knowledge of the river water quality and available respondents. The interview was conducted at a distance of 0 to ~10 km away from the river bank, to capture all the listed land use activities in the basin.

3.4 Selection of Sampling Sites

Primary and secondary Data were employed using a purposive sampling approach to identify and select stations based on perceived land use activities within the river sections. The study focused in the mid reaches of the river basin where unsustainable land use activities such as business units, urban and rural settlement, irrigation, sand harvesting, indiscriminate waste dumps, etc., were common. Covering a distance of 170 km in six (6) sampling stations namely Athi River Town (S1), river Stony Athi (S2), National Youth Service (S3), River Kyawango Confluence (S4), River Thwake Confluence (S5), and Kibwezi Bridge (S6) as shown in Table 1 & Figure 5.

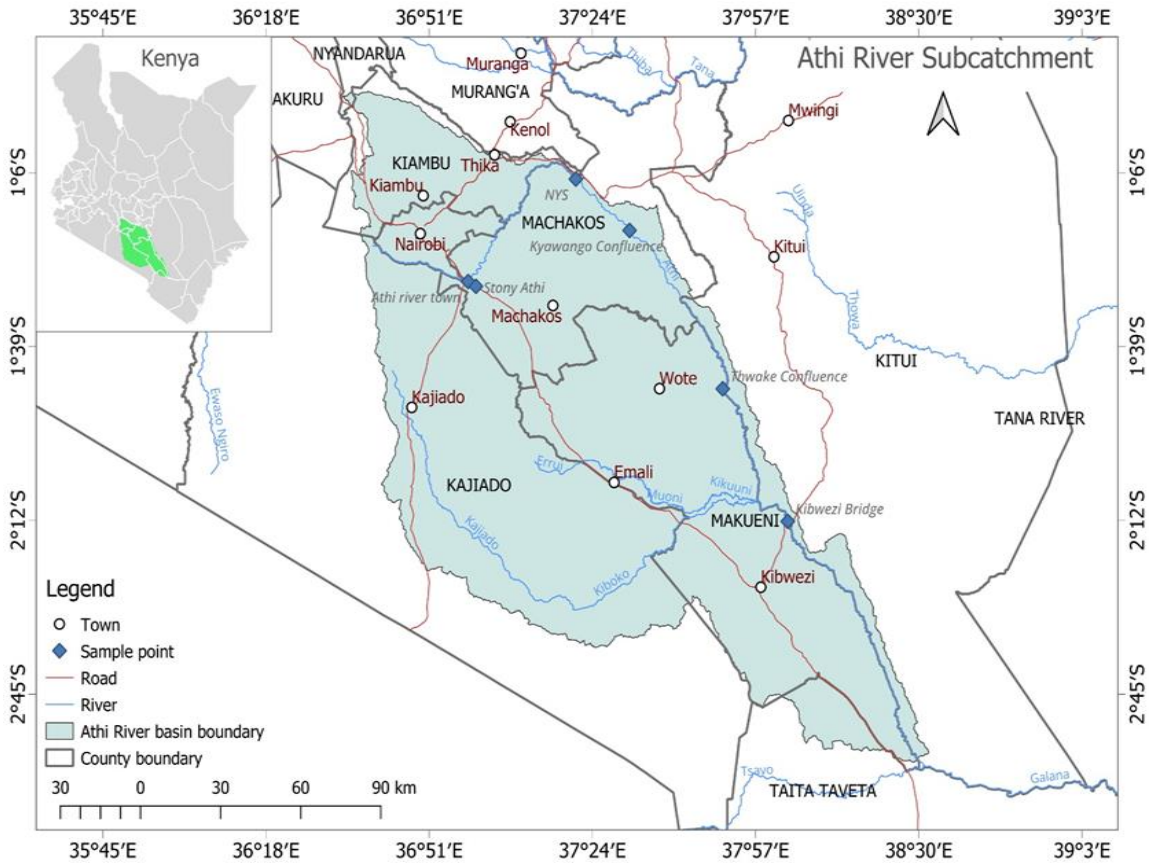

Figure 5: Location of sample stations

The selection of the sample stations are based on land use pattern; urban, peri-urban, industry, settlement, agriculture, including sand mining, Fishing, etc., influenced by natural and anthropogenic activities in the river basin. Table 1 provides a description of the land use activities at the selected monitoring stations.

Table 1: Sampling stations and land use activities

SN	Sampling Stations	GPS Coordinates	Land use Activities	Ecological Salient Features
1	Athi River Town	1 26’38 29’’S 36 58’52.49’’E	Settlement, urban Centre, industry, & commercial	Climatic variability, agro-ecological zone, and Rivers
2	Stony Athi	1 27’32 47’’S 37 00’ 27.34” E	Settlement, urbanization, industry, & commercial	Climatic variability and Riverine ecosystem
3	NYS	1 07' 11.32"S 37 20' 39.06"E	Settlement, agriculture, & commercial	Riparian, agro-ecological zone, fishing species
4	River Kyawango Confluence	1 16' 56.30"S 37 31' 31.33"E	Agriculture, settlement, sand mining, & fishing	Forestland/vegetation, Climate, sedimentation, agro-ecological zone, River & aquatic life
5	River Thwake Confluence (Control)	1 46' 59.64"S 37 50' 21.60"E.	Sand mining & industry	Forestland/vegetation, sand mining
6	Kibwezi Bridge	2 12' 09.45"S 38 03' 30.36"E	Settlement, agriculture & commercial	Grassland/vegetation, & agro-ecological zone

Source: Author (2025)

1. Athi River Town

Athi River Town, situated in the upper mid-reaches of Nairobi and Machakos Counties, is significantly impacted by industrialization, urbanization, and commercial activities (Plate 1). These land use practices result in heavy pollution of the river due to runoff from commercial zones, industrial effluents, and wastewater from residential areas. Rainfall and flood worsens the problem by flushing accumulated pollutants into the river, aggravating downstream contamination (Plate 2). During periods of high rainfall, the Mbagathi River, a tributary of the River Athi, plays a crucial role in carrying these pollutants, impacting

downstream communities, including the National Youth Service (NYS) headquarters and Kibwezi area, before discharging into the Indian Ocean.

Plate 1: Dry River Channel in Athi River Bridge (Left) and Stagnated Water during the Dry Season (Right).

Plate 2: Flooded Settlement (Left) and Irrigation activities (Right) in Athi River Site.

2. Stony Athi River

Stony Athi is a segment of the Athi River Basin that hosts a variety of land use activities, including urbanization, commerce, and human settlements. The Stony Athi River experiences significant water quality degradation due to wastewater discharge from multiple sources, largely driven by human activity and infrastructure development. Commercial enterprises like the Green park Hotel, industrial and agricultural operations, and major projects like the Stony Athi Water Front City (National Housing Corporation Estates) contribute to the river's pollution load (Plate 3).

Plate 3: Stagnant Water at Green Park Estate (Left) and Waste Water from Green Park (Right) During Dry Season at Stony Athi Site

The April-May 2024 rainfall caused significant flooding in the Green Park Estate in Athi River. The heavy rains led to the Stony Athi River overflowing its banks, which resulted in the flooding of the estate and the surrounding areas. This event also caused pollutants from the estate to be carried into the river, raising environmental concerns. The bedrock prevents polluted water from flow during the dry season (Plate 4).

Plate 4: Irrigation Site (Left) and Flooded Green Park Estate during April-May Rainfall (Right) in Stony Athi Site

3. National Youth Service (NYS) Athi River

The Kenya National Youth Service (NYS) is a government organization founded in 1964 to provide youth with vocational training and involve them in community development initiatives. It is situated in the Athi river field unit of Machakos County, along Thika road,

near the Athi River. The NYS encompasses a vast 2,270 acres dedicated to agriculture and livestock production, including crop irrigation for maize, vegetables, fruits, and beans, and the raising of cattle, goats, poultry, and sheep (Plate 5). Additionally, the NYS and its environs support various riparian activities, such as fishing, irrigation, and settlement, all contributing to the region's economic sustainability.

Plate 5: Agro Farm (Left) and Water Pumping Machines for Irrigation (Right)

4. River Kyawango Confluence

The River Kyawango Confluence is located in Machakos County's Kyawango settlement, Mwala sub-county. Particularly during the rainy season, Kyawango, which is primarily used for irrigation and livestock rearing, significantly contributes to the pollution burden of the Athi River. At the Kyawango confluence, runoff carries household and farm waste, often containing pesticides and fertilizers, directly into the river during periods of high rainfall. The river empties into the Athi River Basin after draining the Iyangoni and Nguthuke rivers. Similar to other major and smaller confluence rivers in the Athi Basin, the Kyawango River follows a similar seasonal pattern. The Athi River is crucial for both major irrigation techniques in Kyawango and household uses such as drinking, bathing, and washing. It holds significant economic importance for local agriculture, with large farmlands, such as the French bean farms near Mwala, heavily relying on its water supply (Plate 6, 7 and 8). The sampling station constitutes large sediment discharge during the rainfall period which result to sand harvesting during dry season.

Plate 6: Irrigation Farms

Plate 7: Sand Harvesting Sites at Kyawango & Kamuthakya Communities

Plate 8: Fish Farming (Left) & Processed Fishes Caught in River Athi for Consumption (Right).

5. River Thwake Confluence

The Thwake River, a seasonal tributary of the Athi River, flows only during the rainy season and dries up during the dry season, leading to significant variations in flow patterns. Originating in Athi River Town in Machakos County, the river flows through several Makueni County communities before merging with the Athi River at the Thwake confluence. A notable human activity in the area is sand dredging for a dam construction project by a Chinese company, despite the monitoring station near the Thwake confluence being relatively free from intense anthropogenic activities (Plate 9 and 10). The reduced land use activities in the River Thwake confluence led to its selection as the research control station of this study.

Plate 9: Sand Dredging Activity by Chinese Company at River Thwake Confluence

Plate 10: Dam Construction Site Affected by Flood (Right).

6. Kibwezi Bridge

Plate 11 and 12 indicate Kibwezi sampling station, located along a section of the Athi River that separates Makueni and Kitui Counties, is an essential water source but also absorbs various contaminants accumulated from upstream discharge. Human and animal activities are particularly intense along this part of the river during the dry season, when locals collect water for drinking and other purposes. Activities like cattle rearing, fishing, and sand harvesters introduces pollutants from upper sampling locations, including sediment-bound chemicals. These operations increase the pollution load at this monitoring site by disturbing the riverbed and re-suspending contaminants. To collect filtered water, residents dig shallow trenches into the sand dunes, often with the help of donkeys, which inadvertently introduce garbage into the river and nearby collection points (11). Commercial activities further contribute to the pollution burden by introducing hydrocarbons into the river through the use of tankers and tractors for water transportation (12).

Plate 11: Residents Filtering Drinking Water on Scoop Holes with Cans During The Dry Season

Plate 12: Water Tanker Trucks (Left) and Donkeys Feltching & Drinking Water (Right)

3.5 Sampling Procedure

The water samples were collected in short and long dry and rainy seasons for 8 months period in six sampling stations. The short and long dry season include August-September 2023 and January-February, 2024. The short and long rainy seasons include November-December 2023 and April-May 2024. The short season was sampled two months in dry and two months in rainy seasons, while the long season was also sampled two months in dry season and two months in rainy season for eight (8) months to cover the annual climatic seasons of the study area. This method helped to examine the trend and /or variation in water quality and levels of pollution over time. The sample was collected in the mid reaches sections like Athi river town (S1), Stony Athi (S2), NYS (S3), River Kyawango confluence (S4), River Thwake confluence (S5), and Kibwezi Bridge (S6) of river Athi Basin for trend analysis (Figure 5). The study made use of America Psychology Health Association (APHA) protocol in attaining water sampling and laboratory standard procedures. A manual composite sampling technique was used to collect samples under stable flow conditions. Samples were collected three times at an interval of 30m and combined into a representative samples bottles. The samples were collected in triplicates using 500ml plastic bottles, mixed by pouring 1.5liter plastic bottles, corked and inserted in a cooler (APHA, 2017). A water sampler was used to collect water sample at the river (APHA, 2017). The water quality parameters were collected for 4 days in each sampling month.

3.5.1 Physicochemical Water Quality

Plastic bottles were used for sample collections. The bottles were wash with ultrapure water, soaked in 10% HCl overnight, and rinsed again with ultrapure after pre-cleaned (APHA, 2017; Kalkhajeh *et al*., 2019; Gardolinski *et al*., 2001). The bottles were filled to the top after adding triplicate sample together, leaving no air space and was seal tightly with Cap (Musselman, 2012). Samples were placed in a cooler container with sufficient ice blocks to maintain a temperature of 6°C during transportation to the laboratory (APHA, 2017; EPA, 2022).

3.5.2 Heavy Metal

The plastic sample bottles were used and the bottles were labeled appropriately with water sample description after washing and drying (APHA, 2008; 2017). The bottles were washed with 10% hydrochloric acid. Each sample was acidified with 1.5ml of nitric acid (analytical grade) immediately collected from the river to avoid the adsorption of heavy metals to the container wall (Abdelaal *et al*., 2022; APHA, 2017**).** All samples were inserted in a blue cooler, acidified and refrigerated at 4^0 C for 4 days of sampling and was taken to Water Resources Authority (WRA) laboratory in Nairobi for determination.

Other instruments used are Global Positioning System (GPS) for collection of coordinates of the sampling points and generation of land use/ land cover (LULC) map. In addition, hand gloves, Jotter, biro, masking tape, markers, cooler, and an authorization letter or waiver for the fieldwork were used for the study.

3.5.3 Determination of Physico-chemical Parameters and Heavy Metals

The selected physicochemical parameters indicators were used for the determination of water quality of the river basin. The water parameters were determined in line with international standard analytical methods and procedures (Table 2).

Table 2: Physico-chemical analytical methods

S/N	Parameters	Analytical Methods	
1.	pH	Potentiometric	APHA 4500-H^+
2.	Electrical conductivity (EC)	Iron Electrode Meter	APHA 2510 B
3.	Total dissolved solid (TDS)	Iron Electrode Meter	APHA 2540-C
4.	Nitrate (NO_3)	Spectrophotometer UV/Vis	APHA4500-D
5.	Potassium (K)	Flame Photometer	APHA 3400-KB
6.	Phosphate (PO_4)	Ascorbic acid	APHA 4500-P E.
7.	Chemical oxygen demand (COD)	A Titrimeter	APHA 5200 C
8.	Biological oxygen demand (BOD)	5-Day Test	APHA 5210-B

Source**:** (EPA, 2022; APHA, 2008; 2017).

The standard procedures and methods applied for the determination of water quality parameters are as follows;

1. **pH Value (4500-H+)**

The pH was determined using potentiometric techniques to measure the degree of acidity and alkalinity in a solution on a scale of 0–14 (APHA, 2008; 2017). The quantities of carbon dioxide (CO_2) and bicarbonate ions (HCO_3^-), which affected water's buffering ability, were closely related to pH levels (Tanjung *et al*., 2019). Reagents & Equipment: Polyethylene beakers, standard buffer solutions, and a pH meter with calibrated electrodes. Procedure:

- The pH meter was calibrated using standard buffers.
- A beaker containing 10 mL of the water sample was used.
- The pH was measured with a pH meter after gentle stirring, and the results were recorded.

2. **Nitrate-4500-NO3- D.**

The concentration of nitrate (NO_3) in water which indicates the presence of nitrification, resulting from the breakdown of organic materials was measured (WHO, 2022).

Equipment & Reagents: Nitrate standards (2 ppm, 20 ppm), nitrate buffer [$(NH_4)_2 SO_4$], and an ion meter.

Procedure:

- The nitrate solution was diluted to create standards.
- Buffer was added, and the nitrate electrode was used for measurement.
- Measurements were contrasted to assess and calibrate accuracy (APHA, 2008).

3. Electrical Conductivity 2510-B

Conductivity, a measure of ion concentration in water and its ability to conduct electricity, often linked to total dissolved solids (TDS), was determined, (APHA, 2017).

Apparatus & Reagents: Conductivity cell, thermometer (±0.1°C), and 0.01M KCl solution.

Procedure:

- The conductivity cell was calibrated using KCl solution after rinsing.
- The sample temperature was set to 25°C, and EC was measured in dS/m.
- TDS was calculated using the formula: TDS ≈ EC × 0.64 (APHA, 2017).

4. Potassium-3400-KB

Potassium in water bodies was measured as an essential component.

Equipment & Reagents: Calibration standards for flame photometers (0.1–1.0 mg/L K).

Procedure:

- The potassium stock solution was diluted to create calibration standards.
- Standards were introduced to the flame photometer, and intensity at 589 nm was measured.
- Potassium levels were ascertained by analyzing the water sample and comparing it with calibration (APHA, 2008).

5. Total Dissolved Solids (TDS) 2540-C

TDS, the small amounts of organic materials and inorganic salts dissolved in water, was determined, with sources including sewage, urban and agricultural runoff, industrial wastewater, and natural sources (APHA, 2017).

Apparatus: Evaporating dish, membrane filter funnel, and glass-fiber filter disks (≤ 2-µm pore size).

Procedure:

- Glass-fiber filter disks were cleaned, vacuum-applied, and rinsed with reagent-grade water.
- Samples were filtered, dried in an oven, and weighed.
- TDS content was determined by weighing the dried filtrates (APHA, 2017).

6. Chemical Oxygen Demand (COD) 5220-C

Chemical oxygen demand (COD), is the quantity of oxidant reacting with the sample under controlled circumstances, was measured using Tetrameter.

Apparatus: Pipettes, culture tubes, heating block, digestion vessel, titration tools.

Reagents: Ferrous ammonium sulfate, silver sulfate, sulfuric acid, potassium dichromate, ferroin indicator.

Procedure:

- Samples were digested with sulfuric acid and potassium dichromate, cooled, and titrated with ferrous ammonium sulfate.
- COD levels revealed the amounts of oxidizable pollutants (APHA, 2017).

7. Phosphorus (PO) 4500-P. E

Phosphorus, an essential nutrient for living organisms found as organically bound phosphate particulates, polyphosphates, and orthophosphate, was measured (APHA, 2008). Typically, orthophosphate, total inorganic phosphates, or total Phosphate are used to calculate phosphate concentrations.

Instrument: Spectrophotometer (880 nm).

Reagents: Ascorbic acid, ammonium molybdate, antimony potassium tartrate.

Procedure:

- Samples were exposed to reagent combinations for color development.
- Phosphate concentration was measured spectrophotometrically by comparing absorbance to standards (APHA, 2017).

8. Biological Oxygen Demand-Five Day (BOD5) 5210-B

BOD, the amount of oxygen required by microbes to decompose organic material over five days at 20°C, was measured (APHA, 2017; Gooch, 2007).

Apparatus: Air incubator, oxygen-sensitive probe, incubation bottles.

Reagents: Nitrification inhibitors, calcium chloride, magnesium sulfate, phosphate buffer, Dissolved Oxygen (DO) indicator solutions.

Procedure:

- Samples were diluted in oxygen-saturated water and incubated for 5 days at 20°C.
- Initial and final dissolved oxygen concentrations were measured.
- BOD^5 values reflected the degree of organic pollution (APHA, 2017).

Table 3: Heavy metal instrumentation and methods for micro quantity

Parameters	Analytical Methods	
Arsenic	Atomic Absorption Spectrophotometer	APHA 3113 B
Lead	Atomic Absorption Spectrophotometer	APHA 3113 B
Chromium	Atomic Absorption Spectrophotometer	APHA 3113 B
Cadmium	Atomic Absorption Spectrophotometer	APHA 3113 B

Atomic Absorption Spectrophotometer (AAS) (APHA, 2008; 2017).

Heavy metals like Arsenic, Lead, Chromium, and Cadmium were analyzed using Atomic Absorption Spectrophotometer (AAS).

Apparatus: AAS components included light source, monochromator, flame atomizer, photoelectric detector were used.

Procedure:

- Stock solutions were prepared and diluted to working standards.
- Calibration curves for each metal were created using four points.
- Sample solutions were aspirated into the AAS, and concentrations were validated against spiked sample recovery rates of 115%.

3.6 Quality Assurance/Quality Control (QA/QC)

The sampling and laboratory standard procedures adhered to QA/QC international standard. Quality Assurance (QA) ensured that the water monitoring program generated data with recognized bias and precision or data with known bias and acceptable precision through specified methods and plans. Recognized bias is a systematic errors which are being quantified and accounted for using standard methods.

Quality Control (QC) evaluated the effectiveness of these procedures to ensure accuracy, precision, and proper documentation.

Calibration Methods:

- Blank samples: Deionized water was processed to ensure no drift.
- Calibration standards: Instrument response curves were periodically evaluated.
- Replicates: Laboratory replicates were examined for accuracy.
- Spike Recovery: Known metal concentrations were added to random samples to check procedure accuracy.
- Cleaning of Equipment: All equipment was carefully cleaned to prevent contamination, especially in heavy metal and nutrient analysis.
- SOPs: Methodological consistency and bias reduction were ensured by following APHA and EPA norms.

The adherence to APHA standards ensured comprehensive environmental monitoring approaches (APHA, 2008; 2017).

3.7 Data Analysis

Multiple statistical techniques including multivariate analysis were employed on the basis of research objectives as discussed in the following sections.

3.7.1 The Influence of Land Use/Land Cover on Water Quality

3.7.1.1 Cloud Masking and Generation of Image Composite

Data filtering was done using Google Earth Engine (GEE) for cloud-free imagery relative to the years from the Landsat image collection. The study used a function to handle and detect clouds in a multi-temporal image collection. Google Earth Engine (GEE) provides

many statistical classifiers for pixel-based image classification of land use mapping. Google Earth Engine (GEE) GEE employs various multi-temporal techniques to detect and mask clouds in Landsat imagery (Mateo-García *et al*., 2018).

3.7.1.2 Training Random Forest Classifier

The study implemented and tested random forest, a pixel based supervised machine learning algorithm. To train and test random image classes, data were collected using Landsat images and Google Earth Engine (GEE). High spatial resolution satellite imagery was employed to manually digitize areas of interest (AOI), including bare lands, farmlands, grasslands/vegetation, built-up areas, forests, and water bodies. The study created 100 samples for testing and 129 samples for training. These samples were processed using the Google Earth Engine (GEE), which later imported into the analysis script. The relevant class and number of training samples were as follows: Farmlands 22, Grass-lands 31, Forest 36, Bare-lands 14, Built-up/others 12, and Open-water 14.

The training and sampling were acquired using Google Earth Engine (GEE) and then imported into the analysis script. The production of different land cover categories applied visual interpretation of Landsat ETM backed by a field survey using Google Earth similar to the study conducted by Rotich & Ojwang (2021).

3.7.1.3 Normalized Difference Vegetation Index (NDVI)

To normalize differences, spectral bands of the Landsat mosaics were analyzed, including band 3 band 4. The Normalized Difference Vegetation Index (NDVI) change was calculated to detect land cover change and used as part of the covariates for image classification (Rotich & Ojwang, 2021; Meng *et al*., 2019; Zurqani *et al*., 2018; Elmore *et al*., 2000). NDVI was derived from band 3 (Red Band) and band 4 (Near Infrared Band). According to Elmore et al. (2000), the index quantifies vegetation's reflective difference between the NIR and RED bands and is useful for environmental monitoring, mainly for measuring vegetation growth (Tamiminia *et al*., 2020; Zhu *et al*., 2023). The formula is as follow;

$$NDVI = (NIR + RED) / (NIR + RED) \quad (1)$$

Where;

NIR denote near-infrared and RED denote red wavelengths band, in Landsat Image.

3.7.1.4 Supervised Classification

The study employed a supervised classification technique to develop the spectral signatures of Known categories (Richard & Jia, 2006; Eastman, 2003). Once the area of interest (AOI), also known as the training class, was defined, supervised classification was applied. The study area map was generated using a Digital Elevation Model (DEM) with a 100m x 100m resolution to characterize the river basin, based on coordinates derived from the sample stations.

3.7.1.5 Accuracy Assessment and Image Classification

Accuracy assessment was quantitatively used to assess how effectively the pixels were sampled into the corrected land cover classes (Rwanga & Ndambuki, 2017). It is the most important, difficult, and last stage in the land cover classification process of the images (Foody, 2002). The primary accuracy measure is the overall accuracy, which is calculated by dividing the correctly classified pixels by the total number of pixels checked (Banko, 1998).

This study performed an accuracy assessment for a trained Random Forest (RF) classifier which predicted the generated LULC maps. The classification results were compared with ground truth data using the confusion matrix, which indicated the number of correctly or incorrectly classified pixels in each land cover category. Adjustment were made to improve the accuracy based on error matrix. The RF classifier quantified accuracy by estimating the percentage of correctly classified test Data (Plourde & Congalton, 2003). Accuracy assessment was successfully determined using Kappa coefficient, error matrix, producer accuracy and consumer accuracy. User's accuracy represent the proportion of an area classified on the map which correspond to the actual map on ground. Both user and producer accuracies were calculated using confusion matrix to evaluate the class performance.

To generate accuracy statistics, GEE function techniques were applied using specific equations such as;

$$\text{Overall acuracy} = \left(\frac{1}{N}\right)\sum_{i=1}^{r} nii \quad (2)$$

$$\text{Producer's accuracy} = \left(\frac{nii}{nicol}\right) \quad (3)$$

$$\text{User's accuracy} = \left(\frac{nii}{nirow}\right) \quad (4)$$

Where;

nii denote the number of suitably classified pixels,

N denote the total number of pixels,

r is the number of rows, and

ni col and ni row denote the column and row total.

3.7.1.6 Kappa Coefficient

Kappa coefficient is a measure of the overall agreement of the matrix. The equation below showed the accurate Kappa coefficient for stratified random measurement (Petropoulos *et al*., 2015);

$$\text{Kappa coefficient} = \frac{(\boldsymbol{TxC})-\boldsymbol{G}}{\boldsymbol{T}2-G} \quad (5)$$

Where,

T = denote the test pixels,

C = denote the correctly classified pixels observations, and

G = is the sum of multiplied total value.

3.7.1.7 Temporal Change Detection

The change detection analysis was conducted in ArcGIS software. The classification images were converted to vector format for geoprocessing of the 6-land cover classification through intersection tool. The intersection processing tool allowed the conversion of land cover information for all the required years into one database in tabular form for change detection (Rotich & Ojwang, 2021).

The spatiotemporal change was quantified using gain and loss method. Land cover change was calculated with the equations;

$K_{gain} = S_b - S_a$ (6)

$K_0 = S_{bi} - S_{ai}$ (7)

$K_{loss} = S_a - K_0$ (8)

Where;

S_a and S_b = land cover types at the beginning and end year (time) in a given period (5 years).

S_{ai} and S_{bi} = land cover types with no change between the beginning and end year (time). The total area covered by each class to detect a change was calculated and summarized into percentage change.

3.7.2 Determination of Seasonal Variation in Physicochemical Water Quality

Independent samples t-test was used to determine if there is a significant difference between the means of two independent groups. The study tested the mean levels of physicochemical and heavy metals water quality parameters for dry and rainy seasons using Independent T test. However, researchers have applied independent T test in comparative analysis. Musyoki & Suleiman (2013) applied independent T test analysis on microbial loads in river Nairobi and Athi. Ogbonna & Emenike (2021) employed student T-test to determine the difference between the reclaimed wetland and groundwater quality, using this formula;

$$t = \frac{(\bar{x}_1 - \bar{x}_2)}{s_p\sqrt{1/n_1 + 1/n_2}}$$

Where,

$\bar{x}_1$ and $\bar{x}_2$ are the sample means of groups 1 and 2, respectively

S^2_1 and S^2_2 are the sample variances of groups 1 and 2,

n_1 and n_2 are the sample sizes of groups 1 and 2, respectively.

3.7.3 Assessment of Spatial Variation in Physicochemical and Heavy Metals Water Quality of River Athi Basin

3.7.3.1 One Way Analysis of Variance (ANOVA)

A one-way ANOVA (Analysis of Variance) was used to compare the means of three or more independent groups to determine if there are statistically significant differences

between them. Akpor et al. (2014) compared variable means of water quality using one-way analysis of variance (ANOVA). However, the study applied one way analysis of variance (ANOVA) to compare the mean levels of physicochemical and heavy metal water quality parameters.

The formula for the F-statistic in a one-way ANOVA is:

$$F = \frac{Between - group\ variabilty\ (MSB)}{Within - group\ variability(MSW)}$$

Where;

MSB (Mean Square Between groups) is calculated as:

$$\text{MSB} = \frac{SSB}{K-1}$$

MSW (Mean Square Within groups) is calculated as:

$$\text{MSW} = \frac{SSW}{N-k}$$

SSB (Sum of Squares Between groups) is calculated as:

$$\text{SSB} = \sum_{i=1}^{k} ni(\,X\text{i} - X\text{overall})^2$$

SSW (Sum of Squares Within groups) is calculated as:

$$SSW = \sum_{i=1}^{k} \quad \sum_{j=1}^{k} (X\,ij - Xi)^2$$

k = number of groups.

N = total number of observations across all groups

ni = number of observations in group iii.

Xi = mean of group iii

X overall = mean across all groups.

Xij = represents an individual observation

3.7.3.2 Principal component Analysis (PCA)

I. Standardization (Z-score Transformation)

This transforms your raw data into standardized form, so that all variables contribute equally. It subtracts the mean and divides by the standard deviation for each variable. Kahangwa (2022) used PCA to identify sources of heavy metal contamination (Pb, Cd, Cr, Cu, As, Mn, Ni) in soils around active and abandoned gold mining areas. PCA helped

distinguish between natural and anthropogenic sources. PCA revealed dry-season accumulation of nutrients and metals, in a seasonal variation study on nutrient and heavy metal pollution in surface waters of the Mekong Delta. However, this study seek to identify pollution sources in water quality of River Athi Basin using principal component analysis (PCA). The following analytical formulars will help achieve this objective.

$$Zij = \frac{Xij - \mu j}{\sigma j} \quad 1$$

Where,

Xij: Original value of variable jj in sample ii

μj: Mean of variable jj

σj: Standard deviation of variable jj

Zij: Standardized value (unitless)

II. Covariance or Correlation Matrix

This matrix captures the relationships (co-variation) between standardized variables. It is the foundation for extracting principal components.

$$C = \frac{1}{n-1} Z^{T} Z \quad 2$$

Where,

Z^T: Transpose of the standardized data matrix

n: Number of samples

C: Covariance or correlation matrix

III. Eigen Decomposition (Eigenvalues and Eigenvectors)

$$C\ e_k = \lambda_k e_k \quad 3$$

Where,

Eigenvectors (e_k), which are directions of maximum variance (the axes of new PC space)

Eigenvalues (λ_k), which represent how much variance each principal component explains.

IV. Principal Component Scores

These are the coordinates of each observation in the new principal component space. They tell how each sample "loads" on each PC.

$$PC_k = Z \cdot e_k \quad (4)$$

Where,

Z: Standardized data

e_k: Eigenvector (loading vector) for component kk

PC_k: Principal component score for component k

3.7.3.3 Cluster Analysis (Ward's Method)

I. Euclidean Distance (Dissimilarity between Samples)

Euclidean Distance (ED) measures how far apart two samples i and j are, based on all p variables. This is the basic dissimilarity metric for clustering.. CA grouped stations based on pollution intensity (Shrestha & Kazama, 2007). Another study used CA to assess seasonal and spatial variability in groundwater impacted by agriculture and urbanization (Marin Celestino *et al*., 2018). However, this study used PCA to identify pollution sources, while Cluster analysis (CA) was used to evaluate seasonal and spatial variations and grouped samples in time and space with similar chemical profile and identified clusters of water quality dataset of river Athi basin. To attain the objective, the following analytical tools were used.

$$dij = \sqrt{\sum_{k=1}^{p} (Xik - Xjk)^2} \quad (5)$$

II. Ward's Linkage (Variance Increase Criterion)

Ward's Linkage determines which clusters to merge at each step by minimizing the increase in within-cluster variance. This is why Ward's method tends to create tight, evenly sized clusters.

$$\Delta E = \frac{nA*nB}{nA+nB} * [[X_A - X_B]]^2 \quad (6)$$

Where,

n_A, n_B: Number of samples in clusters A and B

$\bar{x}_A$, $\bar{x}_B$: Centroids (means) of clusters A and B

$\|\cdot\|$: Euclidean norm (distance between cluster centroids)

ΔE: Increase in total within-cluster variance

3.7.3.4 Multiple Linear Regression (MLR) Analysis

Simple linear regression is an analytical model that allows to identify the relationship between two continuous variables, such as response (y), and predictor (x). The model finds a linear function that can help predict the outcome of the dependent variable in relation to the independent one. If the two variables are related, it is possible to predict a response value from a predictor (Valentini *et al.,* 2021; Reham, 2009). However, this study used multiple linear regression analysis to measure the influence of pH, EC, TDS, NO_3, K, and PO_4 on BOD and COD (oxidation parameters) as well as Cadmium and Chromium (heavy metals). This approach allows for examining these factors' impact on spatial and seasonal variations studies.

Multiple Linear Regression is calculated as;

$$yi = \beta_0 + \beta_1 \text{ x } i_1 + \beta_2 \text{ x } i_2 + ... + \beta_p \text{ x } i_p + \epsilon \qquad 7$$

Where,

I = n observation;

y_i =dependent variable,

xi = explanatory variables,

β_0 = y-intercept (constant term),

β_p = slope coefficients for each explanatory variable, and

ϵ =the model's error term (the residuals)

3.7.3.5 Pearson Product-Moment Correlation Coefficient (PPMCC)

Pearson Product-Moment Correlation Coefficient (PPMCC) measures the strength and direction of association between two continuous variables. Abdelaal et al. (2022) used Pearson product moment correlation coefficient to test the relationship between water quality and sediment on heavy metals. Another study used Pearson correlation coefficient on the relationship between water quality and Chlorophyll-a (Xu *et al*., 2022). These studies assessed the relationships between water physicochemical properties and heavy metals using Pearson correlation coefficient.

$$r = \frac{n(\sum XY) - \sum X)(\sum Y}{\sqrt{\ [n\sum X2 - (\sum X)2][n\sum Y2 - (\sum Y)2}}$$

Where,

X and Y are the two variables being compared.

n is the number of paired scores.

∑XY is the sum of the product of the paired scores.

∑X and ∑Y are the sums of the scores for each variable.

$\sum X^2$ and $\sum Y^2$ are the sums of the squares of the scores for each variabl

CHAPTER FOUR

4.0 RESULTS

4.1 Introduction

This chapter presents the results of the study in terms of the influence of land use land cover changes on water quality, seasonal variation in the physico-chemical water quality, and spatial variation in physicochemical water quality of the River Athi Basin.

4.1.1 Impact of Land Use/Land Cover Change on Water Quality of River Athi Basin from 2015 -2023.

This study examined land use/land cover change in mid reaches of the river Athi basin from 2015 to 2023 in order to provide a context in understanding the spatiotemporal variation of the water quality. The study covered part of the Athi River basin at a distance of 170 km from Athi River Town to Kibwezi sampling stations. The land use land cover classification for 2015, 2020, and 2023 from land sat Imagery and resultant maps of the study area are shown in Figure 6. The six (6) land cover classifications were defined, which includes bare-lands, built-up/others, farmlands, forest, grasslands, and open water (Table 4).

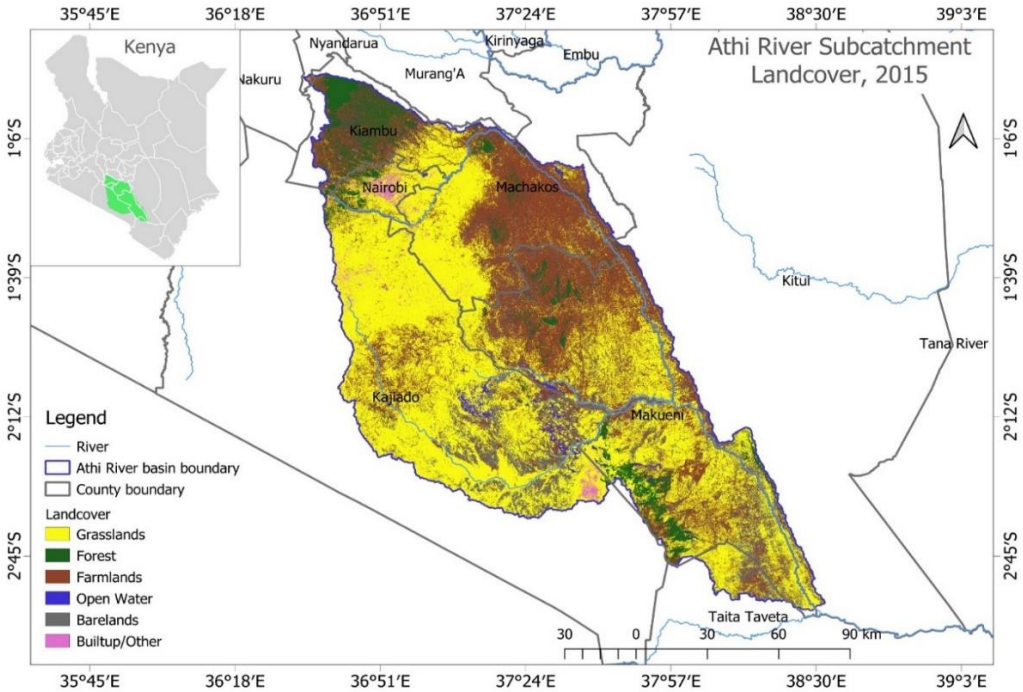

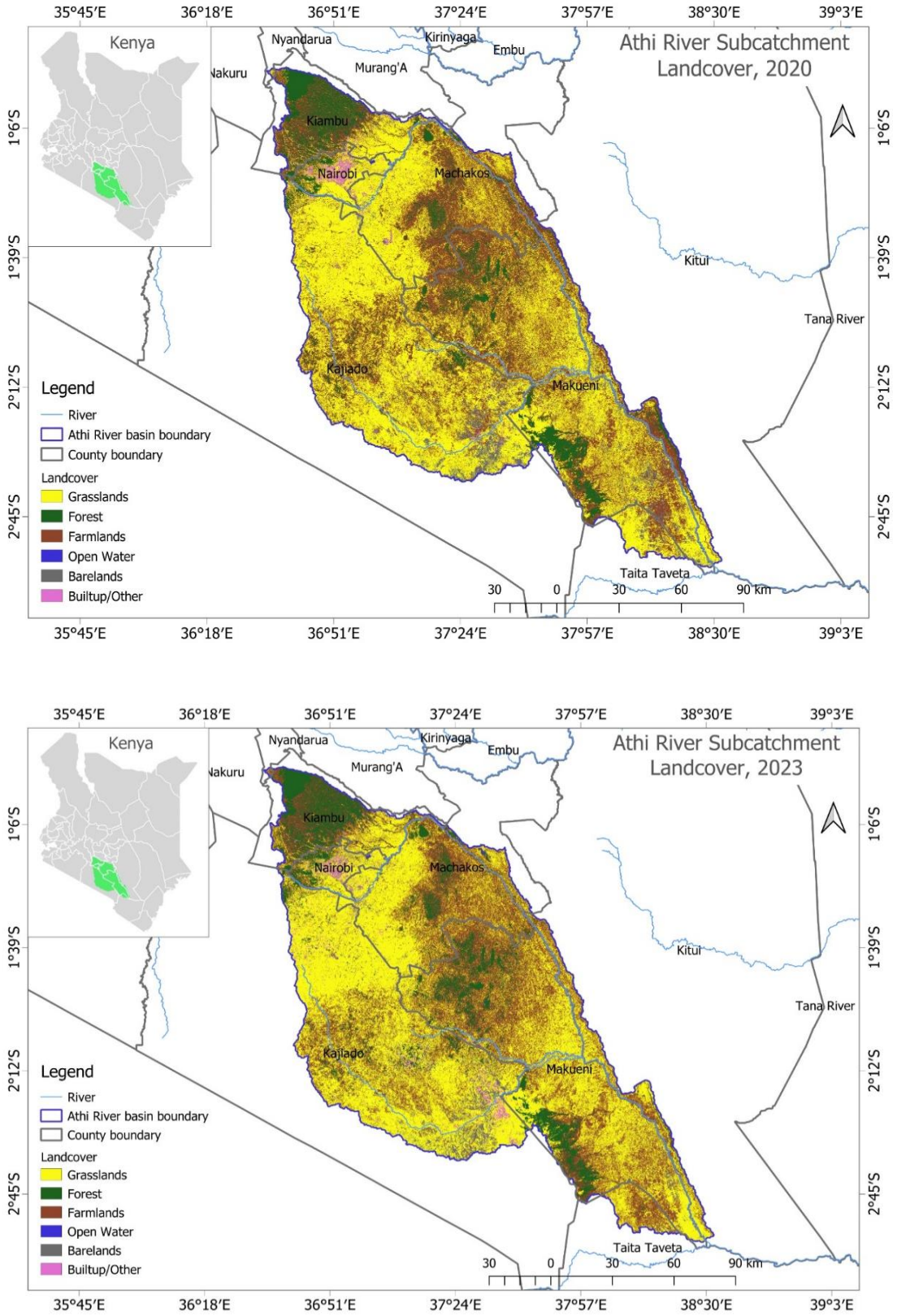

Figure 6: River athi basin land use/land cover (LULC) classification for 2015, 2020, and 2023.

Table 4: Classifications of land use and land cover of the river basin

SN	Definitions	Descriptions
1	Farmlands	Small-scale agriculture, horticulture, rain-fed maize, Farms, garden size, small (< 2 ha) tea orchards, Intercropped, tree/shrub orchards intercrops with Herbaceous crops.
2	Forestlands	Tree height >2 m; crown coverage > 30%; this class includes Bamboo Forest.
3	Grasslands	Grasslands / shrub trees, trees may be present, but less than <30% of crown coverage suitable for pasture.
4	Bare lands	Vegetation cover less than < 15%.
5	Open waters	Lakes and surface water, including waste water treatment plants.
6	Built-up	Built-up and other visible covers

Source: Author, 2025

4.1.1.1 Land Cover Area (Ha) and Gross Percentage Change from 2015 to 2023

Land use/land cover (LULC) percentage change area per hectare between 2015 and 2023 is shown in Table 5. This table illustrates notable changes in the land's use and modification over eight-year periods. Bare land decreased by 7.06% from 2015 to 2023, indicating repurposed for urbanization, reforestation, or agricultural activities. Built-up category remained relatively stable between 2015 and 2020, with a slight increase of 0.29% overall by 2023, reflecting gradual infrastructure development and urbanization. Farmlands expanded by 3.19% from 2015 to 2020, indicating a rise in agricultural activity. However, a 2.67% decrease by 2023 results in a net increase of 0.52% since 2015, suggesting land conversion to other uses such as natural grassland. Forestlands was 11.37% in 2023, showing further growth from 2020. While overall, forest cover increased by 4.54% from 2015, indicating successful conservation efforts and natural regrowth. Grasslands expanded by 2.77% from 2015, demonstrating consistent growth. Open-water category show notable decline by 1.06% since 2015, suggesting trends in water conversion or the impacts of climate change.

Table 5: Land cover area per hectare and percentage (%) change

Land cover	Area (Ha)	% 2015	Area (Ha)	% 2020	Area (Ha)	% 2023
Bare-land	246677.5	10.17%	107746.7	4.44%	75475.66	3.11%
Built-up/other	27048.07	1.12%	26190.68	1.08%	34225.7	1.41%
Farmland	751223.9	30.98%	828480.6	34.17%	763771.9	31.50%
Forest	165602.2	6.83%	238494.6	9.84%	275587.3	11.37%
Grassland	1204176	49.66%	1218805	50.26%	1271276	52.43%
Open-waters	30046.26	1.24%	5055.926	0.21%	4437.723	0.18%

Source: Author, 2025

4.1.1.2 Gross Percentage Change in LULC Classes from 2015 to 2023.

Figure 7 is essential for understanding patterns of land use change in the mid reaches of River Athi Basin. Assessing the socioeconomic and environmental factors capable of inducing changes, and informing future land use regulations to promote sustainable development and conservation in rivers.

The overall changes in the mid reaches of the river basin area coverage vary by land use/land cover (LULC) class. Grassland exhibits the largest area increase, followed by farmland and forestlands, whereas open water and built-up have the smallest area coverage. The Figure highlights variations in multiple land cover categories, indicating areas where specific land use types have expanded or contracted between 2015 and 2023. Notable changes in land cover, such as -31.5% decline in forest areas in 2023, may signal environmental issues like deforestation. This can lead to biodiversity loss, soil degradation, and increased greenhouse gas emissions.

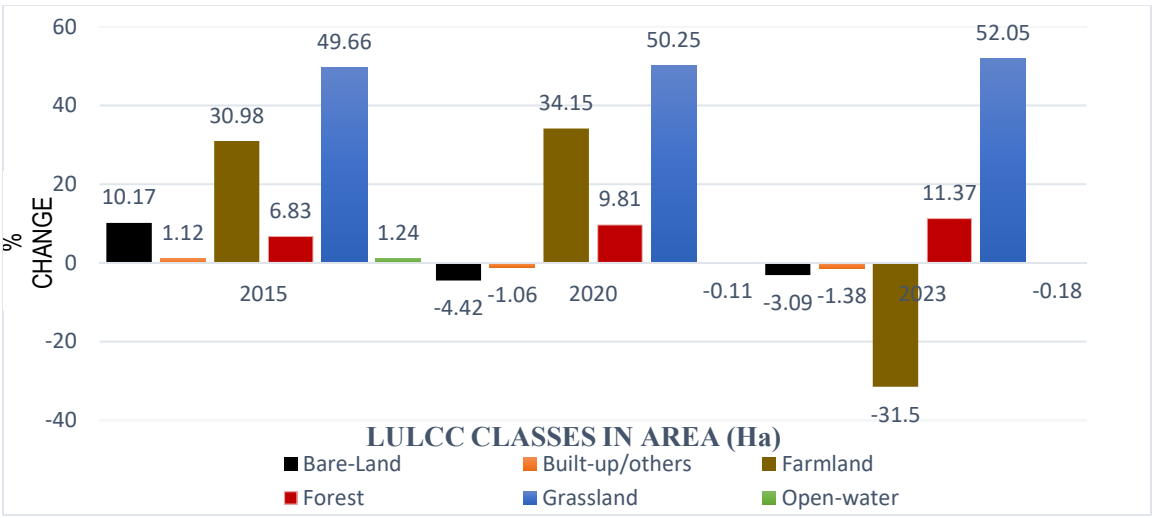

Figure 7: Gross percentage change in LULC of the river basin.

4.1.1.3 Classification Accuracy

The accurate or accuracy shows how many total predictions are correct. A model can have high accuracy but low true positive rate if the dataset is imbalanced. The true positive classification indicate how model used correctly predicts a positive case. The overall accuracy calculation was 77.5%, indicating a good level of accuracy and reliability in differentiating various land cover types in the basin (Table 6). Kappa coefficient value of 72.3% showed large agreement, implying that the model's performance is significantly better than random classification. Land cover data showed 24 true positive classifications of grasslands, 1 was negatively misclassified as forest, 3 misclassified as farmlands, and 2 negatively misclassified as bare lands. However, Grasslands was well-classified, with 24 out of 31 instances correctly identified, resulting in a high class-specific accuracy. The results indicated 23 true positive classifications of Forest and 1 negatively misclassified as Farmlands. However, Forest had an excellent classification, with only 1 instance being misclassified as Farmlands, indicating high precision in detecting forest areas.

The Data indicate that 18 true positive classified as farmlands, 6 were negatively misclassified as grasslands, and 1 negatively misclassified as forest. Farmlands had some confusion with Grasslands, where 6 instances were incorrectly classified. However, the model still identified Farmlands accurately most of the time. The results indicated that Open-waters had perfect classification with all 12 instances correctly identified. The model

was very effective in distinguishing this class. The results also showed 8 true positive classifications of bare-lands, while 5 were negatively misclassified as grasslands, 1 misclassified as farmlands, and 1 was misclassified as built-up. Conversely, Bare-lands had some confusion with Grasslands, where 5 instances were misclassified. Though, the model still managed to identify a majority of Bare-lands correctly. The data indicated 15 true positive classifications of Built-up, while 6 negative or misclassified grasslands and 2 misclassified bare-lands were present, while the majority were correctly identified.

Table 6: Accuracy confusion table

Class	**Cover**	**Class**	**1**	**2**	**3**	**4**	**5**	**6**	**Total**
1	Grasslands	1	**24**	1	3	0	0	2	31
2	Forest	2	0	**23**	1	0	0	0	24
3	Farmlands	3	6	1	**18**	0	0	0	19
4	Open Water	4	0	0	0	**12**	0	0	12
5	Bare-lands	5	5	0	1	0	**8**	1	14
6	Built-up	6	6	0	0	0	2	**15**	16
Total			41	25	23	12	10	18	**100**
	Overall, Class Accuracy								77.5%
	Kappa Coefficient Test								72.3%

Source: Author, 2024

4.1.1.4 Change Detection from 2015 to 2023

Transition between different Land Use/Land Cover (LULC) categories from the base year 2015 to 2020 was examined. Table 7 indicated that bare-lands accounted for 8.45%, due to conversion to farmland and grassland. These findings suggest that growing vegetation or agriculture occupied a portion of previously underutilized or less fertile land, while a tiny amount had been converted to grassland. The results on built-up were comparatively steady, indicating that urban sprawl was minimal. However, some conversions were natural or semi-natural land cover. It showed that while farmland was steady, a sizable amount (3.12%) was reforested and part was converted back to grassland. This suggests that some agricultural land has been abandoned and that natural vegetation, such as grasslands, is

growing. Although there was some conversion to farmland (1.34%). The results demonstrated that forestlands were generally well-maintained, suggesting a change in the priorities for land use.

The results on grasslands indicate a significant level of stability; however, some areas (10.35%) were converted to farmland, indicating continued agricultural activity. The conversion to bare ground (2.44%) may also be a sign of land clearing or deterioration. The findings indicated dramatic decline in open-water areas, with some areas becoming forest (0.35%) and farmland (0.46%). This illustrates the possibility of climate change.

Table 7: Change detection matrix for 2015 and 2020

		2020					
	LULC Type	Bare-lands	Built-up	Farmlands	Forests	Grassland	Open-waters
		Area in %	Area in %	Area in %	Area in %	Area in %	Area in %
2015	Bare-lands	1.33	0.08	4.37	0.31	4.06	0.009
	Built-up	0.12	0.36	0.03	0.001	0.58	0.008
	Farmlands	0.51	0.07	17.60	3.12	9.63	0.031
	Forest	0.003	0.007	1.34	5.24	0.22	0.004
	Grasslands	2.44	0.53	10.35	0.79	35.50	0.036
	Open-waters	0.02	0.017	0.46	0.35	0.26	0.119
	Total	**4.423**	**1.064**	**34.152**	**9.811**	**50.25**	**6**

Researchers' Fieldwork, (2024)

Transitions between different Land Use/Land Cover (LULC) categories from the base year 2015 to 2023 was analysed. Table 8 indicated land use intensification and grassland regeneration, which showed a substantial percentage of bare lands from 2015 with a shift to other land cover types, primarily farming (3.90%) and grassland (4.61%). The results showed that some land uses have been reclassified or resettled, as evidenced by the shifts from the built-up category to grassland (0.66%) and bare land (0.13%). Large stability is shown in the farmlands category, although there are noticeable shifts to grasslands (9.61%) and forests (3.86%), suggesting either land abandonment or reforestation activities.

Findings show that forestlands were largely constant, with only a small percentage (1.13%) being converted to farmlands. The biggest conversions to farmland (9.18%) and forests (1.33%), grasslands remain largely unchanged. A balance between land use conversion and preservation was shown by this transition.

The Data show a notable decrease in open waters, with the majority of the land changing to grassland (0.28%) and forestland (0.45%). These areas suggested that water bodies are drying up or of altered hydrological conditions brought on by the effects of climate change. Significant declines were shown by the open-water data, with a sizable portion shifting to other LULC types, such as forest and grassland. Natural processes affecting the water bodies and flora in the Athi River basin, as well as anthropogenic activities including agriculture, urbanization, and conservation initiatives, were the main causes of these transformations.

Table 8 Change detection matrix for 2015 to 2023

		2023					
	LULC Type	Bare-land	Built-up	Farmland	Forest	Grassland	Open-water
		Area in %	Area in %	Area in %	Area in %	Area in %	Area in %
2015	Bare-land	1.15	0.11	3.90	0.36	4.61	0.013
	Built-up	0.13	0.27	0.02	0.012	0.66	0.002
	Farmland	0.35	0.11	16.99	3.86	9.61	0.028
	Forest	0.003	0.007	1.13	5.32	0.003	0.007
	Grassland	1.46	0.74	9.18	1.33	36.89	0.045
	Open-water	0.004	0.15	0.25	0.45	0.28	0.084
	Total	**3.097**	**1.387**	**31.47**	**11.362**	**52.053**	**0.179**

Researchers' Fieldwork (2025)

4.1.2 Spatial LULC Differences on Water Quality across Sampling Stations in Athi River Basin

Having examined the land use land cover changes in the study area, this section evaluated spatial influence of LULC change on water quality. Pearson correlation analysis was

conducted between the proportional coverage of LULC categories at each sampling station and corresponding water quality parameters. The results reveal strong positive correlations between built-up areas and EC (r = 0.73), TDS (r = 0.81), BOD_5 (r = 0.81), and COD (r = 0.99), indicating that urbanization contributes significantly to pollutant loading. Conversely, forest and grassland cover showed negative correlations with these parameters, suggesting their role in improving water quality, as highlighted in Figures 4.3, 4.4, and 4.5.

4.1.2.1 Built-Up Areas and Urbanization

Figures 4.3 and 4.4 indicate that urban and semi-urban areas, particularly at Athi River Town, Stony Athi, and NYS sampling stations, exhibit elevated levels of EC and TDS, due to reduced runoff. In Built-up areas, urban expansion, also contribute to increase cadmium and chromium levels, with the NYS sampling station exhibiting higher cadmium level as indicated in Figure 4.5. There is strong positive correlations between Built-up areas and EC (0.73), TDS (0.81), BOD_5 (0.81), and COD (0.99) highlighting the contributions of industrial and domestic wastewater pollution.

4.1.2.2 Decrease in Open Water Areas

Reduced open-water areas are correlated with higher concentrations of pollutants such as TDS, EC, BOD, and COD, as indicated by the correlation analysis (Table 4.18). Open water shows strong negative correlations with EC (-0.93), TDS (-0.88, BOD_5 (-0.96, and COD (0.92), indicating the effect river dilution. The decline could also reflects the concentrations of these pollutants across the sampling stations (Figure 4.5). Bare lands are highly vulnerable to erosion because they lack vegetation cover. When these areas decline it means there is increase in vegetation cover that reduce or stabilize sediments or soil. TDS levels become more stable, fluctuating only slightly due to rainfall or minor land-use changes.

4.1.2.3 Bare-Lands and Sediment Runoff

Figure 8 indicates a decline in bare-land areas within the basin, which likely contributes to decreased sediment runoff. This reduction in runoff may account for stable and slight

fluctuations of Total Dissolved Solids (TDS) levels (range from 1125.5 to 1623.3 dS/m) in recent years. The inverse correlations EC (-0.97) and TDS (-0.94), indicate decreasing Barelands due to reduces sedimentation and pollutant runoff, improving water quality.

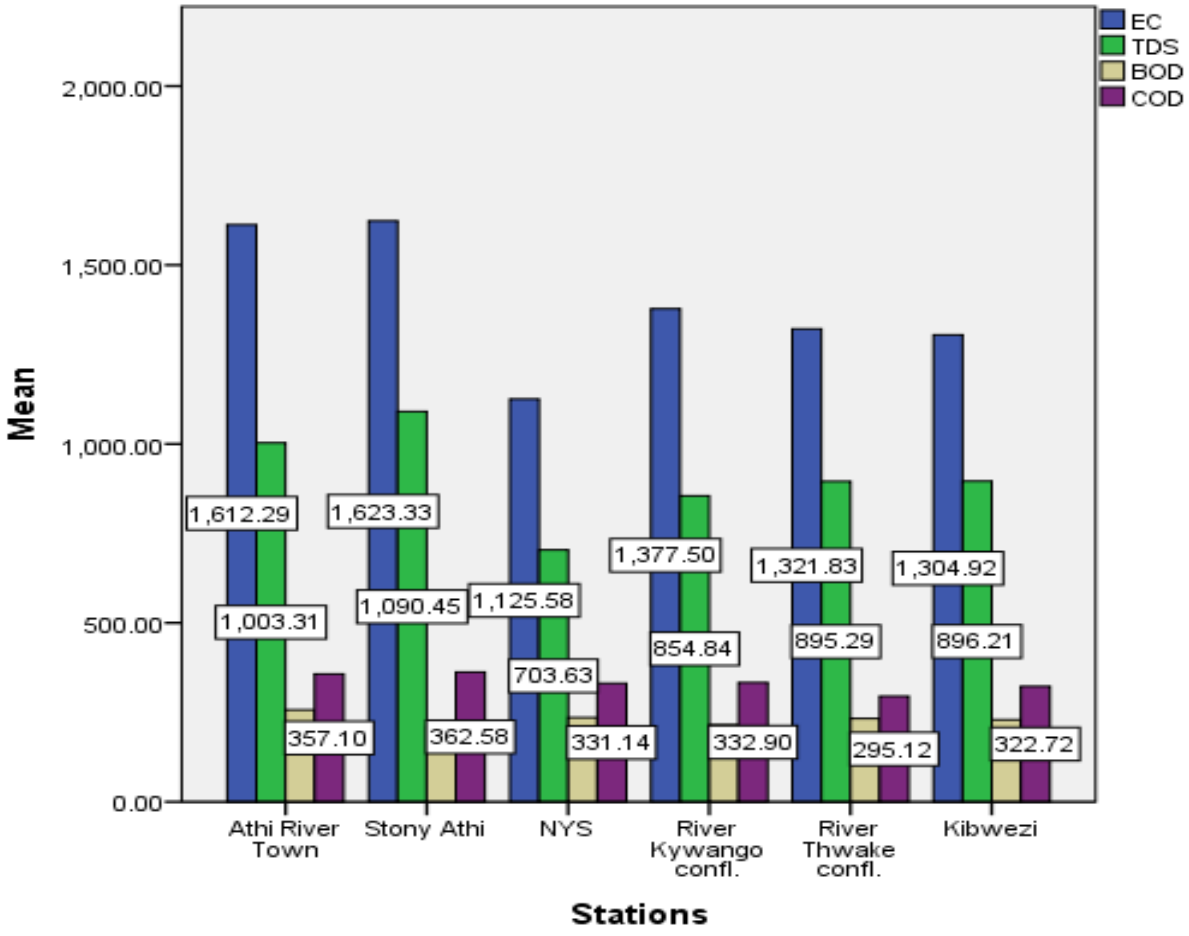

Figure 8: Spatial LULC difference on mean physicochemical water quality parameters across sampling stations in athi river basin

4.1.2.4 Farmlands and Agricultural Expansion

Figure 9 indicated that Athi river Town, Stony Athi and River Kyawango Confluence sampling stations exhibits higher levels of NO_3 and PO_4 than NYS, River Thwake and Kibwezi Bridge sampling stations. Farmlands correlate strongly with NO_3 (0.93), PO_4 (0.93), and Cd (0.97). These higher concentrations are closely linked to nutrient release from agricultural waste into the stagnated water and low flow water at Athi river Town and Stony Athi areas, as well as River kyawango confluence station during the dry season.

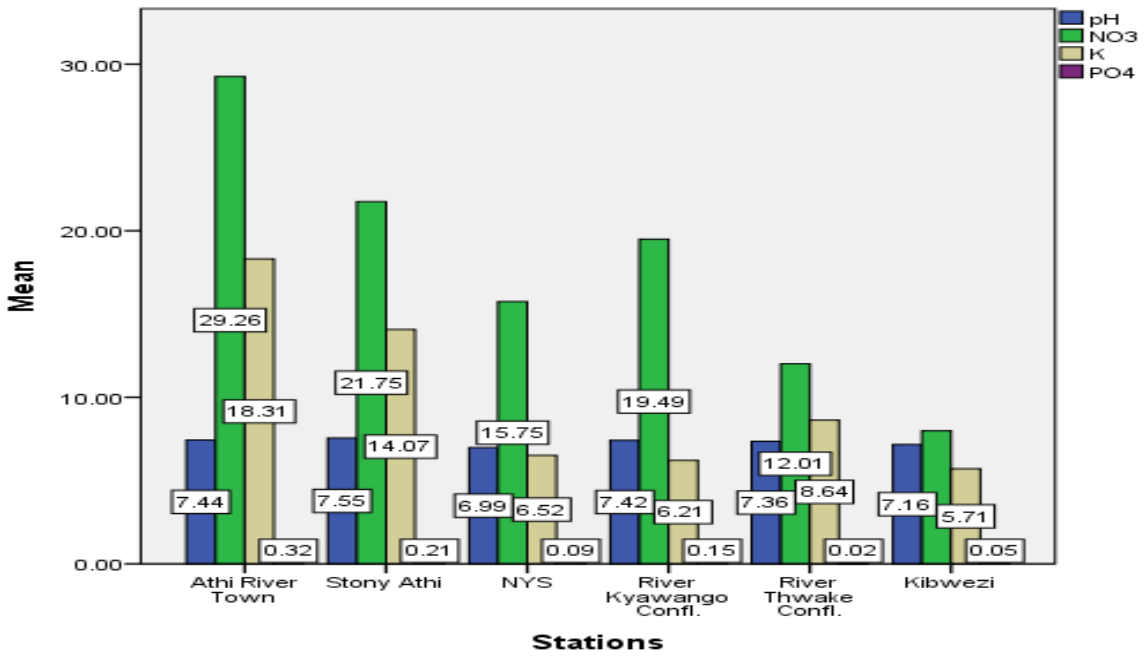

Figure 9: Spatial LULC differences on mean physicochemical water quality parameters across sampling stations in athi river basin.

4.1.2.5 Grasslands and Forests

The findings in Figures 9 and 10 indicate that the Thwake Confluence and Kibwezi rivers contain extensive grassland areas which support cleaner water resulting to reduced levels of BOD, TDS, Cd, and Cr. The evidence is the negative correlations with BOD (-0.48), TDS (-0.61), EC (-0.67), and COD (-0.51), which attributed to improved water quality. Higher levels of Cadmium consentrations was found at NYS sampling station, declined at Stony Athi, and Athi river Town stations. Chromium levels increases at Athi River Town with decreasing levels as the river flow progress downstream to Kibwazi Bridge (Figure 10).

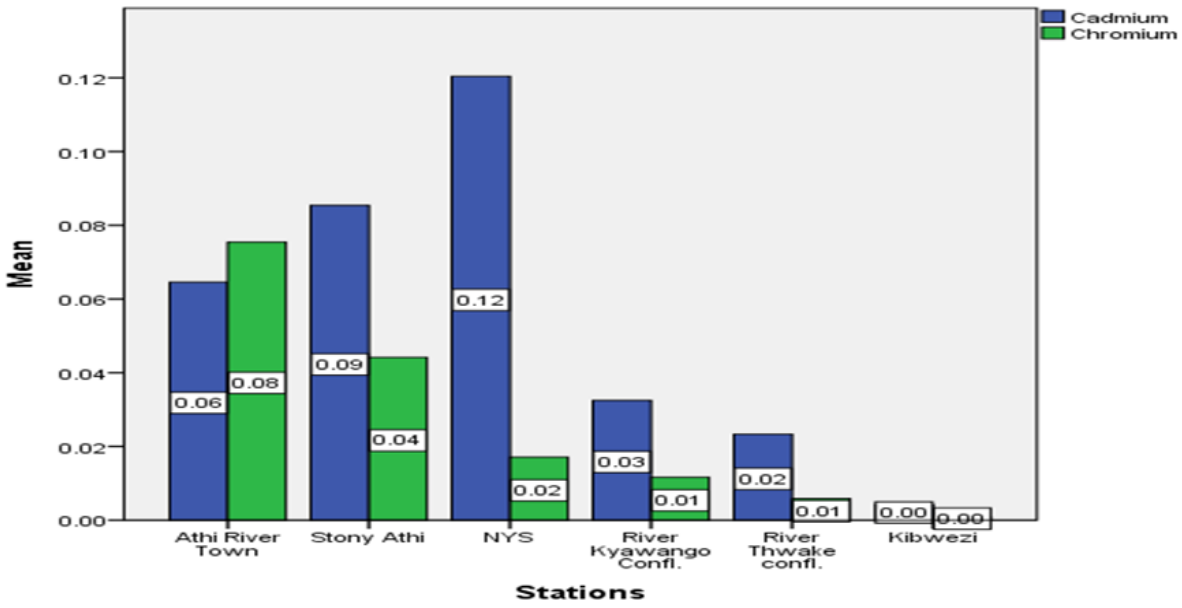

Figure 10: Spatial LULC differences on mean heavy metals water quality across sampling stations in athi river basin

4.1.3 Interview Survey Design on Land Use Drivers of Change in Athi River Basin

The interview survey was conducted within a 0 to 10-kilometer range from the river's edge. The activities outlined in Table 9 include those occurring within the river, such as sand harvesting, fishing, rearing animals, washing, and bathing. 2) Those taking place in the riparian zone and beyond, such as irrigation, settlement, industrial activities, commerce, and population growth. 3) Non-point sources like settlement, seasonal flow, commercial activities, and climatic factors.

Residents from six sampling stations, Athi River Town (S1), Stony Athi (S2), NYS (S3), River Kyawango confluence (S4), River Thwake confluence (S5), and Kibwezi (S6) were assigned twenty interview questions. The highest sampling station S1 with (20) respondents is located in the machakos town, followed by station S2 (17) still found in town. Station S3 with 13 respondents is located in the national youth service headquater and market. Station S4 with 8 respondents is found near farmlands and small village. Station S5 with 3 respondents is located in a pristine ecological area (Thwake confluence) with no settlement nor unsustainable land use activities. While station S6 with 9 respondents is located between two counties comprising villages, with growing population.

Table 9 show that 58.33% of the 70 respondents agreed that water quality contamination in the River Athi basin is attributed to five factors, namely industry, agriculture, settlement, commerce, and climate condition.

Table 9: Interview result on source of athi river pollution

Number of People Targeted and Interviewed				
S.S	No. of Target	No. of Respondents	Number of Factors	Number of listed Drivers
S1	20	20	Industry, agriculture, commercial, settlement and climate.	5
S2	20	17	Industry, agriculture, commercial, settlement, and climate.	5
S3	20	13	Agriculture, settlement, commercial, and climate.	4
S4	20	8	Agriculture, sand harvesting, settlement, and climate.	4
S5	20	3	Sand harvesting, agriculture, and climate	3
S6	20	9	Agriculture, climate, commercial, settlement, and river flow/runoff	5
Total	**120**	**70**		**27**

Researchers' Fieldwork (2025).

The results of the five factors and sub-factors affecting water quality obtained from interview questions was compared with land use/ land cover change classification (Table 10).

Table 10: Relationships between drivers of change and lulc categories

S/N	Natural & Anthropogenic Factors	Land Cover Class Factors
1	Industry: Wastewater treatment plant, cement particles, Sand harvesting, solid waste, plants, and sewages	Open-waters (WWTP) / Barelands, Builtup/others
2	Settlement: population/lifestyle, wastewater, washing & bathing, landscape, plants, waste dumpsites.	Built-up/others, Barelands, Farmlands, and Forest lands
3	Agriculture: irrigation, walking animals, fishing, wastewaters, biological waste, sewages, runoff, and stone burning.	Farmlands, bare-lands, and Open waters
4	Climate: temperature, seasonality (dry and rainfall), and atmospheric deposition.	Bare-lands, Grasslands, and Farmlands
5	Commercial: Road network, Stages, and Vehicular release of CO_2, NO_2, CO, and SO_4	Bare-lands, built-up/others

Researchers' Fieldwork (2025)

The factors or drivers of change and their relationship with land cover classification in percentages were show in Figure 11. It illustrates the five sources of change alongside the percentage classification of land cover associated with each. A detailed examination reveals that, based on their sources and percentage within the basin, the five drivers of water quality degradation and land cover categories reported frequencies of four for industry with openwater, bareland, builtup/others (16%). Six for agriculture with 24% in farmland, barelands, and openwaters, six for commercial with bare-land, and builtup/others (16%). Five for settlement with 20% in builtup/others, barelands, farmlands, and orestlands. Six for climate with 24% in bare-land, grasslands, and farmlands across six land cover categories (Table 5.9). The results indicate that while industrial and commercial activities have some minor or less noticeable effects on the decline in the river water quality, climatic factors such as rainfall (runoff), agriculture, and habitation are the primary drivers.

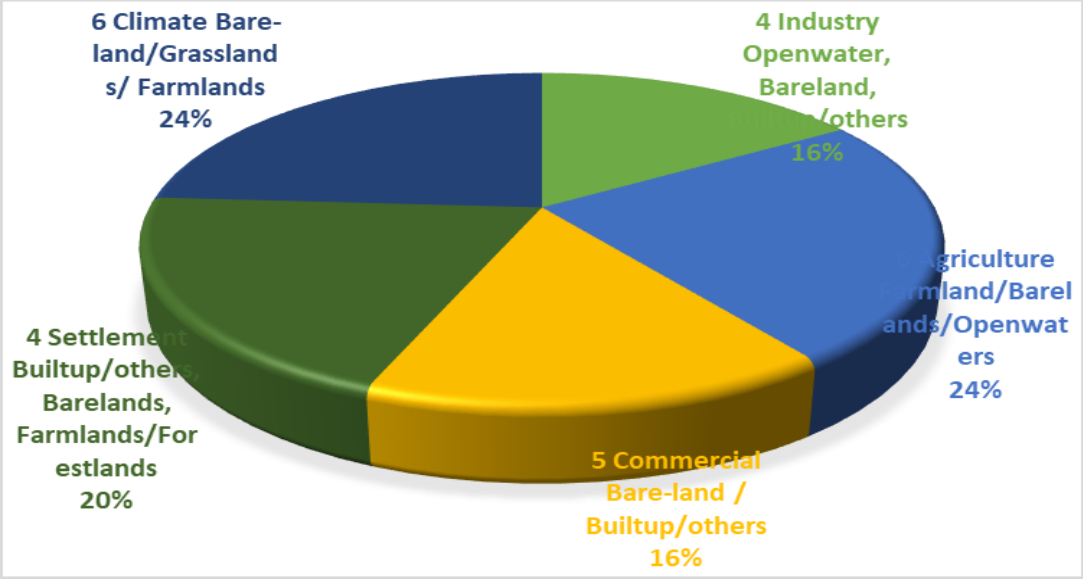

Figure 11: Drivers of change and related land cover classification in percentages

4.2 Spatial and Temporal Variations of Physicochemical Water Quality of River Athi Basin Using Multivariate Analysis.

4.2.1 Identification of Water Quality Dataset Relative Contribution to the Pollution of River Athi Basin.

The data in Table 11 depict the Principal Component (PC) of the water quality variables. The PC1 indicated a general pollution gradient of salinity and organic loads. The variables such as EC (0.38), TDS (0.34), NO_3 (0.34), COD (0.36), BOD (0.34), PO_4 (0.32), highly loaded strong positive. It suggests that PC1 captures overall pollution intensity, from salinity indicators (EC, TDS), Nutrients (NO_3, PO_4,), and organic (BOD, COD). Stations with high PC1 scores likely face urban or mixed-source contamination. PC2 shows a contrast in nutrients and heavy metals. The component indicated positive variables such as Cd (0.51), Cr (0.40), K (0.38), and PO_4 (0.28). At the same time, negative variables include pH (–0.39), BOD, and COD. This group likely separates metal-rich nutrient zones from stations with more acidic or oxygen-demanding conditions. It suggests reflecting industrial vs agricultural gradients. PC3 indicated heavy metals and organic breakdown. Cadmium (Cd) loads strongly (0.68), while Cr is negative (–0.42), BOD and COD are both positive. However, the PC captures a contrast between particulate-bound heavy metals (Cd) and oxygen-demanding organics. PC4 identified chromium dominance. Chromium (Cr) is

dominant (0.71), with lesser contributions from COD, and BOD, suggesting a unique heavy metal-specific pollution axis, from local industrial discharges. PC5 Shows strong negative loading of pH (–0.73), due to geochemical or alkalinity. PC7 identified NO_3 dominant (0.72) pointing to nitrate-driven nutrient zones, induced from agricultural runoff areas. PC8 to PC 10 indicated low-variance components. At the same time, PC9 shows high loadings for COD (0.67) and BOD (–0.60), due to contrasting biodegradable and non-biodegradable organics processes. PC10 was able to fine-tune EC and TDS parameters.

Table 11: Principal component with average water quality parameters

	PC1	PC2	PC3	PC4	PC5	PC6	PC7	PC8	PC9	PC10	WHO 2011
pH	0.28	-0.39	-0.19	-0.22	-0.73	0.19	-0.28	0.09	-0.16	-0.02	6.5-8.5
EC	0.37	-0.18	-0.01	-0.03	0.23	0.27	0.17	0.10	0.32	-0.75	400dS/m
TDS	0.34	-0.27	0.05	-0.08	0.39	0.52	0.21	0.13	-0.21	0.53	500mg/l
NO3	0.34	-0.03	-0.25	-0.11	-0.21	-0.36	0.72	-0.31	-0.01	0.10	50mg/l
K	0.31	0.38	-0.09	-0.45	0.18	0.10	-0.41	-0.58	0.05	0.02	0.3mg/l
PO4	0.32	0.28	-0.25	-0.25	0.18	-0.40	-0.16	0.68	-0.08	0.04	0.2mg/l
BOD	0.34	-0.23	0.34	0.28	0.17	-0.37	-0.18	-0.19	-0.60	-0.19	20mg/l
COD	0.35	-0.19	0.25	0.28	-0.04	-0.	-0.24	-0.02	0.67	0.34	10mg/l
Cd	0.20	0.51	0.68	-0.06	-0.24	0.20	0.19	0.17	-0.05	-0.02	0.003mg/l
Cr	0.25	0.39	-0.42	0.70	-0.10	0.27	-0.08	-0.02	-0.08	0.006	0.05mg/l

Researchers' Fieldwork (2025)

The data in Figure 12 presents an explained variance indicating the two-dimensionality of the study dataset. The PC1 explains 60% of the total variance, driven by dominant pollutants like salinity and minerals (EC, TDS, or NO_3). While PC2 added 20%, to capture 80% of the variability of the water quality.

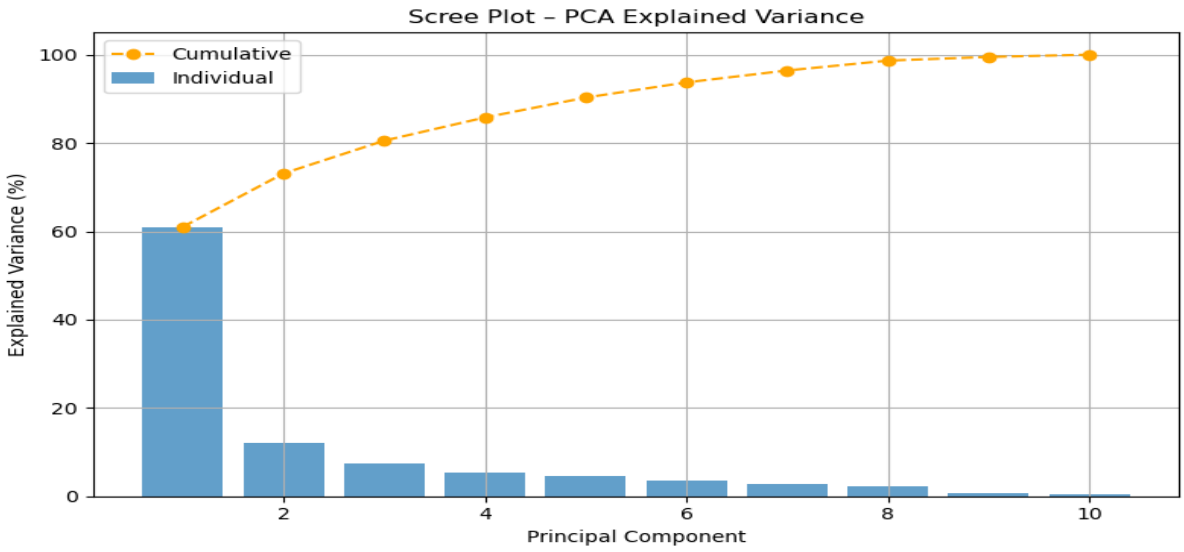

Figure 12: Explained variance in water quality of the mid-river athi basin

4.2.1.1 Spatial Correlation Coefficient of the Dataset

The component loading shows how strongly each original variable influences a principal component (PC). PC1 identified the highest variance (~40–60%) indicating a strong influence of EC, TDS, and Cd, representing Ionic content, salinity, and/or mineral pollution. The higher PC1 scores include Athi River Town and Stony Athi, with elevated EC/TDS due to urban runoff or effluents. PC2 correlates with NO_3, PO_4, BOD, and COD, which reflects organic and nutrient pollutions, such as sewage, agricultural runoff, or decaying biomass. The high scores of the sampling stations might be transitional, or downstream farms or settlements.

Principal Component Scores in Figure 13 depicted sampling stations with combined influence of all the original water quality parameters compressed into two components. PC1 (horizontal axis) explains the largest share of variance, due to salinity or mineral loads as well as overall pollution intensity. PC2 (vertical axis) captures a different gradient, such as nutrients, heavy metals, or organic loads. However, Athi River Town and Stony Athi sampling stations are farthest on the positive side of PC1, exhibiting distinct pollution characteristics. This urban zone is dominated by EC, TDS, COD, NO_3, and heavy metals, emanating from urban-industrial discharge. River Thwake Confluence and Kibwezi Bridge sampling stations are together near the sources or origin, suggesting more moderate or

similar water quality profiles, possibly transitional or mixed-influence zones. NYS sampling station appears slightly separated from the cluster, which may imply unique patterns. Perhaps tied to location, season, or outlier parameters like Cd or PO_4. River Kyawango Confluence station is placed near the center, likely showing a balanced or average signature, making it a good reference point as shown in Figure 13.

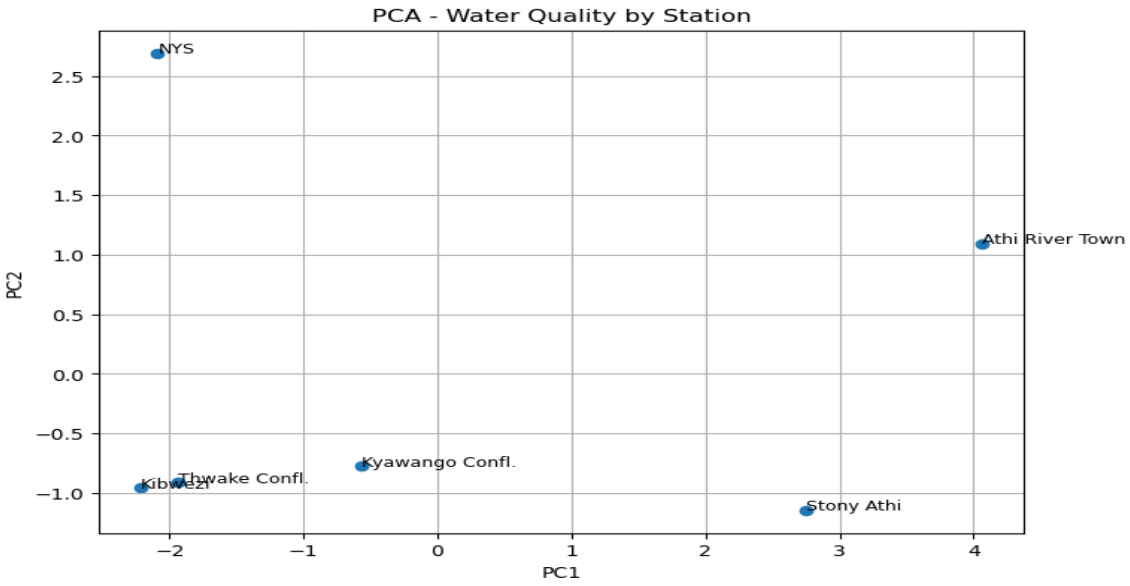

Figure 13: score plot of spatial variation in water quality of the river athi basin

4.2.1.2 Grouping of Sample Stations Based on Similarity in the Water Quality Dataset of the Mid Reaches of River Athi Basin.

The data in Table 12 present average water quality dataset into 3 clusters. Cluster 1 is the most impacted zone. The cluster revealed higher concentration values of EC, TDS, NO_3, K, PO_4, BOD, COD, Cd, and Cr across the sampling stations. It strongly suggests intense pollution, emanating from point sources such as industrial discharge, domestic waste, or concentrated urban runoff. This cluster is suggested to include Athi River Town and Stony Athi, urban-industrial hotspots.

Cluster 2 showed moderate pollution impacts. This cluster indicated that all values are consistently lower than cluster 1, specifically on nutrients (NO_3, PO_4) and heavy metals (Cd, Cr). It relatively increased EC and TDS, but showed improvement compared to cluster

1. The cluster represents transitional or semi-urban stations, such as the River Kyawango confluence sampling station, with minimal impact.

Cluster 3 indicates twist purification or a cleaner zone. The cluster identified low values of pH, EC, and TDS, pointing to less mineralized and fresher waters. However, Cd (0.12) is higher in other clusters, which is typical for cleaner areas. This might indicate a unique local contaminant source, possibly a metal-rich geology affecting the sampling station, like the River Thwake confluence and Kibwezi Bridge. However, the findings indicated that Cluster 1 is the red zone, Cluster 2 is amber, and Cluster 3 is mostly green with a caution flag on cadmium.

Table 12: Spatial mean concentration values of cluster analysis

NS	pH	EC	TDS	NO3	K	PO4	BOD	COD	Cd	Cr
Cluster 1	7.50	1617.81	1046.88	25.50	16.19.	19.27	233.20	359.84	0.07	0.06
Cluster 2	7.31	1334.75	897.67	13.16	6.85	0.07	225.90	316.91	0.02	0.01
Cluster 3	6.99	1125	703.63	15.75	6.52	0.09	235.31	331.14	0.12	0.02
WHO 2011	6.5-8.5	400dS/m	500mg/l	50mg/l	0.3mg/l	0.2mg/l	20mg/l	10mg/l	0.003 mg/l	0.05 mg/l

Researchers'Fieldwork (2025)

The results in Figure 14 depicts the spatial grouping of sample stations into 3 stations using a Dendrogram, which reflects persistent spatial relationship. It shows hierarchical relationships between samples across the six stations. Cluster 1 shows that Athi River Town and Stony Athi sampling stations were grouped together due to high levels of EC, TDS, BOD, and NO_3, characterized by urban-industrial pollution. Cluster 2 grouped NYS and River Kyawango Confluence as possibly transitional sampling stations, influenced by both urban and upstream natural factors. Cluster 3 grouped Kibwezi Bridge and river Thwake Confluence (control station) as purification or geogenically distinct stations, due to low nutrient and heavy metal load.

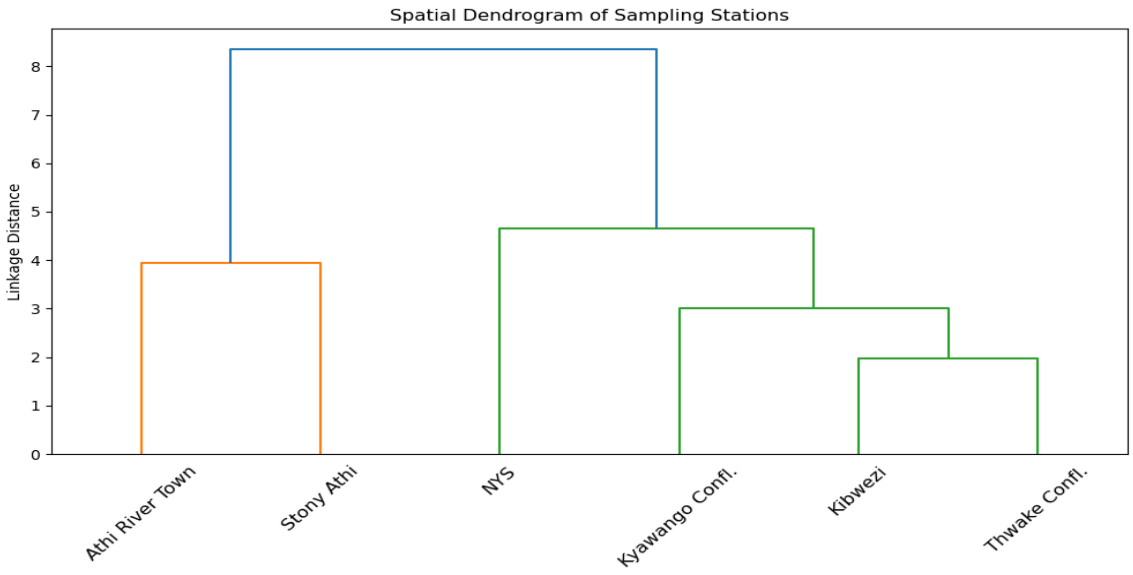

Figure 14: Spatial three clusters of the sample stations of the river athi basin

The data in Figure 15 present a heatmap with spatial concentrations of pollutants across sampling stations or clusters. The Figure shows average values of key water quality parameters across three spatial clusters. Color intensity reveals how high or low each parameter is in each cluster. The darker shades indicate higher concentrations, while lighter shades have lower or cleaner values. Cluster 1 was identified as heavily Impacted Zone. Higher values for EC, TDS, NO_3, K, and PO_4 were observed. Strong coloration for BOD and COD, indicates higher organic and oxygen-demanding matter. Cadmium (Cd) and Chromium (Cr) are moderately elevated. This zone is a highly urbanized and industrially influenced area, possibly Athi River Town and Stony Athi sampling stations, with intense salinity, nutrient, and organic loading. Cluster 2 is moderately affected. Nutrients (NO_3, PO_4) and heavy metals (Cd and Cr) concentrations were decreased in this cluster of heavy metals, with moderate EC and TDS concentrations. There is the presence of organic pollution (BOD, COD) though, it shows subduction. These stations are affected, with less severe impacts. Perhaps the mid-section or peri-urban stations are influenced by both runoff and limited dilution. Cluster 3 shows cleaner waters with a heavy metal twist. Low concentrations of EC, TDS, and nutrient values, were identified, indicating fresher water, though, higher Cd values were noticed. This cluster represents relatively pristine or rural

environments, like Kibwezi Bridge or downstream sites, but with a peculiar spike in cadmium. That suggests localized or geogenic metal inputs.

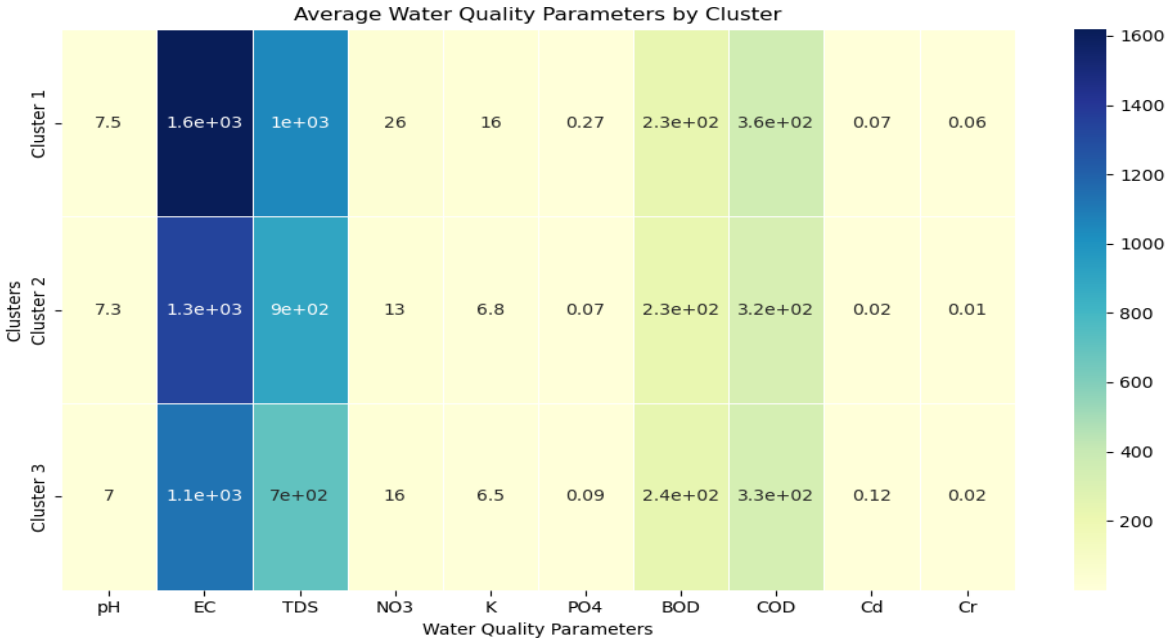

Figure 15: Spatial mean levels in water quality using heatmap in river athi basin

4.2.2 Identification of Monthly Variation of the Water Quality Dataset of the Mid-River Athi Basin.

Explained variance in Figure 16 depicted temporal PCA score plot of water samples from different months and seasons onto two new groups. PC1 captures the most variance in water quality such as mineralization or salinity, and heavy metal influence (EC, TDS, and Cd). Higher PC1 scores indicated pollution potential in dry-season zones. PC2 captures the second-most variance, often linked to nutrient levels and organic content load (NO_3, PO_4, and BOD). However, samples with moderate PC2 scores might experience seasonal runoff. However, the Explained variance revealed how much of the total variability in the multivariate water quality dataset was captured by each principal component (PC). For instance, PC1 and PC2 alone explain approximately 76% of the total variation across months and seasons. These first two components may capture salinity and heavy metal buildup (EC, TDS, and Cd) and nutrient/organic pulses (NO_3, PO_4, and BOD). While PC3 and beyond represent subtle patterns or localized variability, useful but less dominant.

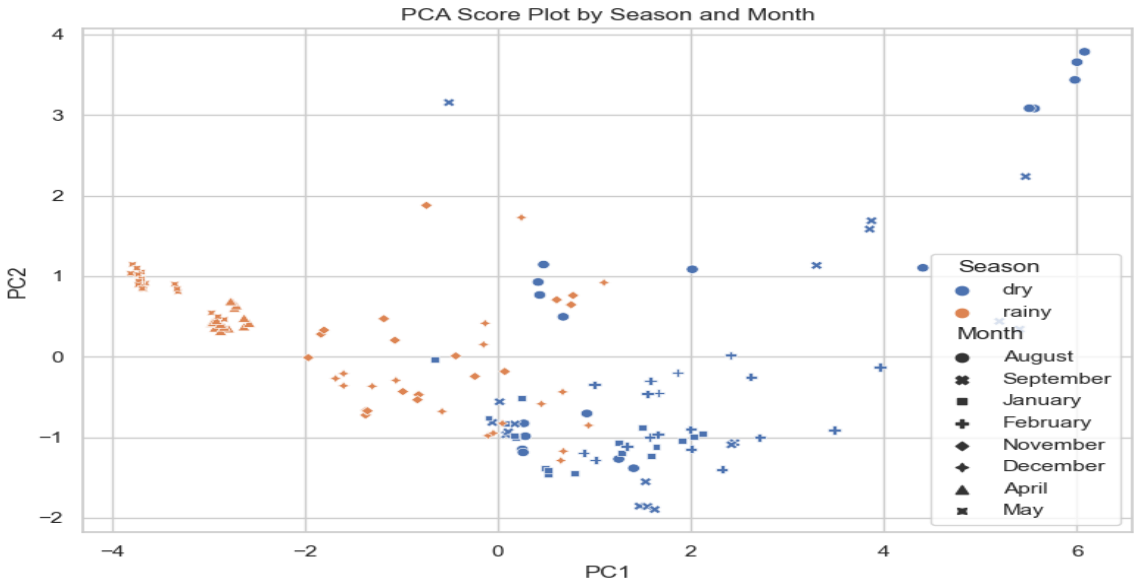

Figure 16: Temporal pca score plot of water quality for 8 months in the river athi basin.

Tmporal cluster analysis (CA) in Figure 17 highlight temporal hierarchical cluster analysison water quality dataset grouped based on similarity. The study analyzed monthly averages and used hierarchical clustering (Ward's method) to build a dendrogram. Cluster analysis shows that Cluster A such as August & September merged at a very low dissimilarity level (~2), indicating identical profiles. High EC, NO_3, and Cd classic dry-season concentration are strongly linked to PC1 loadings, reflecting mineralization and metal buildup. Cluster BNovember & December, also tightly paired (~2 Euclidean units apart). Still in the dry season but shows slightly moderated pollution compared to August–September. The study identified sub-cluster A+B (August–September+November–December), which merged at approximately 6 dissimilarities, forming the core dry-season branch with increased pollution. Cluster C January & February, merged tightly (~2) and then joined Cluster A+B at ~7–8 units. These early-year samples tend to show residual pollution before rainy dilution begins. So this larger Cluster A+B+C captures the entire dry-season continuum. However, Cluster D April & May formed their own cluster, clearly detached, joining the rest at ~10 Euclidean distance. These are rainy-season months with the lowest pollutant levels, confirming dilution effects. Their separation underscores how seasonality drives water chemistry divergence.

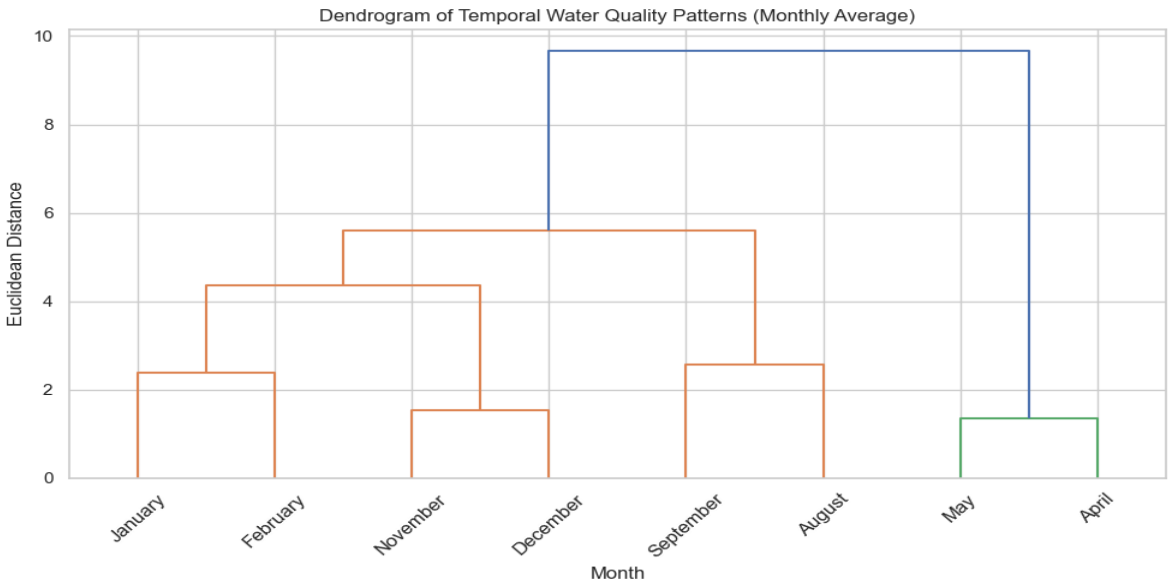

Figure 17: Temporal hierarchical clustering for 8 months average with dendrogram in the river athi basin.

4.2.2.1 Seasonal Contribution of Pollutants in Water Quality of the Mid Reaches of River Athi Basin.

The PCA data in Table 13 highlight that PC1 indicate general pollution load. The axis showed strong positive loading from EC (0.38), TDS (0.35), NO_3 (0.35), COD (0.36), and BOD (0.34). These loading indicates a broad pollution gradient from salinity, nutrient enrichment, and organic content. Likely separates dry season samples (more concentrated) from rainy season ones. PC2 shows heavy metals and potassium (K) concentrations. This PC highlights the strongest contributors of Cd (0.56) Cr (0.44), and K (0.40) in the water quality of River Athi. This component reflects heavy metal contamination, possibly from industrial runoff or seasonal flushing effects. PC3 indicated organic load and heavy metals. This PC shows high positive variables such as Cd (0.63), BOD (0.36), and COD (0.29), with strong negative Cr (-0.45). It contrasts organic pollution with certain metals, possibly distinguishing runoff events (more BOD/COD) from heavy metal hotspots. PC4 showed phosphate dominance and Cr suppression**.** This PC identified high levels of PO_4 (0.57), with low negative Cr (-0.64). Highlighting the impact of domestic waste or fertilizers (rich in phosphate) while being relatively low in Cr in the mid-section of the river basin. PC5 is strongly anti-correlated with pH (-0.77), suggesting a role for acidity/alkalinity control.

PC8 Splits K (+0.68) from PO_4 (–0.60), possibly separating inorganic ions from phosphate-rich effluents. PC9 emphasizes COD (0.65) vs. BOD (-0.60), which indicates oxygen dynamics from different pollution sources. PC10 shows EC (0.73) opposing TDS (–0.51), which is odd and may reflect residual noise or rare conditions. However, PCs 5-10 explained trends variability in the river basin.

Table 13: Contribution of water quality with principle component analysis

Parameters		PC1	PC2	PC3	PC4	PC5	PC6	PC7	PC8	PC9	PC10
1	pH	0.28	-0.32	-0.21	-0.30	-0.77	0.09	-0.20	-0.35	-0.15	0.03
2	EC	0.38	-0.18	0.009	0.05	0.16	0.32	0.14	-0.12	0.34	0.73
3	TDS	0.35	-0.23	0.53	0.008	0.27	0.62	0.16	-0.14	-0.23	-0.51
4	NO3	0.35	-0.00	-031	0.09	-0.07	-0.38	0.75	0.20	-0.01	-0.11
5	K	0.31	0.39	-0.08	0.33	-0.10	0.25	-0.29	0.67	0.08	-0.05
6	PO4	0.32	0.21	-0.19	0.57	-0.04	-0.21	-0.26	-0.60	-0.13	-0.04
7	BOD	0.34	-0.23	0.36	-0.06	0.27	-0.36	-0.19	0.23	-0.59	0.22
8	COD	0.36	-0.19	0.28	-0.15	0.08	-0.34	-0.23	-0.009	0.65	-0.36
9	Cd	0.18	0.56	0.63	-0.17	-0.31	0.08	0.27	-0.19	-0.06	0.03
10	Cr	0.23	0.44	-0.45	-0.63	0.32	-0.03	-0.16	-0.11	-0.05	0.03

Ogbonna *et al.* (2024)

The data in Figure 18 presents principal components with a combined linear of the original variables arranged in order of the amount of variance. PC1 captures the largest amount of variation, while PC2 captures the next largest, and so on.

The explained variance ratio shows the total amount of variability in the dataset as captured by each component (Figure 18). The first two principal components explained 70% of the total variance in water quality, indicating that PCA effectively reduced the multidimensional dataset into two interpretable axes representing key pollution gradients. However, PC1, accounting for 45% of the total variance, was strongly influenced by EC, TDS, and Cd, indicating that it reflects variations related to salinity and metal contamination. PC2, explaining an additional 25%, showed high positive loadings from

NO_3, PO_4, and BOD, likely representing nutrient-enrichment processes linked to runoff or organic load. This orthogonal structure suggests that water quality is shaped by both geochemical and anthropogenic factors acting independently.

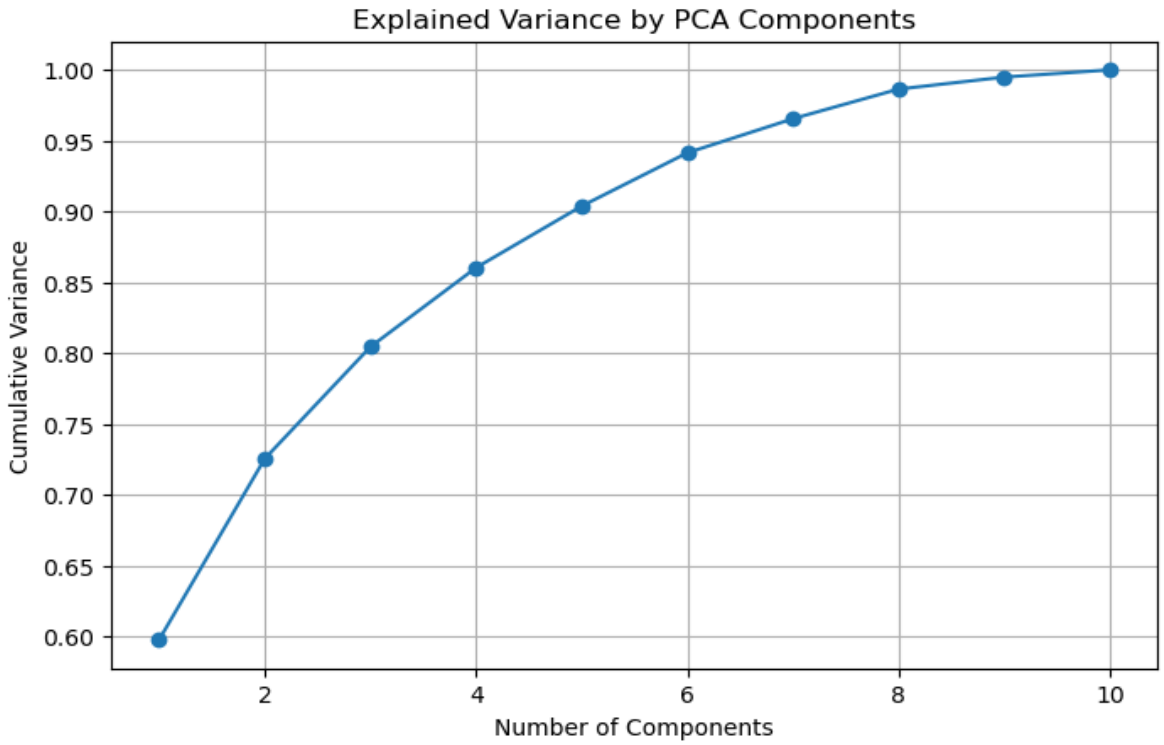

Figure 18: Explained variance of temporal variation in water quality of the river athi basin.

The Data in Figure 19 depict PC1 and PC2 axes, representing the directions of maximum variance captured by PCA. The Colors indicate that each sample of the K-means cluster belongs to PCA, while the shapes represent the seasons. However, the biplot revealed distinct spatial separation between rainy and dry season samples. Dry season grouped largely within Cluster 2, characterized by higher EC, TDS, and BOD values, while rainy season samples clustered separately, associated with lower conductivity and nutrient loads. PC1 and PC2 together explained approximately 70% of the variance, with PC1 strongly influenced by conductivity-related parameters (EC & TDS) and PC2 by nutrient levels (NO_3, PO_4).

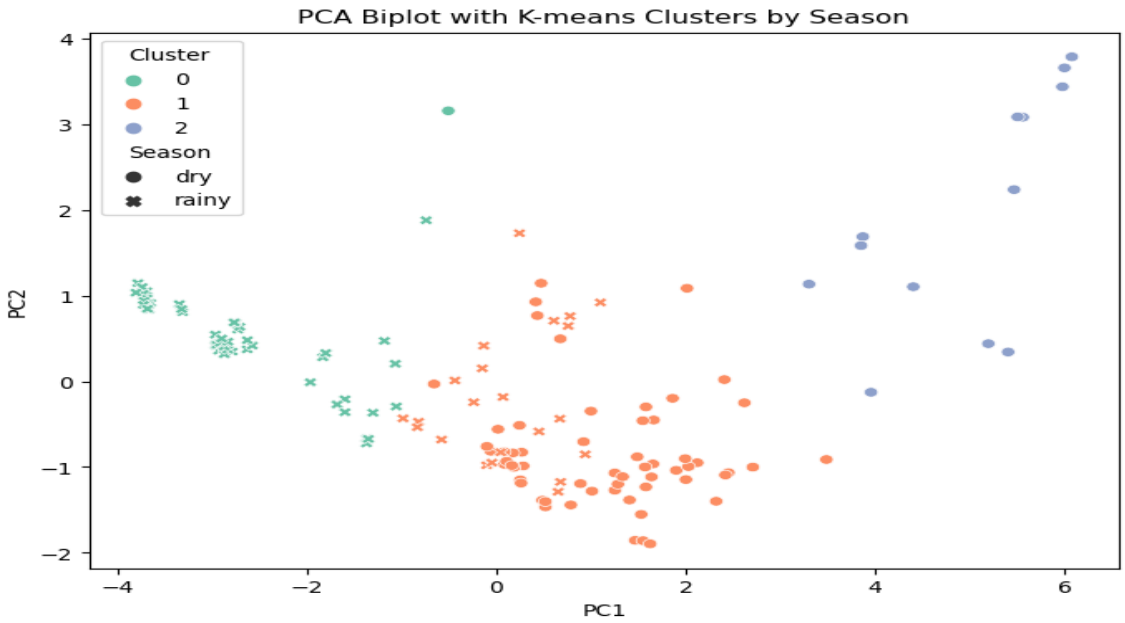

Figure 19: K-means clusters on water quality seasonal variation in the river athi basin

Results in Table 14 highlight Cluster 1 higher seasonal contrast, with severe dry seasonal pollution. This group shows acidic pH in both seasons, with values as low as 4.35 during the dry season. Elevated dry season indicated EC (1220 µS/cm), TDS (750 mg/L), NO_3 (10 mg/L), and particularly Cd (0.50 mg/L) showing intense contamination. Values drop significantly in the rainy season, suggesting seasonal dilution. This cluster represents isolated or pollution-prone hotspots.

Cluster 2 shows stable conditions with moderate pollution. Minor seasonal variation, pH remains near neutral (~7.6), while EC and TDS stay consistently high. Nutrient levels (NO_3, K, and PO_4) are elevated in both seasons, along with detectable Cd and Cr. It indicates steady, annual contamination, emanated from semi-urban or peri-urban sources like runoff or domestic wastewater. Cluster 3 indicated intense pollution zones by industrial or agricultural activities. This cluster is characterized by extreme concentrations in EC (2261 µS/cm), TDS (1458 mg/L), NO_3 (41.76 mg/L), K (~41 mg/L), and PO_4 (~0.63 mg/L). Metals like Cd (0.25 mg/L) and Cr (0.12 mg/L) are also elevated. This likely reflects the dominance of dry season inputs and high-impact land use (e.g., agro-industrial discharges).

Table 14: Cluster analysis on seasonal pollution dynamics

Clusters	Seasons	pH	EC	TDS	NO_3	K	PO_4	BOD	COD	Cd	Cr
1	Dry	4.35	1220.00	750.00	10.00	8.80	0.11	402.00	505.00	0.50	0.06
	Rainy	6.73	786.94	504.20	4.83	3.50	0.06	82.32	132.14	0.012	0.05
2	Dry	7.59	1689.10	1140.50	23.76	9.78	0.17	337.74	454.83	0.04	0.01
	Rainy	7.74	1492.86	940.68	17.13	6.54	0.72	202.35	333.64	0.05	0.05
3	Dry	7.89	2261.00	1458.84	41.76	40.90	0.62	349.76	554.23	0.25	0.11

Researchers' Fieldwork (2025)

4.2.3 Temporal Variation of Physicochemical Parameters and Heavy Metals in Water Quality

4.2.3.1 Monthly Average Rainfall Trend in Athi River Basin

The average rainfall in Figure 20 was used to discuss seasonal trends in the mid river section of Athi basin. The results indicated a notable rainfall peak, with 393 mm falling in April and declining in May, while 425 mm falling in November and lower in December showing bimodal rainfall patterns in the basin. These months experiences the most rainfall, signaling the start of both long and short rains in mid reaches river basin. There is extremely little rainfall in June, July, August, and September, less than 30 mm, especially in September, when there is only about 9 mm. This suggested that these months, which see little precipitation, are part of the dry season. Seasonal fluctuation in precipitation is seen in the fairly high rainfall in March, May, and December, which reaches 184 mm in March, 173 mm in May, and 170 mm in December. With modest rainfall of 57 mm in February and 81 mm in January, there is a noticeable change from the dry to the wet season.

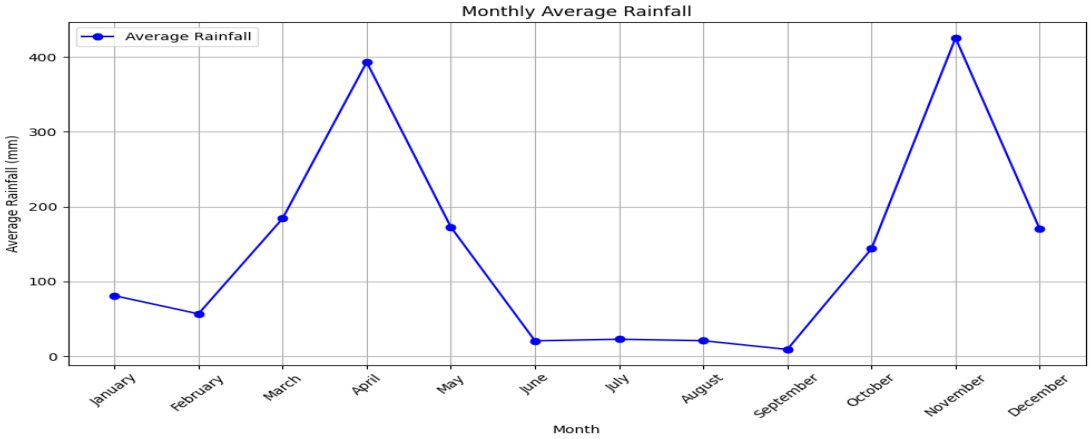

Figure 20: Bimodal rainfall trend of athi river basin

4.2.3.2 Monthly Trend in Water Quality

Potential Hydrogen (pH)

The water pH data collected over an eight-month period, as presented in Figure 21, showed that the pH levels of River Athi remained relatively constant during the months of August, September, November, December, January, and February. This stability may be attributed to hydrological and environmental factors such as reduced rainfall, steady river flow, and minimal anthropogenic pollution during these months. In contrast, a notable decrease in pH was observed in April and May, which is likely due to increased rainfall and surface runoff introducing acidic compounds into the river system.

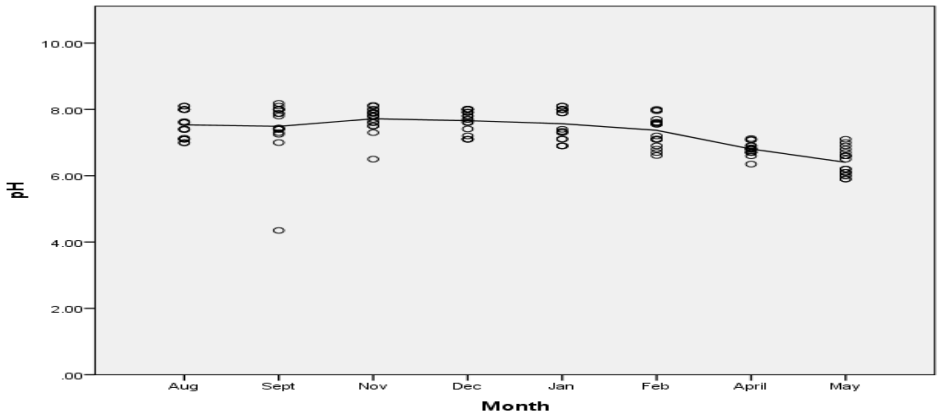

Figure 21: Temporal trend of ph in river athi for a period of eight months

Electrical Conductivity (EC)

The water EC trends for 8 months period presented in Figure 22, showed that the EC of the river Athi exhibited notable fluctuations, rising from August to September, dipping in November, and increasing moderately through December to February. These shifts reflect changes in the concentration of dissolved ions, likely driven by variations in water flow, evaporation rates, and anthropogenic inputs. A pronounced decline in EC was observed in April and May, coinciding with intense rainfall and surface runoff. The resulting dilution effect and downstream flooding likely contributed to the reduced conductivity, underscoring the impact of seasonal hydrological events on river chemistry.

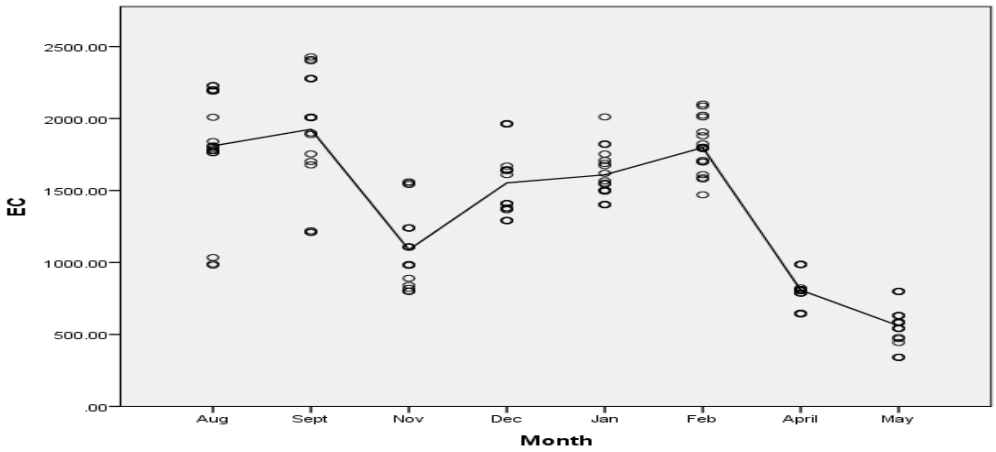

Figure 22: Temporal trend of ec in river athi for a period of eight months

Total Dissolved Solid (TDS)

The trends in water TDS for a period of eight months depicted in Figure 23, showed that TDS levels followed a pattern closely aligned with Electrical Conductivity (EC), rising from August to September, dropping sharply in November, and increasing moderately through December and January, with a peak in February. A significant decline was observed in April and May, likely driven by heavy rainfall and dilution effects from surface runoff and flooding. These fluctuations reflect seasonal changes in the concentration of dissolved solids, influenced by hydrological conditions and environmental inputs. The parallel trends between TDS and EC underscore their shared sensitivity to water flow dynamics and pollutant loading.

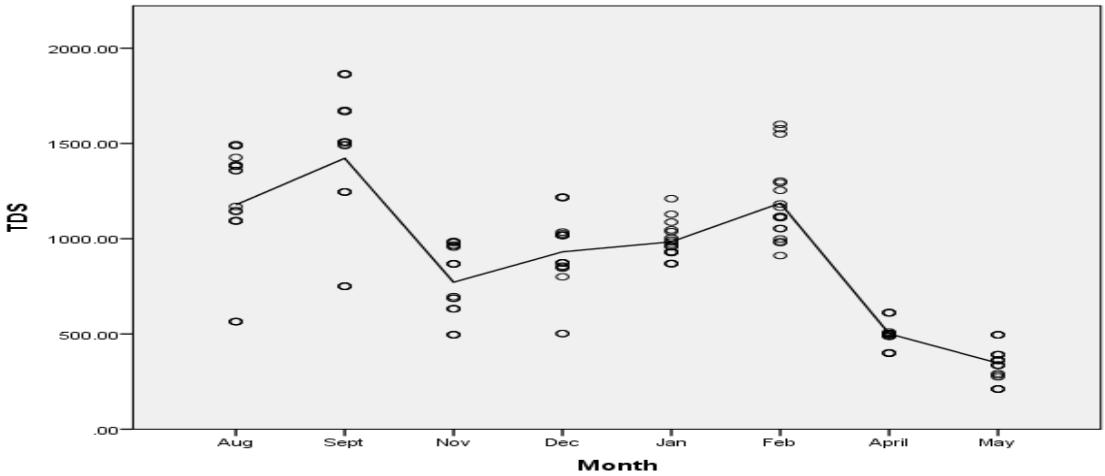

Figure 23: Temporal trend of tds in river athi for a period of eight months

Nitrate (NO_3)

Nitrate (NO_3) concentrations varied for a period of eight months as presented in Figure 24. Highlights dynamic fluctuations, beginning with a slight decrease from August, peaking in September, and declining in November. A sharp rise was observed in December and January, culminating in a February peak, followed by a notable decline in April and May. These variations reflect the complex interplay of seasonal rainfall, surface runoff, and agricultural inputs, particularly fertilizer use and leaching. The observed trends underscore the influence of land-use practices and hydrological cycles on nutrient loading in the river system.

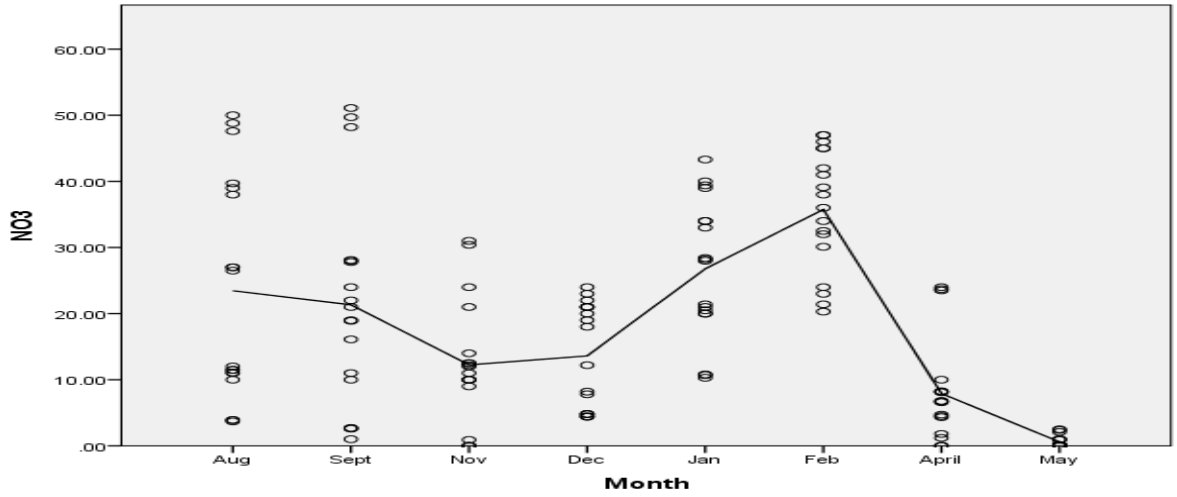

Figure 24: Temporal trend of nitrate in river athi for a period of eight months

Potassium (K)

Water Potassium (K) trends for 8-month period as depicted in Figure 25, showed that Potassium levels remained stable in August and September, followed by a significant decline in November and December. A moderate increase occurred in January, peaking in February, before dropping again in April and reaching the lowest concentration in May. These fluctuations reflect the influence of seasonal rainfall, surface runoff, and agricultural practices, including fertilizer application and soil leaching. The observed pattern highlights the sensitivity of potassium concentrations to hydrological cycles and land-use dynamics within the river basin.

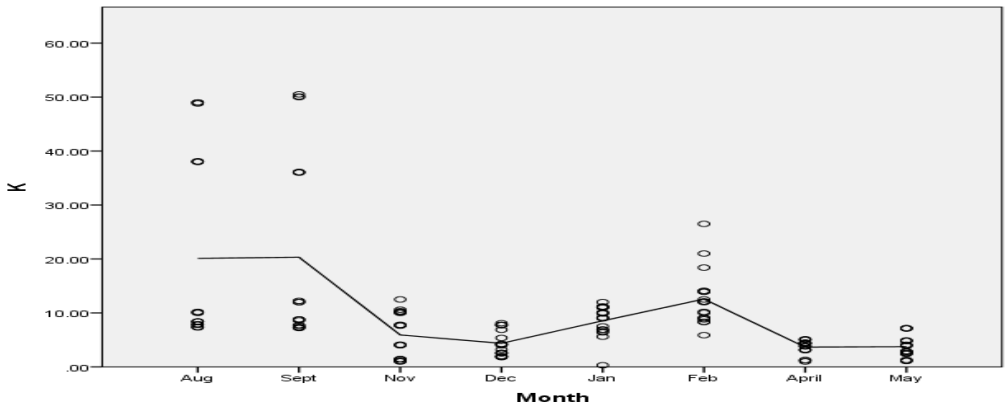

Figure 25: Temporal trend of k in river athi for a period of eight months

Phosphate (PO_4)

The data of water PO_4 dynamics for a period of eight months in Figure 26, indicated that Phosphate levels remained stable in August and September, indicating relatively steady environmental conditions. A decline was observed in November, followed by a gradual increase through December, January, and February. Concentrations dropped again in April, reaching the lowest levels in May. These fluctuations reflect the combined influence of seasonal rainfall, biological uptake, surface runoff, and agricultural activities such as fertilizer use. The observed pattern underscores the role of both natural cycles and human interventions in shaping nutrient dynamics within the river system

.

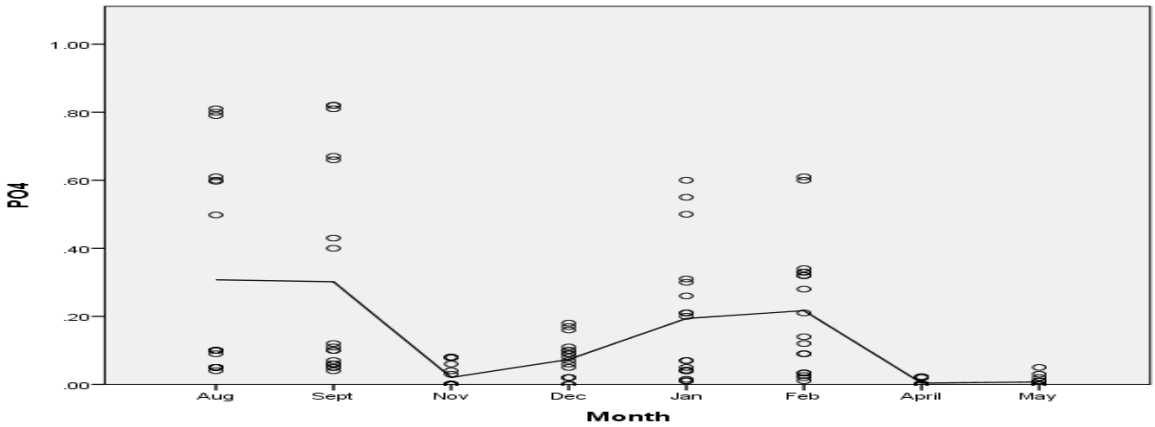

Figure 26: Temporal trend of po_4 in river athi for a period of eight months

Biochemical Oxygen Demand (BOD^5)

Trends in water BOD for 8 months as depicted in Figure 27, indicated that BOD levels fluctuated throughout the monitoring period, with a marked decline from August to September and a further decrease in November. Moderate increases were observed in December and January, peaking in February, followed by a sharp drop in April and the lowest levels recorded in May. These variations suggest the influence of both natural factors, such as temperature, rainfall, and flow rate, and anthropogenic activities including agricultural runoff and organic waste discharge. The observed BOD trends reflect changes in microbial activity and organic matter concentration, highlighting the dynamic interplay between environmental conditions and pollution sources.

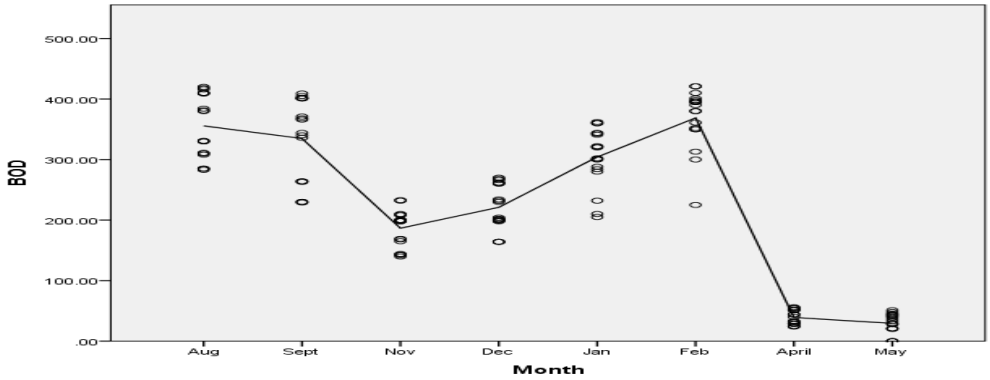

Figure 27: Temporal trend of bod in river athi for a period of eight months

Chemical Oxygen Demand (COD)

Water COD variation over an eight-month period as illustrated in Figure 28, showed a fluctuation pattern similar to BOD. COD levels dropped sharply from August to September, with a further notable decline in November. A moderate rise followed in December and January, peaking in February. In April, COD levels fell significantly and reached their lowest point in May. This decline is likely attributed to heavy rainfall and increased river flow during the wet season, which diluted organic pollutants and reduced COD concentrations.

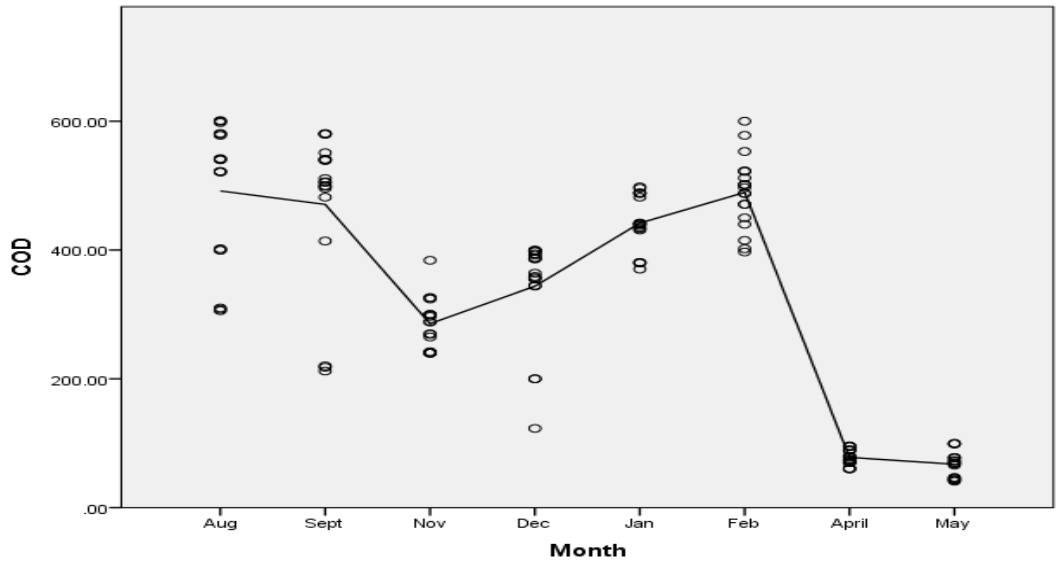

Figure 28: Temporal trend of cod in river athi for a period of eight months

Cadmium (Cd)

The eight-month trend of Cadmium (Cd) concentration in River Athi, as shown in Figure 29, reveals a sharp decline from August through November. Levels rose markedly in December and remained relatively stable during January and February. A significant drop occurred in April, reaching the lowest point in May. This pattern suggests that seasonal variations, likely driven by anthropogenic inputs, changing river flow, and rainfall, play a key role in influencing Cd levels in the river.

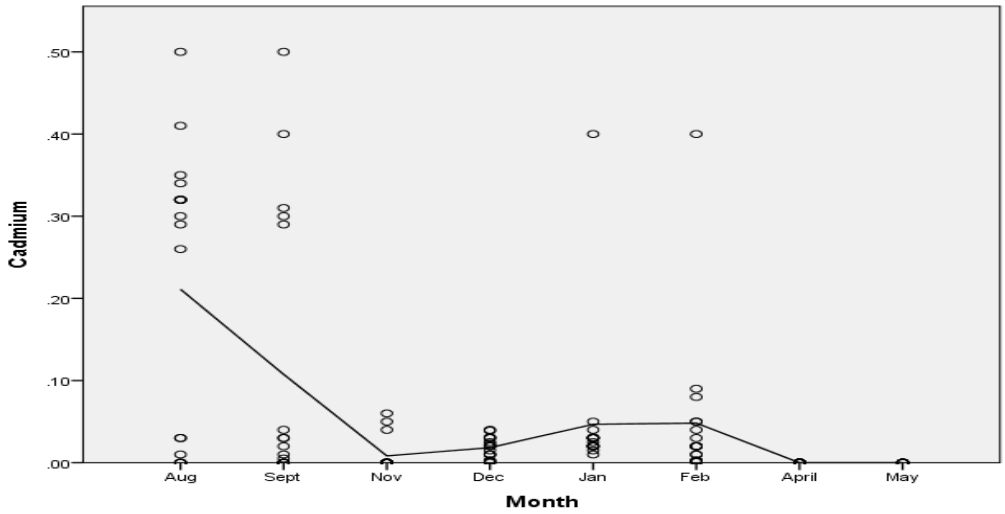

Figure 29: Temporal trend of cadmium in river athi for a period of eight months

Chromium (Cr)

Chromium (Cr) variation in River Athi over an eight-month period, as illustrated in Figure 30, shows a sharp decline from August through November. Concentrations remained steady in December and January, followed by significant decreases in February and April, bottoming out in May. These fluctuations reflect seasonal and temporal influences on water quality, driven by rainfall patterns, anthropogenic activities, and broader environmental dynamics.

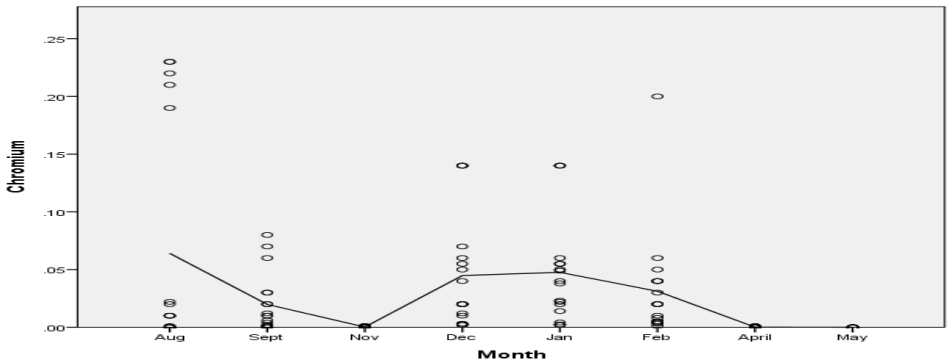

Figure 30: Temporal trend of chromium in river athi for a period of eight months

4.2.4 Seasonal Comparative Analysis of Physicochemical and Heavy Metals Water Quality Parameters in Athi River Basin

The results depicted in Table 4.13 are comparative analysis of mean levels of physicochemical and heavy metals water quality parameters for dry and rainy seasons was done using independent T test. The results showed that water pH differed significantly ($p < 0.00$) between dry and rainy seasons. It varied between 7.03 rainy season and 7.60 dry season below the World Health Organization (WHO) drinking water standard. These seasonal dynamics including dilution, runoff, and evaporation, as well as natural hydrological processes and land use impacts, are all responsible for this pH difference between the rainy and dry seasons. The EC mean levels were significantly different ($p < 0.00$) and varied between 1785.84 ds/m dry season and 1002.63ds/m rainy season, respectively. The mean levels were above WHO standard drinking water limit. The interaction of hydrological processes, land use influences, and dilution effects, indicated a notable seasonal change in EC values between the rainy and dry seasons. TDS mean levels

were significantly different ($p < 0.00$) and varied between 1192.56mg/l dry season and 622.01mg/l rainy season, which was above WHO recommended drinking water limit. The significant seasonal dynamic in the interaction of hydrology, evaporation, and human inputs reflecting variations in TDS levels. NO_3 showed a significant difference ($p < 0.00$) between Nitrate mean levels in dry and rainy seasons. The figures varied between 26.82mg/l dry season and 8.59mg/l rainy season which was below WHO recommended drinking water limit. The combined effects of human, hydrological, and climatic factors are shown in this notable seasonal variation in nitrate levels. The mean levels of potassium (K) were significantly difference ($p < 0.00$) between dry and rainy seasons. The values ranged between 15.38mg/l dry season and 4.42mg/l rainy season, above the WHO standard limit for drinking water. A mixed of anthropogenic, hydrological, and environmental factors are responsible for this notable discrepancy. Phosphate varied between 0.03mg/l dry season and 0.26mg/l rainy seasons which was above WHO permissible drinking water levels (Table 4.13). The figures were significantly different between the two seasons. In the Athi river basin, the combined effects of runoff, erosion, wastewater input, biological processes, and hydrological conditions are reflected in the seasonal variation in phosphate levels. BOD varied significantly between dry and rainy seasons ($p < 0.00$)). The figures ranged from 118.99mg/l dry season to 340mg/l rainy season which was above drinking water permissible limit. The impact of external organic inputs during the rainy season and their decrease during the dry season are reflected in seasonal variations in BOD levels. A significant difference ($p < 0.00$) in COD levels was found in dry and rainy seasons. It was observed to range from 193.71mg/l dry season to 473.47mg/l rainy season which was above WHO drinking water permissible limit. Seasonal changes in pollution inflows are reflected in the notable difference in COD levels between the rainy and dry season

Cadmium mean levels varied significantly between seasons ($p < 0.00$). The figures varied between 0.1034mg/l dry season and 0.0064mg/l rainy seasons which was above WHO drinking water standard limit. The substantial variation in cadmium levels between the rainy and dry seasons is mostly caused by hydrological variables like diluting capacity and river flow. Chromium means levels varied significantly between seasons ($p < 0.00$). The figure ranged between 0.113mg/l dry season and 0.406mg/l rainy seasons which was above

WHO standard for drinking water (Table 15). The primary cause of the notable variation in chromium concentrations between the rainy and dry seasons is variations in river flow and hydrological dynamics.

Table 15: Statistical comparison of temporal mean of water quality parameters

Parameters	Dry Season Mean	Rainy Season Mean	P-value	WHO,2011/2022
pH	7.60(0.53)	7.03(0.59)	0.00	6.5-8.5
EC	1785.84(328.99)	1002.63(418.07)	0.00	400dS/m
TDS	1192.56(304.23)	622.01(251.55)	0.00	500mg/l
NO_3	26.82(14.29)	8.59(8.80)	0.00	50mg/l
K	15.38(13.28)	4.42(2.73)	0.00	0.3mg/l
PO_4	0.26(0.26)	0.03(0.04)	0.00	0.2mg/l
BOD	340.80(59.37)	118.99(90.07)	0.00	20mg/l
COD	473.47(89.42)	193.71(131.85)	0.00	10mg/l
Cd	0.10(0.15)	0.06(0.01)	0.00	0.003mg/l
Cr	0.41(0.61)	0.11(0.03)	0.00	0.05mg/l

Researchers' Fieldwork (2025)

4.3 Spatial Variation of Physicochemical and Heavy Metals Water Quality Parameters in Athi River Basin

4.3.1 Potential Hydrogen (pH)

The pH trend across six sampling stations in River Athi during dry and rainy seasons, as shown in Figure 31, remained stable at Athi River Town and Stony Athi, with a slight decrease observed at NYS. River Kyawango maintained consistent pH levels, while minor variations at River Thwake control station and Kibwezi suggest limited localized pollution. The overall stability at the control station reinforces the minimal impact of anthropogenic activities in that area.

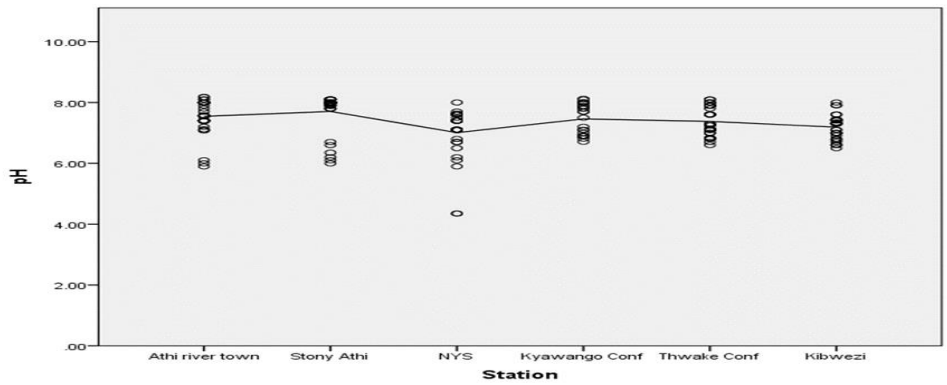

Figure 31: Spatial trend of ph in athi river sampling stations

4.3.2 Electrical conductivity (EC)

Electrical Conductivity (EC) variation across six sampling stations in River Athi during dry and rainy seasons, as depicted in Figure 32, remained stable at Athi River Town and Stony Athi, while a decrease was observed at the NYS station, likely due to dilution effects. EC levels were consistent at Kibwezi, River Kyawango confluence, and River Thwake confluence (control station), suggesting uniform ionic concentration and minimal localized disturbance at these sites.

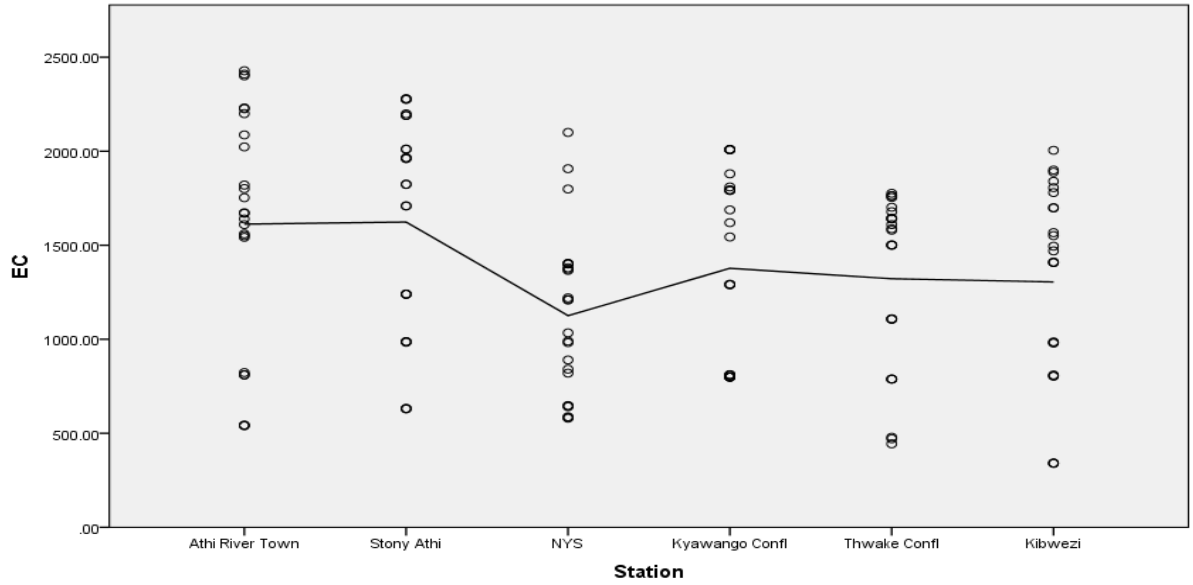

Figure 32: Spatial trend of ec in athi river six sampled stations

4.3.3 Total Dissolved Solid (TDS)

Total Dissolved Solids (TDS) trends across six sampling stations in River Athi during dry and rainy seasons, as shown in Figure 33, reveal a slight increase from Athi River Town, peaking at Stony Athi, followed by a decline at the NYS station. TDS levels remained consistent downstream at River Kyawango confluence, River Thwake confluence, and Kibwezi. The downstream stability suggests possible self-purification or mixing processes, while the peak at Stony Athi may be attributed to localized sources of dissolved solids.

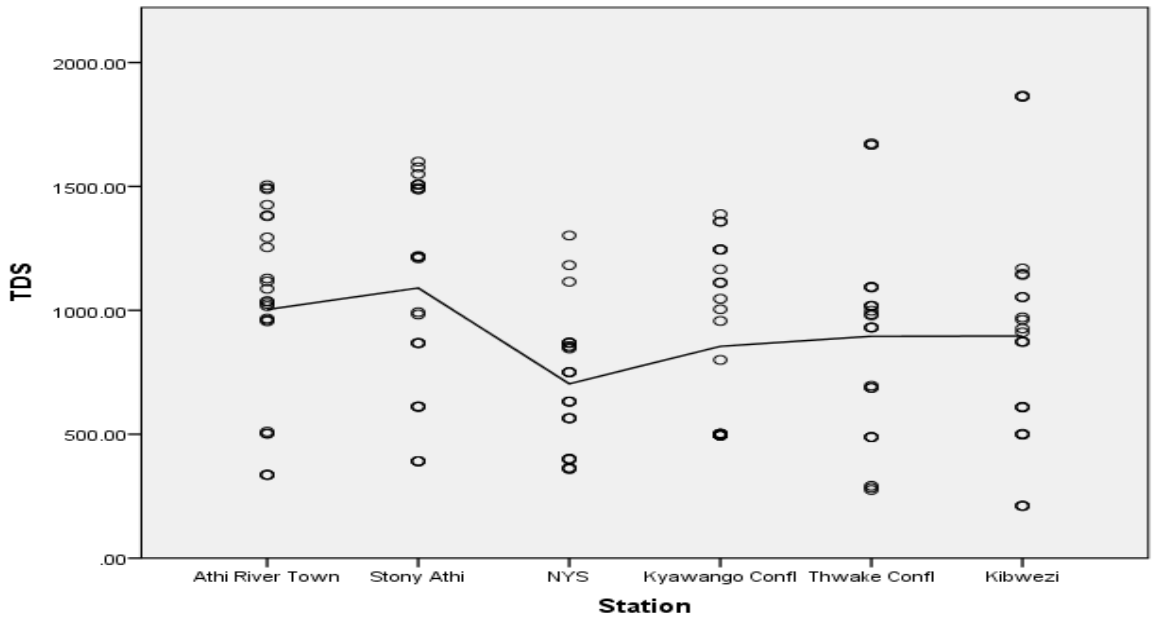

Figure 33: Spatial trend of tds in athi river six sampled stations

4.3.4 Nitrate (NO3)

Nitrate concentration trends across six sampling stations during dry and rainy seasons, as illustrated in Figure 34, show a decline at Athi River Town, Stony Athi, and NYS stations, with a peak observed at the Kyawango confluence. Concentrations dropped significantly at the River Thwake confluence (control station) and Kibwezi Bridge, suggesting possible dilution effects or uptake by aquatic vegetation in downstream areas.

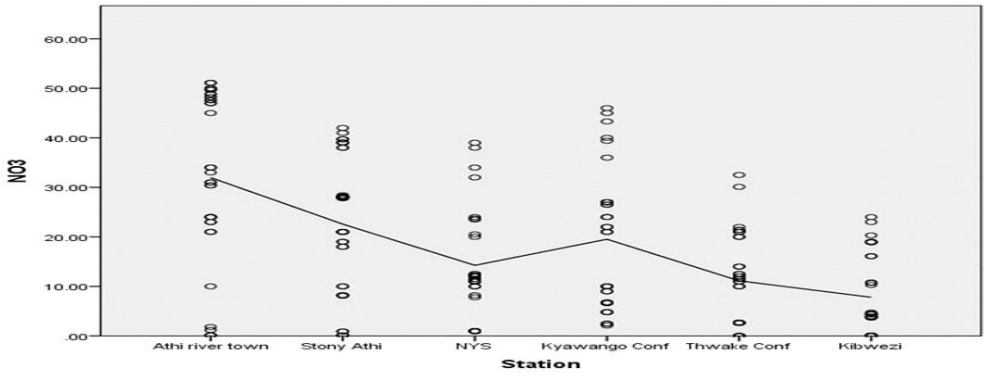

Figure 34: Spatial trend of no_3 in athi river six sampled stations

4.3.5 Potassium (K)

Potassium concentration trends in River Athi across six sampled stations during dry and rainy seasons, as shown in Figure 35, reveal a decline at Athi River Town and Stony Athi, with stable levels at NYS and River Kyawango confluence. A slight increase was observed at River Thwake confluence (control station), followed by a dip at Kibwezi. The rise at Thwake suggests localized inputs, while the decrease at Kibwezi may result from sedimentation or reduced downstream runoff.

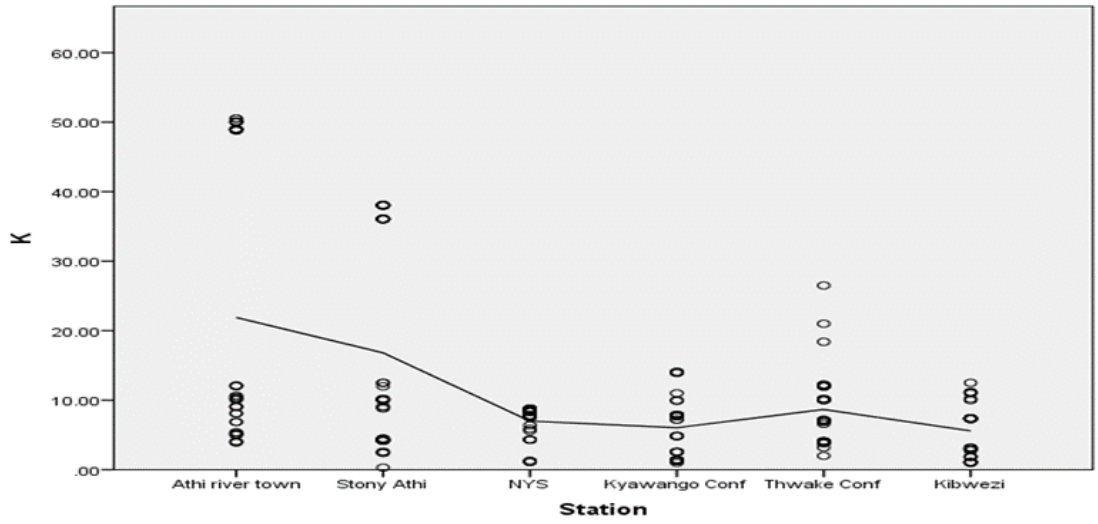

Figure 35: Spatial trend of potassium (k) in athi river six sampled stations

4.3.6 Phosphate (PO4)

Phosphate (PO_4) variation across six sampling stations in River Athi during dry and rainy seasons, as depicted in Figure 36, shows a decline from Athi River Town through Stony Athi to NYS, peaking at the Kyawango confluence. Levels then dropped at the River Thwake confluence (control site) and slightly decreased further at Kibwezi. The peak at Kyawango likely reflects agricultural runoff and domestic wastewater inputs, while the downstream decline may result from dilution, sedimentation, or biological uptake by aquatic plants and algae.

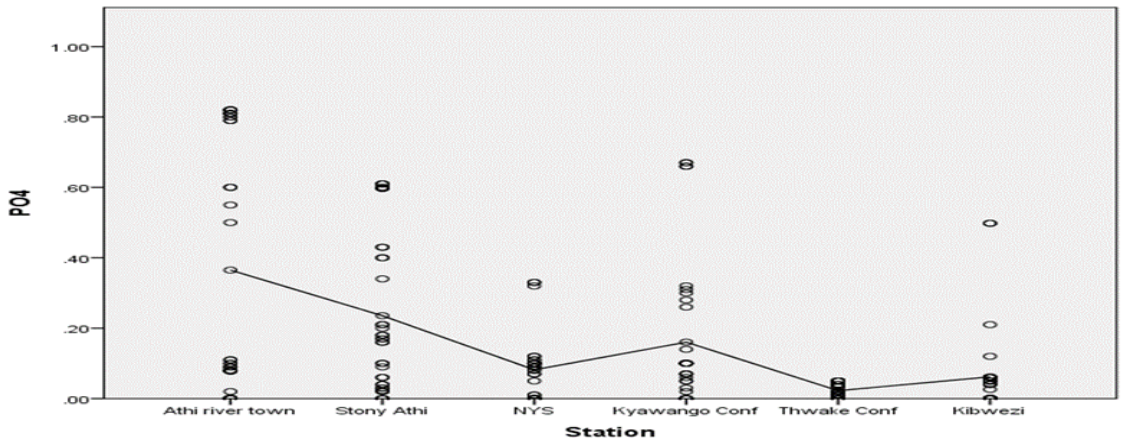

Figure 36: Spatial trend of po_4 in athi river six sampled stations

4.3.7 Biological Oxygen Demand (BOD)

Biochemical Oxygen Demand (BOD) trends in River Athi during dry and rainy seasons across six sampled stations, as shown in Figure 37, exhibit notable fluctuations. BOD levels declined from Athi River Town to Stony Athi, rose at the NYS station, slightly dropped at River Kyawango confluence, and stabilized at River Thwake confluence and Kibwezi Bridge. The elevated BOD at NYS likely reflects increased organic inputs from industrial or urban sources, while the downstream stabilization suggests reduced organic loads or enhanced self-purification processes within the river.

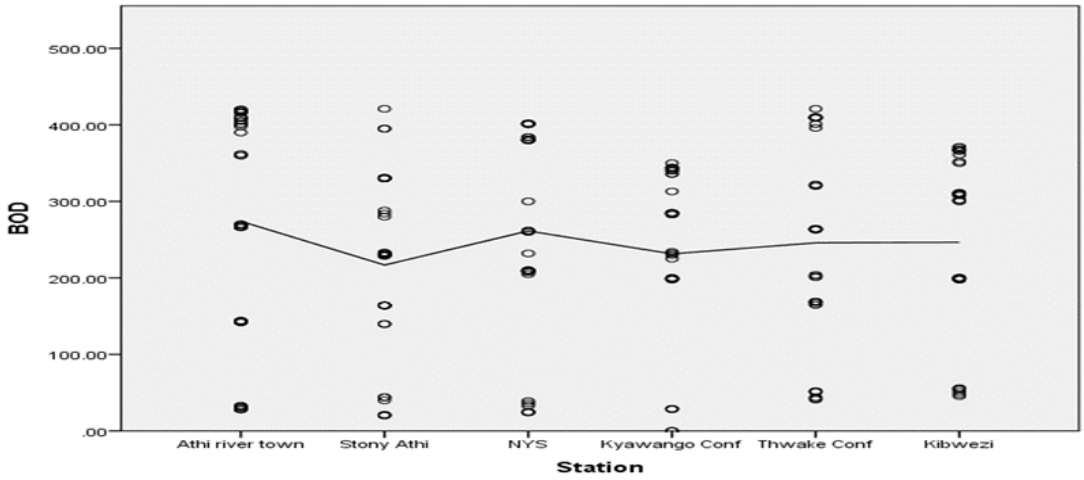

Figure 37: Spatial trend of bod in athi river six sample stations

4.3.8 Chemical Oxygen Demand (COD)

Chemical Oxygen Demand (COD) variation across six sampled stations in River Athi during dry and rainy seasons, as depicted in Figure 38, remained constant at Athi River Town, Stony Athi, NYS, and River Kyawango confluence. A decrease was observed at the River Thwake confluence (control station), while levels peaked at Kibwezi Bridge. The consistent COD values upstream suggest a steady release of organic pollutants or minimal external input, whereas the reduction at the control station may reflect improved water quality due to rainfall-induced dilution.

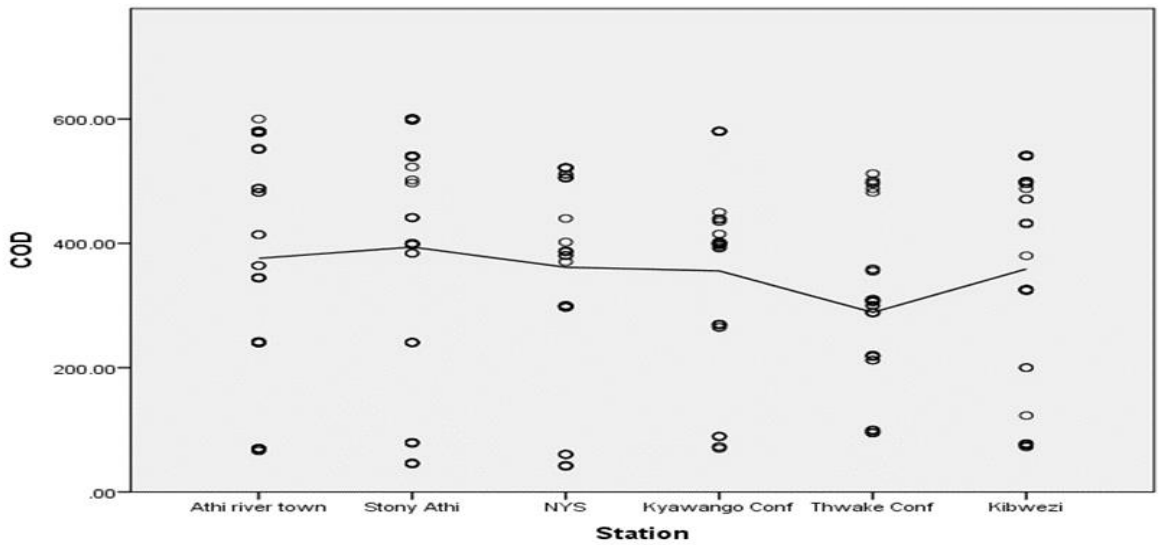

Figure 38: Spatial trend of cod in athi river six sampled stations

4.3.9 Cadmium (Cd)

Cadmium (Cd) variation across six sampled stations in River Athi during dry and rainy seasons, as illustrated in Figure 39, shows an upward trend from Athi River Town and Stony Athi, peaking at the NYS station. Levels then declined at River Kyawango confluence, River Thwake confluence (control station), and Kibwezi. The spike at NYS suggests cadmium input from urban or industrial sources, while the downstream reduction may be attributed to dilution, sediment adsorption, or reduced industrial influence.

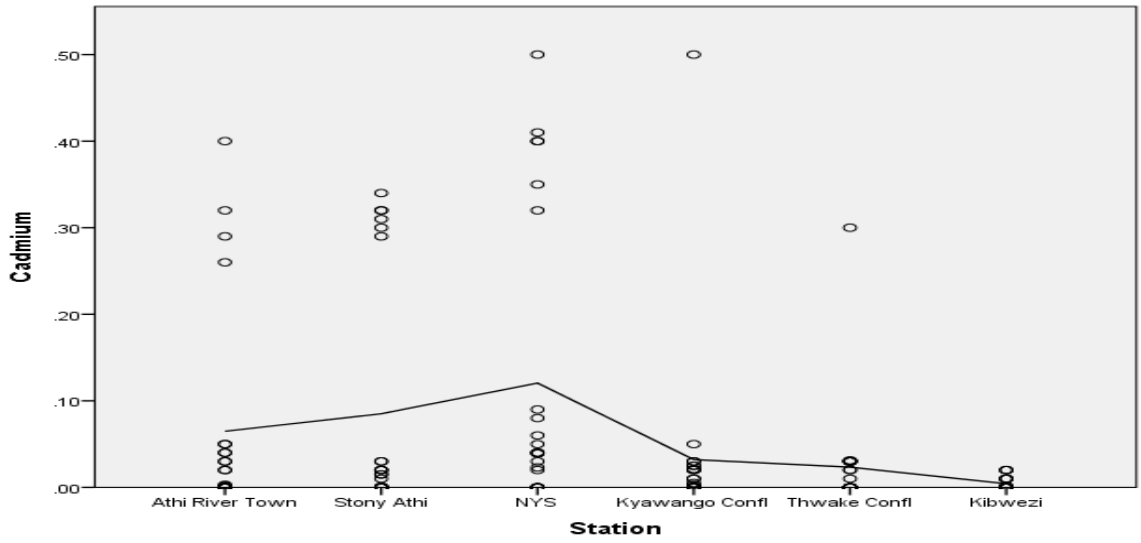

Figure 39: Spatial trend of cadmium (cd) in athi river six sampled stations

4.3.10 Chromium (Cr)

Chromium (Cr) variation across six sampled stations in River Athi during dry and rainy seasons, as shown in Figure 40, reveals a gradual decline from Athi River Town through Stony Athi to NYS, followed by a continued decrease at River Kyawango confluence, River Thwake confluence (control station), and Kibwezi Bridge. This downward trend likely results from natural processes such as sedimentation, which trap chromium in sediments during high flow periods. The consistent decline at the control and downstream stations suggests that natural filtration, rainfall dilution, and sediment binding collectively reduce Cr concentrations in the water column.

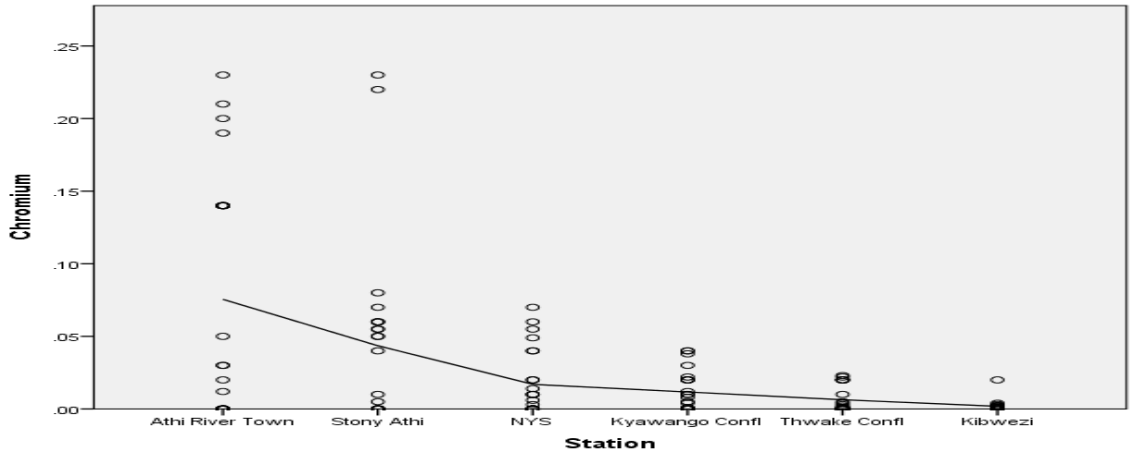

Figure 40: Spatial trend of chromium (cr) in athi river six sampled stations

4.3.11 Spatial Comparison of the Mean Levels of Physicochemical and Heavy Metals Water Quality Parameters in Athi River Basin Using One Way Analysis of Variance (ANOVA)

The results presented in Table 16 depicted a comparison among the sampling stations using a one-way analysis of variance (ANOVA) on mean levels of physicochemical and heavy metals water quality parameters in Athi River Basin. Mean values of water pH in Athi River varied significantly across the sampling stations. The highest level was observed at stony Athi (7.55) sampling station while the lowest was recorded at NYS (6.98) sampling stations. All the mean levels were below the WHO recommended drinking water standard. River Thwake control station showed a dependable baseline due to its consistency in a number of characteristics, which indicates that it is less impacted by localized pollution or sudden changes upstream.

Water EC mean levels varied significantly across the sampling stations. The highest level was detected at stony Athi sampling station (1623.3dS/m) while the lowest was recorded at Kibwezi sampling station (1304.9dS/m). The mean values across the sampling stations are above WHO recommended levels for drinking water. The increase at Stony Athi highlights the necessity for pollution control. However, the lowest EC values observed downstream at Kibwezi and the River Thwake confluence (control station) can be attributed to dilution and natural purification processes.

Mean levels of water TDS in Athi River varied significantly across the six sampling stations. Stony Athi sampling station recorded the highest level (1090.4mg/l) while the lowest levels were detected at NYS sampling station (703.6mg/l). All the mean levels were below WHO recommended drinking water standard. At the River Thwake confluence control station, total dissolved solids (TDS) levels illustrate the cumulative impact of upstream effluents, such as industrial discharges and urban runoff. The consistent ionic loads at this station result from lower flow and seasonal variations concentrating dissolved solids.

Mean water Nitrate (NO_3) levels in Athi River varied significantly in the 6 sampling stations. The highest levels were detected in Athi river town (29.25mg/l) sampling station while the lowest were recorded at Kibwezi (7.98mg/l) sampling station. The mean levels in all the sampling stations where below drinking water recommended levels. Elevated nitrate levels in Athi River Town signal significant anthropogenic pollution. Dilution from tributary mergers and seasonal river flow fluctuations reduce nitrate levels at the River Thwake confluence (control station).

Mean Potassium (K) levels varied significantly across the sampling stations. Athi river town (18.30mg/l) sampling station recorded the highest level while lowest level was detected at Kibwezi (5.70mg/l) sampling station. All the mean levels across the sampling stations were above WHO standard for drinking water levels. High pollution loads along the Athi River are the cause of these elevated levels. Following the confluence of proximity to settlement, industry and irrigation inputs, where flows contribute to the mineral load from storm runoff, potassium concentrations at the Thwake Confluence (control station) are somewhat higher.

The mean PO_4 levels varied significantly in all the six sampling stations. Highest level was recorded at kibwezi (0.52mg/l) sampling station while the lowest level was observed at Thwake confluence (0.02mg/l) sampling station. Mean levels across the sampling stations were above WHO drinking water recommended levels. As the river flows downstream, sedimentation processes and dilution effects at the River Thwake confluence (control

station) reduce the phosphate load, leading to a notable decrease. However, isolated fluctuations, decreased river velocity, and limited dilution capacity in the river's lower reaches are responsible for the higher levels at Kibwezi stations.

Mean levels of water BOD in Athi River could not vary significantly across the sampling stations. Athi river town (256.8mg/l) sampling station detected the highest level while Stony Athi (209.5mg/l) sampling station recorded the lowest level. All the mean levels across the sampling stations were above WHO drinking water recommended standards. Elevated BOD levels in Athi River Town are mainly due to increased organic matter and warmer temperatures. Downstream dilution and reduced inputs of organic pollutants result in constant and lower BOD values at the River Thwake Confluence (control station).

Mean level of COD in Athi River could not vary significantly across the six sampling stations. The highest level was recorded in Stony Athi (362.6mg/l) while the lowest level was observed in Thwake confluence (148.67mg/l). All the sample mean levels were above the WHO standard for drinking water. The elevated COD levels observed at Stony Athi sampling stationare due to anthropogenic activities. As the river flows downstream, processes such as oxidation, adsorption, and dilution reduce the quantities of oxidizable contaminants. Consequently, the River Thwake Confluence (control station) shows a significant decrease in COD levels compared to Stony Athi River sampling station.

The mean Cd levels varied significantly across the 6 sampling stations. All the mean levels were above drinking water recommended levels. The table showed the highest level in NYS (0.1196mg/l) while the lowest was recorded at Kibwezi station (0.0042mg/l). Elevated cadmium levels at the NYS station could be attributed to mineral weathering and industrial effluents. Bioaccumulation, sedimentation, and dilution processes all influence the intermediate cadmium values observed at the River Thwake Confluence (control station). However, mean levels of Athi river water Cr varied in all sampling station. Recording higheer level in Athi river town (0.755mg/l) while the lowest level was observed in Kibwezi station (0.0018mg/l) sampling stations. The mean levels in all sampling stations were above WHO drinking water recommended standard. The River Thwake Confluence

(control station) exhibits lower chromium concentrations than Athi River Town, indicating a decline in chromium levels as the river flows downstream. Conversely, the higher chromium concentrations in Athi River Town are attributed to urban effluents.

Table 16: Results of one way anova on physicochemical and heavy metals water quality parameters' mean levels across sampling stations in athi river basin

Parameters	Athi river town	Stony Athi	NYS	Kyawango Confluence	River Thwake Confluence	Kibwezi Bridge	P-value	WHO,2011/2022
pH	7.44(0.64)	7.55(0.74)	6.98(0.77)	7.42(0.50)	7.36(0.47)	7.163(0.45)	0.02	6.5-8.5
EC	1612.3(621.51)	1623.3(575.25)	1125.5(432.42)	1377.5(498.69)	1321.8(460.40)	1304.9(524.56)	0.01	400dS/m
TDS	1003.3(388.13)	1090.4(421.99)	703.6(264.64)	854.8(354.08)	895.3(403.13)	896.2(765.25)	0.02	500mg/l
NO_3	29.25(18.61)	21.75(14.38)	15.75(11.47)	19.48(15.48)	12.01(10.32)	7.98(7.97)	0.00	50mg/l
K	18.30(18.61)	14.07(13.93)	6.51(2.49)	6.21(4.35)	8.63(6.08)	5.70(3.85)	0.00	0.3mg/l
PO_4	0.32(0.34)	0.22(0.21)	0.09(0.10)	0.15(0.19)	0.02(0.02)	0.52(0.10)	0.00	0.2mg/l
BOD^5	256.8(159.39)	209.5(128.17)	235.3(140.05)	215.3(128.98)	233(137.25)	229.3(120.63)	0.88	20mg/l
COD	357.1(202.40)	362.6(200.12)	331.1(179.92)	332.8(169.59)	148.67(172.01)	322.7(182.97)	0.82	10mg/l
Cadmium	0.65(0.12)	0.85(0.14)	0.12(0.16)	0.03(0.10)	0.23(0.60)	0.0042(0.07)	0.00	0.003mg/l
Chromium	0.755(0.08)	0.0435(0.06)	0.170(0.02)	0.117(0.01)	0.0062(0.08)	0.0018(0.00)	0.00	0.05mg/l

Researchers' Fieldwork (2025)

4.4 Influence of Physicochemical Parameters on BOD, COD, Cd and Cr

Multiple linear regression analysis was conducted to test the influence of pH, EC, TDS, NO_3, K, and PO_4 on BOD and COD (oxidation parameters) and Cadmium and Chromium (heavy metals).

4.4.1 Influence of Physicochemical Parameters on BOD

The results of multiple linear regression analysis indicated that six predictors pH, EC, TDS, NO_3, K, and PO_4 explained 62% ($R^2 = 0.62$) of the variation in BOD levels in the water [$F(6, 137) = 36.7$, p 0.00]. The overall model was statistically significant.

4.4.1.1 Potential Hydrogen (pH)

Data presented in Table 17 denoted that for each one-unit increased in pH, BOD increased by 4.91 units, holding other variables constant. However, the coefficient was not statistically significant ($p > 0.05$). At 95% confidence interval, the true coefficient for pH fell between -26.53 and 36.34.

4.4.1.2 Electrical Conductivity (EC)

The results in Table 17 indicated that for each one-unit increase in EC, BOD increased by .16 units, holding other variables constant. The coefficient was statistically significance ($p < 0.05$), suggesting that EC highly predict BOD. At 95% confidence interval, the true coefficient for pH fell between 0.07 and 0.25.

4.4.1.3 Total Dissolved Solids (TDS)

Results on linear regression analysis denoted that for each one-unit increase in TDS, BOD increased by .02 units, holding other variables constant (Table 17). However, the coefficient was not statistically significant ($p > 0.05$). At 95% confidence interval, the true coefficient for TDS fell between -0.08 and 0.12.

4.4.1.4 NO_3 (Nitrate)

Results on linear regression analysis indicated that for each one-unit increase in NO_3, BOD increased by .98 units, holding other variables constant (Table 17). However, the coefficient was not statistically significant ($p > 0.05$). At 95% confidence interval, the true coefficient for NO_3 fell between -0.64 and 2.60.

4.4.1.5 Potassium (K)

Linear regression analyzed results indicated that for each one-unit increase in K, BOD is expected to decrease by .46 units, holding other variables constant (Table 17). The coefficient was not statistically significant ($p > 0.05$). At 95% confidence interval, the true coefficient for K fell between -2.45, and 1.52.

4.4.1.6 Phosphate (PO_4)

Data presented in Table 17 indicated that for each one-unit increase in PO_4, BOD is expected to increase by 6.09 units, holding other variables constant. However, the coefficient was not statistically significant ($p > 0.05$). At 95% confidence interval, the true coefficient for PO_4 fell between -106.24 and 118.43.

Table 17: Regression results of pH, EC, TDS, NO_3, K, and PO_4 against COD

Coefficient of Estimations			
Parameters	Coefficients	P-value	95% Confidence Interval
Constant	-61.3 (101.3)	0.55	-
pH	4.91(15.75)	0.75	-25.16, 34.97
EC	0.16(0.05)	0.01	0.07, 0.25
TDS	0.02(0.50)	0.65	-0.08, 0.12
NO_3	0.98(0.83)	0.24	-0.64, 2.60
K	-0.46(1.08)	0.65	-2.44, 1.51
Po_4	6.09(57.04)	0.92	-105.69, 117.87

Note the Values in Brackets are Standard Errors.

4.4.2 Influence of Physicochemical Parameters on COD

The result of multiple linear regression analysis indicated that 6 predictors pH, EC, TDS, NO_3, K, and PO_4 explained 70% (R^2 =0. 70) of the variation in chemical oxygen demand (COD) levels in water [$F(6,137) = 53.68$, $p = 0.00$]. The overall model was statistically significant as depicted in Table 18.

4.4.2.1 Potential Hydrogen (pH)

The results presented in Table 18 indicated that for each one unit increase in pH, COD increased by 43.75 units. However, the coefficient was not statistically significant ($p >0.05$). At 95% confidence interval, the true coefficient is likely between -11.974 and 99.474.

4.4.2.2 Electrical Conductivity (EC)

Data presented in Table 18 indicated that for each one unit increase in EC, COD increased by .28 units. The coefficient was statistically significant ($p < 0.05$). At 95% confidence interval, the true coefficient for EC fell between -0.789 and 1.349.

4.4.2.3 Total Dissolved Solid (TDS)

Results on linear regression analysis indicated that for each one unit in TDS, COD decreased .84 units, holding other variables constant (Table 18). However, the coefficient was not statistically significant ($p > 0.05$). At 95% confidence interval, the true coefficient fell between -2.00 and 0.32.

4.4.2.4 Nitrate (NO_3)

Results on Table 18 presaged that for each one unit increase in NO_3, COD increased by .69 units, holding other variable constant. The coefficient was not statistically significant ($p > 0.05$). At 95% confidence, interval, the true coefficient for Nitrate fell between -1.21, and 2.59.

4.4.2 5 Potassium (K)

Data presented in Table 18 indicated that for each one unit increase in K, COD decreased by -0.69 units, holding other variables constant. However, the coefficient was not statistically significant ($p > 0.05$). At 95% confidence interval, the true coefficient was between -1.21 and 2.59.

4.4.2.6 Phosphate (PO_4)

Results on linear regression analysis presaged that for each unit increase in PO_4, COD increased by 43.28 units, holding other variables constant (Table 18). The coefficient was not statistically significant ($p > 0.05$). At 95% confidence interval, the true coefficient for Phosphate fell between -87.07, and 173.53.

Table 18: Regression results of pH, EC, TDS, NO3, K, and PO4 against COD

Coefficient Estimations			
Parameters	Coefficients (ß)	P-value	95% Confidence Interval
Constant	-310.58(119.24)	0.10	-
pH	43.75(18.53)	0.20	-11.97, 99.47
EC	0.28(0.53)	0.00	-0.79, 1.35
TDS	-0.84(0.58)	0.15	-2.00, 0.32
NO_3	0.69(0.97)	0.48	-1.21, 2.59
K	-0.69(1.18)	0.56	-3.08, 1.70
PO_4	43.23(67.12)	0.52	-87.07, 173.53

Note the Values in Brackets are Standard Errors.

4.4.3 Influence of Physicochemical Parameters on Cadmium

The results on linear regression analysis indicated that 6 predictors namely pH, EC, TDS, NO_3, K, and PO_4 explained 36% ($R^2 = 0.36$) of the variation in Cadmium (Cd) level [$F(8, 135) = 9.64$, $p = 0.00$]. The overall model was statistically significant (Table 19).

4.4.3.1 Potential Hydrogen (pH)

Data presented on Table 19 indicated that a unit increased in pH decreased concentration of Cd in water by .35 units. The coefficient was not statistically significant ($p > 0.5$). At 95% confidence interval, the true coefficient for pH fell between .711 and 0.011.

4.4.3.2 Electrical Conductivity (EC)

The results on linear regression results analysis indicated that a unit increased in EC decreased the concentration of Cd in water by 5.04 (Table 19). The coefficient was not statistically significant ($p > 0.05$). At 95% confidence interval, the true coefficient for EC was between -5.04, and -5.04.

4.4.3.3 Total Dissolved Solid (TDS)

The results on Table 19 presaged that for each one unit increase in TDS, decreased the values of Cd in water by 3.87. However, the coefficient was not statistically significant (p

> 0.00). At 95% confidence interval, the true coefficient for TDS was between -3.87, and -3.87.

4.4.3.4 Nitrate (NO_3)

Data presented in Table 19 indicated that for each one unit increased in Nitrate levels, decreased the concentration of Cd in water by .25. The coefficient was not statistically significant ($p > 0.05$). At 95% confidence interval, the true coefficient for NO_3 fell between 0.03, 0.01.

4.4.3.5 Potassium (K)

The results of linear regression analysis indicated that for each one unit increased in K decreased the concentration of Cd in water by .07 (Table 19). The coefficient was statistically significant ($p < 0.5$). At 95% confidence interval, the true coefficient for K declined between 0.05, and 0.09.

4.4.3.6 Phosphate (PO_4)

The result on linear regression analysis presaged that for each one unit increased in Phosphate, decreased the levels of Cd by 0.32 in water (Table 19). The coefficient was not statistically significant ($p > 0.05$). At 95% confidence interval, the true coefficient for PO_4 was between 1.56, and 0.92.

4.4.3.7 Biological Oxygen Demand (BOD_5)

Data presented on Table 19 indicated that for each one unit increased in BOD, Cadmium (Cd) decreased by 5.69 units, on average, holding other variables constant. The coefficient was not statistically significant ($p > 0.05$). At 95% confidence interval, the true coefficient for BOD fell between -5.69, and -5.69.

4.4.3.8 Chemical Oxygen Demand (COD)

The results on linear regression analysis indicated that for each unit increased in COD, Cd decreased in water by .00 (Table 19). The coefficient was statistically significant ($p < 0.00$). At 95% confidence interval, the true coefficient for COD fell between 0.00 and 0.00.

Table 19: Regression results of pH, EC, TDS, NO_3, K, PO_4, BOD, and COD against Cd

Coefficient Estimation			
Parameters	Coefficients (B)	P-value	95% Confidence Interval
Constant	0.24 (0.12)	0.48	-
pH	-0.35(0.18)	0.60	-0.71,0.01
EC	-5.04(0.00)	0.36	-5.04, -5.04
TDS	-3.87(0.00)	0.95	-3.87, -3.87
NO_3	-0.01(0.01)	0.25	-0.03, 0.01
K	.0.07(0.01)	0.00	0.05, 0.09
PO_4	-0.32(0.64)	0.62	-1.56, 0.92
BOD	-5.69(0.00)	0.70	-5.69, -5.69
COD	0.00(0.00)	0.04	0.00,0.00

Note the Values in Brackets are Standard Errors.

4.4.4 Influence of Physicochemical Parameters on Chromium

The results on multiple regression analysis indicated that 6 predictors pH, EC, TDS, NO_3, K, and PO_4 explained 36% ($R^2 = 0.36$) of the variation in Chromium (Cr) level in water [$F(8,135) = 9.49$, $p = 0.00$]. The overall model was statistically significant (Table 4.18).

4.4.4.1 Potential Hydrogen (pH)

Data presented in Table 20 indicated that for each one unit increased in pH, decreased the dependent variable Cr by .04. The coefficient was not statistically significant ($p > 0.05$). At 95% confidence interval, the true coefficient for pH fell between -0.198 and 0.118.

4.4.4.2 Electrical Conductivity (EC)

The results on linear regression analysis indicated that for each one unit increase in EC decreased the concentration of the dependent variable Cr by 6.85 (Table 20). However, the coefficient was not statistically significant ($p > 0.05$). At 95% confidence interval, the true coefficient for EC was between -6.85 and 6.85.

4.4.4.3 Total Dissolved Oxygen (TDS)

Data presented in Table 20 presaged that for each one unit increased in TDS decreased the concentration of the dependent variable Cr by 6.62. The coefficient was not statistically significant ($p > 0.05$). At 95% confidence interval, the true coefficient for TDS was between 6.62 and 6.62.

4.4.4.4 Nitrate (NO_3)

Results of multiple linear regression analysis indicated that for each one unit increased in nitrate levels, increased the concentration of Cr by .01 (Table 20). The coefficient was statistically significant ($p < 0.05$). At 95% confidence interval, the true coefficient declined between 0.01 and 0.01.

4.4.4.5 Potassium (K)

The analyzed results on multiple linear regression indicated that for each one unit increase in potassium, Cr increased by .02 (Table 20). The coefficient was statistically significant ($p < 0.05$). At 95% confidence interval, the true coefficient fell between 0.02 and 0.02.

4.4.4.6 Phosphate (PO_4)

The results on Table 20 indicated that for each one unit in unit increased in phosphate levels, decreased the concentration of Cr by .2. However, the coefficient was not statistically significant ($p > 0.05$). At 95% confidence interval, the true coefficient for PO_4 was between -.076 and 0.36.

4.4.4.7 Biological Oxygen Demand (BOD)

Data presented in Table 20 showed that for each one unit increased in BOD, increased the concentration of Cr by .00. The coefficient was statistically significant ($p < 0.05$). At 95% confidence intervals, the true coefficient for BOD fell between 0.00, 0.00.

4.4.4.8 Chemical Oxygen Demand (COD)

The results on multiple linear regression analysis presaged that for each one unit increased in COD, decreased the concentration of Cr in water by 8.68 (Table 20). The coefficient

was not statistically significant ($p > 0.00$). At 95% confidence intervals, the true coefficient for COD fell between 8.68 and 8.68.

Table 20: Regression results of pH, EC, TDS, NO3, K, PO4, BOD, and COD against Cr

Coefficient Estimations			
Parameters	Coefficients	P-value	95% Confidence Interval
Constant	0.21(0.51)	0.685	-
pH	-0.04(0.08)	0.62	-0.20, 0.12
EC	-6.85(0.00)	0.78	-6.85, -6.85
TDS	6.62(0.00)	0.79	6.62, 6.62
NO_3	0.01(0.00)	0.04	0.01, 0.01
K	0.02(0.00)	0.00	0.02, 0.02
PO_4	-0.2(0.28)	0.57	-0.76, 0.36
BOD	0.00(0.00)	0.05	0.00, 0.00
COD	8.68(0.00)	0.12	8.68, 8.68

Note the Values in Brackets are Standard Errors.

4.5 Relationship between the Physical Athi River Water Quality

A Pearson product-moment correlation coefficient was conducted to assess the relationships between water physicochemical properties and heavy metals.

4.5.1 EC and TDS

There was a significant positive correlation between the two variables, r - .93, $p < .05$, with high levels of EC in water associated with higher concentrations of TDS (Table 21).

4.5.2 EC and BOD^5

Data presented in Table 21 indicated a strong positive correlation between Electrical Conductivity (EC) and Biological Oxygen Demand (BOD) ($r = .78$, $p < .01$). An increase of EC in water will be accompany by rise of BOD^5.

4.5.3 TDS and BOD^5

Data presented in Table 21 indicates a significant correlation between TDS and BOD^5 ($r = .73$, $p < .01$). An increase of TDS in water will be accompany by BOD^5.

4.5.4 Cadmium and Potassium

Data presented in Table 21 indicates a significance correlation between Cd and K ($r = .52$, $p < .01$). An increase of Cd in water will be accompany by potassium.

4.5.5 Chromium and Potassium

There was a significance correlation between Chromium and potassium (K) ($r = .54$, $p < .01$) (Table 21). An increase of Cr will be accompanied by potassium in water.

4.5.6 Cadmium and Chromium

There was a significant correlation between Cadmium and Chromium ($r = .35$, $p < .01$) (Table 21). An increase of Cd in water will be accompany by chromium.

4.5.7 pH and other Parameters

Data presented in Table 21 indicates a moderate and strong positive correlation with EC ($r = .67$, $p < .01$), TDS ($r = .61$, $p < .01$), NO_3 ($r = .61$, $p < .01$), and PO_4 ($r = .43$, $p < .01$). However, a strong positive correlation of pH with COD ($r = .65$, $p < 0.01$) was indicated.

4.5.8 BOD and COD

The results on correlation analysis indicated a correlation between Biological Oxygen Demand (BOD) and Chemical Oxygen Demand (COD) (Table 21). The correlation indicated that BOD and COD had a very high correlation ($r = .91$, $p < 0.01$).

4.5.9 Nitrate (NO_3) and Three Parameters

Data presented in Table 21 suggest a high correlation with EC ($r = .75$, $p < 0.01$), TDS ($r = .65$, $p < 0.01$), and PO_4 ($r = .71$, $p < 0.01$). Moderate positive correlation with Chromium ($r = .51$, $p < 0.01$).

4.5.10 Phosphate (PO_4) and NO_3

The results on correlation analysis indicated a high correlation with K ($r = .74$, $p < 0.01$) and NO_3 ($r = .71$, $p < 0.01$) (Table 21).

Table 21: Pearson correlation matrix of water quality

	pH	EC	TDS	NO_3	K	PO_4	BOD^5	COD	Cd	Cr
pH	1									
EC	0.67**	1								
TDS	0.61**	0.93**	1							
NO_3	0.61**	0.75**	0.65**	1						
K	0.38**	0.62**	0.55**	0.63**	1					
PO_4	0.43**	0.67**	0.57**	0.71**	0.74**	1				
BOD^5	0.55**	0.78**	0.73**	0.63**	0.48**	0.54**	1			
COD	0.65**	0.82**	0.73**	0.67**	0.51**	0.59**	0.91**	1		
Cd	0.10	0.26**	0.23**	0.24**	0.52**	0.35**	0.32**	0.36**	1	
Cr	0.29**	0.47**	0.35**	0.51**	0.54**	0.45**	0.28**	0.36**	0.35**	1

** Correlation is significant at the 0.01 level (2-tailed) (Researchers's Fieldwork, 2025).

CHAPTER FIVE

5.0 DISCUSSION

5.1 Introduction

This chapter provides a comprehensive discussion of the findings, and significance of the literature. It addresses how the findings contribute to the current understanding of the research Topic. It also examines the limitations of the study and suggests areas requires for future researches.

5.1.1 Influence of Land Use/Land Cover Change on Water Quality in River Athi Basin from 2015 -2023.

5.1.1.1 Land Cover Area (Ha) and Gross Percentage Change from 2015 to 2023

1. Bare lands

The bare-land category demonstrates substantial reduction from 10.17% in 2015 to 3.11% in 2023, with overall decrease of 7.1%. This scenario suggests that some bare-lands have been converted to other land uses. Potentially due to urbanization, reforestation, and the growth of industry or agriculture. These patterns conform to broader land management plans aimed at increasing land productivity and reducing soil erosion. A similar finding in a study conducted by Mbayaki (2015) on land use changes in Mumias District, Kenya, demonstrated a significant decrease in bare-lands. Becaues of increase in population, infrastructure development, and changes in agricultural practices. Studies also emphasized the importance of sustainable land management techniques, such as conservation agriculture and integrated soil-crop system management, to maximize land use and environmental degradation (Ismail *et al*., 2016). This approach is essential for preventing land degradation, restoring soil health, and promoting sustainable agricultural productivity (Gaikwad *et al*., 2023).

2. Built-up

The slight reduction in the built-up category from 1.12% in 2015 to 1.08% in 2020, increased to 1.41% in 2023, indicating land use expansion. The overall increase of 0.29% highlights a stable trend of infrastructure development and urbanization. This trend is

consistent with global research on urban sprawl driven by economic growth and population expansion (Chen *et al*., 2014). Similar to a study concluded by Kithiia (2021) that the modest increase in built-up areas may result from ongoing infrastructure development in response to economic and population growth.

3. Farmlands

Farmlands category expanded by 3.19% between 2015 and 2020, is an indication of increase in agricultural activities. In 2020, farmlands had a net increase of 0.52% due to temporary agricultural expansion and land abandonment or conversion to other land uses, such as grasslands or reforestation (JICA, 2012). This finding is consistent with the report by FAO (2020), that agriculture influences land use changes in a river basin. Highlighting how agricultural land expanded by 3.2% from 2015 to 2020, due to increase in agricultural activities, then declined by 2.5%, leading to a net increase. This pattern is similar to findings by Tilman et al. (2002), which identified a dynamic balance between agricultural expansion and conversion to other land uses, such as natural grasslands, due to conservation efforts.

4. Forest lands

The forestlands category had a constant increase from 6.83% in 2015 to 11.37% in 2023, representing an overall gain of 4.54% for 8 years. This growth suggests successful reforestation and conservation programs in the Country and individual aesthetic or commercial land reforestations as well as natural forest regrowth in the basin. Similar to a successful reforestationa and conservation programs in Kenya forest service, which projected an increase in forest from 6.9% in 2015 to 10% in 2022 (Juma & Atieno, 2021). These positive trends are crucial for mitigating climate change impacts, enhancing biodiversity, and supporting ecosystem services (Jwaideh *et al*., 2022).

5. Grasslands

Figures 4.1 and 4.2 illustrate significant growth in the grasslands category between 2015 and 2023, showing a 2.77% increase, with geometric expansion from 49.66% to 52.43% within the study area. This increase indicates a reduction due to agricultural pressure within

the river basin. This might be as a result of changes in land use regulations, low yields, and lack of capital investment. Similar findings indicates that grasslands are increasing as a result of restoration efforts and sustainable management practices, suggests a reduction in agricultural pressure (IUCN, 2024).

According to Pretty (2003), the growth of grasslands indicates biodiversity protection, as grasslands are crucial for preserving ecological balance and providing habitats for various species. Jafarabadi et al. (2018) also noted that trends in grasslands help preserve soil health and minimize erosion. This increase could also be attributed to successful conservation efforts and sustainable land management practices aimed at reducing agricultural expansion and promoting natural habitats.

6. Open-waters

The open-waters category experienced a significant decline, dropping by 1.06% from 1.24% in 2015 to 0.18% in 2023. This decline, especially in surface water, can be attributed to urbanization and the effects of climate change. This is evidently supported by the findings made by NASA (2024) that average amount of freshwater stored on land such as rivers, lakes, and aquifers has decreased drastically between 2015 and 2023 compared to previous years. This phenomenon attributes to series of droughts, exacerbated by climate change and global warming causing surface water deficits and increase in groundwater reliance. The decline in open-water areas not only affects water availability but also has broader implications for ecosystem health and sustainability. Despite the base-flow system of the river basin, the downward trend in open-water bodies is concerning as it could impact groundwater recharge, water supply, aquatic habitats, food production, and the overall health of the river basin ecosystem. According to Kitheka (2019) and Rodell et al. (2024) the loss of open-waters in the basin may have detrimental impacts on local ecosystems, biodiversity, ground water recharge and supply.

5.1.2 Impacts of Spatial LULC Differences on Water Quality across Sampling Stations in Athi River Basin.

Water quality in the mid reaches of Athi River sampling stations are greatly impacted by spatial dynamics in land use/land cover (LULC). Pearson correlation analysis in Table 4.18, shows a high association between spatial differences and variations in water quality, especially at the sampling stations (Athi River Town, Stony Athi, NYS, River Kyawango, River Thwake, and Kibwezi). These variations demonstrate how LULC dynamics significantly affect water quality parameters like pH, EC, TDS, Cd, Cr, NO_3, PO_4, BOD, and COD, reflecting localized impacts and basin-wide trends.

5.1.2.1 Built-up and Urban Areas (Athi River Town, Stony Athi, and NYS)

Urbanization has led to a significant rise in built-up areas, which in turn has increased the concentrations of Cr, Cd, TDS, and EC (Figure 4.4 & Figure 4.5). These increases are attributed to storm water runoff carrying pollutants from commercial, industrial, and residential sources, impermeable surfaces, and industrial emissions from the upper mid-reaches of the study area. The sampling stations at Athi River Town, Stony Athi, and NYS were situated within these built-up or urban and semi-urban areas.

In contrast to more pronounced swings seen in rural areas, urban activities buffer pH variations. These findings are similar to Waturu et al. (2023) who found that an increase in industrial and urban expansions causes encroachments and destructions of wetlands and riparian ecosystems as well as degradations of water quality of the Athi River Basin. Urbanization increases nutrient and organic pollution, reflecting the correlations between built-up lands and parameters like NO_3 (0.75), PO_4 (0.67), and BOD (0.78) (Table 4.15). This is consistent with research by Huang et al. (2022) and Ling et al. (2017) which highlighted how urbanization increases the levels of organic matter, heavy metals, and pollutants in water bodies. Elevated levels of Cd and Cr in these populated areas also suggest that storm water runoff and industrial operations are contributing factors (Figure 4.5). Rainfall worsens the problem by flushing accumulated pollutants into the river, aggravating downstream contamination. During periods of high rainfall, the Mbagathi River, a tributary of the Athi River, plays a crucial role in carrying these pollutants. These

pollutants impacts downstream communities, through the National Youth Service (NYS) headquarters, Kyawango, Wamuyu, and Kibwezi axis, before discharging into the Indian Ocean (Plate 3.1; Plate 3.2; Plate 3.3). These findings align with international research on urban river pollution, highlighting the impact of untreated wastewater and the rapid damage caused by urbanization to river ecosystems (Omer, 2019).

5.1.2.2 Bare-Lands (Throughout the Mid Reaches)

The Bare-land areas, despite being elevated it influences reduction in sediment runoff, which help in maintaining reasonable stable TDS and EC levels. However, bare-lands positively correlate with TDS (0.61), indicating that they contribute to sediments during rainy or dry seasons (Table 4.15). Ndugga (2021) conducted similar study on a stream catchment in Uganda, with a negative correlation, which attributed to factors such as increased runoff, erosion, and lack of filtration, nutrient leaching, and temperature changes. It is clear that bare lands, due to their lack of vegetation contribute to higher runoff and erosion. Ling et al. (2017) found that exposed soil contributes to higher dissolved solids during erosive rainstorm events, which is consistent with these findings. It appears that areas with exposed soil contribute to increased dissolved solids in the river, as indicated by the association between bare-land and TDS (0.61).

5.1.2.3 Farmlands and Agricultural Areas (Athi River Town, Stony Athi, NYS, and River Kyawango Confluence)

The land use of the basin is dominated by agricultural activities, which contribute to high levels of phosphates (PO_4) and nitrates (NO_3) through nutrient loading and fertilizer runoff. Studies have conduted the impacts of agricultural activities on water quality across the Globe (Locke *et al*., 2024). Study concluded that intensive agricultural practice degrade stream water quality due to correlation with nutrients (NO_3 and PO_4) (Crooks *et al.,* 2021). The Athi River Town, Stony Athi, NYS, and River Kyawango Confluence sampling stations observed higher nutrient levels. Farmlands in the River Kyawnago area are evidence of nutrient contaminants. In Kyawango area, the river Athi water is widely used for domestic activities like washing, bathing, and drinking, and it also supports extensive irrigation practices. Large farmlands, such as French bean farms near Mwala, rely heavily

on the river's resources, highlighting the river's economic importance for local agriculture. Additionally, during the dry season, communities in nearby sub-counties like Kiaaoni, Kamuthakya, Wamuyu, and Katangi engages in fishing and sand harvesting at various points along the river, emphasizing the dependence of local livelihoods on the river's resources (Plate 3.4abc). Sand harvesting and frequent use of the river can disrupt aquatic habitats and degrade water quality. However, high levels of nitrate at Athi River town and Stony Athi sampling stations reflect the release of agricultural byproducts through direct discharges.

Peripheral et al. (2020) highlighted how elevated nutrient levels worsen eutrophication, decreasing oxygen availability and lowering water quality. Although a small decline in farming from 31% in 2020 to 30.5% in 2023 would reduce nutrient pollution, these gains might be undone by the shift to urban areas. This dynamic implies that sustainable land use strategies are necessary to strike a balance between protecting water quality and agricultural productivity. These studies have consistently shown that agricultural activities within the river basin, including irrigation, fertilizers and pesticide applications, and livestock farming, contribute significantly to river Athi water pollution.

5.1.2.4 Grasslands (River Thwake Confluence and Kibwezi Bridge)

Grassland as a natural filter, covers up to 52.43% of the basin in 2023 (Figure 4.2), reduces runoff velocities, traps sediments, and buffers pollutants. These areas have a crucial role in reducing both organic and inorganic pollution, as evidenced by their negative connection with BOD (-0.48), TDS (-0.61), EC (-0.67), and COD (-0.51). The efficacy of grasslands in enhancing water quality is supported by sampling stations close to grasslands, such as River Thwake (control station) and Kibwezi Bridge, which exhibit relatively lower pollution levels. The importance of grasslands in improving sediment control, decreasing erosion, and stabilizing soil is further highlighted by Ling et al. (2017). These grasslands are essential for preserving water quality since without them, the basin's TDS and other pollutant levels would probably be greater. According to Editorial Team (2022), grasslands cover roughly 30% of the planet's terrestrial landscape, contributing to a variety of essential ecosystem services. However, the riverbed at these sampling stations acts as a

filtration medium rather than a complete decontaminant, as residents consume the water, this process is insufficient to eliminate all toxins (Plate 3.6ab).

5.1.2.5 Forested Areas (River Kyawango Confluence, River Thwake, and Kibwezi Bridge)

Forests filter pollutants and control sediment and nutrient runoff, among other vital ecosystem services, despite their restricted size. Given the inverse correlations with BOD (-0.48), TDS (-0.61), EC (-0.67), and COD (-0.51), a minor increase in wooded and sedimented areas associated with improved water quality (Table 4.15). These results support research by Omer (2019) and Ling et al. (2017), which highlights the importance of forest conservation as a tactic or strategy for improving water quality. The findings by Forestry (2024), also supported the idea that forests act as natural filters, trapping sediments, nutrients, and pollutants from runoff before they reach the aquatic environment. The proximity to forested areas, which have lower nutrient and sediment loads, is advantageous for sampling stations farther away from urban and agricultural effects. Residents at these stations particularly those at Kibwezi Bridge axis, utilize shallow ditches dug into the sand dunes for filtered water collection, often aided by donkeys, which inadvertently deposit waste into the river and nearby collection points (Plate 3.6ab). Fischer (2024), discussed how forests naturally filter water through vegetation, soil, and organic matter, helps in removing pollutants and managing water flow. The dense vegetation and forest floor litter capture particles and chemicals, preventing them from entering water.

5.1.2.6 Decrease in Open-Water Areas

The decline in open-water areas from 2015 to 2023 will have a big impact on the levels of pollutants. Elevated TDS, BOD, and COD levels result from the loss of open-water areas, which restricts diluting capacity, particularly during the dry season (Figure 4.5). A decrease in open water across the sampling stations suggests low recharge and discharge of groundwater reservoir and aquifer decline during the dry season. This finding is similar to work done by Wang et al. (2020) who found that decrease in water level in the reservoir degrades water quality, leading to increasing pollutants such as Ammonia Nitrogen (NH_3-N), Permanganate index, and total Nitrogen. The trend is consistent with the findings by

Ling et al. (2017), who documented comparable impacts in the Batang Rajang River. Decreased open-water areas make aquatic ecosystems more susceptible to contamination, so specific actions are needed to protect these vital habitats.

5.1.3 Interview Survey and Land Use Change Impacts on Water Quality of the River Athi basin

Studies carried out at the six sampling stations in the mid reaches of the River Basin, provides important information about the perceived cause of the decline or degradation in water quality (Table 4.6 & 4.7). However, by highlighting environmental changes and their effects on water resources, respondents' views offered important insights into the connection between changes in land use and water quality as discussed by Rotich et al. (2022). According to the respondents, the survey shows that several factors are affecting the basin's water quality. Factors like climate, agriculture, and settlements were found to be the main drivers, with industry and commercial activity being mentioned with less effect. Turner et al. (2004) viewpoint is essential for comprehending regional difficulties and guiding management plans.

5.1.3.1 Climate

The data in Table 4.6 indicated that the Climatic factor contributes to contamination of water quality. Studies have demonstrated how rainfall patterns affect river water quality, particularly through runoff that introduces contaminants from different land uses into water bodies (Suma & Srinivasa, 2020; Mngube *et al*., 2020). Additionally, the intensity and frequency of rainfall significantly impact non-point sources of pollution, such as agricultural runoff (Huang *et al*., 2013). Large barelands are created by the extended dry season, particularly in the arid areas of the river basin, where topsoil containing tainted fertilizer from irrigation is leached and vegetation is dried up.

5.1.3.2 Agriculture

The data in Table 4.6 highlight agricultural activities particularly irrigation as a key contributor to water quality pollution of the basin. Similar to a research which showed how agricultural practices contribute to the degradation of water quality through sedimentation,

pesticides, and fertilizer runoff (Tilman *et al*., 2002). Eutrophication in rivers and lakes can result from the high quantities of nitrogen and phosphorus found in agriculture runoff (Smith *et al*., 1999).

5.1.3.3 Settlement

Residents or population generates solid, liguide, and gases wastes in the environment at any giving point in times (Table 4.7). These wastes consists of different pollutants discharged on impervious surfaces and direct to water bodies, are frequently caused by urban and dispersed settlements, which decrease natural infiltration and increase runoff (Paul & Meyer, 2001). Stormwater runoff can introduce sediments, metals, oils, and other contaminants into water bodies (Walsh *et al*., 2005). Apart from this, settlements exhibit lifestyles that generate both liquid and solid wastes containing chemical hazards or less toxic substances, which seep into rivers either directly or through runoff.

5.1.3.4 Industry

According to the results shown in Table 4.6, industrial operations contribute significantly to the pollution of the water quality of the Athi River, although their effects were less significant by the respondents. Low awareness of the possible ramifications of industrial operations and the discharge of harmful chemicals into the environment, or the limited consequences of industrial pollution, could be the cause of this perspective (Plate 3.1a & 3.2a). Nonetheless, heavy metals and other harmful pollutants, which are frequently persistent in the environment, might be strongly present in industrial discharges (Bai *et al*., 2022).

5.1.3.5 Commercial Activities

Commercial activities in the basin may have a modest impact because they are less intensive (Table 4.6). However, some respondents focused on the garbage that is released at motor parks or stages, while others pointed to gasoline stations, hydrocarbons, or vehicle exhausts. Commercial operations may generate trash and contribute to pollution, particularly in places with poor waste management infrastructure, according to Gaston et

al. (2020). However, capturing the complex effects of LULC changes on water quality is made easier by including local knowledge through interviews.

5.1.4 The Relationship between Interview Survey and Land Use/Land Cover Change

Climate with a frequency of six in Table 4.7 & Figure 4.5 showed how changes in grasslands and farmlands may connect to land cover categories and climatic parameters like rainfall and runoff. More rainfall may increase agricultural output, which results in an expansion of farmlands, while increasing runoff may cause soil erosion, reducing woodland and grassland areas to barelands. According to Omondi et al. (2019), rainfall variability is a significant factor in changes in land cover, especially in areas with a preponderance of natural vegetation and agriculture. Trends in Athi River Town can be better understood in light of recent research by Wambugu et al. (2023) that examined the effects of urbanization and land use changes on rainfall patterns and hydrology in Kenyan towns. Farmlands and grasslands have increased, according to LULC data, which is related to the effects of climate-driven causes.

A frequency of six for agriculture indicates that it has a direct impact on farmlands and can cause deforestation, or the loss of forestlands, as more lands have been repurposed for farming. Possible due to contamination and irrigation methods, which may potentially affect open waters (Table 4.7 & Fig 4.6). As more lands are turned over for cultivation to fulfill the rising need for food, agricultural activities lead to land cover change and deforestation (Gibbs *et al*., 2010). This increase in farmlands is consistent with the findings of the interviews, which indicate that agriculture plays a significant role in the alteration of land cover.

According to the data on settlement with five frequencies in Table 4.7 and Figure 4.6, the growth of settlements frequently results in an increase in built-up and other areas, which reduces bare lands and may have an effect on nearby grasslands and forests because of urban sprawl and scattered settlements. According to UN-Habitat (2016), land cover is significantly impacted by urban expansion brought on by settlement growth, which results in the conversion of natural landscapes into built-up regions. Settlement growth is a major

cause of land cover changes, especially in built-up regions, as indicated by the association between increased settlement and the observed changes in land cover types.

According to industry with a frequency of four, higher built-up areas are generally linked to industrial activity (Table 4.7 & Figure 4.6). Nonetheless, the low frequency indicates that the industry's influence on basin-wide LULC changes is somewhat small. Agricultural and urbanization have a greater influence on land cover than industrial and commercial developments, particularly in areas where these activities are concentrated (Lambin *et al*., 2001). The slight alterations seen in populated areas may be a reflection of the small impact of industrial operations. The findings shown in Table 4.7 and Figure 4.6 demonstrates that industry and commercial activities had four frequencies of change. These activities may expand built-up areas and other land uses, as well as have an impact on nearby land uses. The interview results, however, are consistent with the minor changes in built-up areas, suggesting that economic activities have less of an impact on LULC change in the River Athi Basin.

5.2 Spatial and Temporal Variations of Physicochemical Water Quality of River Athi Basin with Multivariate Analysis

5.2.1 Spatial Trends with PCA

The spatial principal component analysis (PCA) revealed strong pollution gradients in the mid-reaches of River River Basin, driven by nutrients, salinity, organic matter, and heavy metal loadings (Table 4.9). High PC1 scores in Athi River Town and Stony Athi ampling stations are associated with elevated electrical conductivity (EC) and biochemical oxygen demand (BOD). Highlighting cumulative pollution from domestic sewage, urban runoff, and industrial effluents (Figures 4.10 & 4.11). These findings correspond with previous multivariate studies by Kazi et al. (2009) and Reza & Singh (2010), where PC1 typically captured generalized pollution associated with salinity, nutrients, and organic load. Furthermore, cadmium-specific loadings observed in PC2 or PC3 suggest inputs from electroplating, battery waste, or combustion residues, often independent of chromium sources, reinforcing spatial segregation of industrial contaminants. Similar observations were reported by Chakraborty et al. (2021) in industrialized river systems.

Moderate PC2 scores in NYS and River Kyawango Confluence suggest dual influences of localized metal discharge and organic load or acidic inputs, possibly tied to sewage or biodegradable waste. This spatial interpretation is supported by Ogbonna et al. (2025), who reported significant land-use impacts on water quality in the Athi Basin, sourcing from urbanization and agriculture, affecting EC, TDS, BOD, Cd, and Cr. Similar to Ashun & Tagoe (2024) who identified artisanal disposal sites as heavy metal hotspots in the Upper Athi Basin. Waturu et al. (2023) also found that EC, DO, Zn, and Pb were spatially associated with urbanized sub-catchments, consistent with PC1 outputs. PC7 revealed high NO_3 and PO_4 loadings, suggesting agricultural runoff from fertilized lands with inadequate erosion control. This pattern has been found in studies across tropical basins, including studiy by Zhou et al. (2007). The influence of pit latrines, livestock rearing, and crop farming on nutrient pollution, in PC2 and PC7, is again substantiated by Ashun & Tagoe (2024). Negative loading of pH in PC5 suggests spatial pH variations linked to acidic or poorly buffered waters, potentially stemming from natural lithology or acidic industrial inputs. Similar interpretations were made by Zhang et al. (2014) in their study on anthropogenic and geological pH controls in river basins. Chromium was found to significantly influence spatial variability, likely due to proximity to tanneries and metal workshops, an observation consistent with Kithiia (2006), who linked Cr enrichment to leather-processing industries in Machakos County. The strong negative score of pH on PC5 (–0.73) reflects acidic inflows or poor buffering, while high NO_3 loadings on PC7 (0.72) identify spatial nutrient hotspots, notably around River Kyawango and Kibwezi Bridge, where irrigated agriculture is prevalent. These observations are corroborated by Ogbonna et al. (2025), who reported nitrate enrichment in similar downstream agricultural zones.

5.2.2 Spatial Cluster Analysis (CA)

The spatial cluster analysis categorized sampling stations along the mid-reach of River Athi Basin into three major pollution regimes (Table 4.10), consistent with regional and global river studies. Athi River Town and Stony Athi sampling stations exhibited high EC, TDS, NO_3, Cd, and Cr, indicating intense point-source pollution from domestic and industrial activities (Table 4.9). These results correspond with Liu et al. (2021), who observed similar polluted clusters in China’s Shuangji River. Comparable patterns were recorded in Iraq's

Euphrates River, where Salah et al. (2012) identified urban zones as the most degraded based on CA outputs. The dense clustering seen on the heat map further supports a strong anthropogenic impact in urban-industrial watersheds (Figure 4.10). This cluster includes River Kyawango Confluence and NYS, characterized by moderate EC, low NO_3, and attenuated heavy metals. Suggesting dilution zones influenced by both natural inputs upstream and urban pressures downstream (Figures 4.12 & 4.13).

Transitional clusters like these have been documented in China by Liu et al. (2021). Additionally, a report on buffer clusters in semi-urban aquifers in Mexico, where mixed pollution potential emerge from dual land-use influence (Marín Celestino *et al*., 2018). Stations like Kibwezi Bridge and River Thwake Confluence Control sites fell in this group, displaying low EC, TDS, and nutrient levels, yet anomalously high Cd. This may point to geogenic sources such as metal-rich soils, or weathering of the river bedrock. This pattern reflect to the findings by Salah et al. (2012), who detected low-nutrient clusters with unexpected heavy metal display in the Euphrates River. Likewise, Le Diem Kieu et al. (2024) found metal anomalies in clean Vietnamese aquifers linked to subsoil geochemistry or upstream gold panning. However, these spatial findings reinforce the role of cluster analysis in detecting pollution gradients and distinguishing urban-industrial sources, transitional buffers, and natural background conditions.

5.2.3 Temporal Principal Component Analysis (PCA)

The PCA results demonstrate that higher PC1 scores were observed during dry season months, particularly August, December, and January (Figure 4.14). This monthly score indicates the accumulation of salinity, heavy metals, and organic matter resulting from reduced river flow and limited dilution capacity. This interpretation corresponds with findings by Shrestha and Kazama (2007), who reported that principal components with strong loadings of EC, TDS, and trace metals typically reflect anthropogenic pollution intensified during low-flow periods.

In contrast, rainy season samples (April and May) tend to cluster tightly near the origin in PCA score space (Figure 4.14). This close grouping reflects chemical homogenization

caused by increased dilution and flushing, as also noted by Simeonov et al. (2003), who found that rainfall reduces both the concentration and variability of pollutants, leading to more compact clusters in PCA plots. Furthermore, the observed temporal grouping in the PCA score plot indicated seasonal hydrological shifts, suggesting that water quality dynamics are deeply shaped by time-linked environmental processes. This relationship is reinforced by Zhou et al. (2007), who highlighted that temporal PCA structures often preserve hydrological seasonality in surface waters. Importantly, the first two principal components, PC1 and PC2, together explain approximately 76% of the total variance in the dataset. These components likely captured pollution associated with salinity and heavy metals (EC, TDS, and Cd), and variability driven by nutrient and organic loading (NO_3, PO_4, and BOD) as shown in Figure 4.15. Subsequent components like PC3 and beyond account for subtle or localized variability, offering insight into minor pollution sources or sporadic events. According to Simeonov et al. (2003), an explained variance exceeding 60% by the first two PCs is typically sufficient to identify the dominant pollution sources in surface water studies. Similarly, Shrestha and Kazama (2007) suggested that capturing 70–85% of total variance in the first few components provides a robust foundation for interpreting spatial and temporal pollution gradients.

In this case, with approximately 80% of the variance explained by PC1 - PC3, the PCA results confirm that a small set of pollution drivers, notably salinity, nutrients, and heavy metals, govern most of the seasonal water quality variation in the River Athi Basin. These patterns are likely shaped by a combination of land use, hydrology, and underlying geological formations.

5.2.4 Temporal Cluster Analysis (CA)

A major finding of this temporal analysis is the emergence of a cohesive dry season cluster, comprised of August, September, November, December, January, and February (Figure 4.15). This branch represents months where water samples exhibited elevated concentrations of pollutants, particularly electrical conductivity (EC), total dissolved solids (TDS), cadmium (Cd), and nitrate (NO_3). The sub-grouping of August and September, merging at the lowest Euclidean distances, indicates a period of maximum contamination,

due to low river flow, evaporation, and accumulation of anthropogenic waste. This trend is consistent with observations by Shrestha and Kazama (2007), who noted that pollution intensity peaks under reduced dilution during dry months. Additionally, the clusters of November and December appear as transitional months, capturing the onset of minor rainfall yet retaining most dry-season chemical signatures (Figure 4.15). January and February extend the dry season's influence, showing residual pollutant load, though possibly moderated by slight shifts in hydrology. This extended dry-season pattern supports the assertion by Zhou et al. (2007) that intra-seasonal shifts can yield persistent but variable chemical stress on aquatic systems.

In contrast, the cluster comprised of April and May is distinctly separated, reflecting low pollutant concentrations and increased hydrological dilution. Their delayed linkage to the dry season cluster (at higher dissimilarity) emphasizing homogenious effect of sustained rainfall, which enhances runoff dispersion and reduces ionic accumulation. Similar to a finding by Simeonov et al. (2003), who observed the clustering of rainy months as chemically stable and less polluted in northern Greek surface waters.

5.2.5 Seasonal Principal Component Analysis (PCA)

The analysis revealed that the first two principal components (PC1 and PC2) together account for approximately 70% of the total variance (Figure 4.16). Indicating that most of the seasonal variations in water quality can be explained along two dominant axes or stages, one capturing salinity and heavy metal accumulation, and the other representing nutrient-organic enrichment in the mid-reaches of the river Basin. PC1 explaining 45% of the variance showed strong positive loadings for EC, TDS, NO_3, COD, and BOD, reflecting a broad pollution gradient, particularly during the dry season(Figure 4.16 & 4.17). These elevated levels suggest that reduced river flow during the dry months concentrates dissolved solids, nitrogen compounds, and decomposing organic matter. Similar seasonal pollution accumulation during low-flow periods was reported by Singh et al. (2005) in the Gomti River, India, where dry-season conditions led to increased EC and BOD values. The PC2 accounting for 25% of the variance, showed high loadings for Cd (0.56), Cr (0.44), and K (0.40) as depicted in Table 4.11. Which suggested that heavy metal mobilization

may occur during the rainy season, emanated from industrial effluents, sediment disturbance, or agricultural runoff. The presence of potassium (K) implies mixed sources, including farming inputs (Figure 4.16). These findings correspond with Marín Celestino et al. (2018), who observed increased heavy metal concentrations in Mexican aquifers during the rainy season, at the downstream of industrial zones. PC3 highlighted a co-loading of Cd, BOD, and COD, contrasting with Cr, which points to complex seasonal dynamics in which organic pollutants and trace metals co-occur during runoff periods (Figure 4.17). Meanwhile, PC4, with a strong positive loading for PO_4 (0.57) and a negative loading for Cr (–0.64), suggests phosphate surges (Table 4.11). These PO_4 surge possibly from fertilizer or domestic waste, occur seasonally, especially in mid-reach zones of the basin. The suppression of Cr in PC4 indicates dilution effects on heavy metals. These nutrient-metal patterns corresponds with findings by Le Diem Kieu et al. (2024), who documented seasonal phosphate enrichment linked to agriculture in Vietnam's Mekong Delta. While PC5 to PC10 accounted for smaller proportions of variance, they still captured subtle seasonal changes driven by biochemical and hydrological processes.

5.2.6 Seasonal Cluster Analysis (CA)

Cluster analysis revealed seasonally distinct groupings in the dataset, including Cluster 2 with mostly dry season samples, associated with elevated EC, TDS, and BOD (Table 4.12). Highlighting pollutant build-up due to reduced flow and evapoconcentration. In contrast, rainy season samples formed separate clusters with lower conductivity and nutrient loads, suggesting dilution effects from runoff. Similar findings were observed by Hammoumi et al. (2024) in Morocco's Nador Canal, where seasonal PCA patterns reflected salinity and nutrient variation between summer and winter months.

Cluster 1 captured seasonal pollution hotspots as shown in Table 4.12. In the dry season, this group exhibited extremely low pH (4.35), high EC (1220 µS/cm), and elevated Cd (0.50 mg/L), indicating acidic, metal-rich waters, likely influenced by dumping sites, stagnant tributaries, or poor buffering capacity. Comparable hotspot behavior was reported by Ituma et al. (2024) in upstream tributaries near refuse dumpsites, where elevated NO_3 and Fe^{2+} were detected during dry season. Cluster 3 marked intense pollution from agro-

industrial sources, especially during the dry season, with EC (2261 µS/cm), NO_3 (41.76 mg/L), K (~41 mg/L), and PO_4 (~0.63 mg/L) all significantly elevated. These hikes likely result from fertilizer runoff and industrial discharges under low-flow conditions. Comparable seasonal peaks were recorded by Le Diem Kieu et al. (2024) in the Mekong Delta, where pollutant inputs in dry months overwhelmed dilution mechanisms.

5.3 Seasonal and Temporal Variations of Physicochemical and Heavy Metals in Water Quality

5.3.1 Potential Hydrogen (pH)

The stability of pH values observed from August to February suggests that external factors, such as surface runoff and anthropogenic influences did not significantly disrupt the water's chemical balance during this period (Figure 4.19). Instead, the river's buffering capacity, the mineral composition of the riverbed, and underlying geological properties played a crucial role in maintaining a pH levels within a neutral range. These findings correspond with Samlafo et al. (2022), who indicated that rivers with strong buffering abilities tend to resist pH fluctuations caused by seasonal changes or pollutant influxes. The ability of the water to regulate pH is largely attributed to the presence of bicarbonates (HCO_3^-) and carbonates (CO_3^{2-}) ions, which are known to stabilize pH by neutralizing acidic and basic components (Tanjung *et al*., 2019; Stumm & Morgan, 2012). In the other hand, natural buffering capacity prevent sudden shifts in pH levels, minor fluctuations do occur due to bedrock weathering, which releases minerals that contribute to pH balance (Fondriest Environmental, 2024).

The study demonstrate a significantly difference in pH levels between the rainy (7.03) and dry (7.60) seasons (Table 4.13). This seasonal shift can be attributed to reduced dilution during the dry season, which allows alkalinity sources such as carbonate rocks and dissolved ions to dominate the river's chemistry as found by Kithiia (2007). Similar pattern were reported by Ngatia et al. (2023) in their study of the Ngong River, where neutral pH values were observed within the range of 6.77 - 7.67 during the dry season and 6.75 -7.72 in the rainy season. These results confirm that seasonal hydrological conditions play a vital role in determining pH stability. Furthermore, temperature fluctuations impact carbon

dioxide (CO_2) solubility, which in turn influences pH levels. Mook (2000) explained that colder water retains more CO_2, shifting the pH toward neutrality, while warmer conditions lead to CO_2 degassing, potentially increasing alkalinity. During low river flow conditions, pH stability is maintained because industrial, agricultural, and household wastewater contaminants accumulate without substantial dilution (Falkenmark & Rockström, 2004). This suggests that seasonal changes in water volume significantly dictate pH behavior, highlighting the importance of hydrological factors in water quality assessment.

In contrast, the river maintains a relatively stable pH throughout most months. April and May exhibited the greatest pH variations, coinciding with the highest recorded rainfall totals (393 mm in April, 172 mm in May) (Figure 4.18). The decline in pH during these months is likely due to the rapid influx of acidic runoff, which temporarily alters the water's chemical profile. The external contaminants including organic acids, dissolved metals, and anthropogenic pollutants, can be introduced through soil leaching and sedimentation during heavy rains (Owino & Owino, 2023; Jafarbadi *et al*., 2018; Owens *et al*., 2005). As fertilizers, industrial discharges, and organic waste enter the water, they release acidic compounds, further contributing to pH reduction.

Despite observed seasonal variations, Table 4.13 confirms that mean pH values remained within WHO drinking water guidelines, corresponding with studies that reported neutral pH ranges from 7.03 to 7.71 (Bhat *et al*., 2018). However, maintaining a neutral pH in aquatic systems is essential as it regulates microbial activity, affects chemical interactions, and determines the solubility and mobility of pollutants.

5.3.2 Electrical Conductivity (EC)

Electrical conductivity (EC) refers to water's ability to conduct electrical current, primarily influenced by the concentration of dissolved salts and ions (Kuang *et al*., 2020). This parameter serves as an essential indicator of water quality, reflecting salinity levels, ion mobility, and anthropogenic influences. EC variations significantly affect freshwater ecosystems, agricultural suitability, and drinking water safety.

The months of August, September, December, January, and February exhibited higher EC values as shown in Figure 4.20. These elevated values align with the mean of 1,785.84 dS/m, significantly higher than the rainy season mean of 1,002.63 dS/m. This seasonal fluctuation is largely driven by increased evaporation rates, lower river discharge, and concentrated dissolved salts and minerals. Several studies has confirm these results. For example, Eze et al. (2018) and Kilonzo et al. (2013) reported higher EC values during dry months, correlating them with reduced water volumes and higher salt concentrations. Ngabirano et al. (2016) and Kibet & Maina (2021) attributed increased EC levels to low precipitation, which leads to reduced dilution and intensified pollutant accumulation. Another findings was Bhat et al. (2018) who emphasized that urban and semi-urban wastewater discharge, combined with mineral weathering, contributes to high EC levels in river baseflow. While Munyaneza et al. (2012) and Ngabirano et al. (2016) highlighted the role of water-rock interactions in amplifying EC concentrations during dry periods.

These studies reinforce that EC elevation in dry seasons is closely linked to anthropogenic waste discharge, decreased water flow, and rising temperatures, which collectively increase salinity and dissolved ion levels, ultimately degrading water quality for residential and agricultural use. Comparative research indicates an increasing trend in EC levels over recent years. Kitheka (2019) reported 1,400 dS/m, while the current dataset in Table 4.13 shows 1,785 dS/m, representing a 27.5% increase over four years. This escalation may stem from intensified land use activities, including agriculture, industrial discharge, and urban expansion, all of which contribute to rising dissolved solid concentrations.

In contrast, EC levels decrease significantly during April and May, coinciding with high rainfall totals that dilute salt and ion concentrations (Figure 4.18). The lowest EC values, 1,002.63 dS/m, correspond with findings by Ngatia & Mutua (2022) and Ngabirano et al. (2016), who observed a dilution effect due to increased river flow. Owens et al. (2005) and Wetzel (2001), explained how ion exchange, sedimentation, and biological uptake regulate EC during high-flow seasons. Similarly, November's moderate EC decline suggests an early onset of seasonal rains, which partially dilute dissolved solids before peak precipitation arrives. Regardless of seasonal fluctuations, mean EC values exceed WHO

drinking water limits, posing potential risks for human health. Chronic exposure to elevated EC levels is associated with cardiovascular stress, hypertension, and kidney disorders (He & MacGregor, 2020; National Research Council, 2005; WHO, 2017). High salinity content affects aquatic life, altering osmotic balance and potentially leading to decreased biodiversity.

5.3.3 Total Dissolved Solids (TDS)

Total Dissolved Solids (TDS) measure the combined content of all inorganic and organic substances dissolved in water, including ions of calcium, magnesium, sodium, potassium, bicarbonates, chlorides, and sulfates(APHA, 2017). The Athi River exhibits distinct seasonal fluctuations in TDS concentration, with values increasing steadily from August to February, peaking during the driest months (Fig. 4.21; Fig. 4.18). This pattern can be explained by several hydrological and anthropogenic processes. Low rainfall during the dry season results in reduced river flow and increased evaporation, concentrating salts and minerals in stagnant or slow-moving water bodies (Dash *et al*., 2021; Huang *et al*., 2022). As water discharge declines, the river's ability to dilute incoming solutes, whether from natural weathering or human activities, decreases, leading to a progressive increase in solute concentration (Bakan *et al*., 2010; Jafarbadi *et al*., 2018). February's spike corresponds to a recession period, where evaporation, continued input from urban runoff, and salt enrichment from mineral weathering or fertilizer residue exacerbate TDS levels (Lemessa *et al*., 2023; Dulo, 2008). TDS mean values of 1,192.56 mg/L in the dry season, reflects this compounded effect of concentration, stagnation, and external loading (Table 4.13). Other factors contributing to the elevated TDS levels are both natural and human-derived sources, which include urban sewage and domestic effluents. These carry salts, detergents, and waste organics, particularly from unregulated discharge points (Tesfaye *et al*., 2021). Fertilizer residue and soil erosion contribute high levels of nitrate, phosphate, and potassium to the dissolved load. The leaching of minerals from volcanic or sedimentary rock formations increases solute content (Khan *et al*., 2016; Ptacek, 2016). Highly acidic or alkaline water can enhance solubility of salts, influencing ionic concentrations (Gadhia *et al*., 2012).

In contrast, the onset of rainfall from March to May and again in November brings a significant decline in TDS values, with a seasonal mean of 622.01 mg/L (Figure 4.21 & Table 4.13). Key processes at play include dilution by rainwater and runoff. Increased water volumes dilute mineral concentrations, especially in early showers (Nguyen *et al*., 2023). Rain enhances river dynamics, flushing out pollutants and disrupting stagnant areas where TDS tends to accumulate. Ion exchange between sediments and water, along with nutrient absorption by aquatic plants, contribute to TDS decline (Ngabirano *et al*., 2016; Wetzel, 2001).

However, despite the dilution, concentrations remain above WHO drinking water guideline, revealing that rainfall's influence, while helpful, cannot fully offset persistent upstream inputs and legacy pollution. Persistently high TDS levels, even during the wet season, raise serious concerns. Aesthetic and infrastructural impacts hike's TDS levels leading to unpleasant taste, scaling in pipes, and appliance wear (Ghosh & Chakraborty, 2018). Long-term intake, especially of water with elevated sodium, sulfate, or nitrate components, may affect renal function and cardiovascular health, particularly among vulnerable populations (Srinivas *et al*., 2019).

5.3.4 Nitrate (NO3)

Nitrate (NO_3^-) plays a fundamental role in the nitrogen cycle, serving as a key nutrient for aquatic ecosystems while also being a potential pollutant when present in excessive concentrations (WHO, 2022). Under oxidizing conditions, nitrate dominates as the main nitrogen form, while ammonium (NH_4^+) prevails in reducing environments (Jamiu *et al*., 2020). Its presence in water originates from natural and anthropogenic sources, including fertilizers, wastewater discharge, industrial runoff, and atmospheric deposition. Nitrate concentrations declined slightly in August, September, and October, as depicted in Figure 4.22, corresponding with reduced water flow and minimal surface runoff (Ngatia *et al*., 2023). The limited rainfall during this period restricts the transport of nitrates from fertilizer applications, organic matter, and industrial pollutants into the river. This pattern continued through November, marking the transition into the rainy season. Limited surface runoff, reducing nutrient transport into water bodies (Ngatia *et al*., 2023). Minimal

fertilizer leaching, as the absence of heavy rains prevents movement of nitrates from agricultural land into rivers (Kilonzo *et al*., 2013). Declined wastewater dilution, leading to reduced nitrogen mobilization (Owens *et al*., 2005).

However, a sharp increase in nitrate levels was observed in February, due to accumulation of pollutants and reduced flow in ongoing dry conditions. This increase correspond with the statistically mean values of 26.82 mg/l in the dry season (Table 4.13). This peak can be attributed to atmospheric nitrogen deposition, where nitrogen compounds settle into surface water (Varma & Jha, 2023). Accumulation of waste discharge, particularly in urban areas like Machakos towns, where sewage and industrial effluents enter the river (Ngatia *et al*., 2023). Stagnant water conditions, allowing microbial decomposition of organic matter to increase nitrate concentrations. This seasonal trend indicates that while external inputs (runoff and fertilizers) reduce in dry months, internal processes (atmospheric deposition and wastewater accumulation) can still lead to increased nitrate levels.

Conversely, from December to March, nitrate concentrations decreased significantly, reaching a statistical mean of 8.59 mg/L, due to higher water levels and stronger river flow (Table 4.13). The influenced of prolonged rainfall in April and May, along with moderate rainfall in November, further diluted nitrate concentrations (Figure 4.22). The increase in precipitation enhances nutrient flushing, reducing localized nitrate accumulation (Bakan *et al*., 2010). Research supporting the causes of nitrate decline in river includes Kaushal et al. (2011) and Lawniczak et al. (2016) who observed that heavy rains decrease fertilizer application, limiting nitrogen introduction into water bodies. Fan et al. (2024) and Moravcová et al. (2013) found that wet soils trap and infiltrate nitrates, preventing their direct entry into rivers. Pericherla et al. (2020) concluded that denitrification increases in saturated soils, further lowering nitrogen content in runoff. Biological uptake, where aquatic organisms utilize nitrate as part of their metabolism (Ngabirano *et al*., 2016; Wetzel, 2001). Furthermore sedimentation prevents nitrate resuspension in turbulent waters (Kilonzo *et al*., 2013). Few among these influencing factors could be responsible to low amount in nitrate concentrations levels in the mid-section of river Athi Basin.

Although average nitrate levels remain below the WHO-recommended threshold for drinking water, sustained nitrate presence can negatively impact ecosystem health and water quality. Barakat et al. (2016) revealed that aquatic organisms experience stress when nitrate levels exceed 1-10 mg/L, affecting growth and reproduction cycles. Nitrate enrichment leads to excessive algae growth, ultimately depleting oxygen and harming aquatic life (Ngatia *et al*., 2023).

5.3.5 Potassium (K)

Potassium (K) is an essential element in aquatic ecosystems, originating from natural geological formations, including sedimentary rocks (clays, silicates, and soils), metamorphic rocks (feldspars), and igneous formations (Mining, Minerals, and Sustainable Development, 2002). It plays a vital role in maintaining water chemistry, biological functions, and ecological balance, yet excessive concentrations can lead to water quality concerns affecting human health and aquatic organisms. High potassium concentrations levels were observed in August, September, and February dry season (Figure 4.23). The temporal elevation correspond with the analyzed mean levels, which demonstrated significantly concentrations (15.38 mg/L) as depicted in Table 4.13. This seasonal increase results from reduced river flow, limited dilution capacity, and enhanced evaporation, all of which concentrate dissolved solutes within water bodies. Pericherla et al. (2020) and Skowron et al. (2018) found elevated temperatures and rock weathering contributing to high potassium concentrations. Paul & Meyer (2001); Galloway et al. (2003), found that urban and agricultural runoff, industrial effluent, and animal waste discharge are major sources of potassium during low river flow periods. Another research by Skowron et al. (2018), observed potassium peaks during summer and fall seasons, reinforcing temperature-driven accumulation. The reduced dilution capacity exacerbates pollutant concentrations, especially potassium.

Furthermore, the February surge in potassium values may be attributed to End-of-January frontal rain events, introducing potassium-rich runoff into rivers. Mineral weathering, where dissolved elements accumulate in surface water. This pattern confirms that

anthropogenic activities, land-use changes, and climatic conditions significantly influence potassium fluctuations in dry seasons.

In contrast, Potassium concentrations were notably lower during November, December, March, April, and May rain fall (Figure 4.18 & 4.23). The declined to 4.42 mg/L was due to increased precipitation and dilution effects (Table 4.13). Similar to conclusion by Owens et al. (2005) and Paul & Meyer (2001) that dilution, sedimentation, and laminar flow dynamics contributes to the reduction of potassium levels. Terrestrial infiltration processes further diminish potassium content in river systems. Fan et al. (2024) found that increased runoff from agricultural areas and irrigated fields enhances potassium removal. Another driver was redox reactions which alter solute availability, lowering potassium mobility in surface waters during dry season.

Despite these reductions, potassium levels remain above WHO drinking water guidelines, indicating persistent pollution sources that rainfall alone does not fully mitigate. Although potassium is essential for cellular function, excessive concentrations pose health risks. Cleveland Clinic (2024) found that higher potassium intake can cause hyperkalemia, potentially impairing heart function, particularly in individuals with kidney disease. Paul & Meyer (2001) excessed that potassium in drinking water can disrupt nutrient balance in human physiology.

5.3.6 Phosphate (PO4)

Phosphates (PO_4) are inorganic compounds composed of phosphorus and oxygen, serving as essential nutrients in aquatic ecosystems (APHA, 2017). Phosphate pollution primarily originates from agricultural runoff, wastewater effluents, industrial discharge, and bedrock weathering, making its regulation crucial for maintaining freshwater ecosystem stability. Phosphate levels remain higher and more stable in August, September, January, and February, due to multiple environmental and anthropogenic factors (Figure 4.24). Reduced river flow, evaporation-driven concentration, and restricted effluent outflow contribute to increased phosphate levels. This findings is consistent with the conclusions made by Sarkar et al. (2016), on the influence in reduced flow living discharged effluents to undergo

biodegrading process. Reduced river flow results in higher phosphate accumulation due to reduced dilution capacity. High temperatures accelerate phosphorus release from soil, enriching rivers with dissolved nutrients (Jiang *et al*., 2008; Zhou *et al*., 2007). Increased evaporation in dry months reduces water volume, intensifying solute concentration effects (Samlafo *et al*., 2022). Additionally, phosphorite minerals from sedimentary rock undergo weathering processes, further increasing phosphate levels in riverbeds. A significant contributing factor in the River Athi Basin is sand harvesting, which disrupts sediment balance and introduces excess phosphates into surface water. Similar to Lwanga et al. (2022) observation on the impact of land mining on water quality.

Conversely, phosphate concentrations decrease to an average of 0.03 mg/L in November, December, April, and May, due to high rainfall levels and increased dilution (Table 4.12; Figure 4.18; 4.24). MacDonald et al. (2016) observed that rainfall facilitates sedimentation, degradation, adsorption, and pH-regulated solute transformation, limiting phosphate mobility. According to Oketola et al. (2013), leaching and nutrient transport redirect fertilizers into river systems, temporarily decreasing phosphate availability. Plate 3.4 indicated high river flow enhances dilution, dispersing contaminants over larger water volumes. Chemical processes such as phosphate co-precipitation with calcium and denitrification further restrict free phosphate levels, limiting eutrophication intensity (Billiah *et al*., 2016). Despite these seasonal fluctuations, phosphate levels remain above WHO drinking water guidelines, raising concerns about long-term water quality risks. Oketola et al. (2013) found that high phosphate levels can increase mortality rates among riverine animals and decrease aquatic biodiversity. Furthermore, excessive phosphate causes eutrophication, leading to toxic algal blooms that threaten human health (Pericherla *et al*., 2020; Conley *et al*., 2019).

5.3.7 Biochemical Oxygen Demand (BOD5)

Biochemical Oxygen Demand (BOD_5) is a key indicator of organic pollution in aquatic environments, representing the amount of dissolved oxygen required by aerobic microorganisms to break down organic matter over five days. In August and September, BOD_5 levels in the River Athi basin peaked at 340 mg/L (Figure 4.25 & Table 4.13). The

peak indicated severe organic pollution in the basin, as observed by Eze et al. (2018) and Kannel et al. (2007) and Zubaidah et al. (2019). These heightened levels are attributed to several interrelated factors. Low river discharge and rainfall reduce the dilution capacity of the river, allowing organic pollutants to accumulate (Ling *et al*., 2017). Stagnation, especially in mid-upper reaches such as Athi River Town and Stony Athi sampling stations, leads to the formation of decomposition zones, where microbial activity intensifies. This microbial breakdown of decaying organic matter consumes large amounts of dissolved oxygen, resulting in hypoxic or even anoxic conditions. As decomposition progresses, the process releases foul-smelling gases and darkens the water, a condition referred to as black-odorization, commonly observed in sluggish urban streams as observed in a study by Liang et al. (2018). This deoxygenation phenomenon not only worsens water quality but also threatens aquatic biodiversity and makes the water unfit for human use.

In contrast, BOD levels dropped significantly during the rainy months (November, December, April, May), averaging 118.99 mg/L (Figure 4.18; 4.25; Table 4.13). Although still high by international standards, this reduction reflects the flushing effect of rainfall. Rain increases river flow and turbulence, dispersing organic loads. Oxygenation improves due to mixing, enhancing microbial efficiency and reducing BOD. The dilution of pollutants by surface runoff and direct rainfall input further lowers BOD concentrations (Kannel *et al*., 2007; Siwek *et al*., 2011). However, despite these benefits, rainy season BOD values remained far above safe limits, indicating that natural dilution alone is not enough to resolve pollution issues. The multiple sources of BOD pollution linkages, including agricultural runoff, untreated sewage, and industrial waste is concern issues. In the Athi River basin, additional variables such as cadmium and chromium contamination compound the stress on water quality. These toxic heavy metals, exacerbated by bedrock weathering, low pH, and fertilizer use, also fluctuate with the seasons. Their interactions with organic material and sediment dynamics further strain the river's oxygen balance, especially during low-flow periods (Pericherla *et al*., 2020; Wu *et al.*, 2010). Despite the diluting effect of rainfall, BOD values remained significantly higher than the WHO drinking water limits, indicating a substantial amount of biodegradable organic material in the water (Table 4.13).

5.3.8 Chemical Oxygen Demand (COD)

Chemical Oxygen Demand (COD) measures the oxygen required to break down both organic and inorganic pollutants in water. Unlike Biochemical Oxygen Demand (BOD), which reflects microbial decomposition of organic matter, COD accounts for chemically oxidizable substances, including industrial waste, agricultural runoff, and domestic pollutants (Varma & Jha, 2023). High COD levels indicate poor water quality, often leading to oxygen depletion, which harms aquatic life and reduces the usability of water for drinking and irrigation. COD levels significantly increase during August, September, January, and February, corresponding with low river flow and pollutant accumulation (Figure 4.26). The mean COD concentration in the dry season was 473.47 mg/L, substantially higher than in the rainy season (193.71 mg/L) as highlight in Table 4.13. Limited water flow restricts dilution capacity, causing increased concentrated pollutants (Ngatia *et al*., 2023). Reduced runoff generates waste accumulations from industrial and household. Geological weathering and air deposition, introduces inorganic carbon and pollutants (Maher & Chamberlain, 2014). Additionally, high temperatures accelerate the breakdown of organic and inorganic materials, further increasing COD levels (Vidal & Vargas, 2008). Research shows that elevated COD reduces dissolved oxygen (DO), compromising aquatic habitat suitability (Gooch, 2007). The highest recorded COD levels in February suggest that pollutants accumulate before seasonal flushing begins with the onset of rains (Figure 4.26). This seasonal increase results from rainfall delays, allowing greater buildup of waste before dilution. Microbial activity, intensifying oxygen consumption and DO depletion. Urban discharge stagnation, leading to localized pollution hotspots.

In contrast, COD levels drop significantly in November, December, April, and May due to rainfall, increasing runoff and dilution effects (Figure 4.18; Table 4.13). Rainwater enhances river velocity, dispersing organic matter and reducing oxygen consumption rates. Siwek et al. (2011) and Owens et al. (2005) found that high river flow improves dilution, lowering COD. Another studies by Varma & Jha (2023) and Ngatia et al. (2023) concluded that rainfall flushes accumulated contaminants, restoring water quality. Zhang et al. (2017) and Mukherjee et al. (2006) found that increased water flow supports reoxygenation, aiding

ecosystem recovery. However, rainfall can introduce phosphate and nitrate fertilizers, which may increase microbial oxygen demand, promoting eutrophication (Plate 3.4).

Despite seasonal reductions, COD levels remain higher than WHO drinking water limits, signaling serious pollution risks. DO depletion, compromising aquatic life survival. Water toxicity, reducing usability for drinking and irrigation. Accelerated eutrophication, disrupting ecological balance. Tang et al. (2023) emphasize that dissolved oxygen regulation is critical for preserving aquatic ecosystems and controlling pollution levels.

5.3.9 Cadmium (Cd)

This variability aligns with hydrological cycles and pollution input dynamics. During August to November, cadmium levels decline due to dilution and sedimentation brought on by early rains. However, a secondary peak in December reflects renewed mobilization, possibly linked to sediment disturbance or renewed anthropogenic inputs (Figure 4.27). Statistical analyses indicate a marked seasonal fluctuation of cadmium levels in the Athi River. The mean concentration during the dry season reaches 0.10 mg/L, sharply varying with 0.0064 mg/L in the rainy season (Table 4.13). Cadmium in the Athi River basin originates from a combination of internal and external sources. Geological Weathering; the river's bedrock contains cadmium-bearing minerals, which are naturally weathered, especially under low-flow and low-pH conditions during dry seasons. The prolonged water-rock interaction releases cadmium into the river (Wu *et al*., 2010). Sediment Dynamics; sediments act as both sinks and sources. During dry seasons, stagnant flows promote resuspension of cadmium-bound particles, intensifying contamination in the water column (Huang *et al*., 2017). Agricultural Inputs; use of phosphate fertilizers common in upstream farmlands, introduces cadmium indirectly. Fertilizer overuse in acidic soils enhances cadmium solubility and mobility (Lawniczak *et al*., 2016). Microbial and Chemical Interactions; the decomposition of organic material in river sediments contributes to acidification, releasing cadmium that was bound to organic complexes (Wu *et al*., 2010). This process is particularly active in low-flow periods when decomposition accelerates.

Conversely, during the April and May rainfall, increased flow velocity and runoff lead to dilution of contaminants, significantly reducing Cd concentrations (Figure 4.18). Sediment burial, effectively locking cadmium in bottom layers. Pollutant flushing, whereby accumulated cadmium is swept downstream or discharged from the system (Patel *et al*., 2018; Pericherla *et al*., 2020). Despite these mitigating effects, heavy rains can also temporarily mobilize cadmium from weathered soils and bedrock, especially in high-slope or recently farmed areas (Tang *et al*., 2023). pH levels play a pivotal role in cadmium behavior: Low pH (acidic conditions) in the dry season enhances cadmium desorption and dissolution from sediments and mineral complexes (Tang *et al*., 2023). Higher pH in the rainy season encourages cadmium precipitation or adsorption onto sediment surfaces, reducing bioavailability (Zhang *et al*., 2017). These chemical equilibria are highly dynamic and respond to temperature, redox potential, and microbial activity, further complicating cadmium mobility.

However, Cadmium levels in the Athi River consistently exceed the WHO drinking water standard limit of 0.003 mg/L, posing significant environmental and public health concerns. The consistently higher cadmium levels in both dry and rainy seasons point to chronic contamination. Given its carcinogenicity and tendency to bioaccumulate, cadmium depletes dissolved oxygen, impairing aquatic ecosystems. It affects fish health through gill and kidney toxicity. Further, poses health risks to local communities relying on untreated water sources, ranging from kidney dysfunction to bone disease and cancer (Khan *et al*., 2016).

5.3.10 Chromium (Cr)

Chromium (Cr) is a naturally occurring heavy metal that poses considerable environmental and health risks when present in elevated concentrations. In aquatic systems, chromium exists primarily in two oxidation states: Cr (III), an essential nutrient in trace amounts, and Cr (VI), a highly toxic and carcinogenic form. The occurrence of chromium in the Athi River basin demonstrates complex spatial and temporal patterns influenced by geology, land use, river hydrology, and anthropogenic activities (Huang *et al*., 2022; Kilonzo *et al*., 2013; Ling *et al*., 2017). Chromium concentrations in the mid-reaches of the Athi River

Basin exhibit a clear seasonal cycle, with peak in August, September, January, and February (Figure 4.28). Highlighting similar findings in the mean values ranging from 0.41 mg/L during the dry season to 0.11 mg/L during the rainy months (Table 4.13). The higher dry season concentrations are driven by reduced river discharge, which limits the dilution of contaminants and creates conditions favorable for pollutant build-up (Guo *et al.,* 2023; Ling *et al*., 2017). The stagnant flow enables prolonged contact between water, sediment, and pollutant sources, enhancing heavy metal accumulation. Geological weathering of the river basin contains chromium-bearing minerals, such as chromite ($FeCr_2O_4$), which release Cr through natural weathering and erosion processes.

These inputs are intensified during low-flow periods, when groundwater interactions mobilize subsurface metals into surface waters (Oze *et al*., 2007; Tumolo *et al*., 2020). Agricultural runoff, due to widespread use of fertilizers rich in nitrogen and phosphorus increases soil acidity, which in turn enhances chromium solubility. This makes Cr more mobile and readily available for runoff into nearby rivers, especially during the early stages of the rainy season (Ngatia *et al*., 2023; Gupta *et al*., 2009). Industrial activities such as sand harvesting, textile dye production, and informal manufacturing contribute significantly to chromium pollution. Effluents from these industries are often discharged untreated into water bodies, elevating Cr levels, particularly in urbanized segments of the river (Guo *et al*., 2023). During dry seasons, low water velocity and volume significantly reduce the river's self-purification capacity. This results in increased residency time of pollutants, higher evapotranspiration, which concentrates solutes, and greater metal-sediment exchange, releasing bound Cr into the water column (Singh & Sharma, 2020).

In contrast, during rainy seasons, Cr levels decreased in November, December, April, and May (Figure 4.28 & 4.18). These lower values are induced by runoff and flood events promoting dilution of dissolved pollutants, sedimentation of suspended particles, and physical scouring of riverbeds, temporarily removing chromium-laden sediments downstream (Huang *et al*., 2022; Owen *et al*., 2005). Yet, it's important to note that heavy rainfall can also mobilize chromium from surface soils and bedrock, generating short-term spikes in pollution (Tang *et al*., 2023). Chromium's solubility and mobility are affected by

redox conditions, pH, and organic matter. Under acidic and oxidizing conditions, Cr(VI) is more soluble, mobile, and bioavailable. Fertilizer-induced acidification of soils near riverbanks elevates Cr leaching into surface runoff. During dry seasons, low water levels and microbial decomposition of organic matter can reduce oxygen availability, potentially converting Cr(VI) to less mobile Cr(III)—though this transformation depends on site-specific redox chemistry (Dash *et al*., 2021).

Despite seasonal dilution, chromium concentrations throughout the year exceed the WHO threshold of 0.05 mg/L for safe drinking water. This poses serious human health implications. Long-term exposure to Cr(VI) is linked to respiratory issues, skin ulcers, and carcinogenic effects, particularly among populations using untreated river water.

5.4 Spatial Variation of Physicochemical and Heavy Metals Water Quality Parameters in Athi River Basin

5.4.1 Potential Hydrogen (pH)

pH is a fundamental water quality parameter that influences chemical solubility, metal mobility, and aquatic ecosystem health (APHA, 2017). In freshwater systems like the River Athi, spatial variation in pH reflects the interaction between geological substrates, hydrological processes, and human activities. River Athi exhibited pH values ranging from slightly acidic (6.98) at NYS (S3) to slightly alkaline (7.55) at Stony Athi (S2) (Table 4.14 & Figure 4.29). Despite this variability, most stations maintained a near-neutral to mildly alkaline profile, consistent with carbonate-buffered freshwater systems. Stony Athi and Athi River Town stations maintained relatively stable and alkaline pH, attributed to low acidity inputs and geological controls. NYS station (6.98) presented a more acidic profile, potentially influenced by localized runoff, wastewater discharge, and redox shifts (Figure 4.29 & Table 4.14). ANOVA results confirm these variations are statistically significant, suggesting spatial differences are not random but stem from identifiable environmental factors. Stability at stations like River Kyawango Confluence and Thwake Confluence (control site) is largely due to bedrock mineralogy (Figure 4.29). Limestone and dolomite dissolution releases bicarbonate (HCO_3^-), carbonate (CO_3^{2-}), calcium (Ca^{2+}), and magnesium (Mg^{2+}) ions, which buffer pH and resist acidification. According to Larson et

al. (2021), these alkaline earth metals neutralize acidic inputs, such as those from organic matter breakdown or sulfide oxidation. In addition, the carbonic acid equilibrium (CO_2-HCO_3^--CO_3^{2-} system) plays a key role in stabilizing pH against sudden fluctuations, particularly in urbanized zones where atmospheric CO_2 interacts with surface water. The higher pH at Stony Athi may reflect buffering from urban sources, while fluctuations in agricultural areas suggest acid-forming fertilizers (high in ammonium and urea) lower pH in soils and runoff. The sampling stations downstream from agriculture-intensive areas often show greater pH variability, as runoff introduces organic acids, nitrates, and agrochemicals. Urban runoff and untreated industrial discharges further modulate pH. Discharged dyeing, tanning, or metal processing containing pH can locally acidify water. Some industrial waste streams may contain alkaline residues, contributing to pH elevation (EPA, 2023; Bakan *et al*., 2010). The overall influence depends on effluent composition, flow volume, and proximity to discharge points.

In contrast, NYS (S3) sample station with significantly slight acidic pH of 6.98 may be due to ion exchange and redox reactions, which decrease hydrogen ion concentrations, as propounded by Singh et al. (2020). Localized acidity sources such as urban runoff or industrial discharges could also contribute to the lower pH. Ion exchange reactions and anaerobic microbial activity (especially during organic decomposition) can generate acidity and alter hydrogen ion dynamics (Singh *et al*., 2020). The stability observed at River Thwake Confluence control station, suggests that the river can neutralize both alkaline and acidic influences over time.

However, most measured pH values fall within acceptable limits for aquatic life (typically 6.5–8.5), the presence of weathered limestone raises concerns about elevated mineral content, including harmful trace elements. According to Akash (2023), prolonged exposure to certain minerals released in alkaline conditions, such as those found in calcite-rich zones, may lead to human health issues, including Kidney dysfunction, nausea and gastrointestinal distress, and bone and muscle complications.

5.4.2 Electrical Conductivity (EC)

Electrical Conductivity (EC) is a key indicator of water quality, representing the ability of water to conduct electrical current, which is directly linked to the concentration of dissolved ions, such as sodium, chloride, calcium, and sulfate (PAHA, 2017). Higher EC levels suggest contamination by anthropogenic sources e.g., industrial discharge, sewage, fertilizers, while natural geologic processes also contribute through mineral dissolution. The upper mid-reaches of River Athi Basin, namely Athi River Town, Stony Athi, River Kyawango Confluence, and Kibwezi Bridge, showed relatively stable EC levels (Figure 4.30 &Table 4.14). The statistical differences point to site-specific influences. Research by Wang et al. (2020), Huang et al. (2022), Owens et al. (2005), and Ling et al. (2017) highlighted similar dynamics in urbanized and semi-urban river systems worldwide, leading to such stability in EC measurements. Stony Athi recorded the highest EC value (1,623.3 µS/cm), attributed to industrial and municipal effluent discharge, and urban runoff from densely populated areas (Table 4.14). Huang et al. (2022) discussed how urban City generates and disposed municipal wastes indiscriminately, which eventually transports by runoff into water body. Kibwezi Bridge, at the downstream, showed the lowest EC level (1,304.9 µS/cm), indicating possible dilution from upstream tributaries or less industrial influence. This stability suggests a constant background load of ionic pollution, likely regulated by bedrock dissolution, limited rainfall recharge, and hydrological retention in low-flow pools (Bucher *et al*., 2017).

During dry seasons, EC levels are significantly influenced by evaporation and stagnation, concentrating salts and minerals. Reduced dilution, allowing pollutants to accumulate in pools or slow-moving reaches. Effluent decomposition, releasing methane, H_2S, and other ions, adding to total dissolved solids (TDS) and EC values (Huang *et al*., 2022; Ling *et al*., 2017). Stony Athi and Athi River Town, located in urbanized zones, become hotspots for EC spikes, fueled by settlement waste and industrial residues. The carbonate-rich and fractured bedrock in segments like Stony Athi enhances mineral dissolution. Water percolates through porous lithology's, picking up calcium and magnesium ions. These geological processes are intensified in dry months, when surface flow decreases but

subsurface interactions increase, elevating EC levels (Gupta *et al*., 2009; Kilonzo *et al*., 2013).

Effluent stagnation and mineral dissolution during dry periods drive EC increases, including detergents and soap residues from riverbank domestic activities. Beyond industrial and urban sources, agricultural runoff introduces dissolved fertilizers (nitrates, phosphates, potassium). These compounds significantly elevate EC values, especially in semi-urban zones where land use is mixed (Wang *et al*., 2020; Bakan *et al*., 2010).

Conversely, sedimentary dissolution from the riverbed and effluent transport during peak flows causes mixed ionic contributions at the River Thwake Confluence (control station), similar to studies conducted by Omer (2019) and Tumolo et al. (2020). However, high mean EC levels, higher than the World Health Organization's (WHO) drinking water limits, may pose health concerns.

5.4.3 Total Dissolved Solid (TDS)

Total Dissolved Solids (TDS) reflect the concentration of all inorganic and organic substances dissolved in water, including minerals, salts, and pollutants (APHA, 2017; WHO, 2022). The mid-section river shows clear spatial gradients in TDS concentrations, with values ranging from 703.6 mg/L at NYS station to 1,090.4 mg/L at Stony Athi sampling stations (Table 4.14 & Figure 4.31). These variations suggested that urban and suburban centers contributes pollutants from domestic wastewater, soaps, industrial effluents, and stormwater runoff as discussed by Tadesse et al. (2018). Stony Athi (S2) recorded the highest TDS levels, directly linked to dense residential settlements like the Greenpark estate and unregulated wastewater discharges. The stagnant pools that form during dry seasons facilitate organic matter decomposition and mineral concentration, as noted by Ling et al. (2017). NYS station (S3) presented the lowest TDS levels, likely due to fewer pollution inputs, increased dilution from tributaries, and ion exchange processes that reduce soluble salt concentrations. Similar to the observation made by Adeleye et al. (2012) and Dash et al. (2021) on water quality studies. The middle and downstream stations, including River Kyawango, River Thwake Confluence (S5), and Kibwezi Bridge

(S6), exhibited more stable TDS values (Figure 4.31). Suggesting a balance between continuous ionic input and natural attenuation mechanisms. Stony Athi and Athi River Town sampling stations are impacted by direct discharge of effluents, particularly during low-flow conditions when rivers stagnate, concentrating TDS. The weathering of minerals from riverbed rocks and soils contributes naturally occurring ions like calcium, magnesium, and bicarbonates, as observed by (Kithiia & Mutua, 2006). Sedimentary dissolution and infiltration during dry seasons enhance mineral concentrations in stagnant pools, elevating TDS levels.

In contrast, rainfall increases dilution, leading to temporary drops in TDS as discussed by Sullivan et al. (2022). In the lower basin, observed stability at River Kyawango and Thwake Confluence suggests the action of several mitigating processes. Adsorption and sedimentation, where suspended particles bind and remove dissolved ions from the water (Owen *et al*., 2005). Microbial oxidation, alters water chemistry and contributes to ionic balance. Neutral pH buffering, aiding in the dissociation or precipitation of some salt forms (Sun *et al*., 2011). These processes together help maintain more consistent TDS levels, despite continuous upstream inputs. Despite spatial variation, mean TDS levels at all sampling stations exceeded WHO recommended limits for potable water (500 mg/L), posing potential health risks. Elevated TDS levels can cause gastrointestinal discomfort, including laxative or constipating effects, depending on the ionic composition (Tesfaye *et al*., 2021). Long-term exposure may lead to taste issues, mineral imbalance, or toxicity, especially in vulnerable populations.

5.4.4 Nitrate (NO3)

Nitrate (NO_3^-) is a prevalent form of nitrogen in freshwater systems, originating largely from agricultural runoff, industrial waste, and domestic effluents (APHA, 2017). Field data from sampling stations stretching from Athi River Town (upper mid-section) to Kibwezi Bridge (low section) show a clear declining trend in nitrate concentrations. Athi River Town recorded the highest NO_3^- levels (29.25 mg/L) due to intense agricultural activity, poor waste management, and sewage inflows (Table 4.14). Stony Athi and NYS stations reflect transitional zones where increasing river flow dilutes nitrate inputs, while

simultaneous organic decomposition processes add complexity to pollutant dynamics. Kibwezi Bridge, at the downstream, recorded the lowest level (7.98 mg/L), influenced by both reduced pollution loading and natural attenuation mechanisms (Table 4.14). These observations are consistent with spatial studies by Wang et al. (2020) and Jafarbadi et al. (2018), which link nitrate variability to flow regulation and pollutant input gradients. Agricultural Inputs in Athi River Town and River Kyawango Confluence sampling stations receive runoff from extensive irrigation farms, where crops like maize, tomatoes, and beans are cultivated (Plate 3.4). These areas apply large quantities of nitrogen-based fertilizers, including urea and ammonium nitrate, which undergo nitrification and contribute significantly to surface water nitrate loads. Wastewater and urban discharge along riverbanks, human settlements discharge organic waste directly into the water (Galloway *et al*., 2003; Torres-Martínez *et al*., 2021). In Athi River Town, over 27.5% of residents engage in riverbank activities, exacerbating nitrate pollution via microbial transformation of organic nitrogen, similar to reports by (Adesse *et al*., 2018; Liang *et al*., 2018). Hydrological dilution and attenuation, as the river flows southward, increased dilution, sediment deposition, and plant uptake help reduce nitrate concentrations (Owen *et al*., 2005; Hu *et al*., 2014). River Thwake Confluence and Kibwezi Bridge stations exemplify this trend, with riparian vegetation, microbial denitrification, and lower fertilizer use playing critical roles in nitrate attenuation. Geological and soil influence, like soil texture, permeability, and ion exchange capacities in different segments of the basin also influence how quickly nitrate leaches into or is removed from the water column (Owens *et al*., 2005; Rivett *et al*., 2008).

In contrast, during low-flow periods, especially in upper mid-section zone, limited water movement enhances nitrate buildup, especially in stagnant pools affected by decomposing organic matter (Fig. 4.32). Rainfall events bring dilution and flushing, helping lower nitrate levels downstream, though sometimes heavy rain can mobilize nitrogen from recently fertilized soils, causing episodic spikes in certain reaches (Higgins *et al*., 2021; Bakan *et al*., 2010).

Although measured nitrate values remain below WHO drinking water limit (50 mg/L), even lower concentrations have been linked to chronic health risks. Levels above 5 mg/L increase the risk of preterm birth by 47%. Long-term exposure above 0.87 mg/L is associated with higher risk of colon, bladder, ovarian, and stomach cancers, as well as endocrine disruption and methemoglobinemia in infants (Sherris *et al*., 2021; Lin *et al*., 2022; Weyer *et al*., 2001).

5.4.5 Potassium (K)

Phosphorus, an essential nutrient for living organisms found as organically bound phosphate particulates, polyphosphates, and orthophosphate, was measured (APHA, 2017; Amadi, 2013). Potassium levels across the mid-section of River Athi varied significantly across sampling stations, with the highest concentration at Athi River Town (18.30 mg/L) and the lowest at Kibwezi Bridge (5.70 mg/L) as seen in Table 4.14. This gradient reflects both geographical proximity to pollution sources and hydrological conditions. Upper mid-sectional zones (Athi River Town and Stony Athi) sampling stations exhibited elevated potassium levels (Figure 4.33). These elevation attributed to dense urban settlements, direct wastewater discharge, industrial effluents, and mineral weathering. The recession of river flows during dry seasons enhances solute-sediment interaction, trapping potassium ions in the riverbed and increasing solute concentrations (Huang *et al*., 2022). Visual signs, such as milky-colored water and algal blooms in stagnant pools, reinforce these findings (Plate 3.1 & 3.2). At midstream and downstream Zones, potassium levels remained relatively stable, likely due to balanced land-use inputs and natural self-purification mechanisms, including sedimentation, ion exchange, and vegetation uptake. The slight increase at Thwake Confluence (control station) may result from localized pollutant release from agriculture or stormwater drains, as found in a study by Bakan et al. (2010). Kibwezi Bridge recorded the lowest levels, influenced by dilution, sediment trapping, chemical precipitation, and seasonal variation (Figure 4.33). Several processes contribute to spatial potassium variability such as anthropogenic Inputs: Domestic waste (detergents, urine), agricultural runoff, and animal waste carry biodegradable and mineral-rich compounds into the river (Wierzba, 2022; Sposito, 2008). Urban runoff and industrial effluents, particularly from treatment plants and local industries, account for heightened upstream concentrations

(Fowler, 2016; Galloway *et al*., 2003). Rock weathering, especially from potassium-rich minerals like feldspars and potash, gradually introduces K^+ ions into surface water. Atmospheric deposition, though minimal, also contributes trace amounts of potassium (Paul & Meyer, 2001). During dry seasons, low flows and warm temperatures intensify chemical reactions, concentrating potassium in stagnant zones. However, rainy seasons, in contrast, enhance dilution, flushing, and sediment coverage, reducing bioavailable potassium levels downstream (Owen *et al*., 2005).

Although potassium is vital for biological function, high levels in drinking water can pose health risks. The mean potassium concentrations exceeded WHO's recommended guideline for individuals with underlying health conditions such as kidney disease, heart conditions, and adrenal insufficiency (WHO, 2009). Ingestion of potassium-rich waters may exacerbate symptoms of hyperkalemia, leading to cardiac arrhythmias or circulatory dysfunction. Long-term ecological risks include altered ion balances in aquatic habitats, potentially stressing freshwater biota (Manning, 2010). Additionally, natural potassium includes a small proportion of radioactive isotope potassium-40, which emits beta radiation. While environmental levels are typically low, prolonged exposure from contaminated sources may increase radiological risks (Britannica, 2024).

5.4.6 Phosphate (PO4)

Phosphate (PO_4^{3-}) is a vital nutrient in aquatic systems, yet excessive concentrations can disrupt ecological balance, trigger eutrophication, and present public health risks (APHA, 2017). The elevated phosphate concentrations were recorded in upper mid-sections, including Athi River Town and Stony Athi sampling stations, where wastewater discharge, industrial effluents, and seasonal river contributions are dominant (Figure 4.34). Sources of Phosphates at these sites include untreated sewage and greywater rich in detergents (EPA, 2023). Agricultural runoff carrying fertilizers and organic debris (Galloway, 2003). Decomposing plant matter and animal waste (Verma & Jha, 2022). The upper midstream is especially prone to phosphate accumulation during dry seasons, when low flow velocity impedes dilution, and stagnation enhances contaminant retention (Ngabirano *et al*., 2016). These conditions promote adsorption of PO_4 into sediment, which may later be

resuspended and released under turbulent flow. Phosphate levels rise again at River Kyawango Confluence (S4), due to inputs from animal husbandry, irrigation schemes, and sand harvesting operations (Figure 4.34). These land use activities introduce nutrient-rich sediments and effluents into the river, supporting algal growth and increasing biochemical demand for oxygen. This observation supports findings by Owens et al. (2005) and Jafarbadi et al. (2018), who noted that small tributaries and human activity-rich sub-basins contribute disproportionately to nutrient hikes in Mainstream Rivers.

Downstream declines due to dilution effects from River Kyawango Confluence to River Thwake Confluence (S5) and Kibwezi Bridge (S6) as depicted in Figure 4.34. A general decline in phosphate concentrations was observed, with River Thwake confluence control station recording the lowest level (0.02 mg/L) as depicted in Table 4.14. This spatial decline is attributed to self-purification mechanisms, including sediment adsorption, microbial uptake, and chemical precipitation (Sun *et al*., 2011). Reduced pollutant input due to decreasing land use intensity and lower industrial activity downstream (Higgins *et al*., 2021). Inundation processes during seasonal flow peaks that aid in dispersing and immobilizing dissolved phosphates. The apparent anomaly at Kibwezi Bridge, where the highest mean concentration (0.52 mg/L) was recorded (Table 4.14). May reflect restricted river flow, localized effluent discharge, or seasonal stagnation, limiting the dilution capacity (Plate 1–6).

However, decline in mean levels at downstream stations exceed WHO drinking water standards, underscoring considerable ecological and health concerns. High phosphates can lead to algal blooms, oxygen depletion, and reduced biodiversity in aquatic systems (Komaba & Fukagawa, 2016). Eutrophication may alter food web structures and impair fisheries and irrigation. Chronic exposure to excess phosphate is linked to hyperphosphatemia, which contributes to vascular calcification, bone deformities, and cardiovascular mortality, especially in patients with chronic kidney disease (CKD) (Cozzolino *et al*., 2001; Kestenbaum *et al*., 2005). Elevated phosphate intake stimulates parathyroid hormone (PTH) secretion, increasing bone resorption and risk of osteoporosis (Almaden *et al*., 1996; Slatopolsky *et al*., 1996). Acute phosphate nephropathy has also

been documented in individuals consuming high-phosphate water sources (Markowitz & Perazella, 2009).

5.4.7 Biological Oxygen Demand (BOD)

BOD levels varied significantly across River Athi Basin sampling stations, reflecting spatial differences in land use, waste input, and hydrological conditions. The results highlight a pattern of organic pollution linked to human activity and reduced natural self-purification capacity in certain river segments. The highest mean BOD concentration was indicated at Athi River Town (S1) sampling station with 256.8 mg/L, while the lowest was observed at Stony Athi (S2) station with 209.5 mg/L (Table 4.14). It decline between S1 and S2 possibly due to dilution effects, aerobic oxidation of organic matter, or increased flow velocity, all of which enhance dissolved oxygen availability, as discussed in a study by Sun et al. (2011). The presence of stagnant pools, mainly in S1 where bedrock formations slow flow, which likely promoted organic accumulation and microbial activity, exacerbating oxygen demand.

During the rainy season, intercatchment flow from the Mbagathi River and surrounding urban settlements such as Komo and Munyu axis, increases pollutant loads, further elevating BOD in upstream and midstream sections. The merging of rivers and runoff from impervious surfaces during rainfall intensifies organic matter input, overwhelming the river's self-purification processes. At the NYS station, a renewed increase in BOD suggests an influx of organic waste from surrounding residential areas, including Kilimambogo and Thika (Figure 4.35). This is consistent with Lemessa et al. (2023), who note that higher organic loading enhances microbial respiration and oxygen consumption. These conditions often produce odorous compounds and support the black-odorization observed in degraded urban rivers (Ling *et al*., 2017). As the pollutants progressively flows towards downstream stations, like River Kyawango Confluence, River Thwake Confluence (control station), and Kibwezi Bridge, it exhibited more stable BOD levels (Figure 4.35). The relative consistency here is attributed to natural dilution, oxidation processes, and a reduction in upstream pollutant inputs (Bhat *et al*., 2018; Sun *et al*., 2011). These sections likely benefit from higher flow volumes, more vegetation, and reduced direct human interference. In

addition, the role of microbial decomposition cannot be overstated particularly, during dry season. As Zubaidah et al. (2019) pointed out, BOD increase is intensified by fully mixed wastewater, which accelerates both aerobic and anaerobic breakdown processes. This rapid consumption of dissolved oxygen can drastically impact aquatic ecosystems, mainly in stretches with limited flow or low re-aeration capacity.

Despite spatial fluctuations, all sampling stations recorded BOD values that far exceeded WHO drinking water standards (Table 4.14). This suggests a pervasive pattern of organic pollution across the basin. High BOD not only signals deteriorated water quality but also fosters the growth of pathogenic organisms, potentially increasing the risk of waterborne diseases such as cholera, gastroenteritis, and dysentery (Geldreich, 2018).

5.4.8 Chemical Oxygen Demand (COD)

Chemical Oxygen Demand (COD) represents the total amount of oxygen required to chemically oxidize both biodegradable and non-biodegradable organic compounds in water. COD concentrations across the six sampling stations reveal distinct gradients and pollution hotspots, particularly in urban-industrial zones. These upper-mid reaches namely Athi River Town (S1) to Stony Athi (S2) sampling stations form the “biodegradable zone”, characterized by high COD concentrations (Figure 4.36). These elevated levels correspond to statistical mean of 362.6 mg/L at Stony Athi sampling station (Table 4.14). The elevated concentrations reflect accumulation of oxidizable wastes from household activities, industrial effluents, decomposing paint, and stormwater runoff (Zubaidah *et al*., 2019; Uddin *et al*., 2016). High temperatures, low flow, and nutrient-rich substrates here accelerate microbial and chemical oxygen demand (EPA, 2012). COD levels remain relatively stable at NYS (S3) and River Kyawango Confluence (S4) stations, due to balanced degradation activity, improved water velocity, and natural sedimentation. These transitional stations benefit from moderate self-purification processes, including adsorption and microbial oxidation (Tchobanoglous *et al*., 2003). COD levels at River Thwake Confluence (S5) Control Station declined significantly to 148.67 mg/L, representing the baseline for recovery and dilution effects in the lower basin (Table 4.14). This reduction indicates lower inputs of complex chemical waste and enhanced dilution,

adsorption, and biological uptake (Lee & Nikraz, 2015; Owens *et al*., 2005). Surprisingly, COD levels increased again at the downstream Kibwezi Bridge (S6) sampling station, likely due to agricultural runoff, animal waste, and residual organic matter, coupled with decreased flow and oxidative capacity. This reflects a reintroduction of pollutant loads and limited breakdown of recalcitrant compounds (Rodriguez *et al*., 2019; Sun *et al.,* 2011).

Several physical, chemical, and biological mechanisms control the spatial distribution of COD. During low-flow periods, pollutants accumulate in stagnant zones, leading to high COD levels. Reduced dilution capacity increases concentrations of organic and synthetic materials, intensifying chemical oxygen demand (Owens *et al*., 2005). Urban and peri-urban areas contribute heavily through mixed wastewater loads, while industrial zones introduce non-biodegradable compounds such as solvents, detergents, and paint residues (Uddin *et al*., 2016). COD breakdown is influenced by microbial respiration, which is itself sensitive to pH, temperature, and nutrient availability. Microbial efficiency tends to improve in neutral to slightly alkaline conditions, especially when supported by stable sedimentation and oxygenation (EPA, 2012; Tchobanoglous *et al*., 2003).

However, downstream sampling stations benefit from natural attenuation processes where oxidizable pollutants are bound to sediments, oxidized, or flushed out during high-flow events, similar to studies by Kaushal et al. (2011) and Pericherla et al. (2020). COD values across many stations exceed WHO recommended thresholds, posing significant water quality and health hazards. High COD indicate the presence of persistent organic pollutants, some of which may be toxic, carcinogenic, or endocrine-disrupting. This impairs not just aquatic life, but also downstream water consumers. Sustained high COD can lead to oxygen depletion, disrupting aquatic habitats and causing fish kills, algal blooms, and other forms of eutrophication. Poorly treated river water used for irrigation, washing, or livestock increases the risk of bioaccumulation of chemical residues, leading to chronic health effects in surrounding communities (Rodriguez *et al*., 2019).

5.4.9 Cadmium (Cd)

Cadmium (Cd) is a non-essential heavy metal with serious toxicological implications, even at trace levels. Between Athi River Town (S1) and NYS Station (S3), cadmium concentrations increase sharply, indicating a region of localized enrichment (Figure 4.37). The peak mean value, 0.1196 mg/L at NYS, indicates critical contamination. These are sourced from mineral weathering of Cd-rich sedimentary formations (Mahmood *et al*., 2019; Tang *et al*., 2016). Discharge of cadmium-laden industrial waste, cement dust, and effluents from the Kilimambogo and Thika zones (ATSDR, 2008). Urban stagnation zones during dry seasons create low-flow conditions that favor cadmium accumulation in bedrock-supported sediment pools (Liang *et al*., 2018; Plate 3.1). Formation of cadmium salts such as CdS and Cd $(NO_3)_2$ increases bioavailability and toxicity in water systems (Zhao & Wang, 2020). These findings correspond with studies identifying industrial activities such as fertilizer production, steelwork runoff, and smelting as major sources of cadmium contamination (Mahmood *et al*., 2019). Beyond NYS, cadmium concentrations begin to decline progressively from River Kyawango Confluence (S4), River Thwake Confluence (S5) control station, and Kibwezi Bridge (S6), which recorded the lowest Cd level at 0.0042 mg/L (Table 4.14). The elevated levels could be due to bioaccumulation and sorption onto sediments (Wierzba, 2022). Ion exchange and desorption processes, which remove cadmium from the dissolved phase (Lee & Nikraz, 2015; Adeleye *et al*., 2012). Elevated ionic strength, shown by increased EC values, which competes with Cd^{2+} ions for adsorption stations, thereby limiting mobility (Chen *et al*., 2021). Dilution and sediment submersion, especially at Kibwezi, where a wider river channel and lower urban pressure support natural purification, similar to study conducted by Zhao & Wang. (2020) on river purification. Interestingly, the River Thwake Confluence control station, although downstream of polluted zones, shows relatively lower cadmium impact (Figure 4.37). Induced by natural attenuation processes are effectively minimizing cadmium mobility.

Despite spatial decline, the mean cadmium concentrations across all stations exceed WHO limits, implying widespread exposure risks. According to researchers, trace Cd exposure can cause renal dysfunction, gastrointestinal damage, and carcinogenesis, with a biological half-life in humans of 25-30 years (Genchi *et al*., 2020; Wang *et al*., 2019). Cd tends to

concentrate in plants, aquatic organisms, and human organs, particularly kidneys, liver, and lungs (Song *et al*., 2015; Bouida *et al*., 2022). Children's vulnerability. Exposure may lead to neurodevelopmental delays, such as hyperactivity and learning impairments (Hunt, 2003). Persistent Cd levels stress aquatic ecosystems, inhibiting enzyme function, damaging gill tissues, and altering species composition.

5.4.10 Chromium (Cr)

Chromium (Cr) is a redox-sensitive trace metal with both essential and toxic forms, commonly introduced into aquatic systems through geogenic weathering and anthropogenic activities (APHA, 2017). The Athi River Town (S1) sampling station displayed the highest chromium levels, reaching 0.755 mg/L, induced by urban and geogenic contributions (Table 4.14). These contributions includes the increased chromium concentrations of industrial discharges from dye manufacturing, metal plating, wood preservation, and textile processing facilities (Anatoly, 2011). Atmospheric deposition of chromium-containing particulates from combustion and manufacturing stations. Geogenic inputs, particularly the weathering of ultramafic bedrock containing chromium-bearing minerals such as chromite ($FeCr_2O_4$) (Bhalerao & Sharma, 2015; Zhitkovich, 2011). Low flow conditions during dry seasons further exacerbate this problem, leading to limited dilution, stagnation, and increased pollutant residence time. As noted by Pericherla *et al*. (2020), such conditions promote chromium accumulation in water and sediments, intensifying its environmental impact. As the river flows downstream from River Kyawango Confluence (S4) to Thwake Confluence (S5) and Kibwezi Bridge (S6) as depicted in Figure 4.30, a steady decline in chromium concentrations is observed, reaching as low as 0.0018 mg/L at Kibwezi in Table 4.14. This gradient highlights the role of dilution from tributary inflows and baseflow contributions. Sediment submersion and sorption onto particulate matter, which reduce chromium's bioavailability. Abiotic transformation, such as Cr (VI) reduction to less mobile Cr(III) under suboxic or anoxic conditions (Sun *et al*., 2011).

Reduced pollution sources further from urban and industrial centers (Rahardjo *et al*., 2021). At the Thwake Confluence, used as a control station, this decline also suggests effective

self-purification. Where adsorption, precipitation, and microbial uptake reduce chromium mobility and toxicity. Chromium exists in the environment primarily as Trivalent Cr (III), it is relatively stable and less toxic, often bound to organic matter or sediment. Hexavalent Cr (VI) is highly soluble, mobile, and toxic is predominant in oxidized environments (Chrysochoou *et al*., 2016). These species interconvert depending on redox potential, pH, and biological activity. Weathering of ultramafic rocks and human interventions e.g., oxidant-rich industrial waste promote the formation of Cr (VI), which poses serious health threats.

Despite the downstream dilution, chromium concentrations across several stations remain elevated relative to safe standards, with implications including carcinogenic risks, chromium exposure, especially Cr(VI), has been associated with lung and gastrointestinal cancers, and respiratory illness (ATSDR, 2012). Systemic toxicity such as prolonged ingestion affects glucose metabolism, reproductive health, and may result in kidney and liver damage (Bahiru, 2020; Chishti *et al*., 2011). In plant toxicity, chromium disrupts photosynthesis, nutrient uptake, and enzyme systems, impairing plant growth and productivity in riparian and irrigated zones (Bhalerao & Sharma, 2015). Cr (VI) resists degradation and bio accumulates in sediments, increasing long-term ecological risk.

5.5 Influence of Physicochemical Parameters on Bod, Cod, and Heavy Metals

The findings of multiple linear regression analysis conducted on the influence of pH, EC, TDS, NO_3, K, and PO_4 on BOD and COD (oxidation parameters) and Cadmium and Chromium (heavy metals) were discussed as follows;

5.5.1 Influence of Physicochemical Parameters on BOD

The overall model was statistically significant, indicating that the predictors have a meaningful influence on BOD levels. The findings highlight the impact of water quality parameters on organic pollution levels.

5.5.1.1 Electrical Conductivity (EC)

This finding demonstrated that BOD levels increase alongside the ion concentration in the water. The rise in EC might be caused by higher organic pollution in the river, which raises BOD levels (Jafarbadi *et al*., 2018). This correspond with the observation that organic pollutants, when dissolved in water, increase the ionic content (measured as EC) and demand more oxygen for microbial breakdown, thus raising BOD levels. Increased availability of dissolved chemicals that elevate oxygen consumption may be responsible for this. Zhou (2022) also found that higher EC values often correspond with increased levels of inorganic and organic pollutants, both of which raise BOD levels. Wu et al. (2010) demonstrated that rising EC often occurs alongside increased nutrient loading, which can stimulate microbial activity and elevate BOD levels.

5.5.1.2 Potential Hydrogen (pH)

The results showed no significant relationship between pH and BOD, suggesting that, when other factors are considered, pH does not significantly affect BOD on its own. While microbial activity and the solubility of organic matter are important in the biodegradation processes that generate BOD, pH alone may not be a reliable indicator of BOD in the River Athi, as indicated by the lack of statistical significance in this result. Findings by Chapman et al. (2013) and Wu et al. (2010) indicate that pH can modify microbial populations and enzyme activity involved in breaking down organic matter, indirectly influencing BOD. Moreover, disparities may be explained by specific pollution sources, such as wastewater discharge, industrial effluents, and urban runoff, which are more prevalent in upper river areas with higher human densities and land use activities, like Stony Athi and Athi River Town.

5.5.1.3 Total Dissolved Solids (TDS)

The non-significant associations suggested that, when other factors are considered, TDS may have a minimal or insignificant direct impact on BOD. Given that water contains both organic and inorganic components, these results align with earlier analyses suggesting a correlation between TDS and BOD. The flow of dissolved organic compounds from the upper Athi River influences the amount of TDS and BOD. Conversely, low flow velocity

and the buildup of organic pollutants during the dry season led to increased levels. The influence of TDS was less noticeable in this instance due to factors such as organic load, microbial activity, and other water quality characteristics that may modify BOD. According to Zhou (2022), higher TDS levels might be linked to higher pollution loads, including organic and inorganic waste, affecting water quality metrics like BOD. Li et al. (2022) reported similar findings, noting that although TDS can serve as a pollutant indicator, the type of dissolved solids often mediates its direct effect on BOD. While TDS's organic components may contribute to BOD, inorganic salts usually do not, which could account for the non-significant correlation.

5.5.1.4 Nitrate (NO_3)

The results showed variability, suggesting that different water conditions may affect how NO_3 influences BOD. Due to seasonal and regional fluctuations in released pollutants, NO_3 concentration levels from seasonal agricultural runoff may not have an immediate or uniform impact on BOD levels over time. Although this study found a positive correlation between NO_3 and BOD, the large confidence range and lack of statistical significance imply that nitrate's impact on BOD is unclear and likely influenced by other environmental factors. High nitrate levels from wastewater discharge and agricultural runoff can cause eutrophication, later elevate BOD levels by promoting algal growth and subsequent degradation. Furthermore, Pericherla et al. (2020) reported that nitrates might indirectly increase BOD level by encouraging algal growth, increasing oxygen demand during decomposition. Variations in land use, pollution sources, and water flow patterns may cause NO_3 and BOD levels to fluctuate from one location to another. However, as the model's non-significant relationship explains, its effect may be overshadowed by other factors.

5.5.1.5 Potassium (K)

According to the data in this study, potassium did not consistently or reliably affect BOD levels since the association between potassium and BOD was not significant. This suggests that seasonal and regional variability in water chemistry may cause potassium's effect on BOD to be minimal or erratic. Falkenmark & Rockström (2004) found that BOD variations

are usually linked to organic contaminants rather than nutrient quantities, and that potassium contributes to the overall chemistry of the water. Although potassium has a negligible direct impact on BOD, it is necessary for biological functions. The lack of significance is supported by the fact that potassium's role in river systems is more closely linked to plant development and nutrient balance than to direct oxygen demand.

5.5.1.6 Phosphate (PO_4)

The non-significance in the association between PO_4 and BOD suggests insufficient evidence to support a consistent influence between these variables. Thus, any observed effect of PO_4 on BOD might be due to random variations or other factors, rather than a true underlying relationship in the Athi River. This random variation could include spatial and seasonal influences on PO_4 and BOD levels in the river basin. These levels may be impacted by long-term changes in land use, such as agricultural operations or wastewater treatment over time. According to Zhou (2022), the direct effect of PO_4 on BOD may vary depending on the water body. Phosphates can contribute to eutrophication, leading to algae development, which increases organic material and potential BOD. Elements such as seasonal and spatial variations, as well as the presence of other nutrients, also play a role. While the amount of biodegradable organic matter has a greater impact on BOD than PO_4 itself, nutrients like phosphates contribute to overall water quality and ecosystem dynamics. Chapman et al. (2013) noted that phosphates can increase BOD by causing eutrophication, triggering algal blooms that significantly increased oxygen demand during decomposition. Other environmental conditions, particularly mineral weathering, can also impact this association. Nevertheless, the strong correlation between BOD and EC suggests that dissolved ionic content is a key factor in organic pollution, and monitoring this parameter can help control organic pollution in water bodies. However, the non-significant findings for pH, TDS, NO_3, K, and PO_4 indicate that these parameters do not directly affect BOD levels within the study range.

5.5.2 Influence of Physicochemical Parameters on COD

The result of multiple linear regression analysis indicated that the predictors collectively have a substantial influence on COD levels.

5.5.2.1 Potential Hydrogen (pH)

The findings displayed a considerable degree of uncertainty, suggesting that pH might not be a reliable indicator of COD. The river basin's pH is generally neutral, with slight variations over time and distance. According to Uddin et al. (2016), factors such as land use, industrial discharge, or atmospheric deposition may impact COD levels if other influencing variables change over time and space. Seasonal variations in temperature, biological activity, and runoff cause fluctuations in pH levels. Wang et al. (2022) noted that pH indirectly impacts COD by affecting chemical reactions during the breakdown of organic materials. The model's lack of statistical significance may result from other dominant factors that have a more direct impact on COD in the water. Additionally, variations in land use, industrial activity, and pollution inputs from nonpoint sources and river sections can affect pH and COD levels in different locations.

5.5.2.2 Electrical Conductivity (EC)

The results showed that COD increases with the concentration of ions in the water, likely due to increased dissolved organic and inorganic materials that elevate chemical oxygen demand. Changes in land use, industrial operations, or pollution sources over time may be linked to a rise in EC and, consequently, an increase in COD levels (Jafarbadi *et al*., 2018). Seasonal variations, including high temperatures, low river flow, and pollution loading, can elevate both COD and EC levels. Soil type, pollution sources, and land use variations can also affect EC in water. This outcome aligns with research by Chen et al. (2023), which found that elevated EC values often correspond with higher concentrations of contaminants, including heavy metals and organic compounds, which can raise COD. This emphasizes the significance of EC as a predictor of COD and confirms its statistical significance.

5.5.2.3 Total Dissolved Solids (TDS)

The non-significant result suggests that the link between TDS and COD is not always affected by historical factors. Seasonal variations in runoff and rainfall can alter TDS levels, which in turn affect the concentration of dissolved solids. Non-significant correlations between seasonal variations in TDS and changes in COD were also noted by

Verma & Jha (2023). Similar conclusion was made by Zhou (2022), that TDS may not substantially impact COD, especially when dominated by inorganic salts. The model's non-significant association supports the understanding that TDS can have varied compositions, with only certain components contributing to COD. Regional characteristics and spatial distribution may still show variations in TDS and COD concentrations.

5.5.2.4 Nitrate (NO_3)

The impact of NO_3 on COD might be context-dependent and insufficiently strong to serve as a meaningful predictor in the model. Heatwaite et al. (2020) suggested that changes in land use, wastewater treatment, or pollution control strategies over time could influence the relationship between NO_3 and COD. Seasonal variations due to runoff, irrigation techniques, and dilution effects in the river can affect NO_3 and COD levels. While nitrates can aid in the breakdown of organic waste, increasing COD, more direct sources of organic pollution often overshadow this effect (Singh *et al*., 2020). The model's non-significant result may reflect this complex relationship, or seasonal fluctuations might have obscured NO_3's direct impact on COD. However, regional interactions and spatial distributions can still influence nitrate and COD levels in the Athi River.

5.5.2.5 Potassium (K)

The negative correlation between K and COD over time suggests that higher potassium levels may coincide with a decrease in COD due to changes in the water's chemical or biological processes. Different land use changes and the gradual natural release of pollutants could also contribute. Potassium, an essential nutrient, does not directly contribute to chemical oxygen demand; instead, it plays a role in biological activities (Zhang *et al*., 2021). The non-significant finding supports the notion that potassium typically has little effect on COD. Unlike other compounds like organic carbon or nitrogenous wastes, potassium is considered a conservative ion and, although essential in biological processes, does not directly impact COD or BOD levels (Aelion & Wartinger, 2010).

5.5.2.6 Phosphate (PO_4)

The trend shown by the non-significant finding may indicate that other factors override PO_4's effect on COD. There is considerable uncertainty, suggesting wide variations in PO_4's impact on COD. Local factors such as wastewater discharge and agricultural runoff, as well as seasonal fluctuations, can affect COD levels. Phosphates can cause COD through eutrophication and subsequent algal breakdown, but the effect varies and depends on other environmental conditions, as proposed by Paerl & Otten (2013). The non-significant and ambiguous results may be explained by this variability. During the rainy season, significant differences in PO_4 and COD levels may occur and vary by location (Sigleo & Frick, 2003). Regression analysis shows that EC and pH significantly affect COD, indicating that controlling these factors may be essential for regulating COD levels in water bodies. However, the effects of the non-significant predictors (TDS, NO_3, K, and PO_4) on COD remain unclear.

5.5.3 Influence of Physicochemical Parameters on Cadmium (Cd)

Given that these physicochemical characteristics affect cadmium levels, the results emphasize the significance of keeping an eye on them. Although these are not the only or most important components in the river, they do help to explain it.

5.5.3.1 Potential Hydrogen (pH)

The Cd level decreased as the pH increased, suggesting that pH and Cd may be inversely related. This relationship is affected by seasonal swings, temporal variations, and changes in pH throughout time. Spatial variances may also show alterations in this relationship. The findings of Tang et al. (2023) are comparable to this one, which found that pH is a key factor in metal solubility and that metals like cadmium are generally more soluble at lower pH values. Nevertheless, the non-significant result might suggest that, without taking into account other interacting factors, pH alone is not enough to predict Cd concentrations.

5.5.3.2 Electrical Conductivity (EC)

The non-significant coefficient suggests inconsistent relationships over time and space. While changes in EC might impact Cd levels, discrepancies or influences from other

factors may make this effect unreliable. There could be a correlation between low cadmium (Cd) concentrations and high Electrical conductivity (EC) levels during dry seasons, but other dominant seasonal factors may overshadow this relationship (Chen *et al*., 2021). Higher EC values, reflecting increased ionic strength in water, can compete with cadmium ions for adsorption sites, thus lowering Cd concentrations (Saeedi *et al*., 2019). However, the non-significant result indicates that EC alone might not be a reliable predictor of Cd levels. Spatial variations in land use and pollution sources, including industrial, agricultural, and natural discharges, can influence both EC and Cd levels, obscuring their relationship. Changes in EC may have varying effects on Cd levels over time, across seasons, and in different locations.

5.5.3.3 Total Dissolved Solids (TDS)

The findings suggested a potential negative correlation between TDS and Cd content, though the non-significant coefficient's impact varied over time. Seasonal variations in temperature, precipitation, and water flow can influence TDS, affecting Cd levels. Additionally, local conditions, such as natural causes, industrial effluents, and agricultural runoff, can impact pollution sources and Cd levels. Zhou (2022) noted that TDS, often comprised of several inorganic salts, may dilute heavy metals like cadmium, leading to lower concentrations. Nonetheless, the non-significant result suggests that TDS does not directly affect Cd levels.

5.5.3.4 Nitrate (NO_3)

This finding suggested a possible inverse relationship where increased NO_3 levels could lead to lower Cd concentrations. Changes in NO_3 levels over time, due to adjustments in agricultural practices and industrial effluent releases, may impact Cd concentrations. However, the non-significant link implies that seasonal variations may not consistently align with changes in Cd levels. Locational sources of pollutants and local characteristics, such as land use, industrial operations, and agricultural methods, may impede a clear link between NO_3 and Cd concentrations (Zhou, 2022). Nitrates can affect metal mobility, often resulting in lower concentrations of heavy metals, especially Cd, in water (Vrzel *et al*.,

2016). The non-significant relationship suggests that other, more influential factors have a greater impact on Cd than nitrate.

5.5.3.5 Potassium (K)

The results showed a strong inverse connection, with higher K levels leading to lower Cd concentrations. Seasonal variations in Cd concentrations may be differently impacted by changes in potassium levels (Varma & Jha, 2023). Local conditions and spatial distributions can affect K and Cd levels; higher K levels in the upper Athi River may correlate with lower Cd concentrations. Aelion & Wartinger (2010) explained that potassium might compete with cadmium for binding sites in sediments or organic matter, reducing Cd levels in water. Potassium may act as a mitigating factor for cadmium exposure, as indicated by the statistical significance.

5.5.3.6 Phosphate (PO_4)

The results indicated a negative correlation between rising PO_4 levels and falling Cd levels; however, the lack of statistical significance suggested that this association might not hold over time. Long-term patterns may not consistently show the impact of potential adjustments. The non-significant result implies that seasonal changes in PO_4 might not consistently and significantly affect Cd levels. Environmental factors, such as pollution sources and seasonal and geographical changes, may overshadow phosphate levels. Phosphate-cadmium binding can form insoluble complexes that precipitate out of the water, lowering Cd concentrations (Paerl & Otten, 2013).

5.5.3.7 Biochemical Oxygen Demand (BOD^5)

The results indicated an inconsistent effect, with an increase in BOD levels over time causing a decrease in Cd levels. Seasonal variations in BOD do not always result in changes in Cd levels, as evidenced by the lack of statistical significance. BOD levels may be impacted by seasonal differences in microbial activity and organic matter loading. The observed connection may be influenced by spatial and local variability in BOD levels and Cd concentrations, following the inputs of organic materials from upstream, midstream, and downstream river sections. Wang et al. (2022) noted that increased BOD levels might

enhance cadmium's adsorption onto organic particles, reducing its concentrations in the water column. The non-significant result suggests that BOD5's impact on Cd varied between the sampling locations.

5.5.3.8 Chemical Oxygen Demand (COD)

The findings showed a strong statistical association, indicating that an increase in COD over time leads to a slight drop in Cd levels. Due to the small magnitude of the change in Cd, seasonal fluctuations in COD levels have little effect on Cd levels (Uddin *et al*., 2016). Furthermore, the minimal impact of geographical fluctuations in COD levels on Cd concentrations indicates a non-random association. This outcome is comparable to the finding by Britannica (2023) that increased COD levels, often linked to higher levels of organic contaminants, can cause heavy metals like cadmium to complex and precipitate, lowering their concentration. Even minor variations in COD can have a noticeable effect on Cd levels, according to the statistical significance. Nonetheless, the multiple linear regression analysis shows that while predictors like COD and potassium (K) have statistically significant effects on Cd levels in water, other parameters like pH, EC, TDS, NO_3, and PO_4 do not. The model only accounted for 36% of the variation in Cd, suggesting that other factors significantly influence cadmium levels in water.

5.5.4 Influence of Physicochemical Parameters on Chromium

The model explained 36% of the variation in the six predictors, showed moderate effects on Cr levels. They contribute to the explanation, thus, are not the only or most significant factors in the river.

5.5.4.1 Potential Hydrogen (pH)

The findings indicated that pH had no discernible impact on Cr levels over time, suggesting that factors other than pH may be responsible for temporal fluctuations in Cr. The Athi River's Cr levels show distinct seasonal cycles that may be unrelated to changes in pH. However, pH remained relatively constant during the study period, with minimal variations over time and seasons. This outcome is consistent with Ngabirano et al. (2017), who found that chromium's solubility and speciation in water can be influenced by pH levels.

Generally, lower pH values make Cr (VI) more soluble and mobile in aquatic environments.

5.5.4.2 Electrical Conductivity (EC)

The lack of a statistically significant correlation between EC and Cr may imply that other factors, such as varying sources of Cr pollution or river solutes, have a greater impact on Cr concentrations. Seasonal variations in EC do not correspond to a discernible shift in Cr concentrations; rather, the effects may be obscured by interactions with other variables. High ionic strength due to elevated EC may result in competitive interactions for adsorption sites, potentially lowering the amount of Cr in water (Wang *et al*., 2020). The non-significant outcome suggests that while EC may affect Cr, it does so in combination with other variables.

5.5.4.3 Total Dissolved Solids (TDS)

The analysis indicated that TDS has a detrimental impact on Cr concentrations, with higher TDS levels resulting in lower Cr concentrations. This effect could source from random variation or additional factors not included in the dataset. Substantial seasonal variation in TDS may influence the relationship between TDS and Cr levels. This finding is consistent with the hypothesis that elevated TDS levels, which include various dissolved salts, can decrease the mobility of heavy metals like chromium by precipitating and complexing them (Zhou, 2022). The non-significant finding suggests that TDS alone may not be a reliable indicator of Cr levels.

5.5.4.4 Nitrate (NO_3)

The correlation between higher nitrate levels and higher Cr concentrations was positive and statistically significant. Notable seasonal fluctuations in nitrate concentrations may affect the correlation between nitrate and Cr. Changes in nitrate levels over time, due to interactions with other factors, can impact Cr levels (Higgins *et al*., 2021). Nitrate can increase the oxidation of Cr(III) to the more mobile and hazardous Cr(VI) in water, potentially raising its concentration (Singh *et al*., 2020; Vrzel *et al*., 2016). These results

are supported by the predictor's statistical significance, indicating that nitrate affects Cr levels.

5.5.4.5 Potassium (K)

There is a positive and statistically significant correlation between increased potassium levels and higher amounts of Cr. Notable seasonal and spatial variations in potassium levels suggest that the Athi River's potassium concentrations are significantly influenced by these factors. Variations in Cr levels may be influenced by temporal changes in potassium, with higher potassium levels during the dry season potentially leading to higher Cr concentrations. This finding is similar to research by Komaba & Fukagawa (2016) and Aelion & Wartinger (2010), which found that potassium can affect the transport and solubility of heavy metals like chromium through ionic interactions, possibly increasing Cr levels in water. The model's statistical significance supports the idea that potassium influences the dynamics of Cr concentration.

5.5.4.6 Phosphate (PO_4)

The inverse correlation between phosphate and Cr suggested that higher phosphate levels are associated with lower Cr levels. Seasonal and spatial fluctuations in phosphate concentrations may impact the relationship between PO_4 and Cr. Phosphate and chromium can form insoluble complexes that precipitate out of the water, lowering Cr concentrations (Chen *et al*., 2023; Paerl & Otten, 2013). This process may exhibit variation depending on the environment, as indicated by the non-significant result.

5.5.4.7 Biological Oxygen Demand (BOD^5)

The statistically significant output that an increase in BOD causes an increase in Cr concentration suggests a reliable impact. Seasonal and spatial factors may influence the link between BOD and Cr concentrations, as evidenced by notable seasonal and spatial changes in BOD levels. More oxygen is needed to decompose organic compounds (Lemessa *et al*., 2023). More organic matter in water may affect chromium behavior, potentially by adsorption onto organic particles, similar to results found with higher BOD

levels (Wang *et al*., 2022). The statistical significance indicates that even minor variations in BOD can affect Cr levels in a quantifiable way.

5.5.4.8 Chemical Oxygen Demand (COD)

The analyzed regression results suggest that, in theory, increased COD would lead to lower Cr concentrations. Temporal and spatial changes in the Athi River may impact notable fluctuations in COD levels and the correlation between COD and Cr. Higher COD levels are frequently linked to greater levels of organic pollutants, which can cause Cr (VI) to be reduced to the less harmful Cr (III), potentially lowering Cr levels in water, according to Ngabirano et al. (2016) and Chen (2023). Nonetheless, the non-significant result suggests that the relationship between COD and Cr concentration is complex and situational.

However, **t**he multiple linear regression model results showed that nitrate (NO_3), potassium (K), and biological oxygen demand (BOD) has statistically significant impact on chromium levels in water. However, pH, EC, TDS, phosphate (PO_4), and COD do not. The model only accounts for 36% of the variation in Cr concentration, suggesting that other factors significantly influence chromium levels in water.

5.6 Relationship between the Physical Mid reaches of River Athi Water Quality

The relationships between EC and TDS; EC and BOD; TDS and BOD; Cd and K; Cr and K; Cd and Cr. Including pH against EC, TDS, NO_3, PO_4, and COD; BOD and COD; NO_3 against EC, TDS, and PO_4; and PO_4 against NO_3 and K where analysed using Pearson correlation snalysis.

The findings showed a correlation between higher EC levels and greater TDS concentrations in water. Water quality deteriorates during the dry season, evidenced by a notable increase in both EC and TDS. This may be due to reduced water levels concentrating dissolved solids and enhancing conductivity. The significant positive association indicates that these two measurements increase together, reflecting higher quantities of dissolved chemicals during the dry season. Variances in EC and TDS levels across different locations indicate various sources of dissolved solids and general water

quality. This result is consistent with earlier research showing a substantial association between EC and TDS, explaining why EC is often used as a proxy for TDS (Rodríguez *et al*., 2019). Higher ion concentrations result in enhanced conductivity, a link frequently observed in water quality investigations.

The rise in BOD^5 will coincide with an increase in EC in the water. The substantial positive relationship between EC and BOD indicates that the amount of organic matter broken down by microorganisms rises in tandem with water's electrical conductivity. During the dry season, smaller water volumes lead to higher TDS values, indicating more concentrated dissolved solids. This consistency is seen in the simultaneous rise of EC and BOD levels during the dry season. Stony Athi's high EC suggests larger amounts of dissolved solids and possibly more pollution than Kibwezi sampling stations. This finding showed that BOD levels rose in tandem with EC. High EC levels, often caused by dissolved salts and organic matter, correlate with increased BOD because these substances raise the organic load in water, thus increasing oxygen demand (Kuang *et al*., 2020; Nguyen *et al*., 2021). Significant organic contamination may also be present in areas with high EC concentrations.

Water with higher BOD will also have higher TDS. The substantial positive correlation between TDS and BOD indicates that organic contamination rises alongside dissolved solids concentrations. Elevated BOD values during the February dry season result from high TDS levels, signaling an increase in organic pollutants. Higher TDS levels at the Athi River town and Stony Athi stations suggest either more organic matter or localized pollution sources. This finding aligns with studies showing that higher TDS increases the amount of biodegradable material in water, hence increasing BOD (Wang *et al*., 2019).
The positive association suggests that potassium levels in water may impact cadmium. This might indicate similar pollution sources or specific biological or geochemical processes affecting both ions. Local factors like industrial discharges or agricultural runoff may influence this association. Seasonal changes in potassium could also impact cadmium levels, with concentrations peaking during the dry season (Skowron *et al*., 2018). Increased levels at Kibwezi may result from sectional discharge of industrial waste, wastewater, or

agricultural runoff. Similar interactions between heavy metals and essential elements such as potassium in aquatic ecosystems were explored (Chen *et al*., 2021). They found that potassium can, under certain conditions, increase the mobility and bioavailability of heavy metals like cadmium. Monitoring potassium levels can help predict cadmium contamination and identify areas at risk of heavy metal pollution.

Potassium levels in water rise in tandem with chromium levels. Higher potassium concentrations are linked to higher chromium levels, likely due to common pollution sources such as industrial waste or fertilizers. The high potassium levels during the dry season suggest that similar factors might affect chromium concentrations. This finding is consistent with research by Singh and Gupta (2023), indicating that potassium can influence chromium behavior in water, especially when interacting with other ions. Potassium can serve as an indicator for potential chromium contamination, guiding cleanup and specific testing efforts.

Higher cadmium levels are often followed by higher chromium concentrations, indicating that cadmium and chromium levels rise together in water. Various mechanisms influence the behavior of these metals, as seen in the significant seasonal variations in their concentrations. During the dry season, dilution reduction, high temperatures, limited flow, and pollution buildup lead to increased Cd and Cr concentrations. Spatial variations between test stations suggest localized pollution issues. High levels of cadmium and chromium at the NYS sampling site and Athi River Town indicate pollution hotspots, possibly due to specific urban and industrial activities. This aligns with findings by Zhou (2022), showing that industrial effluents frequently contain both Cd and Cr, leading to associated contamination in water bodies. Combined cadmium and chromium monitoring can enhance the identification and control of heavy metal pollution sources.

Water chemistry clearly demonstrates the correlations between pH and other water quality measures, including EC, TDS, NO_3, PO_4, and COD. By altering the equilibrium among different species of dissolved chemicals, pH can impact their concentrations and correlations. Each association provides insight into how pH influences other variables,

elements, or solutes in water. The strong positive correlation between EC and pH suggests that the concentration of ions causing EC rises with increasing alkalinity. This is consistent with research indicating that alkaline waters typically contain more ions, which raise EC levels (Singh *et al*., 2019). This connection demonstrates how pH influences the solubility of minerals and salts, which in turn impacts the water's overall conductivity (Pal *et al*., 2015).

A moderately positive relationship between pH and TDS aligns with research by Shrestha & Kazama (2007), who noted that pH variations can affect how solids like salts, metals, and minerals dissolve. Certain compounds may become more soluble at higher pH values, raising TDS levels. Elevated TDS can affect water's flavor, hardness, and suitability for irrigation and consumption, making this relationship crucial for assessing water quality (WHO, 2017).

The positive connection between nitrate (NO_3) and pH means that higher pH values often correspond to higher nitrate levels. More alkaline conditions enhance nitrification, a process converting ammonium into nitrate (Wang *et al*., 2019). This relationship is important for environmental monitoring since elevated nitrate levels can cause eutrophication and water quality deterioration (Gupta *et al*., 2021). The solubility of phosphate compounds, influenced by water pH, explains the mild association between pH and PO_4. Phosphates tend to stay in solution in alkaline waters, resulting in higher concentrations in soils and rivers. This association aligns with research by Hooda et al. (2000), which found that slightly alkaline water increases phosphate availability.

The strong positive association between pH and COD suggests that pH variations can substantially impact the organic load in water by affecting the breakdown of organic matter and chemical oxidation processes. Industrial and agricultural runoff, as well as weathering of rock minerals, contribute to the basin's high COD levels, indicating stable pH and increased organic contaminants. According to this correlation, pH can help determine overall water quality and potential organic pollution (Crittenden *et al*., 2012).

The findings showed a relationship between BOD and COD. Following intense rains that may carry organic waste into the river, BOD and COD levels are predicted to rise in February, during significant effluent discharge. Temporal variations in pollution sources, such as Agricultural runoff and periodic industrial discharges, can also cause variations in BOD and COD levels. The link between BOD and COD is particularly noticeable during the rainy season due to increased organic pollution (Nguyen *et al*., 2021; Sun *et al*., 2011). Higher levels of both BOD and COD were found in the upper mid sections of the Athi River with high organic pollution sources, as indicated by the high correlation between the two parameters across sample stations. Lacalamita et al. (2024) noted that BOD and COD are frequently associated since they both evaluate the organic content of water, consistent with their findings. While BOD measures the oxygen needed for microbial breakdown, COD offers a more comprehensive assessment of oxidation potential. High BOD often indicates high COD, and vice versa.

The moderate connection between NO_3, EC, TDS, and PO_4 indicates that these parameters rise or fall together over time, likely due to common pollution sources like agricultural and industrial runoff. The strong correlation between NO_3 and EC reflects nitrates' substantial influence on the water's ionic load and electrical characteristics, particularly in areas like Kyawango with fertilizer runoff and upstream regions with congested sewage discharge during the dry season.

In the Athi River Basin, substantial agricultural activity and wastewater discharge containing nitrate pollution make this link particularly noticeable. The robust associations between nitrate and both EC and TDS indicate that nitrate significantly impacts the overall ionic composition and dissolved solids of water. However, seasonal factors influence these correlations, such as nitrate input during wet seasons and ion concentration during dry periods (Higgins & Worrall, 2021). The relationship between nitrate levels, EC, and TDS varies by location due to human activities and proximity to pollution sources. Given that nitrate and phosphate are major contributors to nutrient-enriched runoff, their association represents the effects of agriculture and nutrient pollution (Gibbs, 2000). Elevated phosphate and nitrate levels in freshwater systems can interact, causing negative water

quality consequences like reduced dissolved oxygen (DO) and increased biological oxygen demand (BOD) (Schindler, 2006). Liu et al. (2023) found that nitrate frequently co-occurs with other anions, like phosphate, in water, resulting in strong correlations. Nitrates ionic character likely causes its relationship with EC and TDS.

Significant positive correlations between potassium, phosphate, and nitrate indicates that when one of these nutrients rises, the others are likely to rise as well. This is common in aquatic ecosystems, where pollution sources and nutrient cycles often cause simultaneous fluctuations. Phosphate and potassium have a significant association due to their sources and presence in fertilizers and agricultural runoff. This finding correspond with Omoruyi & Oghuvwu (2015), Oremo et al. (2020) and Anderson et al. (2002) who found a strong positive correlation between phosphate (PO_4) and nitrate (NO_3) concentrations in both water and sediment, due to similar pollution sources and nutrient cycles in aquatic ecosystems. Correll, (1998) discussed that the concentrations of PO_4 and NO_3 rise in tandem when they seep into adjacent water bodies. Areas with high potassium concentrations, possibly due to intensive farming methods, are also likely to have higher phosphate levels. Though potassium is less reactive than phosphate in aquatic environments, it can still lead to eutrophication, particularly when phosphate concentrations are high. Potassium promotes overall nutrient availability, while phosphate, a limiting factor for algal growth, drives eutrophic conditions (Dodds *et al*., 2002).

The high positive association between phosphate and nitrate suggests they come from similar sources, including animal waste, sewage discharge, and agricultural fertilizers. In water bodies affected by human activity, these nutrients are frequently found together, especially in regions with high fertilizer application rates. Phosphorus and nitrates in aquatic systems can cause eutrophication, leading to algal blooms and oxygen depletion (Smith *et al*., 1999). High nitrate levels often cause phosphate concentrations to rise, exacerbating eutrophic conditions and causing ecological effects like fish kills and biodiversity loss (Dodds *et al*., 2002). The strong positive connections among phosphate, potassium, and nitrate suggest these nutrients often come from similar sources, such as waste pollution and agricultural runoff. However, even if organic fertilizers are released

into the water due to river flow, nitrate levels in this study remain below the WHO drinking water threshold. These connections highlight the potential for nutrient enrichment, where high concentrations of potassium, phosphate, and nitrate can cause eutrophication and water quality degradation.

CHAPTER SIX

6.0 CONCLUSION AND RECOMMENDATIONS

6.1 Conclusion

These studies highlights land use and land cover (LULC) changes in the mid river section, seasonal, and spatial dynamics on water quality of the river Athi basin. The findings revealed LULC transitions for 8 years from 2015 to 2023 and spatial difference of LULC change on water quality across the sampling stations. The studies identified urbanization, agricultural expansion, and climate factors as key drivers of water quality degradation, with elevated pollutants like TDS, EC, BOD, cadmium, and chromium.

The finding identified seasonal variability in physicochemical water quality driven by hydrological factors, geological influences, and anthropogenic factors, and geochemical interactions. The findings highlights temporal fluctuations and higher pollution concentrations in February including EC, TDS, BOD, and COD above WHO drinking water thresholds.

Studies on spatial variation in the physicochemical water quality of the River Athi Basin, identified urban and semi-urban areas as major pollution sources across the sample locations (e.g, Athi River Town, Stony Athi, and NYS). However, NYS sampling station highlighted higher levels of organic pollutants, heavy metals, and low nutrients (BOD, COD, Cr, Cd, PO_4, and NO_3) due to urban and industrial discharges. While Kibwezi Bridge sampling station mitigation pollutants, due to effective natural self-purification.

6.2 Recommendations

This study successfully identified significant pollution sources and potential in the Athi River Basin, considering LULC changes, seasonal water quality variations, and spatial water quality differences. Despite numerous strategies and regulations, pollution issues persist, attributing to the basin's geology, urban centers, topography, and river location. The study makes the following recommendations in light of natural and anthropogenic

factors, including rock weathering, seasonal cycles, spatial land use, and LULC changes' effects on water quality:

1. The Kenya National Environmental Management Authority (NEMA) should implement water resource management techniques that balance ecological sustainability and human needs, including actions to reduce pollution, enhance water conservation, and mitigate climate change effects on freshwater supply.
2. The NEMA & National Environmental Policy (NEP) should establish buffer zones along riverbanks to restrict agricultural activities near water bodies. These zones should incorporate native plants to enhance biodiversity, filter pollutants, and reduce soil erosion. Additionally, tighten and enforce regulations on industrial discharges, urban waste management, and agricultural runoff to significantly reduce pollutant loads entering the Athi River and improve overall water quality.
3. The MWSSP should implement targeted awareness campaigns along the downstream sections of the Athi River, particularly in Kibwezi and surrounding communities to educate the public on the health risks of contaminated water and promote safe water usage practices, including appropriate treatment methods.

6.3 Recommendations for Further Research

1. Research should be conducted on temporal analysis of LULC changes and their impacts on water quality in the River Athi Basin for 30 years period with Land use policy implication.
2. Research should be conducted on seasonal rock-water interactions and the role of geological formations in heavy metal, potassium, and phosphate pollution in river Athi basin.
3. Further study should Model natural river purification processes and predicting pollution reduction efficiency under low-flow conditions using hydrological and environmental parameters.

REFERENCES

Abdelaal, A., Abdelkader, A., Alshehri, F., Elatiar, A., & Almadani, S. A. (2022). Assessment and Spatiotemporal Variability of Heavy Metals Pollution in Water and Sediments of a Coastal Landscape at the Nile Delta. *Water, 14*(23), 3981.

Adeleye, A. O., Shelle, R. O. D., & Akinnigbaghe, A. E. (2012). Pollutant Dynamics and Distribution in Sediments North of Lagos Lagoon Ecosystem. *Journal of Natural and Science, 9*(5), 13-16.

Aelion, C. M., & Wartinger, M. A. (2010). Potassium and its relationship to other cations in urbanized coastal watersheds. *Journal of Environmental Quality, 39*(5), 1663-1670. https://doi.org/10.2134/jeq2009.0485

Agency for Toxic Substances and Disease Registry (ASTDR). (2012). *Toxicological Profile for Lead*. Agency for Toxic Substances and Disease Registry.

Agency for Toxic Substances and Disease Registry (ATSDR). (2008). Toxicological Profile for Cadmium. Draft for Public Comment. U.S. *Department of Health and Human Services.*

Ahogle, A.M.A., Korir, N.K., Houngnandan, P., Abu-Ghunmi, L. and Letema, S. (2023). Bacte-rial Hazards in Urban Stream Irrigation in Peri-urban Interface of Nairobi-Machakos Counties, Kenya. *International Journal of Environmental Studies.* 1-17.

Akash, M. S. (2023). Environmental Impact Assessment and Pollution Control Strategies. *Journal of Environmental Management, 295*, 113209.

Akintunde-Alo, D. A., Owoeye, Y. T., Oyediran, A. E., & Komolafe, O. O. (2020). *Land use land cover dynamics of Ise Forest Reserve, Nigeria*. Faculty of Agriculture International Conference (FAIC), Nnamdi Azikiwe University. https://journals.unizik.edu.ng/faic/article/download/3477/2807/8055

Akpor, O. B., Olaolu, T. D., & Okolie, E. C. (2014). The Effect of Temperature on Nitrate and Phosphate Uptake from Synthetic Wastewater by Selected Bacteria Species. *British Microbiology Research Journal, 4*(3), 328-342.

Anderson, D. M., Glibert, P. M., & Burkholder, J. M. (2002). Harmful algal blooms and eutrophication: Nutrient sources, composition, and consequences. *Estuaries, 25*(4b), 704–726.

Almaden, Y., Duwel, K., & McElroy, W. D. (1996). Environmental and Health Implications of Trace Elements. *Journal of Environmental Health Science and Engineering, 3*(2), 235-246. https://doi.org/10.1007/BF03325869.

Amadi, E. K. (2013). Nutrient Loads and Heavy Metals Assessment along Sosiani River, Kenya. *Chemistry and Materials Research, 3*(12), 14-20.

American Public Health Association (APHA). (2008). Standard Methods for the Examination of Water and Wastewater (20th Ed.). Washington, DC.

American Public Health Association (APHA). (2017). Standard methods for the examination of water and wastewater (23rd Ed.). Washington, DC.

An, M., Song, Y., Jiang, J., Fu, G., Wang, Y., & Wan, X. (2023). Water quality evaluation, spatial distribution characteristics, and source analysis of pollutants in Wanquan River, China. *Applied Sciences*, *13*(7982).

Anatoly, Z. (2011). Chromium in drinking water: Sources, Metabolism, and Cancer Risks. *Chemical Research in Toxicology, 24*(12), 1617–1629.

Apudo, M.G., Odhiambo, K.O., & Rop, S.K. (2016). Impact of Land Use Activities on Itare River Bank Stability and Water Quality in South West Mau Water Catchment, Kenya. *Journal of Environmental Science, Toxicology and Food Technology*. *10*(6), 15-27.

Ashun, E., & Tagoe, N. D. (2024). Anthropogenic drivers of spatial trends in groundwater quality in the Upper Athi River Basin of Kenya, East Africa. *International Journal of Environmental Monitoring and Analysis, 12*(4), 58–73. https://doi.org/10.11648/j.ijema.20241204.11

Aywa, J. O., Njuru, P. G., & Muendo, P. (2016). Suitability of Athi River Water for irrigation within Athi River Town and its Environs. *Archives of Current Research International, 6*(4), 1-13. https://doi.org/10.9734/acri/2016/25193.

Bagnis, S., Boxall, A., Gachanja, A., Fitzsimons, M., Murigi, M., Snape, J., Tappin, A., Wilkinson, J., & Comber, S. (2019). Characterization of the Nairobi River catchment impact zone and occurrence of pharmaceuticals: Implications for an impact zone inclusive environmental risk assessment. *Science of the Total Environment*, *703*, 134925.

Bahiru, D.B. (2020). Determination of heavy metals in wastewater and their toxicological implications around Eastern Industrial Zone, Central Ethiopia. *Journal of Environmental Chemistry and Ecotoxicology*, 12(2), 72-79.

Bai, B., Bai, F., Li, X., Nie, Q., Jia, X., & Wu, H. (2022). The remediation efficiency of heavy metal pollutants in water by industrial red mud particle waste. *Environmental Technology & Innovation, 28*, 102944. https://doi.org/10.1016/j.eti.2022.102944.

Bakan, G., Ozkoc, H. B., Tülek, S., & Cuce, H. (2010). Integrated environmental quality assessment of kizil irmak river and its coastal environment. *Turkish Journal of Fisheries and Aquatic Sciences, 10*, 453–462.

Banko, G. (1998). A Review of Assessing the Accuracy of Classifications of Remotely Sensed Data and of Methods Including Remote Sensing Data in Forest Inventory. *Interim Report IR-98–081*. https://www.silvaprojects.com/

Barakat, A., Baghdadia, M. E., Rais, J., Brahim Aghezzaf, B., & Slassi, M. (2016). Using multivariate statistical techniques to assess spatial and seasonal water quality variation of Oum Er Rbia River (Morocco). *International Soil and Water Conservation Research, 4*, 284–292. https://doi.org/10.1016/j.iswcr.2016.08.005

Bhalerao, S. A., & Sharma, A. S. (2015). Chromium: As an environmental pollutant. *International Journal of Current Microbiology Applied Science, 4*(4), 732-746.

Bhat, B. N., Parveen, S., & Hassan, T. (2018). Seasonal assessment of physicochemical parameters and evaluation of water quality of river Yamuna, India. *Advances in Environmental Technology*, *1*, 41-49.

Billiah, M., Hossain, M. K., & Hasan, M. M. (2016). Assessment of water quality and impact on human health in the Tangail District, Bangladesh. *Journal of Environmental Science and Engineering, 10*(3), 457-468.

Bouida, L., Rafatullah, M., Kerrouche, A., Qutob, M., Alosaimi, A. M., Alorfi, H. S., & Hussein, M. A. (2022). A Review on cadmium and lead contamination: sources, fate, mechanism, health effects and remediation methods. *Water, 14*, 3432. https://doi.org/10.3390/w14213432

Britannica. (2023). Water pollution. *Animals and Nature*. Encyclopedia Britannica. Retrieved from https://www.britannica.com/science/water-pollution.

Bucher, K., Zhou, W. & Stober, I. (2017). Rocks Control the Chemical Composition of Surface Water from the high Alpine Zermatt area (Swiss Alps). *Swiss Journal of Geoscience, 110*:811–831.

Chapman, P.J., Kay, P., & Mitchell, G.N. (2013) .Surface water quality. In: Holden, J, (ed Water resources: an integrated approach. *Routledge*, 79-122.

Chen, M., Zhang, H., Liu, W., & Zhang, W. (2014). The global pattern of urbanization economic growth: Evidence from the last three decades. *PLoS ONE, 9*(8), e103799. https://doi.org/10.1371/journal.pone.0103799.

Chen, P., Wang, S., Liu, Y., Wang, Y., Wang, Y., & Zhang, T. (2023). Water availability in China's oases decreased between 1987 and 2017. *Earth's Future, 11*, e2022EF003340. https://doi.org/10.1029/2022EF003340

Chen, Y., Yang, K., & Zhao, W. (2021). Spatial Variations of Water pH in Urban River Systems: Influences and Implications. Water Research, 202, 117458.

Chepkorir, J. K., Ogendi, G. M., M'erimba, C. M., & Maina, G. M. (2021). Spatial and temporal variations in land use and land cover in the Njoro and Kamweti river catchments, Kenya. *East African Journal of Science, Technology and Innovation, 2*(3), 1–16. https://doi.org/10.37446/eajst/2.3.2021.1-16.

Chishti, K.A., Khan, F.A., & Hassan, S.S.M. (2011). Estimation of heavy metals in the seeds of blue and white capitalism's of *Silybum marianum* grown in various districts of Pakistan. *Journal of Basic and Applied Science*, 7(1), 45-49.

Chrysochoou, M., Theologou, E., & Bompoti, N., Dermatas, D., & Panagiotakis, I. (2016). Occurrence, Origin and Transformation Processes of Geogenic Chromium in Soils and Sediments. *Current Pollution Rep, 2*, 224–235. DOI 10.1007/s40726-016-0044-2.

Chu, X., Wu, D., Wang, H., Zheng, F., Huang, C., & Hu, L. (2021). Spatial distribution characteristics and risk assessment of nutrient elements and heavy metals in the Ganjiang River Basin. *Water, 13*(23), 3367.

Cleveland Clinic. (2024). Hyperkalemia (High Potassium). https://my.clevelandclinic.org/health/diseases/15184-hyperkalemia-high-blood-potassium.

Conley, D. J., Paerl, H. W., Howarth, R. W., Boesch, D. F., Seitzinger, S. P., & Havens, K. (2019). Controlling eutrophication: Nitrogen and phosphorus. *Science, 339*(6114), 775-776. https://doi.org/10.1126/science.1231653.

Connor, R., & Chaves Pacheco, S. M. (2024). Global employment trends and the water dependency of jobs. *UNESCO*

Conserve Energy Future. (2020). *Top 19 most polluted rivers in the world in 2020*. https://www.conserve-energy-future.com/most-polluted-rivers-world.php

Constitution of Kenya. (2010). *Laws of Kenyan*. National Council for Law Reporting. Retrieved from https://www.kenyalaw.org

Correll, D. L. (1998). The role of phosphorus in the eutrophication of receiving waters: A review. *Journal of Environmental Quality, 27*(2), 261-266.

Cozzolino, M., Dusso, A. S., & Slatopolsky, E. (2001). Role of calcium-phosphate product and bone-associated proteins on vascular calcification in renal failure. *Journal of the American Society of Nephrology, 12*(11), 2511–2516.

Crittenden, J. C., Trussell, R. R., Hand, D. W., Howe, K. J., & Tchobanoglous, G. (2012). *MWH's water treatment: Principles and design* (3rd Ed.). John Wiley & Sons, Inc.

Crooks, E. C., Harris, I. M., & Patil, S. D. (2021). Influence of land use land cover on river water quality in rural North Wales, UK. *Journal of the American Water Resources Association, 57*(3), 357-373.

Curtis, E., Comiskey, C., & Dempsey, O. (2016). Importance and use of correlational research. *Nurse Researcher, 23*(6), 20-25.

Dash, S., Borah, S. S., & Kalamdhad, A. S. (2021). Heavy metal pollution and potential ecological risk assessment for surficial sediments of Deepor Beel, India. Ecological Indicators, 122, 107265. https://doi.org/10.1016/j.ecolind.2020.107265

Dodds, W. K., Smith, V. H., & Lohman, K. (2002). Nitrogen and phosphorus relationships to benthic algal biomass in temperate streams. *Canadian Journal of Fisheries and Aquatic Sciences, 59*(5),

Dulo, S. O. (2008). Determination of some physico-chemical parameters of the Nairobi River, Kenya. *Journal of Applied Science & Environmental Management, 12*(1), 57–62.

Duong, V. N., Le, H. V., & Nguyen, H. T. L. (2022). Seasonal and tidal influence on surface water quality – A case study in the Hau River segment, Vietnamese Mekong Delta Province. *Journal of Ecological Engineering, 23*(8), 290–298. https://doi.org/10.12911/22998993/151155.

Eastman, J. R. (2003). *Guide to GIS and Image Processing* (14th ed., pp. 239-247). Clark University Manual, USA.

Economic Commission for Africa. (2012). *The Africa Water Vision for 2025: Equitable and sustainable use of water for socioeconomic development*. United Nations Economic Commission for Africa.

Editorial Team. (2022, April 12). Nature-based benefits in focus: Protecting grasslands reduces soil erosion and improves water quality. *The Climate Trust*. Retrieved from The Climate Trust website: https://www.climatetrust.org.

Elmore, A. J., Mustard, J. F., Manning, S. J., & Lobell, D. B. (2000). Quantifying vegetation change in semiarid environments. *Remote Sensing of Environment, 73*(1), 87–102. https://doi.org/10.1016/S0034-4257 (00)00059-8.

Eneji, I. S., Onuche, A. P., & Sha'Ato, R. (2012). Spatial and temporal variation in water quality of River Benue, Nigeria. *Journal of Environmental Protection, 3*, 915-921. doi:10.4236/jep.2012.32810.

EPA (2012). *Quality assurance, quality control, and quality assessment measures*. EPA841-B-96-003. Environmental Protection Agency, Office of Water, Washington, DC. Retrieved from https://www.epa.gov

EPA. (2022). *Approved methods for the sampling and analysis of water pollutants in NSW*.Environmental Impact Authority. Retrieved from https://www.epa.nsw.gov.au

EPA. (2023). Drinking water standards. U.S. Environmental Protection Agency. https://www.epa.gov/dwstandardsregulations.

Eze, O. C., Tukura, B. W., Atolaiye, B. O., & Opaluwa, O. D. (2018). Spatial and temporal variations in physicochemical properties of an aquatic environment. *Chemical Science International Journal, 23*(1), 1–8. https://doi.org/10.9734/csji/2018/40942.

Falkenmark, M., & Rockström, J. (2004). Balancing water for humans and nature: The new approach in ecohydrology. Routledge.

FAO & IWMI. (2017). *Water pollution from agriculture: A global review*. Food and Agricultural Organization (FAO) and International Water Management Institute (IWMI). Retrieved from https://www.fao.org

Fan, H., Zhang, W., Wu, L., et al. (2024). Soil nitrogen biogeochemistry and hydrological characteristics shape the nitrate levels in a river. *Environmental Geochemistry and Health, 47*(4).

Fischer, R. (2024). The role of forest ecosystems in regulating hydrological cycles and water quality. *Opinion Journal of Biodiversity, Bioprospecting and Development, 10*(3).

Food and Agriculture Organization of the United Nations. (2020). *World food and agriculture 2020: Statistical yearbook*. Retrieved from http://www.fao.org/publications/yearbook.

Fondriest Environmental. (2024, November 23). pH of water. Fondriest Environmental Learning Center. https://www.fondriest.com/environmental-measurements/parameters/water-quality/ph/?utm

Foody, G. M. (2002). Status of land cover classification accuracy assessment. *Remote Sensing of Environment, 80*(1), 185-201.

Forestry. (2024, August 15). *Forest ecosystem services: Carbon sequestration, water filtration, and more*. Forestry.

Fowler, K. J. A., Peel, M. C., Western, A. W., Zhang, L., & Peterson, T. J. (2016). Simulating runoff under changing climatic conditions: Revisiting an apparent deficiency of conceptual rainfall-runoff models. *Water Resources Research, 52*.

Frankfort-Nachmias, C., & Nachmias, D. (2009). *Research methods in the social sciences* (5th Ed.). London, England: Holder Education.

Gadhia, M., Surana, R., & Ansari, E. (2012). Seasonal variations in physico-chemical characteristics of Tapi Estuary in Hazira industrial area. *Our Nature, 10*, 249–257.

Galloway, J. N., Aber, J. D., Erisman, J. W., Seitzinger, S. P., Howarth, R. W., Cowling, E. B., & Cosby, B. J. (2003). The nitrogen cascade. *BioScience, 53*(4), 341–356.

Gardolinski, P. C. F. C., Hanrahan, G., Achterberg, E. P., Gledhill, M., Tappin, A. D., House, W. A., & Worsfold, P. J. (2001). Comparison of sample storage protocols for the determination of nutrients in natural waters. *Water Research, 35*(14), 3670-3678.

Gaston, K. J., Davies, T. W., Bennie, J., & Hopkins, J. (2020). Impacts of artificial light at night on biological timings. *Annual Review of Ecology, Evolution, and Systematics, 51,* 337-360. https://doi.org/10.1146/annurev-ecolsys-011720-103218.

Geldreich, E. E. (2018). Water Quality and Its Control. *Environmental Science and Technology, 45*(11), 4575-4582. https://doi.org/10.1021/es020027g.

Genchi, G., Sinicropi, M. S., & Lauria, G. (2020). Environmental and Health Impacts of Heavy Metals. *Environmental Monitoring and Assessment, 192*(2), 162.

Ghosh, S., & Chakraborty, P. (2018). Impact of High Total Dissolved Solids in Drinking Water on Human Health. *Journal of Environmental Management, 227,* 256-261.

Gibbs, M. M. (2000). Nitrate Contamination in Freshwater Systems: Sources, Effects, and Management. *Science of the Total Environment, 246*(2-3), 127-136.

Gituara, S. M. (2021). Effects of land use distribution on the surface water quality in the upstream section of Nairobi River (C50/5008/2017) [Unpublished master's thesis]. University of Nairobi.

Global Institute for Water Security. (2022). *Global assessment of private sector impacts on water*. Valuing Water Initiative. Ceres.org.

Gobry, J. J., Twisa, S. S., Ngassapa, F., & Kilulya, K. F. (2023). Impact of land-use/cover change on water quality in the Mindu Dam drainage, Tanzania. *Water Practice & Technology, 18*(5), 1086.

Gooch, M. R. (2007). Water Quality Monitoring in the Global Context. *Journal of Water and Climate Change, 8*(2), 112-125.

Gopalan, M., Rosinger, K. O., & Ahn, J. B. (2020). *Use of quasi-experimental research designs in education research: Growth, promise, and challenges*. Review of Research in Education, 44(1), 218–243. https://doi.org/10.3102/0091732X20903302

Government of Kenya (GOK). (2007). Ministry of Water and Irrigation: National Water Service Strategies (NWSS) 2007-2015. Government of the Republic of Kenya (GRK), Vision 2030.

Government of Kenya (GOK). (2013). National Environment Policy (NEP). Kenya Ministry of Environment, Water and Natural Resources (MEWNR).

Government of Kenya (GOK). (2016). Kenya Environmental Sanitation and Hygiene Policy 2016-2030. Ministry of Health.

Government of Kenya (GOK). (2016). Kenyan Water Act Reform. Arrangement of Sections Part I-Preliminary.

Government of Kenya (GOK). (2018). Sector Plan for Environment, Water, Sanitation and Regional Development. Kenya Vision 2030.

Guo, X., Xiao, Y., Zhao, L., Yang, T., Tang, C., Luo, W., Huang, C. and Zheng, F. (2023). Spatiotemporal Analysis and Health Risk Assessment of Heavy Metals in Water from the Fuhe River, South China. *Water*.*15*, 641.

Gupta, D., Sunita, & Saharan, J. (2009). Physicochemical analysis of groundwater of selected areas of Kaithal city (Haryana), India. Researcher, 1(2), 1-5.

Hammoumi, D., Al-Aizari, H. S., Alaraidh, I. A., Okla, M. K., Assal, M. E., Al-Aizari, A. R., Moshab, M. S., Chakiri, S., & Bejjaji, Z. (2024). Seasonal variations and assessment of surface water quality using water quality index (WQI) and principal component analysis (PCA): A case study. *Sustainability, 16*(13), 5644.

He, H., Zhou, J., Wu, Y., Zhang, W. and Xie, X. (2008). Modeling the response of surface water quality to urbanization in Xi'an China. *Journal of Environmental Management*. 86, 731-749.

He, F. J., Tan, M., Ma, Y., & MacGregor, G. A. (2020). Salt reduction to prevent hypertension and cardiovascular disease: JACC state-of-the-art review. *Journal of the American College of Cardiology, 75*(6), 632–647.

Heathwaite, A. L., & Sleigh, P. A. (2020). Understanding Nitrate Dynamics in Agricultural Catchments. *Journal of Environmental Quality, 49*(2), 450-463.

Higgins, R. P., & Worrall, F. (2021). Seasonal and Spatial Variations in Nitrate Concentrations in River Systems. *Water Research, 196*, 117042.

Hooda, P. S., Edwards, A. C., Anderson, H. A., & Miller, A. (2000). A review of water quality concerns in livestock farming areas. *Science of the Total Environment, 250*(1-3), 143–167.

Hou, S., Zhao, X., Liu, Y., Tillotson, M. R., Weng, S., Wang, H., Li, Y., Liu, B., Feng, K., & Zhang, N. (2022). Spatial analysis connects excess water pollution discharge, industrial production, and consumption at the sectorial level. *Npj Clean Water*, *5*(4), 1-9.

Hu Y, Fernández V., & Ma L. (2014). Nitrate transporters in leaves and their potential roles in foliar uptake of nitrogen dioxide. Front Plant Sci 5:360.

Huang, H., Winter, J. M., Osterberg, E. C., Horton, R. M., & Beckage, B. (2017). Total and extreme precipitation changes over the Northeastern United States. *Journal of Hydrometeorology, 18*(6), 1783–1798.

Huang, J., Zhan, J., Yan, H., Wu, F., & Deng, X. (2013). Evaluation of the Impacts of Land Use on Water Quality: A Case Study in the Chaohu Lake Basin. *The Scientific World Journal,* 329187.

Huang, M., Zou, H., & Tan, J. (2022). Spatial water quality analysis of the watercourses in Northwestern New Territories (Hong Kong). *Water Supply*, *22*(8), 6895.

Hunt, J.R. (2003). Bioavailability of iron, zinc, and other trace minerals from vegetarian diets. *American Journal of Clinical Nutrition*, 78(3), 633S-639S.

International Institute for Sustainable Development (IISD). (2024). Zero draft of HLPF outcome commits to accelerated action in years to 2030. *IISD SDG Knowledge Hub*. https://sdg.iisd.org/

International Union for Conservation of Nature (IUCN). (2024, December 20). *Grasslands rising: Restoring vital ecosystems for a sustainable future*. Riyadh, Saudi Arabia.

Islam, M. S., & Mostafa, M. G. (2021). Suitability of Water Quality Index Methods for Assessing Groundwater Quality in the Ganges River Basin area. *H_2 Open Journal, 5*(2), 198. https://doi.org/10.1007/s11356-021-15353-9

Ismail, A., Toriman, M. E., Juahir, H., Md Zain, S., Abdul Habir, N. L., Retnam, A., Kamaruddin, M. K. A., Roslan Umar, R., & Azid, A. (2016). Spatial Assessment and Source Identification of Heavy Metals Pollution in Surface Water Using Several Chemometric Techniques. *Marine Pollution Bulletin, 107*(1), 292-300. https://doi.org/10.1016/j.marpolbul.2016.03.060.

Ituma, S. I., & Anijiofor-Ike, C. S. (2024). Evaluating seasonal variations and quality of surface water in refuse dumpsite-proximal areas using statistical analysis. Rxploremetic *Journal of Innovative Engineering and Technology, 5*(2).

Jafarabadi, A. R., Bakhtiari, A. R., Spano, N., & Cappelloc, T. (2018). First Report of Geochemical Fraction Distribution, Bioavailability and Assessment of Potentially Toxic Inorganic-Elements in Sediments of Coral Reef Islands of Persian Gulf, Iran. *Marine Pollution Bulletin, 137*, 185-197.

JICA (2012). The Development of the National Water Master Plan, 2030. Draft Report: Kenya. Japan International Cooperation Agency.

Jiang, W., Li, L., & Wu, S. (2008). Evaluation of Water Quality in the Taihu Lake Region Using Multivariate Statistical Methods. *Water Research, 42*(8-9), 2022-2032. https://doi.org/10.1016/j.watres.2008.01.027.

Juma, A., & Atieno, S. (2021.). Africa news, climate change, environment, top stories in Science Africa. *Science Africa*. Retrieved from [https://scienceafrica.co.ke/](https://scienceafrica.co.ke/

Jwaideh, M. A. A., Sutanudjaja, E. H., & Dalin, C. (2022). Global Impacts of Nitrogen and Phosphorus Fertilizer Use for Major Crops on Aquatic Biodiversity. *International Journal of Life Cycle Assessment, 27*, 1058-1080.

Kahangwa, C. A. (2022). Application of principal component analysis, cluster analysis, pollution index and geoaccumulation index in pollution assessment with heavy metals from gold mining operations*, Tanzania*. *Journal of Geoscience and Environment Protection*, *10*(4), 303–317.

Kalkhajeh, Y. K., Amiri, B. J., Huang, B., Khalyani, A. H., Hu, W., Gao, H., & Thompson, M. L. (2019). Methods for Sample Collection, Storage, and Analysis of Freshwater Phosphorus. *Water, 11*, 1889.

Kaniz, F., Wan, M. W. O., & Mansor, M. I. (2014). Spatial and Temporal Variation of Physicochemical Parameters in the Merbok Estuary, Kedah, Malaysia. *Tropical Life Sciences Research, 25*(2), 1–19.

Kannel, P. R., Lee, S., & Kanel, S. R. (2007). Application of Multivariate Statistical Techniques to Evaluate Spatial and Temporal Variations in Water Quality of the Bagmati River Basin, Nepal. *Environmental Monitoring and Assessment, 130*(1-3), 121-141.

Kazi, T. G., Arain, M. B., Jamali, M. K., Jalbani, N., Afridi, H. I., Sarfraz, R. A., Baig, J. A., & Shah, A. Q. (2009). Assessment of water quality of polluted lake using multivariate statistical techniques: A case study. *Ecotoxicology and Environmental Safety, 72*(2), 301–309.

Kemper, E. A., Stringfield, S., & Teddlie, C. (2003). Mixed methods sampling strategies in social science research. In A. Tashakkori & C. Teddlie (Eds.), *Handbook of mixed methods in social and behavioral research* (pp. 273–296). Sage Publications.

Kenya National Bureau of Statistics. (2019). *2019 Kenya population and housing census. Volume II: Distribution of population by administrative units* (p. 270). KNBS.

Kestenbaum, B., Sampson, J. N., & Rudser, K. D. (2005). Serum phosphate levels and mortality risk among people with chronic kidney disease. *Journal of the American Society of Nephrology, 16*(2), 520–528.

Khan, M. Y. A., Khan, B., & Chakrapani, G. J. (2016). Assessment of Spatial Variations in Water Quality of Garra River at Shahjahanpur, Ganga Basin, India. *Arabian Journal of Geosciences, 9*, 516.

Kibet, S., & Maina, J. (2021). Influence of Land Use and Seasonal Patterns on River Water Quality in Kenya. *Journal of Environmental Sciences, 98*, 215-224.

Kilonzo, F., Masese, F. O., Griensven, A. V., Bauwens, W., Obando, J., & Lens, P. N. L. (2013). Spatiotemporal Variability in Water Quality Macro-Invertebrate Assemblages in the Upper Mara River Basin, Kenya. *Journal of Physics and Chemistry of the Earth,* 67-69, 75-86.

Kitheka, J. U. (2019). Salinity and salt fluxes in a polluted tropical river: the case study of the Athi River in Kenya. *Journal of Hydrology: Regional Studies, 24*, 100614. https://doi.org/10.1016/j.ejrh.2019.100614.

Kitheka, J. U., Kitheka, L. M., & Njogu, I. N. (2022). Suspended sediment transport in a tropical river basin exhibiting combinations of land uses/land covers and hydro-climatic conditions: A case study of up-per Athi Basin, Kenya. *Journal of Hydrology: Regional Studies, 38*, 100614.

Kithiia, S. M., & Mutua, F. M. (2006). Impacts of land-use changes on sediment yields and water quality within the Nairobi River sub-basins, Kenya. *IAHS Publication, 306*, 582–588.

Kithiia, S. M. (2007). An Assessment of Water Quality Changes within the Athi and Nairobi River Basins during the Last Decade. Water Quality and Sediment Behavior of the Future: *Predictions for the 21st Century. Proceedings of Symposium HS2005 at IUGG2007.*

Kithiia, S. M. (2012). Effects of Sediments Loads on Water Quality within the Nairobi River Basins, Kenya. *International Journal of Environmental Protection, 2*(6), 16-20. https://doi.org/10.1080/03067310902922490.

Kithiia, S. M. (2021). *A critical analysis of the water quality impacts on water resources in the Athi River drainage basin, Kenya*. IntechOpen.

Kokoi, B., Kaluli, J. W., Ndiba, P., & Thiong'o, G. (2015). Seasonal Variation of Surface Water Quality in the Nairobi River System. *Water, Energy, Environment, and Climate. The 2015 JKUAT Scientific Conference,* 221-230.

Komaba, H, Fukagawa, M. (2010). FGF23-parathyroid interaction: implications in chronic kidney disease. *Kidney International, 77*, 292–298.

Kuang, Y., Guo, X., Hu, J., Li, S., Zhang, R., Gao, Q., Yang, X., Chen, Q., & Sun, W. (2020). Occurrence and Risks of Antibiotics in an Urban River in Northeastern Tibetan Plateau. Science Rep.10, 20054.

Kaushal, S. S., Likens, G. E., Jaworski, N. A., Pace, M. L., Sides, A. M., Seekell, D., Belt, K. T., Secor, D. H., & Wingate, R. L. (2011). Rising stream and river temperatures in the United States. *Frontiers in Ecology and the Environment, 9*(9), 461–466.

Lacalamita, D., Mongioví, C., & Crini, G. (2024). Chemical oxygen demand and biochemical oxygen demand analysis of discharge waters from laundry industry: Monitoring, temporal variability, and biodegradability. *Frontiers in Environmental Science, 12*, Article 1387041.

Lambin, E. F., Geist, H. J., & Lepers, E. (2001). Dynamics of land-use and land-cover change in tropical regions. *Annual Review of Environment and Resources, 28*, 205-241.

Langat, P.K., Kumar, L., Koech, R., & Kumer, M. G. (2019). Monitoring of Land Use/Land -Cover dynamics using remote sensing: A case of Tana River Basin, Kenya. *Geocarto International*, 1-29.

Lanmandjèkpogni, M.P.S., De Paule Codo, F., Yao, B.K., & Aina, M.P. (2018). Seasonal Variation of Nutrient Pollution and Suspended Solids in the Drainage Network of Okpara Basin in Parakou (North-East of Benin). *Journal of Environmental Protection. 9*, 1359-1371.

Lawniczak, A. E., Zbierska, J., Nowak, B., Achtenberg, K., Grześkowiak, A., & Kanas, K. (2016). Impact of agriculture and land use on nitrate contamination in groundwater and running waters in central-west Poland. Environmental Monitoring and Assessment, 188(172).

Le Diem Kieu, & Pham Quoc Nguyen. (2025). *Effects of season and aquifer on groundwater quality in the Mekong delta: A case study in Dong Thap province*. *Ecological Engineering & Environmental Technology*, *26*(6), 321–336.

Lee, A., & Nikraz, H. (2015). BOD: COD ratio as an indicator for river pollution. International Proceeding of Chemical, Biological, and Environmental Engineering, 88, 89-94.

Lei, C., Wagner, P. D., & Fohrer, N. (2021). Influences of Land Use Changes on the Dynamics of Water Quantity and Quality in the German Lowland Catchment of the Stör, *Hydrology Earth System. Science. 26*, 2561–2582.

Lemessa, F., Simane, B., Seyoum, A., & Gebresenbet, G. (2023). Assessment of the impact of industrial wastewater on the water quality of rivers around the Bole Lemi Industrial Park (BLIP), Ethiopia. *Sustainability, 15*(4290), 1-15.

Li, D., Chang, F., Wen, X., Duan, L., & Zhang, H. (2022). Seasonal Variations in Water Quality and Algal Blooming in Hypereutrophic Lake Qilu of Southwestern China. *Water. 14*, 2611.

Liang, Z., Siegert, M., Fang, W., Sun, Y., Jiang, F., Lu, H., Chen, G.-H., & Wang, S. (2018). Blackening and odorization of urban rivers: A bio-geochemical process. FEMS Microbiology Ecology, 94(3), fix180.

Ling, T.Y., Soo, C.-L., Phan, T.-P., Nyanti, L., Sim, S.-F., & Grinang, J. (2017). Assessment of water quality of Batang Rajang at Pelagus Area, Sarawak, Malaysia. *Sains Malaysiana, 46*(3), 401–411. http://dx.doi.org/10.17576/jsm-2017-4603-07.

Liu, J., Zhang, D., Tang, Q., Xu, H., Huang, S., Shang, D.,& Li, Y. (2021). Water quality assessment and source identification of the Shuangji River (China) using multivariate statistical methods. *PLOS ONE, 16*(1), e0245525. https://doi.org/10.1371/journal.pone.0245525

Liyanage, C. P., & Yamada, K. (2017). Impact of population growth on the water quality of natural water bodies. *Sustainability, 9*(8), 1405.

Locke, K. A. (2024). Impacts of land use/land cover on water quality: A contemporary review for researchers and policymakers. *Water Quality Research Journal, 59*(2), 89. https://doi.org/10.2166/wqrj.2024.002

Lwanga, A., Tsingalia, H., Agevi, H., & Shilenje, Z. (2022). Effects of sand-harvesting on river water quality and riparian soil physico-chemical properties. *Open Journal of Ecology, 12*, 570-583. https://doi.org/10.4236/oje.2022.128032.

Ma, X., Wang, L., Yang, H., Li, N. and Gong, C. (2020). Spatiotemporal Analysis of Water Quality Using Multivariate Statistical Techniques and the Water Quality Identification Index for the Qinhuai River Basin, East China. *Water.12*, 2764.

MacDonald, A. M., Shamsudduha, M., Taylor, R. G., & Scanlon, B. R. (2016). *Groundwater and resilience to climate change in sub-Saharan Africa*. *Nature Geoscience*, 9(3), 163–167. https://doi.org/10.1038/ngeo2650

Mbayaki, H. (2015, December). *Assessment of land use land cover change and decline in sugarcane farming using GIS and remote sensing - A case study of Mumias District, Kenya* (Master's thesis). Dedan Kimathi University of Technology.

Maher, S., & Chamberlain, A. (2014). Water quality assessment in semi-arid regions: Challenges and strategies. *Environmental Science and Pollution Research, 21*(5), 3096-3107. https://doi.org/10.1007/s11356-013-2266-5.

Mahmood, Q., Asif, M., Shaheen, S., Hayat, M.T. and Ali, S. (2019). Cadmium Contamination in Water and Soil. Cadmium Toxicity and Tolerance in Plants. *Elsevier.* 141-161.

Maja, M.M., Ayano, S.F. (2021). The Impact of Population Growth on Natural Resources and Farmers' Capacity to Adapt to Climate Change in Low-Income Countries. *Earth System Environment. 5*, 271–283. https://doi.org/10.1007/s41748-021-00209-6.

Manning, D. A. C. (2010). Mineral sources of potassium for plant nutrition: A review. *Agronomy for Sustainable Development, 30*(2), 81–294.

Marín Celestino, J. L., Martínez Cruz, D. A., Otazo Sánchez, E. M., Gavi Reye, F., & Vásquez Soto, D. (2018). Groundwater quality assessment: An improved approach to K-means clustering, principal component analysis and spatial analysis, A case study. *Water, 10*(4), 437.

Markowitz, G.S, & Perazella, M.A. (2009). Acute phosphate nephropathy. *Kidney Int, 76*, 1027–1034.

Marthe, Y.K., Lanciné, G.D., Bamory, K., Aristide, D.G. and Ardjouma, D. (2015). Seasonal and Spatial Variations in Water Physicochemical Quality of Coastal Potou Lagoon (Côte d'Ivoire, Western Africa). *Journal of Water Resource and Protection. 7*, 741-748.

Masime, P., K'Oreje, K.K., Chebii, F., Okoth, M., Lutta, S., Demeestere, K. and De Wispelaere, P. (2022). Physical-chemical water quality assessment of rivers within the athi river basin area, Kenya. *Africa Environmental Research Journal*. *5*(2), 144-155.

Mateo-García, G., G´omez-Chova, L., Amor´os-L´opez, J., Mu˜noz-Marí, J. and Camps-Valls, G., (2018). Multitemporal cloud masking in the Google Earth Engine. *Remote Sens. 10* (7), 7–9.

Mei, K., Liao, L., Zhu, Y., Lu, P., Wang, Z., Dahlgren, R.A. and Zhang, M. (2014). Evaluation of spatial-temporal variations and trends in surface water quality across rural-suburban-urban interface. *Journal of Environmental Science Pollution Resource. 21*, 8036–8051.

Meng, Y., Liu, X., Wu, L., Liu, M., Zhang, B., & Zhao, S. (2019). Spatio-temporal variation indicators for landscape structure dynamics monitoring using dense normalized difference vegetation index time series. *Ecological Indicators*, *107*, 105607.

Ming, M. M., Gao, L., Zhang, H., Ge, J., Zhang, Z., Qiu, Y., & Zhao, Y. (2023). Effects of land use on water quality at different spatial scales in the middle reaches of Huaihe River. *Journal of Freshwater Ecology*, *38*(1), 2176373. https://doi.org/10.1080/02705060.2023.2176373

Mkude, I. T., Kodom, K., Afolayan, A. O., Saria, J., & Mihale, M. J. (2018). Spatial and temporal variations of physicochemical parameters in surface water of Wami River, Tanzania. *International Journal of Development and Sustainability*, *7*(6), 1936-1945.

MMSD (2002). Potash Case Study. *Mining, minerals, and Sustainable Development. International Fertilizer Development Center and United Nations Industrial Development Organization, Fertilizer Manual*. (1-9). Muscle Shoals, AL: IFDC.

Mngube, F. M., Kapiyo, R., Aboum, P., Anyona, D., & Dida, G. O. (2020). *Subtle impacts of temperature and rainfall patterns on land cover change overtime and future projections in the Mara River Basin, Kenya*. *Open Journal of Soil Science*, 10(9), 327–358. https://doi.org/10.4236/ojss.2020.109018

Molekoa, M. D., Avtar, R., Kumar, P., Minh, H. V. T., Dasgupta, R., Johnson, B. A., Sahu, N., Verma, R. V., & Yunus, A. P. (2021). Spatiotemporal analysis of surface water quality in Mokopane area, Limpopo, South Africa. *Water*, *13*, 220.

Mook, W. G. (2000). Introduction to isotope hydrology: A review. Springer.

Moravcová, J., Pavlíček, T., Ondr, P., Koupilová, M., & Kvítek, T. (2013).Comparison of parameters influencing the behavior of concentration of nitrates and phosphates during different extreme rainfall-runoff events in small watersheds. *Hydrology and Earth System Sciences Dis- cussions, 10*, 12105–12151. https://doi.org/10.5194/hessd-10-12105-2013

Muia V. K., Opere A. O., Ndunda E.,& Amwata D. A. (2024). Rainfall and Temperature Trend Analysis using Mann-Kendall and Sen's Slope Estimator Test in Makueni County, Kenya, *Journal of Material and Environmental Science, 15*(3), 349-367.

Mukherjee, M., & Nelliyat, P. (2006). Groundwater Pollution and Emerging Environmental Challenges of Industrial Effluent Irrigation in Mettupalayam Taluk, Tamil Nadu. Comprehensive Assessment of Water Management in Agriculture Discussion Paper 4. *International Water Management Institute*. P O Box 2075, Colombo, Sri Lanka.

Mukherjee, P., Kumar, P., Gupta, S. K., & Kumar, R. (2022). Seasonal variation in physicochemical parameters and suitability for various uses of Bouli pond water, Jharkhand. *Water Science*, *36*(1), 125-131. https://doi.org/10.1080/11104929.2022.2021456

Munyaneza, O., Wenninger, J., & Uhlenbrook, S. (2012). Hydrological Earth System Science, 16, 1991-2004.

Musselman, R. (2012). *Sampling procedure for lake or stream surface water chemistry* (Res. Note RMRS-RN-49). U.S. Department of Agriculture, Forest Service, Rocky Mountain Research Station.

Musyoki, M. A., Suleiman, A. M., Mbithi, N. J., & Maingi, J. M. (2013). Water-borne bacterial pathogens in surface waters of Nairobi River and health implication to communities' downstream Athi River. *International Journal of Environmental Studies*, *70*(1), 4-10.

MWSI and WRA (2020). Athi Integrated Water Resources and Management and Development Plan, Final Report. Technical report prepared for The Ministry of Water, Sanitation, and Irrigation, Republic of Kenya, by Aurecon Amei Limited, Ebene Mauritius, 307.

National Aeronautics and Space Administration. (2024). NASA satellites reveal abrupt drop in global freshwater levels. *NASA's Earth Science News Team.* By James R. Riordon.

National Research Council. (2005). *How students learn: Science in the classroom*. The National Academies Press.

Ndugga, P. (2021). *Correlation between land use and stream water quality: A \case study of Kinawataka stream catchment in Uganda* (Master's thesis). *Kyambogo University.*

Ngabirano, H., Byamugisha, D., & Ntambi, E. (2016). Effects of seasonal variations in physical parameters on quality of gravity flow water in Kyanamira Sub-County, Kabale District, Uganda. *Journal of Water Resource and Protection, 8*(11), 1297-1309. https://doi.org/10.4236/jwarp.2016.811104.

Ngatia, L. W., & Mutua, B. M. (2022). Impacts of agricultural runoff on river water pH during rainy seasons. *Water Resources Management, 36*(4), 987-1001. https://doi.org/10.1007/s11269-022-03073-1.

Ngatia, M., Kithiia, S. M., & Voda, M. (2023). Effects of anthropogenic activities on water quality within Ngong River Sub-Catchment, Nairobi, Kenya. *Water, 15*(3), 660. https://doi.org/10.3390/w15030660.

Nguyen, T. N., Nguyen, T. X., Pham, T., & Nguyen, D. T. (2021). Applying the Soil and Water Assessment Tool model for integrated lake basin management in Northern Vietnam: Case study of the Thac Ba Reservoir Basin. *Environmental Engineering Science, 38*(11), 695–705.

Nguyen, M. H., Tran, T. A., Van, H. T., Hoang, T. H. N., Phan, P. C. M., Nguyen, C. L., Nguyen, D. T., & Pham, T. H. (2023). Surface water quality assessment in the Bach Dang river basin, Vietnam: Using water quality index and geographical information system methods. *Environmental Research Communications*, *5*(075015).

Nimi, G. D., Marc, J. M., & Andrew, P. C. (2018). Urban land-use dynamics in the Niger Delta: The case of Greater Port Harcourt Watershed. *Journal of Urban Science, 2*(1), 108.

Njuguna, S. M., Yan, X., Gituru, R. W., Wang, Q., & Wang, J. (2017). Assessment of macrophyte, heavy metal, and nutrient concentrations in the water of the Nairobi River, Kenya. *Environmental Monitoring and Assessment, 189*, 454. https://doi.org/10.1007/s10661-017-6161-7.

Ogbonna, V. A., & Emenike, A. C. (2021). Assessment of reclaimed wetland groundwater quality in Omuoko Aluu, Ikwerre Local Government Area, Rivers State, Nigeria. *International Research Journal of Modernization in Engineering Technology and Science, 3*(10), 11-39.

Ogbonna, V. A., Kauti, M., Ndungu, C., & Kiruki, H. (2025). Impact of land use land cover change on water quality of Athi River Basin, Kenya. *Journal of Geography, Environment and Earth Science International, 29*(4), 67–91. https://doi.org/10.9734/jgeesi/2025/v29i4879

Ojok, W., Wasswa, J., & Ntambi, E. (2017). Assessment of seasonal variation in water quality in River Rwizi using multivariate statistical techniques, Mbarara Municipality, Uganda. *Journal of Water Resource and Protection, 9*(1), 83-97. https://doi.org/10.4236/jwarp.2017.91006

Oketola, A. A., Adekolurejo, S. M., & Osibanjo, O. (2013). Water quality assessment of River Ogun using multivariate statistical techniques. *Journal of Environmental Protection, 4*(466), 466-479.

Okoth, P. F. (2003). *A hierarchical method for soil erosion assessment and spatial risk modelling: A case study of Kiambu District in Kenya* (Doctoral dissertation, Wageningen University). Wageningen University and Research Centre. p. 232.

Olang, L.O and Josef, F. (2011). Effects of Land Cover Change on Flood Peak Discharges and Runoff Volumes: Model Estimates for the Nyando River Basin, Kenya. *Hydrological Processes. 25*(1), 80-89.

Omer, N. H. (2019). Water quality parameters: Science, assessments, and policy. *IntechOpen Journal*, 1–18.

Omondi, O. C., Ndolo, J. I., Nyandega, I. A., & Ang'u, C. (2019). Impact of rainfall variability on surface water resources in Homa Bay County, Kenya. *Journal of Sustainable Environment and Peace, 1*(3), 84–90.

Omoruyi, C. I., & Oghuvwu, P. O. (2015). Concentration level of phosphate and nitrate in Ikpoba River of Edo State, Nigeria. Proceedings of the 11th Annual National Conference of The Association for Encouraging Qualitative Education in Nigeria, Adeyemi College of Education Ondo, Ondo State, 7E01D2. *Academic Journals.*

One Earth. (2022). Persistent Degradation: Global Water Quality Challenges and Required Actions. *One Earth Commentary*, *5*(2), 129-131.

Ontumbi, G. M., & Sanga, J. K. (2018). Spatial-Temporal Variation of Selected Water Quality Parameters along River Sosiani, Uasin Gishu County. *Africa International Journal of Multidisciplinary Research*, 2(5), 1-9.

Oremo, J., Orata, F., Owino, J., & Shivoga, W. (2020). Assessment of available phosphates and nitrates levels in water and sediments of River Isiukhu, Kenya. *Applied Ecology and Environmental Sciences, 8*(3), 119–127.

Owens, P. N., Batalla, R. J., Collins, A. J., Gomez, B., Hicks, D. M., Horowitz, A. J., & Walling, D. E. (2005). Fine-Grained Sediment in River Systems: Environmental Significance and Management Issues. *River Research and Applications*, 21(7), 693-717.

Owino, J. A., & Owino, F. O. (2023). Seasonal Variations and Their Influence on Water Quality in Tropical Rivers. *Environmental Monitoring and Assessment, 195*(2), 145.

Oze, C., Bird, D. K., & Fendorf, S. (2007). Genesis of hexavalent chromium from natural sources in soil and groundwater. *Proceedings of the National Academy of Sciences, 104*(16), 6544–6549.

Padedda, B. M., Lugliè, A., Lai, G. G., Giadrossich, F., Satta, C. T., & Pulina, S. (2022). Land-Based Impact of Nutrient Loads and Eutrophication on an Ancient Mediterranean Natural Lake. *Hydrology*, 9(7).

Paerl, H. W., & Otten, T. G. (2013). Harmful Cyanobacterial Blooms: Causes, Consequences, and Controls. *Microbial Ecology*, *65*(4), 995–1010.

Pal, M., Samal, N. R., Roy, P. K., & Roy, M. B. (2015). Electrical conductivity of lake water as environmental monitoring: A case study of Rudrasagar Lake. *IOSR Journal of Environmental Science, Toxicology and Food Technology, 9*(3), 66–71.

Patel, P., Raju, N. J., Reddy, B. C. S. R., Suresh, U., Sankar, D. B., & Reddy, T. V. K. (2018). Heavy metal contamination in river water and sediments of the Swarnamukhi River Basin, India: Risk assessment and environmental implications. Environmental Geochemistry and Health, 40, 609–623. https://doi.org/10.1007/s10653-017-0006-7.

Paul, M. J., & Meyer, J. L. (2001). Streams in the urban landscape. *Annual Review*

Pericherla S, Karnena MK, Vara S. (2020). A review on impacts of agricultural runoff on freshwater resources. *International Journal on Emerging Technologies, 11*, 829–833.

Petropoulos, G. P., Kalivas, D. P., Georgopoulou, A., & Srivastava, P. K. (2015). Urban Vegetation Cover Extraction from Hyperspectral Imagery and Geographic Information System Spatial Analysis Techniques: Case of Athens, Greece. *Journal of Applied Remote Sensing*, 9(1), 096088.

Plourde, L., & Congalton, R. G. (2003). Sampling method and sample placement: How do they affect the accuracy of remotely sensed maps? *Photogrammetric Engineering & Remote Sensing*, *69*(3), 289-297.

Poore, J. and Nemecek, T. (2018). Reducing Food's Environmental Impacts through Producers and Consumers. *Science*. *360*, 987–992.

Prasol Training and Consulting Ltd. (2012). *Environmental and social impact assessment study report – Proposed multipurpose Thwake Dam*. Report to Tanathi Water Services Board and Ministry of Water and Irrigation, 89.

Ptáček, P. (2016). Phosphate rock. In *Handbook of Environmental Materials Management* (pp. 335-381). IntechOpen. https://doi.org/10.1016/B978-0-08-097397-2.00019-7.

Putri, R. J., Florensia, A. S., Asmara, A. A., Yulianto, A., & Brontowiyono, W. (2021). A spatiotemporal analysis of water quality and land use in Tambayakbayan River, Yogyakarta. *IOP Conference Series: Earth and Environmental Science*, *933*(1), 012045. https://doi.org/10.1088/1755-1315/933/1/012045.

Rahardjo, D., Djumanto, & Manusiwa, W.S., Prasetyaningsih, A. (2021). The chromium concentration downstream of the Opak River, Yogyakarta, Indonesia. *Applied Ecology and Environmental Research*, 14(1), 569-602.

Rahman, A., Jahanara, I., & Jolly, Y.N. (2021). Assessment of physicochemical properties of water and their seasonal variation in an urban river in Bangladesh. *Water Science and Engineering*, 14, 139–148.

Rahman, K., Barua, S., & Imran, H. M. (2009). Assessment of water quality and apportionment of pollution sources of an urban lake using multivariate statistical analysis. *Journal of Cleaner Engineering and Technology*, *5*(100309), 100309.

Ratemo, M. K. (2018). Investigating the impact of anthropogenic activities on the water quality of the Athi River in Machakos County, Kenya. *Journal of Environmental Science, Toxicology and Food Technology*, *12*(4), 01-29.

Ren, Q., & Hui, L. (2021). Spatiotemporal effects and driving factors of water pollutants discharge in Beijing-Tianjin-Hebei region. *Water*, *13*(8), 1174.

Reza, R., & Singh, G. (2010). Heavy metal contamination and its indexing approach for river water. International *Journal of Environmental Science and Technology, 7*, 785–792. https://doi.org/10.1007/BF03326187.

Richards, J., & Jia, X. (2006). *Remote sensing digital image analysis: An introduction* (4th Ed.). Springer.

Rivett, M. O., Buss, S. R., Morgan, P., Smith, J. W. N., & Bemment, C. D. (2008). Nitrate attenuation in groundwater: A review of biogeochemical controlling processes. *Water Research, 42*(16), 4215–4232.

Rodell, M., Barnoud, A., Robertson, F. R., Allan, R. P., Bellas-Manley, A., Bosilovich, M. G., Chambers, D., Landerer, F., Loomis, B., Nerem, R. S., O'Neill, M. M., Wiese, D., & Seneviratne, S. I. (2024). An abrupt decline in global terrestrial water storage and its relationship with sea level change. *Surveys in Geophysics, 45*(1875–1902).

Rodríguez, M., García, C., & López, P. (2019). Evaluating the Impact of Land Use on Water Quality in aRiver Basin. *Journal of Environmental Quality, 48*(5), 1420-1429.

Rotich, B., & Ojwang, D. (2021). Trends and drivers of forest cover change in the Cherangany hills forest ecosystem, western Kenya. *Global Ecology and Conservation, 30*, e01755.

Rotich B, Kindu M, Kipkulei H, Kibet S, Ojwang D. (2022). Impact of land use/land cover changes on ecosystem service values in the Cherangany Hills water tower, Kenya. *Environ Challenges, 20*; 100576.

Rwanga, S. S., & Ndambuki, J. M. (2017). Accuracy assessment of land use/land cover classification using remote sensing and GIS. *International Journal of Geosciences, 8*(4), 611-622.

Saeedi, M., Li, L. Y., & Salmanzadeh, M. (2019). Heavy metals and their adsorption characteristics in soil: A review. *Environmental Monitoring and Assessment, 191*(2), 120. https://doi.org/10.1007/s10661-019-7217-5.

Salah, E. A. M., Turki, A. M., & Al-Othman, E. M. (2012). Assessment of water quality of Euphrates River using cluster analysis. *Journal of Environmental Protection, 3*(12), 1621–1625.

Samlafo, V. B., Tordzro, K. G., Ankudze, B., & Mahama, A. (2022). Assessment of seasonal variations in water quality of River Tordzie, Ghana. *Journal of Resources and Environment, 12*(2), 59-65.

Sarkar, A., Mohanty, B. P., & Pattnaik, S. K. (2016). Assessing the effects of anthropogenic activities on the water quality of the Mahanadi River, India. *Environmental Monitoring and Assessment, 188*(6), 349.

Shadish, W. R., Cook, T. D., & Campbell, D. T. (2002). *Experimental and quasi-experimental designs for generalized causal inference*. Houghton Mifflin.

Schindler, D. W. (2006). Recent advances in the understanding and management of eutrophication. *Limnology and Oceanography, 51*(1, part 2), 356–363. https://doi.org/10.4319/lo.2006.51.1 part_2.356.

Sherris, A. R., Baiocchi, M., Fendorf, S., Luby, S. P., Yang, W., & Shaw, G. M. (2021). Nitrate in drinking water during pregnancy and spontaneous preterm birth: A retrospective within-mother analysis in California. *Environmental Health Perspectives, 129*(5), 57001. https://doi.org/10.1289/EHP8205.

Shortle, J. S., Mihelcic, J. R., Zhang, Q., & Arabi, M. (2019). Nutrient control in water bodies: A systems approach. *Journal of Environmental Quality, 49*(2), 517-533.

Shrestha, S., & Kazama, F. (2007). Assessment of surface water quality using multivariate statistical techniques: A case study of the Fuji River basin, Japan. *Environmental Modelling & Software, 22*(4), 464–475.

Shrestha, S., Kazama, F., & Nakamura, T. (2007). Use of principal component analysis, factor analysis, and discriminant analysis to evaluate spatial and temporal variations in the water quality of the Mekong River. *Journal of Hydroinformatics, 10*(1), 43-56. https://doi.org/10.2166/hydro.2008.008/.

Sidhu, N., Pebesma, E., & Câmara, G. (2018). Using Google Earth Engine to detect land cover change: Singapore as a use case. *European Journal of Remote Sensing, 51*(1), 486-500.

Sigleo, A., & Frick, W. (2003). Seasonal variations in river flow and nutrient concentrations in a northwestern USA watershed. *Water Research, 37*(2), 370-375.

Simeonov, V., Stratis, J. A., Samara, C., Zachariadis, G., Voutsa, D., Anthemidis, A., Sofoniou, M., & Kouimtzis, T. (2003). Assessment of the surface water quality in Northern Greece. *Water Research, 37*(17), 4119–4124.

Singh, A. K., & Gupta, S. K. (2023). *Removal of chromium ion by chemically modified kinnow peel and its isotherm study*. *International Journal of Environmental Research, 17*(2), 145–158. https://doi.org/10.31838/ijers.2023.17.2.145.

Singh, K. P., Malik, A., Mohan, D., & Sinha, S. (2005). Water quality assessment and apportionment of pollution sources of Gomti river (India) using multivariate statistical techniques: A case study. *Analytica Chimica Acta, 538*(1–2), 355–374.

Singh, P., Kumar, R., & Sharma, R. (2020). Impact of Point Sources on pH Levels in River Water: A Case Study. *Environmental Monitoring and Assessment, 192*(9), 543.

Singh, S. K., Das, S., Singh, S., Pradhan, N., Gajamer, V. R., Kumar, S., Lepcha, Y. D., & Tiwari, H. K. (2019). Physicochemical parameters and alarming coliform count of the potable water of Eastern Himalayan State Sikkim: An indication of severe fecal contamination and immediate health risk. *Frontiers in Public Health, 7*, 174.

Siwiec, T., Kiedryńska, L., Abramowicz, K., Rewicka, A., & Nowak, P. (2011). BOD measuring and modeling methods – Review. *Land Reclamation, 43*(2), 143–153.

Skowron, P., Skowrońska, M., Bronowicka-Mielniczuk, U., Filipek, T., Igras, J., Kowalczyk-Juśko, A., & Krzepiłko, A. (2018). Anthropogenic sources of potassium in surface water: The case study of the Bystrzyca river catchment, Poland. *Agriculture, Ecosystems & Environment, 265*, 454-460. https://doi.org/10.1016/j.agee.2018.07.006.

Slatopolsky, E., Finch, J., & Denda, M. (1996). Phosphorus restriction prevents parathyroid gland growth. High phosphorus directly stimulates PTH secretion in vitro. *Journal of Clin Invest. 97*, 2534–2540.

Smith, V. H., Tilman, G. D., & Nekola, J. C. (1999). Eutrophication: Impacts of excess nutrient inputs on freshwater, marine, and terrestrial ecosystems. *Environmental Pollution, 100*(1-3), 179-196.

Song, J. K., Luo, H., Yin, X.H., Huang, G.L., Luo, S.Y., Lin, D.R., & Yuan, D.B. (2015). Association between cadmium exposure and renal cancer risk: A meta-analysis of observational studies. *Scientific Reports*, 5, 17976.

Sposito, G. (2008). "The Chemistry of Soils." Oxford University Press. Link

Srinivas, N., Das, A., & Satyanarayana, V. (2019). Impact of electrical conductivity on drinking water quality and human health. *Water Resources Management, 33*(4), 1341-1353.

Stumm, W., & Morgan, J. J. (2012). *Aquatic chemistry: Chemical equilibria and rates in natural waters* (3rd Ed.). Wiley.

Sudarshan, P., Mahesh, M. K., & Ramachandra, T. V. (2019). Assessment of seasonal variation in water quality and water quality index (WQI) of Hebbal Lake, Bangalore, India. *Environment and Ecology, 37*(1B), 309–317.

Sullivan, D., Burn, R., & Johnson, J. (2022). "Variation in Electrical Conductivity in River Systems: Factors and Implications." *Hydrology Research, 53*(4), 745-756.

Suma, R., & Srinivasa, G. (2020). *Influence of rainfall patterns on river water quality in tropical regions*. In D. Ayejoto et al. (Eds.), *Influence of Seasonal Changes on the Quality of Water Resources in Southwestern Nigeria* (pp. 423–447). Springer.

Sun, K., Jiang, B., & Jiang, X. (2011). Electrochemical desorption of self-assembled monolayers and its applications in surface chemistry and cell biology. *Journal of Electroanalytical Chemistry*, 656(1), 223-230.

Sutherland, W. J., Fleishman, E., Clout, M., Gibbons, D. W., Lickorish, F., Peck, L. S., Pretty, J., Spalding, M., & Ockendon, N. (2019). Ten years on: A review of the first global conservation horizon scan. *Trends in Ecology & Evolution, 34*(2), 139–153.

Tahiru, A. A., Doke, D. A., & Baatuuwie, B. N. (2020). Effect of land use and land cover changes on water quality in the Nawuni catchment of the White Volta Basin, Northern Region, Ghana. *Applied Water Science, 10*, 198.

Tamiminia, H., Salehi, B., Mahdianpari, M., Quackenbush, L., Adeli, S., & Brisco, B. (2020). Google Earth Engine for geo-big data applications: A meta-analysis and systematic review. *ISPRS Journal of Photogrammetry and Remote Sensing, 164*, 152–170.

Tang, J., Song, P., Hu, X., Chen, C., Wei, B., & Zhao, S. (2023). Coupled effects of land use and climate change on water supply in SSP–RCP scenarios: A case study of the Ganjiang River Basin, China. *Ecological Indicators, 154*, 110745.

Tanjung, R.H.R., Hamuna, B., & Alianto, A. (2019). Assessment of water quality and pollution index in coastal waters of Mimika, Indonesia. *Journal of Ecological Engineering*, 20(2), 87–94.

Tchobanoglous, G., Burton, F. L., & Stensel, H. D. (2003). Wastewater engineering: Treatment and reuse. McGraw-Hill.

Tesfaye,T,, Tesfau, H., Balcha, A. and Hassen, M. (2021). Assessment of the Level of Some Selected Heavy Metals and Physicochemical in Abzana Water , Kibet Woreda, Ethiopia. *Research Square*. 1-15.

Tokareva, I. V., & Prokushkin, A. S. (2022). Seasonal and spatial variability of dissolved nutrients in the Yenisei River. *Water, 14*, 3935.

Toriman, M. E., Alssgeer, H. M. A., Gasim, M. B., Kamarudin, K. A., Daw, M. M., & Alabyad, L. O. M. (2018). Impacts of land-use changes on water quality by an application of GIS analysis: A case study of Nerus River, Terengganu, Malaysia. *International Journal of Engineering and Technology, 7*(3.14), 155-164.

Torres-Martínez, J. A., Mora, A., Mahlknecht, J., Daesslé, L. W., Cervantes-Avilés, P. A., & Ledesma-Ruiz, R. (2021). Estimation of nitrate pollution sources and transformations in groundwater of an intensive livestock-agricultural area (Comarca Lagunera), combining major ions, stable isotopes and MixSIAR model. Environmental Pollution, 269, 115445.

Tumolo, M., Ancona, V., De Paola, D., Losacco, D., Campanale, C., Massarelli, C., & Uricchio, V. F. (2020). Chromium pollution in European water: Sources, health risk, and remediation strategies: An overview. *International Journal of Environmental Research and Public Health, 17*(15), 5438.

Turner, B. L., Skole, D., & Sanderson, S. (1994). Land-use and land-cover change: Science/research plan. *International Geosphere-Biosphere Programme*.

Uddin, M. G., Moniruzzaman, M., Al-Amin Hoque, M., Hasan, M. A., & Khan, M. (2016). Seasonal variation of physicochemical properties of water in the Buriganga River. *World Journal of Applied Sciences, 34*, 24–34.

United Nations Environment Programme (UNEP). (2022). *Monitoring water quality: GEMS/Water programme*. United Nations Environment Programme. https://www.unep.org/gemswater

United Nations (UN). (2016). *Step-by-step methodology for monitoring water quality (SDG indicator 6.3.2)*. UN-Water. https://www.unwater.org/publications/step-step-methodology-monitoring-water-quality-632

UNESCO (2021). Water Quality and Wastewater. UN-Water.

UN-Habitat. (2016). World cities report 2016: Urbanization and development- Emerging futures. United Nations Human Settlements Programme.

United Nations (UN). (2016). *Sustainable Development Goal 6: Ensure access to water and sanitation for all*. UN.

UN-Water. (2011). *Policy Brief on Water Quality. UNEP.*

UN-Water. (2021). *International Initiative on Water Quality (IIWQ)*. UNESCO.

UN-Water. (2021). Summary progress update 2021: SDG 6 – water and sanitation for all. United Nations. https://www.unwater.org/publications/summary-progress-update-2021-sdg-6-water-and-sanitation-all.

UN-Water. (2023). *Water quality and wastewater*. UN.

Valentini, M., Santos, G. B. d., & Bruno Muller Vieira, B. M. (2021). Multiple linear regression analysis (MLR) applied for modeling a new WQI equation for monitoring the water quality of Mirim Lagoon, in the state of Rio Grande do Sul-Brazil. *SN Applied Sciences, 3*(70), 1-11.

Varma, K., & Jha, P. K. (2023). Spatial and seasonal variations in nutrient load and trophic status of Ganga and Yamuna rivers in Uttar Pradesh, India. *Water Supply, 23*(6), 2553-2569.

Varma, K., & Jha, P. K. (2024). Phosphorus distribution in the water and sediments of the Ganga and Yamuna Rivers, Uttar Pradesh, India: Insights into pollution sources, bioavailability, and eutrophication implications. *Environmental Monitoring and Assessment, 196*(336). https://doi.org/10.1007/s10661-024-12499-0.

Vidal, M., & Vargas, R. (2008). Water quality assessment of surface water resources using multivariate analysis: A case study in the Atacama Desert, Chile. Environmental Monitoring and Assessment, 137(1-3), 373-384. https://doi.org/10.1007/s10661-007-9705-3.

Vrzel, J., & Ogrinc, N. (2015). Nutrient Variations in the Sava River Basin. *Journal of Soils and Sediments, 15*, 2380–2386.

Wafula, M. S. M., Owuor, P. O., Kengara, F. O., Ofula, A. V. O., & Matano, S. A. (2018). Influence of land use practices on water physicochemical parameters and nutrients loading along the Mara River of East Africa. *African Journal of Environmental Science and Technology, 12*(7), 235-243. https://doi.org/10.5897/AJEST2015.2021.

Walsh, C. J., Roy, A. H., Feminella, J. W., Cottingham, P. D., Groffman, P. M., & Morgan II, R. P. (2005). The urban stream syndrome: Current knowledge and the search for a cure. *Journal of the North American Benthological Society, 24*(3), 706-723. https://doi.org/10.1899/04-028.1

Wambugu, W., Nyandega, I., & Kıthiia, S. (2017). Spatiotemporal dynamics of land-use practices on rivers in tropical regions: A case study of Ruiru and Ndarugu basins, Kiambu County, Kenya. *African Journal of Environmental Science and Technology, 11*(8), 426-437. https://doi.org/10.5897/AJEST2017.2383

Wang, M., Strokal, M., Burek, P., Kroeze, C., Ma, L., & Janssen, A. B. G. (2019). Excess nutrient loads to Lake Taihu: Opportunities for nutrient reduction. *Science of the Total Environment, 664*, 865–873. https://doi.org/10.1016/j.scitotenv.2019.02.051.

Wang, Z., Chen, J., & Zhou, Y. (2020). Assessment of Electrical Conductivity Levels in Urban Rivers: Case Study and Management. Science of the Total Environment, 735, 139212.

Water Resources Authority (WRA). (2022). *Basin area: Athi River Basin. Accounting for every drop*. WRA, Kenya.

Water.org. (2023). *Empowering families in Kenya with access to water*. Water.org.

Waturu, M., Sitoki, L., Lalah, J., Chasia, S., & Mbao, E. (2023). Effect of land use/land cover changes on water quality in the upper Athi River sub-catchment in Kenya. *African Journal of Aquatic Science*, 1-13. https://doi.org/10.1080/16085914.2023.2210153

Wetzel, R. G. (2001). *Limnology: Lake and river ecosystems* (3rd Ed.). Academic Press.

Weyer, P. J., Cerhan, J. R., Kross, B. C., Hallberg, G. R., Kantamneni, J., Breuer, G., Jopnes, M. P., Zheng, W., & Lynch, C. F. (2001). Municipal drinking water nitrate level and cancer risk in older women: The Iowa Women's Health Study. *Epidemiology, 12*(3), 327-338.

WHO. (2017). *Guidelines for drinking-water quality* (4th ed., incorporating first addendum). Geneva, Switzerland: World Health Organization.

WHO. (2022). Guidelines for drinking-water quality. World Health Organization. https://www.who.int/water_sanitation_health/dwq/gdwq3/en/

Wierzba, P. (2022). Water quality monitoring and assessment: An integrated approach. Springer.

Wilson, M. M., Michieka, R. W., & Mwendwa, S. M. (2021). Assessing the influence of horticultural farming on selected water quality parameters in Maumau Stream, a tributary of Nairobi River, Kenya. *Heliyon, 7*(12), E08593. https://doi.org/10.1016/j.heliyon.2021.e08593

Wokeh, O., Okey-Wokeh, C., & Orose, E. (2023). Water quality assessment and spatial variation in Aba River water, South-Eastern Nigeria. *African Journal of Pure and Applied Sciences*, *4*(1), 36-41.

Wu, Y., Wang, X., & Chen, J. (2010). Long-term changes in COD, BOD and nitrogen levels in the main stem of the Yangtze River (China) as a consequence of management strategies. *Environmental Monitoring and Assessment, 165*(1-4), 429-444.

Xu, W., Duan, L., Wen, X., Li, H., Li, D., Zhang, Y., & Zhang, H. (2022). Effects of seasonal variation on water quality parameters and eutrophication in Lake Yangzong. *Water, 14*(17), 2732. https://doi.org/10.3390/w14172732.

Zelenakova, M., Purcz, P., Pintilii, R. D., Blistan, P., Petr Hlustik, P., Oravcova, A., & Hashim, M. A. (2018). Spatiotemporal variations in water quality parameter trends in river waters. *REV.CHIM. (Bucharest), 69*(10). https://doi.org/10.37358/Rev.Chim.69.10.6742

Zhang, H., Tang, Y., & Ma, H. (2014). Characterization of river water buffering capacity based on natural and anthropogenic factors. *Environmental Science and Pollution Research, 21*(11), 6980–6990. https://doi.org/10.1007/s11356-014-2556-x.

Zhang, W., Jin, X., Liu, D., Lang, C., & Shan, B. (2017). Temporal and spatial variation of nitrogen and phosphorus and eutrophication assessment for a typical arid river - Fuyang River in Northern China. *Journal of Environmental Science, 7*(4), 41-48. https://doi.org/10.1016/j.jes.2016.08.001.

Zhang, Y., Wang, W., Yang, Y., Liu, J., & Tian, C. (2021). Influence of Nutrient Concentrations on Algal Growth and Oxygen Dynamics in Aquatic Systems. *Environmental Science and Pollution Research, 28*(4), 4735–4748. https://doi.org/10.1007/s11356-020-10947-6.

Zhao, L., & Wang, J. (2020). Sources and Distribution of Cadmium in River Systems: A Review. *Environmental Science and Pollution Research, 27*, 2351-2364.

Zhitkovich, A. (2011). Chromium in drinking water: Sources, metabolism, and cancer risks. *Chemical Research in Toxicology*, 24, 1617–1629.

Zhou, L. (2022). A study of spatial distribution of water pollutants and water quality in Puget Sound Basin, Washington State, U.S. based on GIS. *International Journal of Frontiers in Engineering Technology*, *4*(4), 73-8.

Zhou, X., Liu, Y., & Zhao, X. (2007). The use of multivariate statistical techniques for the assessment of water quality in a river basin. *Water Research, 41*(15), 3421-3432.

Zhu, L., & Zhang, Y. (2023). Assessment of Water Quality and Land Use Changes in the Yellow River Basin, China. *Environmental Science and Pollution Research, 30*, 28052–28064. https://doi.org/10.1007/s11356-023-27191-3.

Zubaidah, T., Karnaningroem, N., & Slamet, A. (2019). The self-purification ability in the rivers of Banjarmasin, Indonesia. *Journal of Ecological Engineering, 20*(2), 177–182.

Zurqani, H. A., Post, C. J., Mikhailova, E. A., Schlautman, M. A., & Sharp, J. L. (2018). Geospatial analysis of land use change in the Savannah Rive Basin using Google Earth Engine. *International Journal of Applied Earth Observation and Geoinformation, 69*, 175–185.

APPENDICES

Appendix i: Permission to proceed for data colection

SOUTH EASTERN KENYA UNIVERSITY
OFFICE OF THE DIRECTOR
BOARD OF POST GRADUATE STUDIES

P.O. BOX 170-90200
KITUI, KENYA
Email: info@seku.ac.ke

TEL: 020-4213859 (KITUI)
Email: directorbps@seku.ac.ke

Our Ref: B502/KIT/30016/2021

DATE: 27th November 2023

Ogbonna Vincent Anaboro
Reg. No. B502/KIT/30016/2021
Doctor of Philosophy in Environmental Management
Email: Vintofoundation@yahoo.com

Dear Anaboro

RE: PERMISSION TO PROCEED FOR DATA COLLECTION

This is to acknowledge receipt of your Doctor of Philosophy in Environmental Management Proposal document entitled: ***"Spatio-temporal Variations in Water Quality of River Basin, Kenya"***

Following a successful presentation of your Ph.D Proposal, the School of Agriculture, Environment, Water and Natural Resources Board of Examination in conjunction with the Directorate, Board of Postgraduate Studies (BPS) have approved that you proceed to research data collection in accordance with your approved proposal.

During the research work, you will be supervised by Dr. Charles Ndung'u and Dr. Matheaus K. Kauti You should ensure that you liase with the supervisors at all times. In addition, you are required to fill in a Progress Report ***(SEKU/ARSA/BPS/F-02 and SEKU/ARSA/BPS/F-14,))*** which can be downloaded from the University Website.

The Board of Postgraduate Studies wishes you well and successful research data collection, analysis and project report writing.

r. Carol Hunja
Director, Board of Postgraduate Studies

Copy to: Deputy Vice Chancellor, Academic, Research and Innovation (Note on File)
Dean, School of Agriculture, Environment, Water and Natural Resources
Chairman, Department of Environmental Science and Land Resources Management
Dr. Charles Ndung'u
Dr. Matheaus K. Kauti

Appendix ii: Interview Survey

Interview Survey Using Open-Ended Questions on Participants' Thoughts, Observations, and Experiences Regarding Water Quality of the Mid Reaches of River Athi Basin.

- **Interview Questions on Community Perception of River Athi Water Quality Issues**

Table 4.1 *Changes noticed in the Athi river water quality over time and space*

Q/N	Open Ended interview	Purpose of the Question
1.	Can you describe yourself and role in your village based on River Athi Issues?	To understand the respondent background knowledge in River Athi
2.	How would you describe the current water quality in your village?	To gather perceptions of water status
3.	How long did you started experiencing physical changes?	To know when the river changes color
4.	What are the materials common found in the river and what time?	To understand the types of usually flow and the period
5.	Do you drink the water?	To know if the water is used for consumption
6.	Is there fish in the river? If yes do you eat it and other aquatic organisms?	To know whether there is fish used for food

Table 4.2 *The causes of water pollution of the river athi basin*

Q/N	Open Ended Interview	Respondents
1.	Is the river polluted?	
2.	Can you describe your experience with water pollution area?	
3.	What do you think are the major causes of the river pollution?	
4.	What are the role of government to avert the pollution?	
5.	Is there any awareness campaign on health implication in drinking the water and eating Fishes in the river?	

Appendix iii: Apparantus/Field Tools Use for This Study

Plate 1. Plastic Bottles Used For Water Samples & An Improvise Sampler

Plate 2. Sealed Water Samples and Ice Cooler

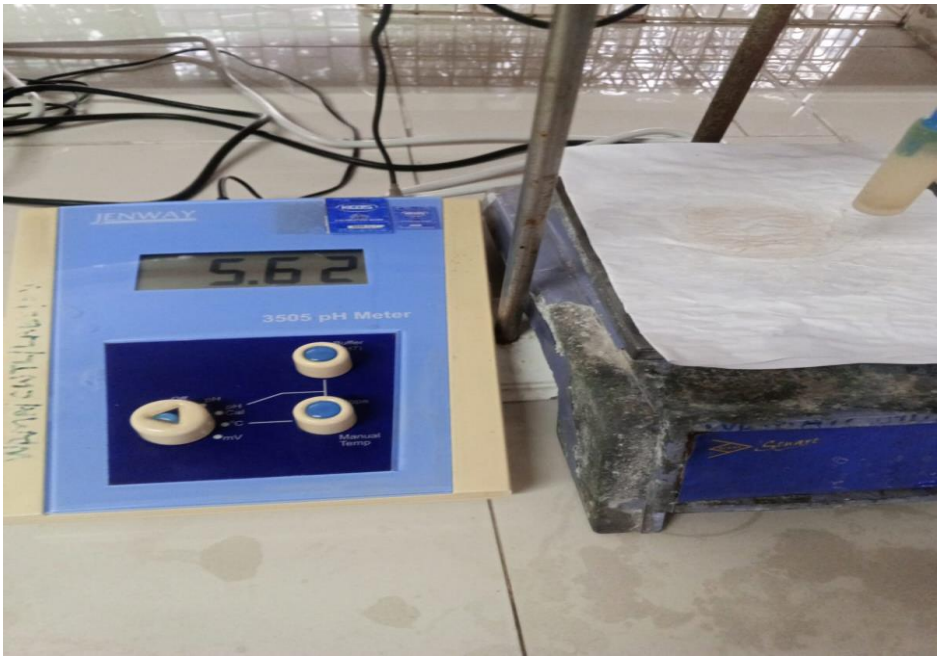

Plate 3: Electric pH Meter Used for The Analysis